Application of machine learning to quantify forest cover loss in the Congo Basin and its implications for large mammal habitat suitability

Yisa Ginath Yuh

A Thesis

in

The Department

of

Geography, Planning and Environment

Presented in Partial Fulfillment of the Requirements

for the Degree of Doctor of Philosophy (Geography, Urban and Environmental Studies)

at Concordia University

Montreal, Quebec, Canada

August 2023

CONCORDIA UNIVERSITY

SCHOOL OF GRADUATE STUDIES

This is to certify that the thesis prepared

By: Yisa Ginath Yuh

Entitled: **Application of machine learning to quantify forest cover loss in the Congo Basin and its implications for large mammal habitat suitability**

and submitted in partial fulfillment of the requirements for the degree of

Doctor of Philosophy (Geography, Urban and Environmental Studies)

Complies with the regulations of the University and meets the accepted standards with respect to originality and quality.

Signed by the final Examining Committee:

_____ Chair
Dr. Eric Pederson

_____ Examiner
Dr. Robert Weladji

_____ Examiner
Dr. Angela Kross

_____ Examiner
Dr. James Grant

_____ External Examiner
Dr. Travis Steffens

_____ Supervisor
Dr. Sarah Turner

_____ Supervisor
Dr. Damon Matthews

Approved by _____
Dr. Pascale Biron, Graduate Program Director

September 05, 2023 _____
Dr. Pascale Sicotte, Dean of Faculty

Abstract

Application of maching learning to quantify forest cover loss in the Congo Basin and its implications for large mammal habitat suitability.

Yisa Ginath Yuh, Ph.D.
Concordia University, 2023

Machine learning (ML) models are a powerful tool for land use and land cover (LULC) mapping. In the African tropics, and particularly in the Congo Basin, there is a need to better assess the performance and reliability of ML-based LULC classification using coarse-resolution satellite images. In the context of ongoing climate change and socioeconomically-driven forest disturbances, it is important to understand and quantify the extent of forest cover loss in the Congo Basin, as well as the impact of this loss on suitable habitat for key wildlife species. In this dissertation, I address these key issues in three manuscript-based chapters. In Chapter 2, I compared the classification performance of four ML algorithms (k-nearest neighbor (kNN), support vector machines (SVM), artificial neural networks (ANN), and random forests (RF)) for LULC mapping within a tropical region in Central Africa (the Mayo Rey department of northern Cameroon). All four classification algorithms produced high accuracy (overall classification accuracy > 80%), with the RF model (> 90% classification accuracy) outperforming the other algorithms. In Chapter 3, I used the RF model, together with the Idrissi TerrSet land change modeler, to map and project LULCC for the Congo Basin under historical and future scenarios of socioeconomic impacts and climate change. I found that over 352642 km^2 of dense forests have been lost in this region between 1990 and 2020, with projected continued loss of about 174860 - 204161 km^2 by the year 2050. In Chapter 4, I produced spatially explicit species distribution models to map habitat suitability for great apes (chimpanzees and gorillas) and elephants within the Dzanga Sangha Protected Areas (DSPA) of the Congo Basin. I found that priority habitat areas for the three mammal species mostly occurred and overlapped spatially within the DSPA national parks. However, priority habitat areas for the three species declined by 4, 4.5 and 9.8 percentage points respectively between 2015 and 2020, mostly due to increased human pressures. This research provides a new understanding of the extend and implications of forest cover loss in the Congo Basin, highlighting the critical conservation challenges that remain in this region.

Acknowledgements

My first and greatest acknowledgement goes to Drs. Sarah Turner and Damon Matthews for giving me the opportunity to work with them as a grad student. They believed in me from the beginning of my grads program till date, and gave me the opportunity to always knock on their office and home doors whenever I was in need. They did not only give me the best mentoring I have ever received in a research environment, but gave me the opportunity to work and visit them as a family. Their sense of humility and love is so exceptional that I will always live to say thank you. Like many other researchers, undergrad and grad students in your Labs, you gave me the opportunity and possibility to discover and believe in my research potentials. Thank you both for being wonderful and exceptional supervisors to my PhD studies.

My sincere thanks further go to Dr. Paul N'goran, the regional biomonitoring coordinator for the WWF Congo Basin program. You believed in my project from the onset, and provided me with the mentoring, financial, and office resources to successfully accomplish my PhD studies as an intern. You were not only a colleague to me during my time at WWF, but a friend, and model for success. Your commitments, hard work and consistent follow-ups gave me the opportunity to work hard, and successfully finish my internship and PhD research tasks on time. I owe you every respect and gratitude.

I also acknowledge the efforts of WWF Germany for their continuous funding and support to the Congo Basin Biomonitoring Program. Sincere thanks also go to the University of Concordia for supporting my research activities within the Congo Basin through the Canadian MITACS Accelerate funding program. I give lots of credits to Anna-Maria Moubayed for a great role towards my MITACS funding success, and to Jessica Park and WWF Canada for providing matching funds. Special thanks also goes to the German

Academic Exchange Service (DAAD), and the British Ecological Society for respectively supporting my research activities through the British Ecological Society (BES) ecologist for Africa award, and the DAAD short term research grants. We also acknowledge the collaboration and support offered to this project by the Wildlife Ecology Lab at the University of Freiburg, Germany.

Sincere thanks further goes to all my external collaborators, especially Dr. Wiktor Tracz; who was my Master Thesis supervisor at the Warsaw university of Life science, and who believed in my academic and research potentials from the onset, and is still collaborating with me till date. You are also a wonderful mentor, and I will never cease to say thank you for your support and confidence bestowed in me. I also want to say thank you to all my Lab colleagues for their collaborations, and sense of diversity and inclusion in our working environment.

Sincere thanks also goes to my committee members (Drs. Robert Weladji and Angela Kross) for their commitments towards reviewing my dissertation project, as well as open their doors for guidance and advice towards a successful completion. Special thank you also goes to all external reviewers of my work, including those that reviewed my dissertation proposal, final thesis, and published manuscripts.

Finally, I want to say thank you to my wife (Tangwa Juliette), my daughter (Yuh Rhemaleah), my parents (Mr. Nikang Stephen and Mrs. Kumbong Tilda), my friends (Teboh Godlove, Ngale Xavier, Samuel Lyonga, Herve Nundo Brice, and Stephan Mbukam), and all other family members who supported me in one way or the other towards my academic achievements.

Dedication

I dedicate this to my wife (Tangwa Juliette), my daughter (Yuh Rhemaleah), and my parents (Mr. Nikang Stephen and Mrs. Kumbong Tilda). To the entire WWF Congo Basin team for their exceptional contributions towards my academic achievements, and to Dr. Sarah Turner and Damon Matthews for their wonderful guidance and mentorship.

Contribution of Authors

As the corresponding author, I contributed in the conceptualization, data acquisition, data analysis and validation, and manuscripts and thesis preparation, writing, revision and editing. Dr. Sarah Turner and Damon Matthews contributed in the conceptualization, supervision, and manuscripts and thesis revision and editing. Dr. Wiktor Tracz contributed in the conceptualization, supervision, revision and editing of chapter one, while Dr. Kouame Paul N'Goran contributed in the conceptualization, supervision, revision and editing of chapters two and three. Dr. Ilka Herbinger coordinated all field operations for chapter three, as well as assisted in editing chapters two and three. Dr. Marco Heurich assisted in the revision and editing of chapter two, while Ghislain Brice Beukou, Janika Wendefeuer, Terence Fuh Neba, Aristide Mesac Ndotar, Denis Lambert NdombaA, and Albert Christian Junior Ndadet collected and contributed field data for Chapter 4.

Chapter two has been published in the Journal *Ecological Informatics* as:

Yuh, Y. G., Tracz, W., Matthews, H. D., & Turner, S. E. (2023). Application of machine learning approaches for land cover monitoring in northern Cameroon. *Ecological Informatics*, 74, 101955. https://doi.org/10.1016/j.ecoinf.2022.101955

Chapter three is in preparation to be submitted to the journal *Science Advances* as:

Yuh, Y. G., N'Goran, K. P., Herbinger, I., Heurich, M., Matthews, H. D., & Turner, S. E. Monitoring Forest cover and land use change in the Congo Basin under IPCC climate change scenarios.

Chapter four has been published in the journal *Global Ecology and Conservation* as:

Yuh, Y. G., N'Goran, K. P., Beukou, G. B., Wendefeuer, J., Neba, T. F., Ndotar, A. M., NdombaA, D. L., Ndadet, A. C. J., Herbinger, I., Matthews, H. D., & Turner, S. E. (2023). Recent decline in suitable large mammal habitats within the Dzanga Sangha Protected Areas, Central African Republic. *Global Ecology and Conservation*, 42, e02404. https://doi.org/10.1016/j.gecco.2023.e02404

Table of Contents

List of Figures and Illustrations

Chapter 2: Application of machine learning approaches for land cover monitoring in northern Cameroon

Chapter 3: Monitoring Forest cover and land use change in the Congo Basin under IPCC climate change scenarios

Chapter 4: Recent decline in suitable large mammal habitats within the Dzanga Sangha Protected Areas, Central African Republic

List of Tables

Chapter 2: Application of machine learning approaches for land cover monitoring in northern Cameroon

Chapter 3: Monitoring Forest cover and land use change in the Congo Basin under IPCC climate change scenarios

Chapter 4: Recent decline in suitable large mammal habitats within the Dzanga Sangha Protected Areas, Central African Republic

List of Supplementary Figures

Chapter 2: Application of machine learning approaches for land cover monitoring in northern Cameroon

Chapter 3: Monitoring Forest cover and land use change in the Congo Basin under IPCC climate change scenarios

Chapter 4: Recent decline in suitable large mammal habitats within the Dzanga Sangha Protected Areas, Central African Republic

List of Supplementary Tables

Chapter 2: Application of machine learning approaches for land cover monitoring in northern Cameroon

Chapter 3: Monitoring Forest cover and land use change in the Congo Basin under IPCC climate change scenarios

Chapter 4: Recent decline in suitable large mammal habitats within the Dzanga Sangha Protected Areas, Central African Republic

List of Abbreviations and Nomenclature

Abbreviations

ANN, Artificial Neural Networks

AR, Apparent Reflectance model

AUC, Area Under the Curve

CAR, Central African Republic

CART, Classification and Regression Trees

CBD, Convention on Biological Diversity

CI, Confidence Interval

CMIP6, Coupled Model Inter-comparison Project phase 6

CMR, Cameroon

COMIFAC, Commission for the Forests of Central Africa

COST, Cosine estimation of atmospheric transmittance

DOS, dark object subtraction

DRC, Democratic Republic of Congo

DSPA, Dzanga Sangha Protected Areas

DT, Decision Trees

ETM+, Enhanced Thematic Mapper Plus

FAO, Food and Agricultural Organization

GAM, Generalized Additive Model

GB, Gabon

GEDI, Global Ecosystems Dynamics Investigation service

GEE, Google Earth Engine

GHoA, Green Heart of Africa

GIS, Geographic Information Systems

GLM, Generalized Linear Model

HS, Habitat Suitability

ILCM, Idrissi Land change modeler

IPCC, Intergovernmental Panel on Climate Change

IPCC-AR6, Intergovernmental Panel on Climate Change Sixth Assessment Report (AR6)

IUCN, International Union for Conservation of Nature

kNN, K-Nearest Neigbours

LULCC, Land use and Land cover change

Mha, Million hectares

ML, Machine Learning

MLC, Maximum Likelihood classification

MODIS, Moderate Resolution Imaging Spectroradiometer

MP-ANN, Multiperceptron Artificial Neural Networks

NA, Not Applicable

NASA, National Aeronautics and Space Administration

NDVI, Normalized Differential Vegetation Index

NDWI, Normalized Differential Water Index

NIR, Near Infra-red

NOAA, National Oceanic and Atmospheric Administration

NPs, National Parks

NS, Non-significant

OA, overall accuracy

OLI, Operational Land Imager

OLS, Ordinary Least Square

PAs, Protected Areas

PCA, Principal Component Analysis

PP, Percentage Point

QA, Quality Assessment bands

radCor, Radiometric Calibration and Correction

RC, Republic of Congo

RCP, Representative Concentration Pathway

REDD+, Reduce Emissions from Deforestation and Forest Degradation

RF, Random Forests

ROC, Receiver Operator Characteristics

SDM, Species Distribution Model

SDOS, simple dark object subtraction

SINFOCAM, Société Industrielle des Forêts Centrafricaines et d'Aménagement

SMART, Spatial Monitoring and Reporting Tool

SSP, Shared Socioeconomic Pathways

STBC, Société de Transformation de Bois en Afrique Central

SVM, Support Vector Machines

TNS, Sangha Tri-National Landscape

TOA, top of atmosphere

UNESCO, United Nations Educational, Scientific and Cultural Organization

UNFCCC, United Nations Framework Convention on Climate Change

USGS, United States Geological Survey

VIF, Variance Inflation Factor

WCS, Wildlife Conservation Society

WWF, World Wildlife Fund

ZCC, Community Hunting Zone

Nomenclature

African forest antelope, *Tragelaphus euryceros*

African forest elephant, *Loxodanta cyclotis*

African savanna elephant, *Loxodanta africana*

Bonobo, *Pan paniscus*

Central chimpanzee, *Pan troglodytes troglodytes*

Cross River gorilla, *Gorilla gorilla diehli*

Eastern chimpanzee, *Pan troglodytes schweinfurthii*

Eastern lowland gorilla, *Gorilla beringei graueri*

Forest buffalo, *Syncerus caffer nanus*

Mountain gorilla, *Gorilla beringei beringei*

Nigeria-Cameroon chimpanzee, *Pan troglodytes ellioti*

Western chimpanzee, *Pan troglodytes verus*

Western lowland gorilla, *Gorilla gorilla gorilla*

Chapter 1: General Introduction and Literature review

General Introduction

Deforestation and land degradation is accelerating worldwide as a result of increased socioeconomic pressures combined with changing disturbance regimes resulting from human-driven climate change (Curtis et al., 2018). As a consequence, the need to predict and map ecosystem changes has become increasingly important for conservation biologists, land use planners and other decision makers. At the level of forest cover and land use, much research has focused on understanding changes in land use and land cover dynamics, as well as the underlying drivers of change (e.g. reviewed in Chang et al., 2018; Nedd et al., 2021; Wang et al., 2023). Results from studies that have applied remote sensing, quantitative and modeling techniques have shown that large proportions of the world's forests are being converted to other land use types (e.g. grasslands, savannahs, barelands, croplands, built-up areas), with much of these conversions predicted to be caused by logging and forest clearing, infrastructural developments, forest fires and other potential disturbances resulting from global warming (Geler Roffe et al., 2022; Kumar, 2011; Ritchie & Roser, 2021), and human population density (Cafaro et al., 2022); a partial indicator for a combination of anthropogenic drivers, impacts and pressures arising from economic neocolonialism (e.g. forest logging and resource exploitation by higher income countries, increased agricultural productivity for export to higher income countries, and socioeconomic inequalities amongst and within nations) and Neo-Malthusianism (i.e. population growth outspaces food supply, hence leading to rapid deforestation for increase agricultural productivity) (Hughes et al., 2023). Neocolonialism, an instrument of imperialism, is defined as the exploitation of the less developed parts of the world by powerful and higher income countries in a way that impoverishes (rather than developing) the less developed world, with investments increasing

rather than decreasing the gap between the higher and low income countries of the world (Nkrumah, 1976). Problems with economic neocolonialism, Neo-Malthusianism and climate change are particularly acute in the African tropics, especially in the Congo Basin, where the intensity of human activities is increasing, and the effects of global warming are expected to increase in severity i.e., mean annual temperatures are expected to rise by 2-4°C by the end of the 21st century (Aloysius et al., 2016; Diedhiou et al., 2018; Fotso-Nguemo et al., 2017; Mba et al., 2018; Tamoffo et al., 2019).

The Congo Basin is a global biodiversity hotspot. The region is reported to face continued deforestation, with average annual rates estimated at approximately 1 million hectares (Mha) (Tyukavina et al., 2018). Socioeconomic (e.g. industrial selective logging, small scale clearing for agriculture, large scale agro-industrial clearing, and construction of roads and houses); and climate-related disturbances (e.g. forest fires) are reported to be the main contributing factors (Juárez-Orozco et al., 2017; Kleinschroth et al., 2019; Tyukavina et al., 2018), with these problems causing large-scale changes in land use and land cover (LULC) patterns, and consequently, habitat fragmentation and decreased habitat connectivity. Fragmentation and land use change problems are expected to increase substantially in the future, as conversion of forested land to agricultural land continues, and with increased global warming (Estrada et al., 2017). However, several important issues remain poorly documented. First, although socioeconomic and climate-related factors are reported to contribute to forest cover loss in this region (Tyukavina et al., 2018), their effects have not been fully incorporated in land use and land cover change (LULCC) mapping in this region (e.g. Ludwig et al., 2013, but see Tyukavina et al., 2018). Moreover, limited information is available in the scientific literature on the contributions of climate change to LULCC in this region. Climate change in particular has been shown to cause changes in land cover patterns in several regions across the globe. For example, in the Amazon Basin of South America,

López et al., (2022) expect that climate change will lead to approximately 30-35% loss in forest cover in this region by the year 2050. In the United States of America, Mu et al., (2017) modeled potential impacts and found that climate change could lead to substantial reductions in croplands, and pasture lands by the year 2070. In Europe, Carozzi et al., (2022) found that climate change could cause approximately 6 and 7% loss in crop and grasslands respectively by the year 2099. In other regions of the world, climate change has been projected to interact with other drivers of land use change (e.g. socioeconomic variables such as wood extraction, domestic costs for land, labor and timber, price increase for cash crops, agricultural and infrastructural expansions; soil erosion; topography; institutional factors related to neocolonial forest policies and poor forest governance; and human population density (a proxy to economic neocolonialism)) to substantially alter land use and land cover change in the long-term (Geist & Lambin, 2002, 2004; Hellwig et al., 2019). Thus, the impact of climate change needs to be considered in present and future LULCC mapping in order to provide accurate assessments of land cover change dynamics within the Congo Basin.
Second, most studies have mapped and quantified forest cover and land use changes at relatively small geographical scales (e.g., country and landscape scales) (Molinario et al., 2017; Potapov et al., 2012; Yuh et al., 2019) or over shorter time periods (e.g., 1 – 15 years) (deWasseige et al., 2009; Ernst et al., 2013; Mayaux, 2004; Mayaux et al., 2002; Molinario et al., 2017; Potapov et al., 2012; Tyukavina et al., 2018; Verhegghen et al., 2012; Yuh et al., 2019). However, to date, to the best of my knowledge, no study has made a comprehensive projection of future conditions that incorporates the predicted increase in impacts of socio-economic, demographic, and climate-related effects for the Congo Basin. There is therefore a need to map and project present and future changes in forest cover and land use patterns in this region, as well as document the associated impacts of socioeconomic factors and climate changes. Mapping tools and quantitative models can help describe and predict such large

scale spatiotemporal changes, and using this integrated approach, baseline information required for landscape conservation and management could be provided for the Congo Basin, and inform our understanding of global climate change and biodiversity loss.

Over the last two decades, Machine Learning (ML) models have been identified as powerful computational tools for mapping LULCC. Prominent examples of models proven to be successful include Artificial Neural Networks (ANN) (Alshari et al., 2023; Díaz-Pacheco & Hewitt, 2014; Megahed et al., 2015; Silva et al., 2020; Zerrouki et al., 2019), Support Vector Machines (SVM) (Adam et al., 2014; Cardoso-Fernandes et al., 2020; Dabija et al., 2021; Gong et al., 2013; Paneque-Gálvez et al., 2013; Thakur & Panse, 2022; Zerrouki et al., 2019), Random Forests (RF (Adam et al., 2014; Cutler et al., 2007; Gong et al., 2013; Magidi et al., 2021; Thakur & Panse, 2022; Zerrouki et al., 2019), Decision Trees (DT) (Teodoro, 2015), K-Nearest Neigbours (kNN) (Samaniego & Schulz, 2009; Zerrouki et al., 2019), Classification and Regression Trees (CART) (Basheer et al., 2022), and the Maximum Likelihood classification (MLC) (Guermazi et al., 2016). These models generally use non-linear statistical or probabilistic modeling approaches to automatically predict and detect patterns in data through a supervised learning process, and with high degrees of accuracy (Breiman, 2001b). They are very powerful in dealing with large and complex datasets, as well as spatial layers with missing data.

Because of the complexity in LULC classification uncertainties or accuracies between ML methods, Khatami et al., (2016) conducted a large-scale meta-analysis of pixel based supervised classification extracted from over 266 published articles. They found that SVM, ANN, kNN and RF improve LULC classification accuracy as compared to other supervised classification approaches (e.g. MLC, DT, CART etc.). To continue to improve LULC mapping accuracies for effective land use planning, the classification performances of two or more of these algorithms have been recently compared in many regions across the globe. For

example, in Asia, Alshari et al., (2023) have used the Multiperceptron Artificial Neural Network (MP-ANN) and RF modeling algorithms to accurately map and document land cover patterns within the Sana'a city of Yemen for the year 2016. In Europe, Dabija et al., (2021) applied SVM and RF to improve the Corine land cover mapping and classification accuracy for selected landscapes within Poland and Romania. Pacheco et al., (2021) compared the classification performance of the kNN and RF classifiers in mapping land cover change within Central Portugal. In North America, Basheer et al., (2022) compared the classification performance of the RF and SVM classifiers in accurately mapping LULCC for the city of Charlottetown in Canada, for 2017 – 2021. In South America, Volke & Abarca-Del-Rio, (2020) compared the classification performance of SVM and RF in mapping LULC within earthquake and Tsunami affected areas in Chili for the year 2010. For Africa, however, limited considerations have been given to the application of these approaches for the effective monitoring of changes in LULC, especially within tropical rainforest regions, where coarse resolution satellite images are often the only available option. Those studies that do exist have generally relied on applying only a single method (Brink & Eva, 2009; Matlhodi et al., 2019; Midekisa et al., 2017; Zoungrana et al., 2015), which in effect, can increase classification uncertainties relative to the use of multiple ML methods. There is therefore the need to compare the classification performance of these ML algorithms, so as to improve long-term land cover change mapping in this region.

One of the regions of Africa where limited considerations have been given for comparing ML approaches for effective LULC monitoring is Central Africa. Satellite images in this region are well known for having high levels of cloud cover (Basnet & Vodacek, 2015), making analysis difficult as cloud-free satellite images are required for analysis. Together with image coarseness, a lack of availability of cloud-free images increases LULC classification uncertainties (Basnet & Vodacek, 2015). To minimize uncertainties with LULC

classification in this region, there is a need to first, compare the classification performance of ML algorithms on smaller and cloud-free or less cloudy geographical areas; and second, to use the most performant algorithm for large scale LULC mapping. Such methodological approaches would foster the advancement of knowledge in the application of ML algorithms for LULC monitoring within tropical rain forest regions across Africa, especially with the use of coarse-resolution Landsat images.

Forest cover change, land use change, climate change and forest fragmentation constitute major threats to wildlife biodiversity (Andrén & Andren, 1994; Crooks et al., 2017). Thousands of species across the globe are facing population declines due to changing environmental conditions, with a large majority of mammal species facing higher risks of extinction than are many other taxa (Andrén & Andren, 1994; Crooks et al., 2017). These devastating effects are particularly severe in the Afro-tropics, especially in the Congo Basin. Several large mammalian species in the region appear on the International Union for Conservation of Nature's (IUCN) Redlist of Threatened Species (https://www.iucnredlist.org/), many with Endangered or Critically Endangered status (e.g. Western Gorillas (*Gorilla gorilla*) are Critically Endangered; Bonobos (*Pan paniscus*) and Chimpanzees (*Pan troglodytes*) are Endangered, and the Western sub-species of chimpanzee (*Pan troglodytes verus*) is Critically Endangered; Western red colobus monkeys (*Piliocolobus badius*) are Endangered; African forest elephants (*Loxodonta cyclotis*) are Critically Endangered, and the list goes on.

Because of the severity of biodiversity loss within Congo Basin landscapes, the six countries surrounding the Congo Basin (Republic of Cameroon, Central African Republic (CAR), the Democratic Republic of Congo (DRC), Equatorial Guinea, Gabon, and Republic of the Congo) identified a number of transboundary landscapes for conservation, and established agreements for these transboundary conservation landscapes in the year 2000,

based on the Commission for the Forests of Central Africa (COMIFAC) agreement (http://www2.ecolex.org/server2neu.php/libcat/docs/TRE/Full/En/TRE-154456.pdf) . Among these landscapes, the Sangha Tri-National Landscape (TNS) established between the Republic of Congo, the Republic of Cameroon and the (CAR), was identified as one of the key areas requiring urgent management intervention. To assess conservation efforts and effectively measure conservation impacts on wildlife and suitable habitats for wildlife species within this landscape, the World Wide Fund for Nature (WWF, also known in some countries as World Wildlife Fund) developed an ecological monitoring program (N'Goran et al., 2014) as part of the Green Heart of Africa (GHoA) monitoring & evaluation framework (https://origin-congo.wwf-sites.org/what_we_do/). The objectives of the WWF ecological monitoring program are to operationalize an adequate system for the monitoring and evaluation of conservation activities, support the management of priority landscapes, and demonstrate conservation impacts in the Congo Basin (N'Goran et al., 2017). As part of its conservation strategy, the WWF ecological monitoring program focuses on medium and large size mammals (in particular, but not limited to, the forest elephants (*Loxodanta cyclotis*) and great apes (*Pan troglodytes troglodytes*, *Pan paniscus*, and *Gorilla gorilla gorilla*)).

Great Apes are large-bodied mammal species in the Primate Order, and are our closest animal relatives (Wilson & Reeder, 2005). African great ape species occur within tropical forests and woodland savannah regions across equatorial Africa (Strindberg et al., 2018). They are divided into several different subspecies based on their geographic distribution and taxonomic status. For example, chimpanzees are divided into four subspecies (Groves, 2001): *Pan troglodytes verus* (western chimpanzee) that occur within tropical and savannah woodlands across West Africa (IUCN, 2016c); *Pan troglodytes troglodytes* (central chimpanzees) that live within Central African forests (IUCN, 2016a); *Pan troglodytes schweinfurthii* (eastern chimpanzees) that live within East African forests (Plumptre, 2016)

and *Pan troglodytes ellioti* (Nigeria-Cameroon chimpanzees) that occur west of the Sanaga River between Nigeria and Cameroon (IUCN, 2015; Morgan et al., 2011). Gorillas are divided into two species; Western gorillas (*Gorilla gorilla*) and Eastern Gorillas (*Gorilla beringei*), each with two subspecies: the eastern lowland gorilla (*Gorilla beringei graueri*) and mountain gorilla (*Gorilla beringei beringei*) (IUCN, 2018; Roy et al., 2014) and the western lowland gorillas (*Gorilla gorilla gorilla*) and cross river gorillas (*Gorilla gorilla diehli*) (Oates et al., 2007, 2002; Strindberg et al., 2018; Sunderland-Groves, 2003). Bonobos constitute only a single species (*Pan paniscus*) found only South of the Congo River throughout the extensive forest belt across the Democratic Republic of Congo (DRC) (IUCN, 2016b).

African elephants (*Loxodanta spp*.) are the largest land mammals and inhabit tropical and woodland savannah regions across equatorial Africa. They are divided into two species of African elephant, the African forest elephant (*Loxodanta cyclotis*) that inhabits forested and woodland savannah regions across West and Central Africa (IUCN, 2020); and the African savanna elephant (*Loxodanta africana*) that inhabits forested and woodland savannah regions across East and Southern Africa, as well as some parts of West and Central Africa (IUCN, 2008).

Great apes (specifically chimpanzees and gorillas) and forest elephants are facing increasing threats within the Dzanga Sangha Protected Areas (DSPA) of the TNS (N'Goran et al., 2014, 2017). According to consultations conducted by the International Union for the Conservation of Nature (IUCN) and the United Nations Educational, Scientific and Cultural Organization (UNESCO), these large mammal species are losing the suitable habitats required for their survival, and therefore their conservation requires urgent management intervention (UNESCO, 2015, 2017, 2019; UNESCO/IUCN, 2016). In general, habitat suitability for these large mammals have been shown to be strongly impacted by climatic

factors (e.g. temperature (Hill, 2006; Kosheleff & Anderson, 2009; Pruetz et al., 2002; Thomas & Bacher, 2018) and precipitation (Reed & Fleagle, 1995)); landscape factors such as topography (Fitzgerald et al., 2018) and presence and distribution of water bodies (Plumtre, 2010); the type of land cover (dense forests, swampy forests, grasslands) (Ginath Yuh et al., 2020; Morgan et al., 2019; Strindberg et al., 2018; Yuh et al., 2019); human activities such as hunting (Araújo et al., 2004; Chase et al., 2016; Ginath Yuh et al., 2020; Humle et al., 2016; Kyale et al., 2011; Maingi et al., 2012; Peres & Lake, 2003; Wittemyer et al., 2014), human population density (Strindberg et al., 2018; Zhao et al., 2018), anthropogenic deforestation (Estrada, 2013; Humle et al., 2016; Isabirye-Basuta & Lwanga, 2008; Sá, 2012; Yuh et al., 2019) and anthropogenic habitat fragmentation (e.g. caused by permanent land use change and road construction) (Fotang et al., 2021; Wittemyer et al., 2014); and the enforcement of laws associated with conservation and protection, such as those enforced with the presence of eco-guard patrols (Kablan et al., 2019; Morgan et al., 2018; N'Goran et al., 2012). Yet, to our knowledge no study has evaluated the potential impacts of these environmental and human factors on species distribution within the DSPA, a problem that I fully address in one of my dissertation research chapters.

In this dissertation therefore, I aimed to: 1) compare the classification performance of four ML algorithms (MP-ANN, RF, SVM, and kNN) in accurately mapping LULCC within a tropical forest region in Central Africa; 2) use the most performant ML algorithm for large scale LULC mapping for the Congo Basin; and 3) document the influence of land use factors and human activities on the spatial distribution of large mammal species within the DSPA. To fulfill these aims, I present here three manuscript-based chapters. In Chapter 2 of this dissertation, I applied machine learning approaches to monitor LULCC in Northern Cameroon. The specific objective in this chapter was to apply statistical and machine learning approaches using four classification algorithms (ANN, kNN, SVM, and RF) to effectively

map and quantify LULCC within a tropical rainforest region in Central Africa (the Mayo Rey department of northern Cameroon), thereby providing a first attempt in comparing these algorithms within such a setting. In Chapter 3, I used the machine learning algorithm with the highest classification performance identified in Chapter 2 to map and project LULCC for the Congo Basin under IPCC climate change scenarios. Specifically, I mapped land cover patterns for the Congo Basin for the period 1990 – 2020, and quantitatively assessed decadal changes in land cover patterns. I used the 1990 – 2020 LULC results as baseline data to model and project LULCC to the year 2050, under various scenarios of socioeconomic impacts, demographic factors, and climate change. In Chapter 4, I documented the recent decline in suitable large mammal habitats within the Dzanga Sangha Protected Areas of the Congo Basin. Specifically, I produced spatially explicit species distribution models to map the spatial variability and changes in ape and elephant habitat suitability within the DSPA between two survey years (2015 and 2020), using spatial datasets of eco-guard patrol activities, habitat fragmentation, land cover, human pressure, topography, and climatic variability, as model predictors. I identified priority habitats, as well as key factors affecting species distribution, quantified priority habitat loss and gain, evaluated the contributions of key factors to these changes, evaluated the relationship between suitable habitats among species, and finally, identified overlapping priority habitats for conservation.

Literature review

Forest cover and Land use change

Forests cover are an integral part of the earth's surface and are defined as land areas that contain trees with height greater than 5m, spanning more than 0.5 ha, and with canopy closures ≥ 20% (FAO, 2000; Friedl & Sulla-Menashe, 2019; Hansen et al., 2010, 2013; Potapov et al., 2021). They are categorized and classified according to canopy closures, landscape patterns and ecozones or continental assignments. For example, in Africa, forests are categorized and classified as closed or dense tropical rain forests, closed evergreen montane and sub-montane forest, savannah woodlands, and swampy and mangrove forest (Cuni-Sanchez et al., 2016; Fisher et al., 2013; Malhi et al., 2013; Mayaux et al., 2003; Mengist, 2020). In Europe, they are categorized as broadleaf, coniferous and mixed forests (Büttner, 2014). In North America, they are classified as mixed forests, temperate or sub-polar needle leaf forest, broadleaf deciduous forest, tundra forests, and sub-polar taiga needle leaf forests (Fry et al., 2011; Latifovic, 2019; Homer et al., 2007, 2015, 2020).

Land use involves the exploitation of various land cover types by humans, either for settlement or socioeconomic reasons (FAO, 2000). They are generally classified similarly across continental scales even though differ in some ecozones. For example, in Africa, various land use types include croplands, grazed lands, pastureland, bare soils, barren lands, built-up areas (e.g. roads, residential areas, railways), grasslands, shrublands and water bodies (Mayaux et al., 2003). In North America, land use types have been classified as wetlands, shrublands, croplands, barrenlands, burnt areas, water bodies, snow and ice, wetlands, grasslands, lichens and moss and built-up areas (Fry et al., 2011; Latifovic, 2019; Homer et al., 2007, 2015, 2020). In European regions, land use types involve pastures,

vineyards, agro-forestry areas, bare rocks, sparse vegetation, burnt areas, peat bogs, water bodies, salt marshes, grasslands, croplands, built-up areas etc. (Büttner, 2014).

Changes in forest cover and land use are characterized by changes in land cover and are usually defined by the interconversion of different forest cover types (e.g. the conversion of dense forests to swampy forests; woody savannas to mangrove forests; and mixed forests to coniferous forests), different land use types (e.g. the conversion of bare lands to built-up areas, grasslands to grazed lands, and grazed lands to croplands), and the conversion of forest cover categories to different land use types (e.g. the conversion of savanna forests to bare lands; dense tropical forests to built-up areas; and mixed forests to sparse vegetation) (e.g. Büttner, 2014; Homer et al., 2020). These changes can be monitored at both local, regional, and global scales, to improve our knowledge and understanding of LULCC dynamics and potential impacts on biodiversity loss.

Forest cover and land use change are driven by socioeconomic (Aguiar et al., 2007; Armenteras et al., 2006, 2019; Chen et al., 2014; Hellwig et al., 2019; Tyukavina et al., 2018; Walsh et al., 2008; Xie et al., 2005), demographic (Armenteras et al., 2006, 2019; Hellwig et al., 2019; Shi et al., 2010; Tyukavina et al., 2018; Walsh et al., 2008) and ecological or climate-related factors (Armenteras et al., 2006, 2019; Serra et al., 2008; Tyukavina et al., 2018; Walsh et al., 2008). Socioeconomic factors are societal and economically related land use change factors, most often arising from issues related to economic neocolonialism, poverty, poor governance, and Neo-Malthusianism (Hughes et al., 2023). Examples include small-scale large-scale clearing for agriculture, large-scale agro-industrial clearing, industrial logging, resource exportation to high income countries, socioeconomic inequalities, mining, construction of roads, dams and settlements, and the use of forest resources for food, medicine, and firewood (Aguiar et al., 2007; Armenteras et al., 2006; Hellwig et al., 2019; Lambin et al., 2001; Tyukavina et al., 2018; Xie et al., 2005). Demographic factors include

human population density (Armenteras et al., 2006, 2019; Cafaro et al., 2022; Hellwig et al., 2019; Tyukavina et al., 2018) that is often used as a partial indicator for a combination of anthropogenic drivers, impacts and pressures arising from economic neocolonialism (Hughes et al., 2023). Ecological or climate-related factors include forest fires (Morgan et al., 2020; Tyukavina et al., 2018), changing temperature and precipitation patterns (deWasseige et al., 2015; Hellwig et al., 2019), and landscape topography (Armenteras et al., 2019; Bakker et al., 2005; Zgłobicki et al., 2016). These factors generally interact together to influence forest cover and land use change (Li et al., 2016; Serra et al., 2008), and because they constitute important change drivers, they are predicted to significantly alter the states of future forest cover and land use patterns across several geographical scales (Ameray et al., 2023; Beaumont & Duursma, 2012; Carozzi et al., 2022; Chaturvedi et al., 2011; Chen et al., 2020; Cox et al., 2004; Geist & Lambin, 2002, 2004; Hellwig et al., 2019; Hurtt et al., 2011; Kolden & Abatzoglou, 2012; Liang et al., 2018; Liu et al., 2017; Mu et al., 2017; Stralberg et al., 2018; Upgupta et al., 2015; Zgłobicki et al., 2016). These problems are particularly acute for the African tropics, especially in the Congo Basin, where anthropogenic land-use activities are highly alarming (Tyukavina et al., 2018).

The Congo Basin is a global biodiversity hotspot. A recent study by Tyukavina et al., (2018), has shown that the region annually loses approximately 1Mha of its total forest cover as a result of socioeconomic land use activities, and climate-related impacts. 45-90% of forest cover change in this region come from socioeconomic activities such as industrial logging and small and large-scale clearing for agriculture, while forest fires and construction activities (e.g. roads, settlements and commercial constructions) contribute between 4-16% (Tyukavina et al., 2018). Climate change impacts have not been fully investigated in this region, though some studies have reported changes in vegetation dynamics in western and central Sahel regions, as a result of changing precipitation patterns and drought conditions

(Anchang et al., 2019; Brandt et al., 2019), as well as the exacerbation of climate-driven vegetation change due to socioeconomic land use change activities (Aleman et al., 2017). Substantial temperature increases are expected for this region, where mean annual temperatures are expected to rise by 2-4^{o}C by the end of the 21st century (Aloysius et al., 2016; Diedhiou et al., 2018; Fotso-Nguemo et al., 2017; Mba et al., 2018; Tamoffo et al., 2019). Associated with this temperature rise, vegetation productivity is expected to be negatively affected, with many ecosystem services altered (Pörtner et al., 2022). The need to map and continuously monitor forest cover and land use change in this region, under the direct influence of socioeconomic activities and climate change is vital for addressing these issues. Several endangered wildlife species are already facing these impacts, with prominent examples being large mega faunas such as forest elephants and great apes (chimpanzees, gorillas and bonobos) (UNESCO/IUCN, 2016).

Overview of African Ape and Elephant conservation biology

Great apes (our closest animal relatives) and forest elephants are large mammal species respectively classified under the Order Primates and Order Proboscidea. In Africa, they are reported to mostly occur within protected areas (PAs), with low density estimates reported for certified logging concessions (Blake et al., 2008; Douglas-Hamilton et al., 2005; IUCN, 2014; N'Goran et al., 2014, 2015, 2016, 2017; Nzooh Dongmo et al., 2016a, 2016b; Ordaz-Nemeth et al., 2021; Strindberg et al., 2018; Wall et al., 2021). In the Congo Basin for example, approximately 64% of ape species are reported to occur within PAs, with only about 20% reported within certified forestry concessions (Strindberg et al., 2018). In Western equatorial Africa, about 17% of chimpanzees are reported to occur within PAs while approximately 10% live in nearby forest concessions (Heinicke et al., 2019). In the African

continent as a whole, over 33% of all elephant species are predicted to occur within PAs, with no reliable information presented for forestry concessions, though range estimates predict a 57% occurrence out of PAs (Wall et al., 2021). These large mammal species have been generally reported to face continued population declines as well as reductions in habitats suitable for their survival (Heinicke et al., 2019; Junker et al., 2012; Strindberg et al., 2018; Wall et al., 2021), with effects highly linked to hunting (Araújo et al., 2004; Chase et al., 2016; Ginath Yuh et al., 2020; Humle et al., 2016; Kyale et al., 2011; Maingi et al., 2012; Peres & Lake, 2003; Wittemyer et al., 2014; Maisels et al., 2013), deforestation through logging and agricultural expansions (Estrada, 2013; Isabirye-Basuta & Lwanga, 2008; Morgan et al., 2019; Robson et al., 2017; Strindberg et al., 2018; Yuh et al., 2019), and climate change (Barratt et al., 2021; Hill, 2006; Kosheleff & Anderson, 2009; Thomas & Bacher, 2018).

Efforts to conserve the population of great apes and elephants, as well as other endangered wildlife species are ongoing across their respective geographic ranges (D'udine et al., 2016; IUCN, 2014), however, several important issues related to the effective conservation of these species have not been fully reported in the Central African region. For example, anti-poaching patrols, developed as one of the most important conservation measures to deter the activities of poachers have been frequently implemented in many landscapes across the Congo Basin (Kablan et al., 2019; Morgan et al., 2018; N'Goran et al., 2012), however, the role of anti-poaching patrols in the effective conservation of species within highly threatened PAs have not been fully assessed in this region. Moreover, information on the short or long-term changes in species biogeographic information are still missing within many PAs, especially those identified by the IUCN and UNESCO as facing increasing threats (UNESCO/IUCN, 2016). Mapping tools and quantitative models (e.g., remote sensing applications and machine learning models) can therefore, help describe and

predict the spatial patterns of change in suitable species habitats, as well as the contributions of anti-poaching patrols and other human activities within such PAs. Using this integrated approach, information on species biogeographic patterns can be achieved, and the contributions of patrolling efforts assessed.

Machine Learning (ML) models and remote sensing applications

Machine learning models (a branch of artificial intelligence) are powerful computational tools most often designed with linear or non-linear statistical or probabilistic modeling approaches to train, recognize and predict patterns in a given dataset, using either a supervised or unsupervised modeling approach (Breiman, 2001). They generally perform a series of tasks, including regression analysis; where the model creates either a linear or non-linear relationship between a target or dependent variable and a set of independent or predictor variables to predict or forecast patterns in a given set of data, and classification analysis; where the model filters, categorizes and classifies patterns in a data, following a supervised or unsupervised classification approach (Sarker, 2021). They are very powerful in dealing with large and complex datasets, as well as spatial layers with missing data. They thus guide users in drawing important conclusions and making management recommendations on real world problems, based on current and future outcomes predicted from given datasets.

Several machine learning models have been developed to deal with real world data mining problems. Prominent examples include artificial neural networks (ANN) (Lek et al., 1996), support vector machines (Drake et al., 2006; Keerthi et al., 2001), random forests (Breiman, 2001a; Cutler et al., 2007), K-nearest neighbors (kNN) (Aha et al., 1991), Decision tree (DT) (Quinlan, 1993), Adaptive Boosting (AdaBoost) (Freund et al., 1996), K-

means clustering (MacQueen et al., 1967), Linear Discriminant Analysis (LDA) (Pedregosa et al., 2012) and Ecological Niche Models (ENMs) or species distribution models (SDMs) (Elith & Leathwick, 2009; Franklin, 2013; Guisan & Zimmermann, 2000; Phillips et al., 2006; Phillips & Dudík, 2008). In the context of remote sensing (specifically in LULCC mapping), models such as ANN, SVM, RF, kNN, CART, DT and MLC have been successfully applied (Adam et al., 2014; Alshari et al., 2023; Basheer et al., 2022; Cardoso-Fernandes et al., 2020; Cutler et al., 2007; Dabija et al., 2021; Díaz-Pacheco & Hewitt, 2014; Gong et al., 2013; Guermazi et al., 2016; Magidi et al., 2021; Megahed et al., 2015; Paneque-Gálvez et al., 2013; Samaniego & Schulz, 2009; Silva et al., 2020; Teodoro, 2015; Zerrouki et al., 2019). Amongst these models, ANN, SVM, RF, and kNN have been proven to outperform other ML models in several remote sensing studies (as reviewed in Khatami et al., (2016)).

Artificial Neural Networks (especially the Multi-perceptron type) are ML models that use a set of inter-connected nodes to accurately classify satellite images using a backpropagation (backward transmission of errors) approach, and following a supervised training of sampled datasets (Silva et al., 2020). The model uses an input layer, and one or more hidden layers, as well as output layers to carry out this backpropagation of training samples. SVM are ML models mostly built with a radial basis function (RBF) to identify optimal decision boundaries that separate two or more LULC classes in a given satellite image (Cortes & Vapnik, 1995; Kuhn & Johnson, 2016). RF is an ensemble of ML models that uses bootstrap techniques to build many single decision tree models (Breiman, 2001a; Mellor et al., 2013; Rodriguez-Galiano et al., 2012). The model uses subsets of explanatory variables (e.g. Landsat bands) to split observation datasets into subsets of homogenous samples to build each decision tree (Mellor et al., 2013). kNN is a non-parametric model that

performs LULC classification based on the distance between k closest samples drawn from training datasets (Kuhn & Johnson, 2016).

Like with LULCC mapping, one of the most important areas of remote sensing and ecology where ML models have been proven useful and successful in informing decision making is in the domain of wildlife species distribution monitoring. As a means of solving issues with global biodiversity loss, and informing our understanding of where species occur or are likely to occur in the future, especially under land use and climate change conditions, Ecological Niche Models (ENMs) have been developed and successfully applied to tackle these issues (Franklin, 2013; Guisan & Thuiller, 2005; Guisan & Zimmermann, 2000; Phillips et al., 2006). In a more general context, they are stochastic models designed to predict the relationship between environmental and human disturbance variables (spatial layers) and species occurrence across a given landscape, and over a specified time frame (Franklin, 2013; Guisan & Thuiller, 2005; Guisan & Zimmermann, 2000; Phillips et al., 2006). They relate species presence/absence data with these environmental layers in a non-linear or logistic regression approach to predict species presence or occurrence in areas where data is both presents and limited within a given landscape (Elith & Leathwick, 2009; Franklin, 2013; Guisan & Thuiller, 2005; Guisan & Zimmermann, 2000). Prominent examples of these models include MaxEnt (Phillips et al., 2006; Phillips & Dudík, 2008); Random Forest (Cutler et al., 2007), Boosted Regression Trees (BRT) (Elith et al., 2008), Generalized Linear Models (GLMs) and Generalized Additive Models (GAMs) (Leathwick et al., 2005), and Bayesian Regression Models ((McCarthy, 2007). In the context of wildlife ecology and conservation biology, they have been widely used in predicting wildlife species distribution in several regions across the globe e.g., such as the prediction and mapping of primate species distribution (Brown & Yoder, 2015; Condro et al., 2021; Fitzgerald et al., 2018; Ginath Yuh et al., 2020; Gouveia et al., 2016; Hill & Winder, 2019; Junker et al., 2012;

Meyer et al., 2014; Meyer & Pie, 2022; Sales et al., 2020; Sesink Clee et al., 2015; Struebig et al., 2015; Vu et al., 2020; Zhang et al., 2019), and elephant species distribution (Chibeya et al., 2021; Dejene et al., 2021; He et al., 2023; Kanagaraj et al., 2019). Results from such modeling studies provide reliable information on species biogeography and paleoecology, as well as basis for estimating and evaluating changes in species distribution over time; information highly relevant for aiding conservation decision making.

Chapter 2: Application of machine learning approaches for land cover monitoring in northern Cameroon

Published as:

Yuh, Y. G., Tracz, W., Matthews, H. D., & Turner, S. E. (2023). Application of machine learning approaches for land cover monitoring in northern Cameroon. *Ecological Informatics*, 74, 101955. https://doi.org/10.1016/j.ecoinf.2022.101955

Abstract

Machine learning (ML) models are a leading analytical technique used to monitor, map and quantify land use and land cover (LULC) and its change over time. Models such as k-nearest neighbour (kNN), support vector machines (SVM), artificial neural networks (ANN), and random forests (RF) have been used effectively to classify LULC types at a range of geographical scales. However, ML models have not been widely applied in African tropical regions due to methodological challenges that arise from relying on the coarse-resolution satellite images available for these areas. In this study, we compared the performance of four ML algorithms (kNN, SVM, ANN and RF) applied to LULC monitoring within the Mayo Rey department, North Province, Cameroon. We used satellite data from the Landsat 7 Enhanced Thematic Mapper Plus (ETM+) combined with 8 Operational Land Imager (OLI) images of northern Cameroon for November 2000 and November 2020. Our results showed that all four classification algorithms produced relatively high accuracy (overall classification accuracy >80%), with the RF model (> 90% classification accuracy) outperforming the kNN, SVM, and ANN models. We found that approximately 7% of all forested areas (dense forest and woody savanna) were converted to other land cover types between 2000 and 2020; this forest loss is particularly associated with an expansion of both croplands and built-up areas. Our study represents a novel application and comparison of statistical and ML approaches to LULC monitoring using coarse-resolution satellite images in an African tropical forest and savanna setting. The resulting land cover maps serve as an important baseline that will be useful to the Cameroon government for policy development, conservation planning, urban planning, and deforestation and agricultural monitoring.

Keywords: land use and land cover change, machine learning, remote sensing, land cover classification, African forest and savanna.

Introduction

Human activities are continually modifying the Earth's land surface. Changes in anthropogenic land use and land cover (LULC) are particularly acute in tropical regions, where rapid rates of deforestation, agricultural expansion, industrial development, migration, growth in population density and urbanization often manifest as an outcome of neocolonial extractivism and associated geopolitical conflict (Escobar, 2011; Pereira & Tsikata, 2021; Romijn et al., 2015; Watson et al., 2001; Yeshaneh et al., 2013). Monitoring and mitigating the negative consequences of changing LULC has become a priority for researchers and policymakers worldwide. To monitor these changes successfully, there is a need to produce reliable and accurate LULC maps. Such maps provide vital information required for policy development, conservation planning, urban planning, and deforestation and agricultural monitoring (Gebhardt et al., 2014; Wessels et al., 2003).

Satellite image processing is one of the most important tools used by researchers for generating LULC maps (Chavez, 1996; Cracknell & Reading, 2014; Mohajane et al., 2018; Xia et al., 2015). Using satellite images is cost efficient and provides Earth surface data that cover large geographical areas. Datasets derived from satellite images enable accurate classification of land cover types, and can be used to detect changes in land cover at different spatial scales (Gómez et al., 2016; Kavzoglu & Colkesen, 2009). However, the processing time needed to generate accurate LULC maps using satellite image processing still represents a major challenge to remote sensing researchers, particularly when using coarse-resolution satellite images (i.e., Landsat, from the National Aeronautics and Space Administration (NASA) and U.S. Geological Survey (USGS) program that provides publicly available satellite image data) (Gómez et al., 2016; https://landsat.gsfc.nasa.gov).

To improve accuracy and decrease processing time, several Machine Learning (ML) algorithms have been tested for LULC mapping using remote sensing data. Prominent examples include: k-Nearest Neighbors (kNN) (Samaniego & Schulz, 2009; Thakur & Panse, 2022; Zerrouki et al., 2019); Support Vector Machines (SVM) (Adam et al., 2014; Cardoso-Fernandes et al., 2020; Gong et al., 2013; Paneque-Gálvez et al., 2013; Thakur & Panse, 2022; Zerrouki et al., 2019); Artificial Neural Networks (ANN) (Díaz-Pacheco & Hewitt, 2014; Megahed et al., 2015; Silva et al., 2020; Zerrouki et al., 2019); Random Forest (RF) (Adam et al., 2014; Gong et al., 2013; Thakur & Panse, 2022; Zerrouki et al., 2019); the Maximum Likelihood Classification (MLC) (Guermazi et al., 2016); and Decision Trees (DT) (Teodoro, 2015; Thakur & Panse, 2022; Törmä, 2013). These algorithms combine computer science and data mining to solve classification, clustering, regression and other pattern recognition problems (Cracknell & Reading, 2014; Hastie et al., 2009). They employ supervised classification systems using training datasets to minimize classification errors that could otherwise be caused by the internal structure of the algorithms (Bousquet et al., 2004; Hastie et al., 2009). As a result, ML algorithms can be used to improve classification performance without needing to articulate the underlying mechanisms and assumptions of traditional statistical models (Clarke, 2013; Hastie et al., 2009). They can therefore, be trained using both balanced datasets (with the same amount or number of pixels sampled for each LULC) and imbalanced datasets (with different amount or number of pixels sampled for each LULC class) without major classification uncertainties. Here, we focus on four ML algorithms, kNN, SVM, ANN, and RF, which have been shown to be well suited to LULC classification and to outperform other algorithms such as MLC and DT (Khatami et al., 2016; Thanh Noi & Kappas, 2017). The kNN model is a non-parametric model that performs LULC classification based on the distance between k closest samples drawn from training datasets. The approach depends on thorough image (predictor) pre-processing so as to reduce sampling

bias and ensure equal treatment of predictors when computing distance (Kuhn & Johnson, 2016). The SVM model uses support vectors (i.e. based on a subset of training data points closest to decision boundaries) to locate optimal decision boundaries that separate two LULC classes (Cortes & Vapnik, 1995; Kuhn & Johnson, 2016). The ANN model is a mathematical model developed as an analogy of the human brain. Using an interconnected group of responsive and conducting nodes, the ANN model mimics, in a very simplified fashion, the functionality of the human brain for knowledge acquisition, recall, synthesis and problem solving (Kubat, 1999; Yang, 2009). In LULC classification, the Multi-Layer Perceptron (MLP) type of ANN has been used most often (Silva et al., 2020). MLP carries out backpropagation of training samples to accurately classify LULC. The RF was developed as an ensemble of ML models that use bootstrap techniques to build many single decision tree models (Breiman, 2001a; Mellor et al., 2013; Rodriguez-Galiano et al., 2012). The RF model uses subsets of predictor variables (e.g. Landsat bands) to split observation datasets into subsets of homogenous samples to build each decision tree (Mellor et al., 2013).

The kNN, SVM, ANN, and RF learning approaches have proven successful in improving LULC classification performance (Khatami et al., 2016; Thanh Noi & Kappas, 2017), but the application of these methods requires considerable image preprocessing (particularly with coarse resolution images) in order to reduce uncertainties in LULC classifications. Furthermore, there has been limited application of these approaches to effective monitoring of changes in LULC within tropical forest areas across Africa, for which coarse resolution satellite images are often the only available option. Those studies that do exist have generally relied on applying only a single method (Brink & Eva, 2009; Matlhodi et al., 2019; Midekisa et al., 2017; Zoungrana et al., 2015), which can increase classification uncertainties relative to the use of multiple ML methods.

In this study, our goal is to apply statistical and ML approaches using four classification algorithms (kNN, SVM, ANN, and RF) to map and quantify changes in LULC within a tropical forest and savanna region in Central Africa (the Mayo Rey department of North Province, Cameroon), and to provide a novel comparison of these algorithms in an African forest setting. Changes in LULC patterns in this part of Cameroon are strongly affected by socio-economic factors such as changing farming practices, legal and illegal logging, and increases in the practice of pastoral nomadism. Describing and understanding the impacts of socio-economic and demographic changes on land use is vital for developing integrated, socially and economically sustainable environmental management and biodiversity conservation. Therefore, in addition to comparing classification algorithms, a goal of this study is to produce accurate LULC maps and estimates of land cover changes over the past 20 years. The result of this analysis can serve as baseline information that is required by the Cameroon government for policy development, biodiversity and forest conservation planning, urban planning, and deforestation and agricultural monitoring within this region.

Materials and Methods

The study area

Our study area consists of the northern portion of the Mayo Rey department, located in the North Region of Cameroon (Figure 1). We chose this region because: (1) It is a sub-Saharan tropical region with mostly cloud-free Landsat images that are freely available, and easy to acquire and preprocess; and (2) the region is experiencing large scale deforestation and agricultural expansion, and a rise in migration associated with political tensions in neighboring countries (Chad and the Central African Republic) (Njidda, 2001; Tchotsoua, 2006; Tchobsala & Mbolo, 2010).

The Mayo Rey department covers a total surface area of approximately 36,000 km^2. The population of the Mayo Rey is ~242,000 people, and this region borders on two countries: Chad in the north east and the Central African Republic to the south east. Our study area covers approximately 800,000 ha in northern Mayo-Rey, located between longitudes 13.7°E and 15°E and latitudes 8.4°N and 9.4°N (Figure 1). Annual mean rainfall ranges between 800-1000 mm and typical temperatures range from 25-30°C, though maximum temperature can reach values as high as 45°C. Elevations range between 348-794 m above sea level. This region is part of the Afro tropic biome and supports savanna and forest ecoregions, with the largest intact tracts of savanna forest found within the Bouba Njida National Park (Olson et al., 2001). This national park contains a wide variety of ecosystems, some of which include: open and mixed wooded savanna grasslands, semi-evergreen riparian forests and thick dry savanna forests. Our study region also supports a diversity of large mammalian fauna including elephants, lions, spotted hyena, buffalo, and many species of monkey and antelope.

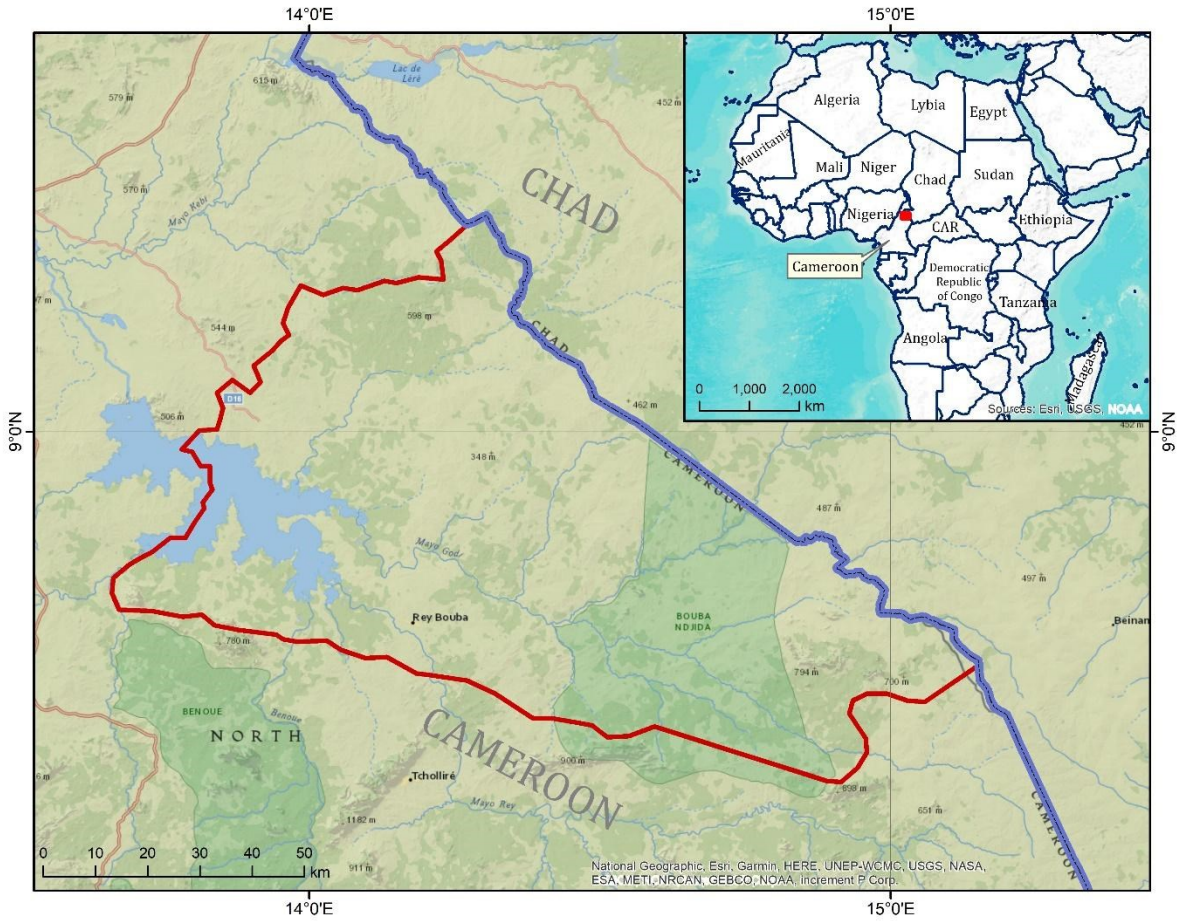

Figure 1. Location of the study area within the Mayo Rey department of northern Cameroon.

.

Image acquisition and pre-processing

We downloaded Landsat 7 Enhanced Thematic Mapper Plus (ETM+) and Landsat 8 Operational Land Imager (OLI) images of northern Cameroon from https://earthexplorer.usgs.gov/, for the dates 17 November 2000 and 29 November 2020, and with a 10% maximum cloud threshold. The images were loaded and preprocessed in R (R Core Team, 2016) using the "raster", "rgdal" and "RStoolbox" packages (a full description of packages is shown in Table M2).

Image preprocessing was conducted using radiometric corrections (Jensen, 2005). Radiometric corrections convert digital satellite numbers to radiance measures; this process corrects internal sensor errors and reduces atmospheric noise. To perform radiometric

corrections, we applied four techniques using the radCor (Radiometric Calibration and Correction) function from the "RStoolbox" package (Leutner & Horning, 2017): 1) the apparent reflectance model (AR) (Caselles & López García, 1989); 2) simple dark object subtraction (SDOS) (Chavez, 1988); 3) dark object subtraction (DOS) (Chavez, 1988); and 4) Cosine estimation of atmospheric transmittance (COST) (Chavez, 1996). In combination, these four radiometric processing techniques provided the necessary image preprocessing for our analyses.

We first converted the Landsat 7 and 8 digital numbers to at-satellite radiance. We then applied the AR model, which helps correct the spectral band irradiance and solar zenith angle of the acquired images, to convert the at-satellite radiance to top of atmosphere (TOA) reflectance. However, the AR model does not correct for atmospheric scattering and absorption, and we therefore applied the SDOS to carry out haze reduction, followed by the DOS approach, which assumes that scattering is highest in the blue bands and gradually decreases towards the near infra-red (NIR) bands. We used DOS to remove atmospheric scattering, and corrected for atmospheric additive scattering, spectral band irradiance and solar zenith. The main limitation to these approaches is that they do not produce correct band reflectance values after removing atmospheric scattering (Chavez, 1996). To address this limitation, we completed the radiometric corrections with the COST model to correct for the multiplicative effects of atmospheric scattering and absorption, and produce images with correct band reflectance values. We then extracted the study area from the corrected images, and selected six bands as independent variables for image processing. We used Landsat 7 band numbers 1, 2, 3, 4, 5 and 7, which correspond to wavelengths of 0.45–0.52 μm, 0.52–0.60 μm, 0.63–0.69 μm, 0.77–0.90 μm, 1.55–1.75 μm and 2.08–2.35 μm, respectively, and Landsat 8 band numbers 2, 3, 4, 5, 6 and 7, which correspond to wavelengths of 0.45–0.51 μm, 0.53–0.59 μm, 0.64–0.67 μm, 0.85–0.88 μm, 1.57–1.65 μm and 2.11–2.29 μm,

respectively. More details about these wavelength values are found in https://www.usgs.gov/landsat-missions/landsat-7 and https://www.usgs.gov/landsat-missions/landsat-8.

Image processing (classification and change detection)

To process (classify) the atmospherically corrected surface reflectance images of the study area for both years, we used a series of R packages, including: "randomForest", "caret", "kknn", "rpart", "rgdal", "raster", "sp", "e1071", "RStoolbox", "nnet", "kernlab", "ggplot2" and the "NeuralNetTools" packages. Full descriptions of packages are shown in Table S1.

Generating training (test and validation) datasets

We used three steps for image classification: 1) the establishment of training datasets, 2) classification, and 3) accuracy assessment. In generating training datasets, we first identified eight LULC classes in our study area, including croplands, dense forest, grassland savanna, open savanna/barelands, built-up areas, water bodies, wetlands, and woody savanna (see Table S2 for a full description of the LULC classes). We identified and selected these eight LULC classes to be consistent with the land cover types used by Moderate Resolution Imaging Spectroradiometer (MODIS) Global Land Cover products for the years 2010 and 2020. These MODIS data are generated by NASA, and mapped at a 500 m pixel resolution (Friedl & Sulla-Menashe, 2019). We also incorporated results from published datasets that examined and mapped single land cover types, i.e., global forest cover data (Hansen et al., 2013; Potapov et al., 2021), and global croplands and built-up areas data (Potapov et al., 2021, 2022). These published datasets have been validated through statistically significant correlations with ancillary datasets from the United Nations Food and Agricultural

Organization (FAO), as well as with other global land cover products generated by the NASA Global Ecosystems Dynamics Investigation (GEDI) service (Potapov et al., 2022).

Next, using these previously published datasets as reference, we carried out a balanced land cover data sampling approach by randomly sampling approximately 500 pixel points (representing approximately 5% of image pixels) for each land cover class, in each year of study, based on sampling approaches for each class applied in Potapov et al., (2021), Potapov et al., (2022) and Friedl & Sulla-Menashe, (2019). For example, we sampled forest pixels from areas of land with trees ≥5 m in height (Potapov et al., 2021, 2022), and a canopy cover ≥20% (FAO, 2000; Friedl & Sulla-Menashe, 2019). We then separated dense forest pixel samples from woody savanna pixel samples by following the criteria of Friedl & Sulla-Menashe, (2019) (i.e. dense forest had >60% canopy cover, and woody savannas had between 30% and 60% canopy cover (Table 1) (see Table S2 for more details)). We loaded the training datasets in R, using the "sp" vector package, then allocated 80% of the data as test files and the remaining 20% as validation files using the createDataPartition () function from the "caret" package. The test datasets enabled us to check optimal model parameters and initial model performance based on repeated cross-validation, while the validation dataset enabled us to check final model accuracy (Qian et al., 2014).

Table 1. Land use classifications and definitions used for sampling pixels

Land Use Class	**Land Use Class definition criteria for sampling pixels**	**Source**
Croplands	Cultivated crops > 60% of area	Pixel points extracted from Potapov et al., (2021); selected only points that matched the criteria defined in Friedl & Sulla-Menashe, (2019)
Dense forest	Canopy height ≥ 5m Canopy cover > 60%	Potapov et al., (2021, 2022) Friedl & Sulla-Menashe, (2019)
Grassland savanna	Canopy height of <5m Herbaceous non-agricultural vegetation or grassland cover >10%	Friedl & Sulla-Menashe, (2019)
Open savanna/ barelands	Vegetation cover of <10%	Friedl & Sulla-Menashe, (2019)
Built-up areas	Human-made land surfaces associated with built structures, such as commercial and residential infrastructures, and roads.	Potapov et al., (2020)
Water bodies	Inland areas covered with at least 60% permanent water, and not obscured by objects above the surface such as buildings, tree canopies, and bridges.	Potapov et al., (2022) and Friedl & Sulla-Menashe, (2019)
Wetlands	Vegetated and non-vegetated lands inundated with between 30-60% water, and usually forming swampy or peatlands	Friedl & Sulla-Menashe, (2019)
Woody savanna	Canopy height ≥ 5m Canopy cover between 30% and 60%	Potapov et al., (2021), Potapov et al., (2022) and Friedl & Sulla-Menashe, (2019)

Performing LULC classifications and change detection

Using the remaining 80% test data alongside the image subset for the study area, we applied four image classification models (kNN, SVM, ANN and RF) to classify the test data by applying the train () function from the "caret" package. In order to clarify what we used as training vectors for all four classification approaches, we used the names of the eight LULC classes identified (croplands, dense forest, grassland savanna, open savanna/barelands, built-up areas, water bodies, wetlands, and woody savanna) as target variable values. For predictor variables, we used the six Landsat image bands mentioned in Section 2.2. as predictors for our analysis. Before training each model, we defined a set of model tuning parameters using the trainControl () function of the "caret" package. Each modeling algorithm had at least one tuning parameter that controlled model performance, and the trainControl () function helped to evaluate these tuning parameters for model performance. Table S3 shows the parameterization settings (i.e. model type, number of tuning parameters/iterations, tuning methods and description) for each of the four ML algorithms.

kNN: k-nearest neighbour classification

In classifying pixels into land use categories with the kNN model, we used the "kknn" package. This model considers a group of k samples that are closest to the unknown sample, with the class of each unknown sample deduced by calculating the average of the k nearest neighbors (Akbulut et al., 2017; Wei et al., 2017). In training the kNN classifier, we defined the LULC classes of the test datasets as target (response) variables and the subset of image band reflectance values as predictors. Prior to performing model runs, we centered and scaled the predictor variables in order to reduce sampling bias during distance computation (Kuhn & Johnson, 2016). Centering and scaling of predictors were done using the center_scale () function of the "caret" package.

SVM: support vector machines classification

In classifying with the SVM model, we used the packages: "e1071", "kernlab" and "svmRadial". These packages use the radial basis function (RBF) kernel of the SVM classifier to accurately perform LULC classification (Knorn et al., 2009; Shi & Yang, 2015). We carried out automatic tuning and again centered and scaled our predictor variables in order to reduce sampling bias.

ANN: artificial neural networks classification

In classifying with the MLP ANN model, we used the package "nnet", which provides possibilities for adjusting weighted decay and size, thereby countering the effects of model overfitting. We used an MLP ANN architecture with 1 hidden layer established as a default setting within the "nnet" package, and with 6 neurons defined for our model inputs. The number of neurons in the input layer was equal to the number of used bands (6), and the output layer had 8 neurons (representing 8 LULC classes). A back propagation learning algorithm was used during the training phase of the model. Size and decay were used to define the primary model tuning parameters, and the control () function was used to control for model runs. As with the kNN approach, we defined the LULC classes of the test datasets as target variables and the band reflectance values as predictors, and equally centered and scaled the predictor variables in order to reduce sampling bias.

RF: random forest classification

With the RF approach, we used the "randomForest" package. We allowed the model to set the number of trees (ntree) and number of features in each split (mtry) by default so as

to ensure satisfactory model performance (Duro et al., 2012; Matlhodi et al., 2019; Zhang & Roy, 2017), . i.e. about 500 decision trees were created by the model under default settings, with over 3000 training samples randomly selected for training purposes under default settings.

Estimating classification accuracy

To produce and validate our LULC maps from all ML models, we applied two different approaches. In the first approach, classification accuracies for all four models (kNN, SVM, ANN, and RF) were computed and compared with the test and validation datasets using the confusion Matrix () function from the "caret" package. We computed four commonly used accuracy: overall accuracy (OA), producer's accuracy, user's accuracy and Kappa coefficients, with OA values validated through statistical significant tests, and at 95% confidence intervals (CI). The OA defines the overall percentage of correctly classified LULC classes, calculated as the number of correctly classified land cover pixels divided by the total number of pixels in the dataset (Congalton, 1991). The producer's accuracy defines the percentage accuracy of each LULC class in a LULC map, calculated by dividing the number of correct pixels in a given land cover class by the total number of pixels of that land cover class from the reference data. In producer's accuracy, misclassified pixels are referred to as an error of omission. The user's accuracy defines the reliability of a given land cover map with respect to how close the derived map is to ground observations, calculated by dividing the number of correctly classified pixels in a given land cover class by the total number of pixels classified in that class. In user's accuracy, misclassified pixels are also referred to as an error of omission. The kappa coefficient describes the percentage agreement between the test and validation data in a generated land cover map. It is based on the probability that the test data will be close to the validation data in the land cover mapping

process. The kappa coefficient is highly correlated to the overall accuracy. In general, these accuracy scores determine the degree to which a classified land cover map agrees with reality or conforms to the truth (Campbell, 1996, 2011; Smits et al., 1999). They have been successfully used to validate land cover maps generated at different geographical scales (Liu et al., 2021; Sari et al., 2021; Wang et al., 2013; Yang et al., 2021; Yuh et al., 2019), and therefore produce a robust approach for validating land cover. From the kNN, SVM, ANN, and RF accuracy assessments, we generated LULC maps by predicting model results with the subset image of the study area, using the predict () function from the R "prediction" package.

In a second approach, we performed a Pearson's correlation test between our generated LULC products (i.e. the land cover product from the model with the best classification accuracy) and datasets from already published studies such as the Hansen et al., (2013) global forest cover map, the 2020 MODIS global land cover products Friedl & Sulla-Menashe, (2019), and the global built-up and cropland data published in Potapov et al., (2021) and Potapov et al., (2022). We used these published datasets because they have been generated with high degrees of accuracy, and have been properly validated through statistically significant correlations with ancillary datasets from the United Nations Food and Agricultural Organization (FAO), as well as with other global land cover products generated by the NASA Global Ecosystems Dynamics Investigation (GEDI) service (Potapov et al., 2022). The validated datasets were then converted to vector layers using the raster to polygon conversion tool in GIS software (ArcMap 10.8), and the attribute tables for both years of study were intersected for change detection analysis (Yuh et al., 2019). Detected changes between LULC types (i.e. change from one LULC type in the year 2000 to another in the year 2020) were quantified in hectares using spatial statistics with the ArcGIS geometry tool.

Results

Model performance and LULC mapping

The LULC maps produced by the four ML classification algorithms are shown in Figure 2. All four ML models performed well at producing LULC classifications for both years of study (2000 and 2020) with OA scores of >80%, and statistically significant ($p < 0.05$) correlations with existing LULC maps. The model accuracies for all four models (producer's, user's and overall accuracies, as well as kappa values) are shown in Table 2, Table 3, Table 4, Table 5. The RF model had the best overall performance (OA of 90% for the year 2020 and 99% for the year 2000), and it outperformed the kNN, SVM and ANN models which had OAs of between 80% and 90% for both years of study. Because the RF model produced the best OA, we used the RF LULC maps from both years of study for further processing. To further validate the RF LULC maps, we correlated them with existing LULC maps (result shown in Table 6, Table 7), and then quantified the areas affected by LULC change between 2000 and 2020 using these validated maps. Pearson's correlation tests show that our land cover classes were strongly and significantly correlated with map products published in Hansen et al., (2013), Friedl & Sulla-Menashe, (2019), and Potapov et al., (2021), Potapov et al., (2022). For example, our woody savanna areas were strongly and significantly correlated with woody savannas extracted from Potapov et al., (2021) and Hansen et al., (2013) (correlation strength, $R = 0.98$, $p < 0.05$ for the year 2020, and $R = 0.99$, $p < 0.05$ for the year 2000). Furthermore, we found a 90% correlation with our croplands and those from the 2020 MODIS global land cover dataset ($R = 0.9$, $p < 0.05$), and 98% correlation with croplands published in Potapov et al., (2022). For built-up areas, we also found relatively strong correlations between our datasets and datasets from Potapov et al., (2021) ($R = 0.8$, $p < 0.05$ for the year 2020, and $R = 0.7$, $p < 0.05$ for the year 2000). We found a 99% correlation with water bodies and wetlands from the 2020 MODIS data ($R = 0.99$, $p < 0.05$). For grassland

savanna and open savanna/barelands, average correlation strengths where $R = 0.5$, $p < 0.05$ and $R = 0.48$, $p < 0.05$ respectively. Fig. 3 and 4 show comparisons between our land cover maps and existing land cover maps published in Hansen et al., (2013), Friedl & Sulla-Menashe, (2019), and Potapov et al., (2021), Potapov et al., (2022).

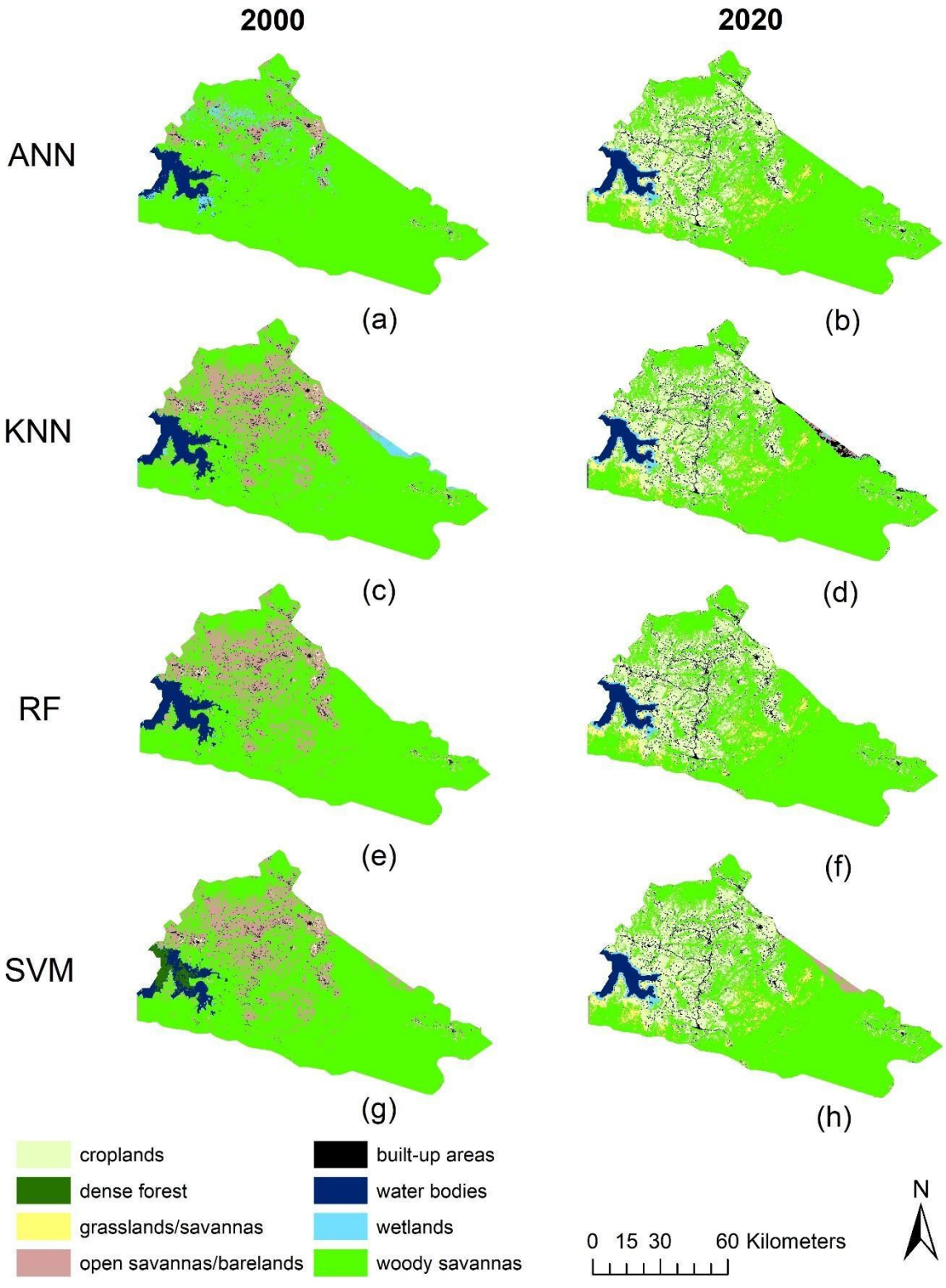

Figure 2. Comparison of LULC classification of the study area between the years 2000 (left) and 2020 (right) based on the four models. Figures a-b illustrate ANN classification maps; c-d illustrate kNN maps; e-f illustrate RF maps and g-h illustrate SVM maps

Table 2. Accuracy assessment for the kNN classification.

2020								
LULC class	Croplands	Dense forest	Grassland savanna	Open savanna/ barelands	Built-up areas	Water bodies	Wetlands	Woody savanna
Croplands	80	0	0	0	0	0	0	9
Dense forest	0	5	0	0	0	2	1	0
Grassland savanna	1	0	12	0	0	0	0	0
Open savanna/barelands	0	0	0	5	0	0	0	0
Built-up areas	0	0	0	3	3	0	0	1
Water bodies	4	0	0	0	0	221	9	0
Wetlands	0	0	0	0	0	0	29	0
Woody savanna	0	0	0	0	0	0	0	412
Total	**85**	**5**	**12**	**8**	**3**	**223**	**39**	**422**
Overall producer's accuracy (%)	**94.3**	**100**	**100**	**63**	**100**	**99.1**	**74.4**	**97.6**
Overall accuracy = 91.1% 95% CI (89%, 92%); Kappa statistics = 89%; p < 0.05								
2000								
LULC class	Croplands	Dense forest	Grassland savanna	Open savanna/ barelands	Built-up areas	Water bodies	Wetlands	Woody savanna
Croplands	20	0	0	0	0	0	0	33
Dense forest	0	296	0	6	1	11	0	0
Grassland savanna	0	0	40	0	1	0	1	0
Open savanna/barelands	5	0	1	35	68	0	4	1
Built-up areas	0	0	0	0	4	0	0	0
Water bodies	0	0	0	0	0	75	0	0
Wetlands	0	1	0	0	0	1	77	0
Woody savanna	0	0	0	0	0	0	0	149
Total	**25**	**297**	**41**	**41**	**74**	**87**	**82**	**183**
Overall producer's accuracy (%)	**80**	**99.7**	**99**	**85.4**	**91.9**	**86.2**	**93.9**	**81.4**
Overall accuracy = 89.7% 95% CI (85%, 91%); Kappa statistics = 88%; p < 0.05								

Table 3. Accuracy assessment for the ANN classification.

2020								
LULC class	Croplands	Dense forest	Grassland savanna	Open savanna/ barelands	Built-up areas	Water bodies	Wetlands	Woody savanna
Croplands	80	0	0	0	0	1	0	9
Dense forest	0	5	0	0	0	0	1	0
Grassland savanna	1	0	12	0	0	0	0	0
Open savanna/barelands	0	0	0	5	0	0	0	0
Built-up areas	0	0	0	3	3	0	0	1
Water bodies	4	0	0	0	0	223	9	0
Wetlands	0	0	0	0	0	0	29	0
Woody savanna	0	0	0	0	0	0	0	412
Total	**85**	**5**	**12**	**8**	**3**	**223**	**39**	**422**
Overall producer's accuracy (%)	**94.3**	**100**	**100**	**100**	**100**	**100**	**74.4**	**97.6**
Overall accuracy = 95.8% 95% CI (93%, 97%); Kappa statistics = 94%; p < 0.05								
2000								
LULC class	Croplands	Dense forest	Grassland savanna	Open savanna/ barelands	Built-up areas	Water bodies	Wetlands	Woody savanna
Croplands	79	0	0	0	0	0	0	0
Dense forest	24	38	0	2	0	3	1	282
Grassland savanna	4	0	41	0	1	0	0	0
Open savanna/barelands	0	0	0	15	15	0	7	36
Built-up areas	0	1	0	0	31	0	0	0
Water bodies	0	0	0	0	0	77	0	0
Wetlands	0	0	0	0	0	1	84	0
Woody savanna	0	0	0	0	0	0	0	415
Total	**107**	**38**	**41**	**17**	**47**	**81**	**92**	**733**
Overall producer's accuracy (%)	**73.8**	**100**	**100**	**88.2**	**70**	**95**	**91.3**	**56.6**
Overall accuracy = 84.4% 95% CI (80%, 87%); Kappa statistics = 83%; p < 0.05								

Table 4. Accuracy assessment for the RF classification.

2020								
LULC class	Croplands	Dense forest	Grassland savanna	Open savanna/ barelands	Built-up areas	Water bodies	Wetlands	Woody savanna
Croplands	80	0	0	0	0	0	0	8
Dense forest	0	9	0	0	0	6	0	0
Grassland savanna	1	0	12	0	0	0	0	0
Open savanna/barelands	0	0	0	5	0	0	0	0
Built-up areas	0	0	0	0	3	0	0	1
Water bodies	4	0	0	4	0	221	9	0
Wetlands	0	0	0	0	0	0	30	0
Woody savanna	0	0	0	0	0	0	0	413
Total	**85**	**9**	**12**	**9**	**3**	**227**	**39**	**422**
Overall producer's accuracy (%)	**94.3**	**100**	**100**	**56**	**100**	**97.4**	**76.9**	**97.9**
Overall accuracy = 90.3% 95 CI (94%, 97%); Kappa statistics = 94%; p < 0.05								
2000								
LULC class	Croplands	Dense forest	Grassland savanna	Open savanna/ barelands	Built-up areas	Water bodies	Wetlands	Woody savanna
Croplands	20	0	0	0	0	0	0	0
Dense forest	0	38	0	0	0	0	0	0
Grassland savanna	0	0	41	0	0	0	0	0
Open savanna/barelands	0	0	0	17	0	0	0	2
Built-up areas	0	0	0	0	47	0	0	0
Water bodies	0	0	0	0	0	76	0	0
Wetlands	0	0	0	0		0	92	0
Woody savanna	0	0	0	0		0	0	33
Total	**20**	**38**	**41**	**17**	**47**	**76**	**92**	**35**
Overall producer's accuracy (%)	**100**	**100**	**100**	**100**	**100**	**100**	**100**	**94.3**
Overall accuracy = 99.3% 95 CI (94%, 99%); Kappa statistics = 97%; p < 0.05								

Table 5. Accuracy assessment for the SVM classification.

2020								
LULC class	Croplands	Dense forest	Grassland savanna	Open savanna/ barelands	Built-up areas	Water bodies	Wetlands	Woody savanna
Croplands	237	0	1	0	0	0	0	9
Dense forest	0	42	3	0	0	0	0	0
Grassland savannas	0	8	20	0	3	0	0	0
Open savanna/barelands	0	0	1	75	0	0	0	0
Built-up areas	0	1	5	1	24	0	0	2
Water bodies	0	0	0	0	0	47	10	0
Wetlands	0	0	0	0	0	0	29	0
Woody savanna	0	0	0	0	0	0	0	401
Total	**237**	**51**	**30**	**76**	**27**	**47**	**39**	**412**
Overall producer's accuracy (%)	**100**	**82.4**	**66.7**	**98.7**	**88.9**	**100**	**74.4**	**97.3**
Overall accuracy = 88.6% 95% CI (87%, 90%); Kappa statistics = 87%; p < 0.05								
2000								
LULC class	Croplands	Dense forest	Grassland savanna	Open savanna/ barelands	Built-up areas	Water bodies	Wetlands	Woody savanna
Croplands	20	0	133	0	0	0	0	0
Dense forest	0	41	1	0	5	0	0	0
Grassland savanna	0	0	158	0	0	0	0	1
Open savanna/barelands	0	0	0	3	0	0	0	2
Built-up areas	0	0	0	0	11	0	0	0
Water bodies	0	2	0	0	0	76	0	0
Wetlands	0		2	0	0	0	92	33
Woody savanna	0		0	0	0	0	0	613
Total	**20**	**43**	**294**	**3**	**16**	**76**	**92**	**649**
Overall producer's accuracy (%)	**100**	**95.3**	**53.7**	**100**	**68.8**	**100**	**100**	**94.5**
Overall accuracy = 89% 95% CI (84%, 91%); Kappa statistics = 87%; p < 0.05								

Table 6. Accuracy validation for the year 2020. This table shows correlation strengths between our land cover data from the RF model, and datasets from other published results for the year 2020. Correlation strengths are only determined for land cover classes that are available from the cited studies.

Land cover class	Modis global land cover products		Global forest cover data		Global croplands data		Global built-up data	
	Data available ?	Correlation strength	Data available ?	Correlation strength	Data available ?	Correlation strength	Data available ?	Correlation strength
Croplands	Yes	0.9	No	NA	Yes	0.4	No	NA
Dense forest	No	NA	No	NA	No	NA	No	NA
Grassland savanna	Yes	0.5	No	NA	No	NA	No	NA
Open savanna/ barelands	Yes	0.48	No	NA	No	NA	No	NA
Built-up areas	Yes	NA	No	NA	No	NA	Yes	0.8
Water bodies	Yes	0.99	No	NA	No	NA	No	NA
Wetlands	Yes	0.99	No	NA	No	NA	No	NA
Woody savanna	No	NA	Yes	0.98	No	NA	No	NA
Overall correlation		**0.77**		**0.98**		**0.4**		**0.8**

Modis global land cover products (Friedl & Sulla-Menashe, 2019; Global forest cover data (Hansen et al., 2020; Potapov et al., 2020); Global croplands data (Potapov et al., 2021); Global built-up data (Potapov et al., 2020); NA = Not Applicable; NS = Non-significant

Table 7. Accuracy validation for the year 2000. This table shows correlation strengths between our land cover data from the RF model, and datasets from other published results for the year 2000. Correlation strengths are only determined for land cover classes that are available from the cited studies. Global Modis land cover datasets do not exist for the year 2000, and are therefore excluded from the Table.

Land cover class	Global forest cover data		Global croplands data		Global built-up data	
	Data available ?	Correlation strength	Data available ?	Correlation strength	Data available ?	Correlation strength
Croplands	No	NA	Yes	0.98	No	NA
Dense forest	No	NA	No	NA	No	NA
Grassland savanna	No	NA	No	NA	No	NA
Open savanna/ barelands	No	NA	No	NA	No	NA
Built-up areas	No	NA	No	NA	Yes	0.98
Water bodies	No	NA	No	NA	No	NA
Wetlands	No	NA	No	NA	No	NA
Woody savanna	Yes	0.99	No	NA	No	NA
Overall correlation		**0.99**		**0.98**		**0.98**

Modis global land cover products (Friedl & Sulla-Menashe, 2019; Global forest cover data (Hansen et al., 2020; Potapov et al., 2020); Global croplands data (Potapov et al., 2021); Global built-up data (Potapov et al., 2020); NA = Not Applicable; NS = Non-significant

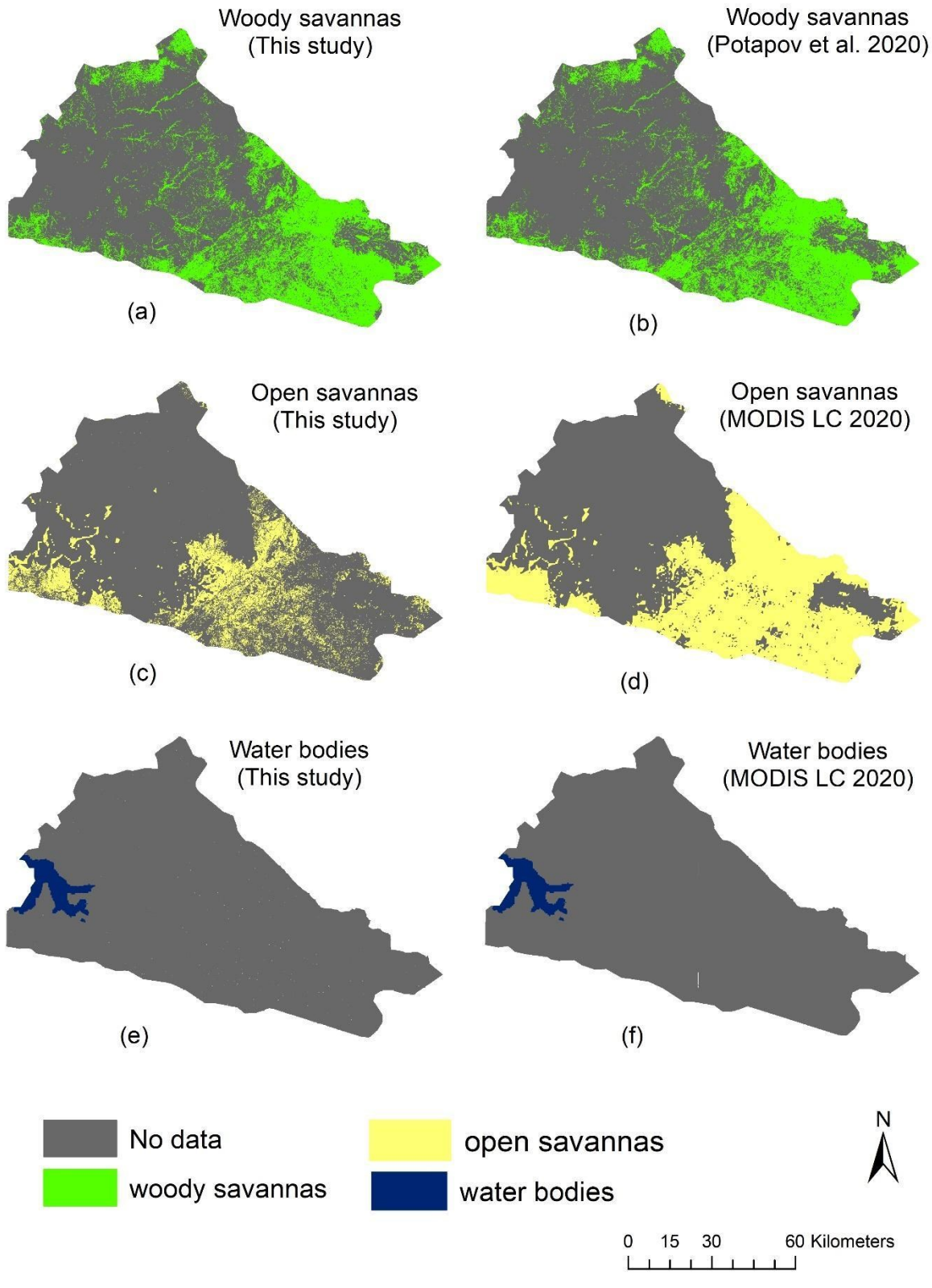

Figure 3. Maps showing comparison in LULC between our study and products extracted from the MODIS global LULC products (Friedl & Sulla-Menashe, 2019), as well as products published by Potapov et al., (2021). Map comparisons are for the year 2020, and represent a comparison between water bodies (e-f), open savanna (c-d) and woody savanna (a-b).

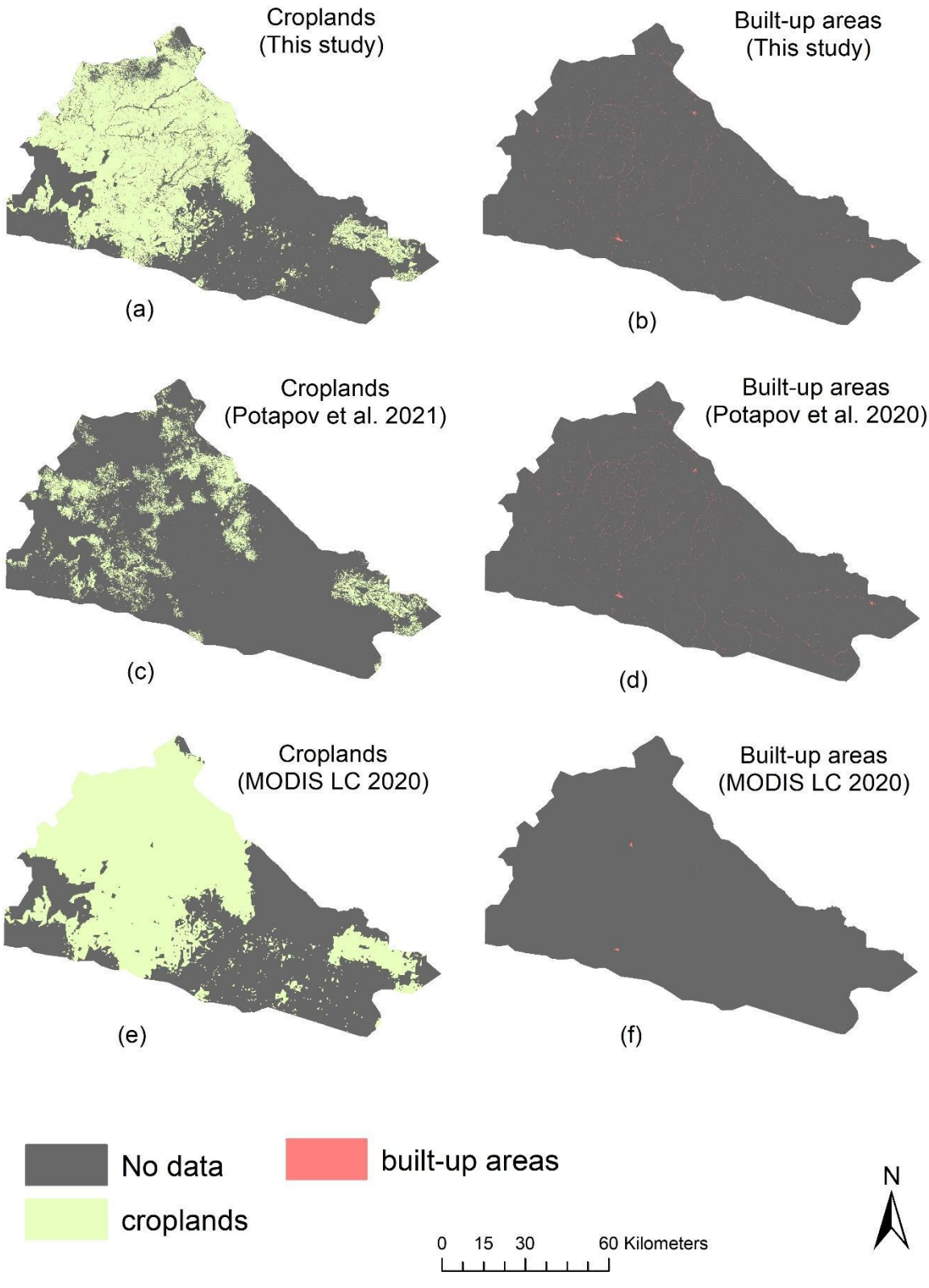

Figure 4. Maps showing comparison in LULC between our study and products extracted from the MODIS global LULC products (Friedl & Sulla-Menashe, 2019), as well as products published by Potapov et al., (2020, 2021). Map comparisons are for the year 2020, and represents a comparison between croplands (a, c and e), and built-up areas (b, d and f).

Quantification of LULC classification

The results from the different LULC classification approaches conducted for both years of study (2000 and 2020) show that the total LULC area for this section of the Mayo Rey department is approximately 793,000 ha. The areas of individual land cover types and the changes that we detected between the years 2000 and 2020 are summarized in Table 8. We found a significant loss in woody savanna within the study area, and an almost complete loss of what little dense forest cover existed in the study area. In the year 2000, woody savanna covered a total land area of about 304,976 ha in our study area, which constituted approximately 39% of the land area analyzed. Woody savanna declined to approximately 253,903 ha (32%) in the year 2020, accounting for approximately 51,073 ha loss in woody savanna area within the study region. While dense forests covered only 291 ha of our study area in the year 2000, it had declined to about 9 ha by the year 2020, suggesting an almost complete loss in dense forest cover area within the study area.

The Mayo Rey department has experienced a large-scale expansion in cropland areas and grassland savanna in the 20 years of the study period. In the year 2000, croplands covered a total land area of approximately 50,000 ha, constituting about 6.3% of our study area. Croplands increased to approximately 376,184 ha (47% of our study area) in the year 2020, for a total increase in cropland area of approximately 326,184 ha. Grassland savanna increased by approximately 126,268 ha within the study period (from ~756 ha (0.1% of the study area) in the year 2000 to ~127,000 ha (16% of the study area) in the year 2020). With the loss in forest cover (both dense forest and woody savanna) and expansion of agriculture, there has also been a significant expansion in built-up areas in this portion of Mayo Rey. Built-up areas expanded by approximately 3538 ha within the 20-year study period (~1748 ha (0.2% of the study area) in the year 2000, to ~ 5286 ha (0.7% of the study area) in the year 2020). We also found that the Mayo Rey department of northern Cameroon has experienced

dramatic declines in inland water bodies over the study period. Water bodies have declined from covering approximately 42,829 ha (5.4% of the study area) in the year 2000 to approximately 24,095 ha (3% of the study area) in the year 2020, leaving a loss of inland water bodies of approximately 18,733 ha.

Table 8. Quantified LULC class areas and change areas between the years 2000 and 2020. Percentages represent the fraction of the study area represented by the land cover class in each year, as well as the fraction of study area represented by the change in area between 2000 and 2020.

	2000		**2020**		**2020-2000**	
Land cover class	Area (ha)	Area (%)	Area (ha)	Area (%)	Changed area (ha)	Changed area (%)
croplands	50099.9	6.3	376184.6	47.3	326084.7	41.0
dense forest	291.0	0.0	9.1	0.0	-281.9	0.0
grassland savanna	756.2	0.1	127024.3	16.0	126268.2	15.9
open savanna/barelands	390180.9	47.3	2526.5	0.3	-387654.4	-48.9
built-up areas	1747.7	2.1	5285.9	0.7	3538.3	0.4
water bodies	42828.5	5.4	24095.1	3.0	-18733.4	-2.4
wetlands	2134.1	0.3	5460.3	0.7	3326.2	0.4
woody savannas	304975.9	38.5	253902.8	32.0	-51073.1	-6.5

Quantification of changes in LULC

The changes in LULC between the years 2000 and 2020 are shown in Figure S1 and Table S4. To highlight these results, we generated thematic hotspot maps for gains and losses in three of the LULC classes identified: woody savanna, croplands and built-up areas (Figure 5). Overall, changes in LULC over this period were dominated by an expansion of cropland areas. We calculated a gain of 326,084 ha of cropland area over the 20-year period, with over 71,266 ha of open savanna/barelands, and 41,900 ha of woody savanna converted to croplands. A smaller amount of cropland area (14,989 ha) has been lost to other LULC types, with most cropland loss occurring where abandoned croplands have been converted to grassland savannas (approximately 1046 ha), and some cropland loss associated with the expansion of built-up areas (653 ha). An expansion in the build environment has also

occurred over the 20 years of study, with a total of 3994 ha of built-up expansion. Of the land converted to built-up areas, over 653 ha came from abandoned croplands, and another 2982 ha from open savanna/barelands. Of the 282 ha of dense forest cover lost between 2000 and 2020, over 218 ha was converted to croplands, while of the 51,000 ha net loss in woody savanna areas, over 41,900 ha was converted to croplands. Despite this conversion of woody savanna, over 20,000 ha of woody savanna have also been gained, (with open savanna/bareland changing to woody savanna in over 18,894 ha of those 20,000 ha).

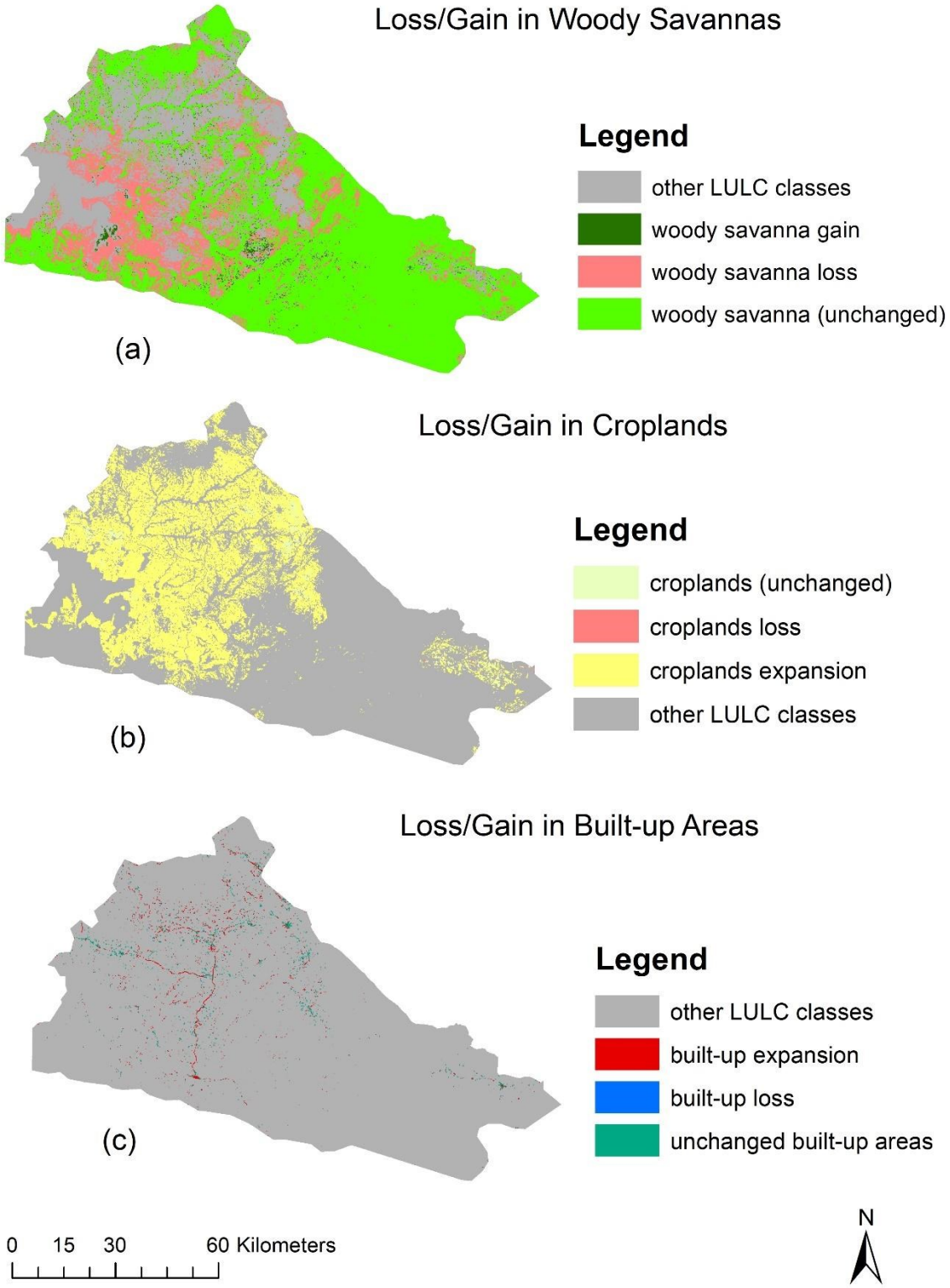

Figure 5. Hotspot maps for gains and loss in three LULC classes identified to show the highest environmental values in the Mayo Rey department of northern Cameroon. They include: woody savanna, croplands and built-up areas

Discussion

Comparison and validation of ML classification models

In this study, we have provided an analysis and comparison of land cover classifications produced by four ML algorithms for a portion of the Mayo Rey Department of Northern Cameroon. A recent syntheses and meta-analysis demonstrated that tropical regions are underrepresented in current studies, especially across equatorial Africa (Khatami et al., 2016). Furthermore, previous studies conducted within tropical regions across Africa have most often used the MLC supervised approach (Díaz-Pacheco & Hewitt, 2014; Yuh et al., 2019), however, this approach poses several methodological challenges or classification uncertainties when coupled with the coarse-resolution satellite images (i.e., Landsat) used by most remote sensing researchers in Africa. Unlike in Europe or North America, many African countries do not have advanced space agencies with national satellite data collection programs, or large budgets for large-scale land surveys; most African-based remote sensing research relies on freely available Landsat data. Developing methods for reducing classification uncertainties associated with the use of coarse-resolution Landsat images is therefore particularly pertinent for research on land use change in Africa.

Our results show that the four ML classification models used here (kNN, SVM, ANN and RF) are robust approaches that could potentially improve classification uncertainties within tropical forest regions globally. It is worth noting however, that we did not consider potential non-linearities that could arise from ecosystem dynamics in this region, which could be addressed in future analyses using models such as Convergent Cross Mapping or Optimal Information Flow (Li & Convertino, 2021). Nevertheless, our results are consistent with other studies that have shown that the four algorithms we used here are able to produce a high degree of classification accuracy (Adam et al., 2014; Ghosh & Joshi, 2014), and as such, they

can potentially outperform other supervised classifiers (e.g. MLC) in other tropical contexts as well (Khatami et al., 2016).

We found further that the RF model performed the best for both years of study compared to the other three models: RF showed greater than 90% accuracy compared to between 80 and 90% accuracy generated for the SVM, ANN and kNN models. These results show that RF could be the most suitable approach for LULC mapping within tropical regions across Africa, even though some studies have found that the kNN model outperformed RF, as well as the other two algorithms, in some other contexts (Heydari & Mountrakis, 2018; Pouteaua et al., 2011). However, consistent with our findings, RF is generally accepted as the best ML approach for mapping LULC (Belgiu & Drăguţ, 2016; Pelletier et al., 2016), based on its superior modeling performance when compared to other ML algorithms (Gislason et al., 2006; Rodriguez-Galiano et al., 2012).

The RF algorithm specifically solves problems associated with using freely available coarse-resolution Landsat images, by using Landsat bands to split observation datasets into a subset of homogenous samples, which are then used in building single decision trees (Mellor et al., 2013). The best decision trees are automatically selected by the model in an ensemble approach to predict land cover maps following a pixel to pixel sampling approach. Given its high computation power, the RF model is a powerful LULC prediction tool that should be prioritized in LULC mapping within afro tropical regions. Despite this evidence however, the ANN and SVM models still remain the most frequently used classification algorithms for monitoring LULC and its change over time using Landsat images (Adam et al., 2014; Gong et al., 2013; Khatami et al., 2016).

We validated our RF results by correlating the resulting land cover classifications with existing global land cover products. Although this approach is robust, an alternate

validation approach could be to compare results with ground-truthed data or datasets classified at a local level. Local level classification of land surface features and ground-truth mapping can provide more realistic land use and land cover class category identification as compared with using global land cover products for validation. However, we are not aware of any ground-truthed or local level datasets available for our study area. As such, we followed a standardized protocol that was developed for mapping the MODIS global land cover products, as well as for the Hansen et al., (2013), and Potapov et al., (2021), Potapov et al., (2022) global forest cover, global croplands and built-up datasets respectively. We cross validated our results with these products, as these products (especially the Hansen and Potapov datasets) have been mapped with high levels of accuracy, and were validated with more conventional validation datasets from the United Nations Food and Agricultural Organization (FAO). We do interpret our results with some caution, as the MODIS global land cover data has several limitations due to misclassification of some land cover features (Friedl & Sulla-Menashe, 2019), and so direct comparisons may produce some erroneous results. Nevertheless, our overall results provide a novel analysis and maps that can be usefully applied for policy development and sustainable land use planning in Cameroon.

Changes in land cover between 2000 and 2020

The result of our comparison of the RF LULC classifications between 2000 and 2020 showed substantial changes in land cover in the Mayo Rey department over this 20-year period, characterized by increased croplands and built-up areas, and corresponding decreases in forested areas. It is notable here that the area of dense forest in this region decreased from an area in the year 2000 that was comparable to that of Central Park in New York City (340

ha; Britannica, n.d.) to a forested area in 2020 that is was only 9 ha, about half the size of the Buckingham Palace grounds in London (Royal Collection Trust, n.d.).

It is likely that political tensions in neighboring Chad and the Central African Republic have contributed to the increased population density that is associated with some of the land use changes we documented in our study. The expansion in croplands and built-up areas, and the loss of dense forests and woody savannas in the Mayo Rey have occurred in parallel with a rapid rise in migration into this region, as refugees flee political tensions from neighboring countries (Chad and the Central African Republic). A lack of economic opportunities for migrants and displaced people has contributed to ecological pressures in a part of the world already economically disadvantaged by neocolonial extractivism. This region has seen a rise in illegal logging, and conversion of forest and woody savanna land for agriculture and nomadic pastoral use (Njidda, 2001; Tchobsala & Mbolo, 2010; Tchotsoua, 2006). These tensions and land use changes are an outcome of extractivism embedded in contemporary global capitalism and associated geopolitical conflict, where resources flow unequally and unsustainably to the global north (Escobar, 2011; Pereira & Tsikata, 2021).

Furthermore, many people in this region depend on fuel wood for heating and cooking (Megevand & Mosnier, 2013), which can also contribute to deforestation when coupled with rapid social and demographic shifts. In addition, an increase in the number of people practicing nomadic pastoralist livelihoods may be contributing to a loss in forest cover and woody savanna and associated expansion of grassland savanna, croplands and open savanna/barelands in a context where local traditional ecological knowledge is being lost due to human displacement. Traditionally, mobility has been a strategy Indigenous pastoralists have used in order to reduce negative impacts on the land, and to respond sustainably to change (Kongnso, 2022). However, geopolitical pressures disrupt sustainable traditional practices and lifeways, leading to over-grazing of lands by cattle, which can then lead to

desertification and deforestation (Asner et al., 2004; Kongnso, 2022). When combined with geopolitical tensions and human displacement, cattle grazing and other forms of agriculture, especially industrial agriculture, may have led to a large-scale reduction of surrounding water bodies through irrigation changes and desertification (Fonteh, 2013).

The loss in water bodies that we documented could also be related to climate changes (Fonteh, 2013) considering that the study area faces high seasonal temperatures with relatively low precipitation rates. Increasing temperatures resulting from climate change are associated with increased evapotranspiration (Cheo et al., 2013), which can contribute to reduced lake area and altered surface runoff patterns (Frederick, 2002). In addition to climate change effects, inland water loss could also be attributed to flood mitigation and post-flooding reconstruction projects in the Far North region of Cameroon (https://www.worldbank.org/en/results/2020/11/10/flood-management-in-the-far-north-of-cameroon). The Northern region of Cameroon experienced high levels of flooding in the year 2012 as a result of high rainfall, causing extensive damage to property and crops. As a consequence, the Cameroon government and the World Bank implemented an emergency rehabilitation plan (2014–2020). This plan oversaw the building of more than 7000 ha of dykes, 2700 ha of dams, and 7500 ha of irrigation schemes. Our study found significant decreases in the area of inland water bodies near these rehabilitated areas, suggesting that they may have had unintended negative consequences for the Mayo Rey and surrounding ecosystems.

Conclusions and future research directions

Our study provides a first attempt, to our knowledge, to apply and compare four statistical and ML models (kNN, ANN, RF and SVM) as potentially robust means of monitoring changes in LULC using coarse resolution satellite images within a tropical African biome. By testing these approaches with cloud free Landsat images from the northern section of the Mayo Rey department of northern Cameroon, we showed that all four classification algorithms provided significant and relatively high degrees of accuracy in LULC classification (i.e. all models had >80% OA), supporting similar findings from other regions of the world. As a result, highly accurate LULC maps and quantified change detection derived through the application of these ML approaches are possible. Our findings show that the RF model outperformed the kNN, SVM and ANN models, and produced highly accurate LULC maps, which produced statistically significant correlations when validated against other existing global LULC products.

We showed further that significant areas of forest (dense forest and woody savanna) have been lost through conversion to other LULC types within the 20-year study period. In particular, large proportions of these forest areas were converted to croplands and built-up areas between 2000 and 2020. We suggest that many of the LULC changes we observed are related to increased population density within the study area, without an associated increase in economic and social support systems required to alleviate poverty. In particular, there have been high rates of immigration in this area as a result of armed conflicts in the neighboring countries Chad and the Central African Republic – a situation that requires attention and resource allocation so that all the people involved can support themselves sustainably in the region while maintaining important ecosystem services and relationships with land, water and forests based on local ecological knowledge systems.

Our results provide baseline information required by the Cameroon government for policy development, conservation planning, urban planning, and deforestation and agricultural monitoring in northern Cameroon. Our methodological approaches will foster the advancement of knowledge in the application of ML algorithms for LULC monitoring within tropical rain forest regions across Africa, especially with the use of coarse-resolution Landsat images. We recommend that these mapping approaches be tested further in forested areas across other African regions that remain underrepresented in the remote sensing literature.

Chapter 3: Monitoring Forest cover and land use change in the Congo Basin under IPCC climate change scenarios

To be submitted as:

Yuh, Y. G., N'Goran, K. P., Herbinger, I., Heurich, M., Matthews, H. D., & Turner, S. E. Monitoring Forest cover and land use change in the Congo Basin under IPCC climate change scenarios.

Abstract

The Congo Basin has been a global hotspot for forest fragmentation and loss. Yet, very little has been done to document the region's rapid deforestation, to assess its effects and consequences, or to project future forest cover loss to aid in effective planning. Here we applied the Random Forest (RF) supervised classification algorithm in Google Earth Engine (GEE) to map and quantify decadal changes in forest cover and land use in the Basin between 1990 and 2020. We cross-validated our land use/land cover maps with existing global land cover products, and projected our validated results to the year 2050, under three climate change scenarios, using the Idrissi Land Change modeller from TerrSet. We assessed that, between 1990 and 2020, over 5.2 percentage points (215938 km^2), 1.2 pp (50046 km^2), and a 2.1 pp (86658 km^2) of dense forest cover were lost in the Basin, totalling approximately 8.5 pp (352642 km^2). For the period 2020 – 2050, we estimate a projected 3.7-4 pp (174860 – 204161 km^2) loss in dense forest cover under all three climate change scenarios, suggesting that approximately 12.3 pp (556803 km^2) of forest cover could be lost in this region over a 60-year period (1990-2050).

Keywords: Climate change, Forest cover change, Idrissi Land Change modeler, Land use change, Random Forest model

Introduction

Forests cover approximately one third of the Earth's surface and serve as home to diverse species of plants, animals and fungi, however these ecosystems are threatened due to increased human socioeconomic needs and demands, as well as natural disturbance conditions which are becoming more frequent and intense with climate change (IPCC, 2023; Tyukavina et al., 2018). According to the United Nations Food and Agricultural Organization (FAO), over 420 million hectares (Mha) of forest cover has been lost globally since the beginning of 1990, with an approximate 110 Mha loss recorded between 2010 and 2020 (FAO, 2020). Africa alone has lost over 3.9 Mha over the last 10 years, with a continuation of these trends predicted for Sub-Saharan Africa, especially in the Congo Basin where the activities of humans are increasing (Réjou-Méchain et al., 2021).

The Congo Basin, with its tropical forests home to many endemic and endangered species, is a global biodiversity hotspot. The region is home to over 10000 tropical plant species, and over 1000, 400, 280, and 700 species of birds, mammals, reptiles, and fish respectively (Environment, 2005), distributed within dense forest belts covering a total surface area of approximately 178 Mha (Mayaux et al., 2013). However, the Congo Basin is losing over 1Mha of forest cover per year as a result of often externally operated neocolonial economic activities (e.g. industrial logging, small and large-scale clearing for agriculture, and development projects such as the construction of roads and houses). Changes in human population density (used as a partial indicator for a combination of anthropogenic drivers, impacts and pressures arising from economic neocolonialism) and human-driven climate change are also contributing factors in forest declines (Tyukavina et al., 2018). This forest loss is connected to large-scale changes in land use and land cover (LULC) patterns, resulting not only in reduction in overall forest cover, but also in habitat fragmentation and loss in habitat connectivity. Fragmentation and land use change problems are expected to increase

substantially in the future, with increased human pressure, and with the related overarching global warming (Estrada et al., 2017).

Many studies have monitored forest cover and land use changes in the Congo Basin (deWasseige et al., 2009; Ernst et al., 2013; Mayaux, 2004; Mayaux et al., 2002; Molinario et al., 2017; Philippe & Karume; Potapov et al., 2012; Tyukavina et al., 2018; Verhegghen, 2015; Verhegghen et al., 2012; Ygorra et al., 2021; Yuh et al., 2019). However, several important variables remain poorly documented, and interactions among socioeconomic and demographic pressures, biophysical disturbances and climate change are often unexamined and have not been fully incorporated in land use and land cover change (LULCC) mapping in this region. Climate change, in particular, has been shown to impact land use and land cover (LULC) patterns in several regions across the globe. For example, in the Amazon Basin of South America, López et al., (2022) expect that climate change will lead to approximately 30-35% loss in forest cover in this region by the year 2050. In the United States of America, Mu et al., (2017) modeled potential impacts on ecosystems and found that climate change could lead to substantial reductions in croplands and pasture lands by the year 2070. In Europe, Carozzi et al., (2022) concluded that, by the year 2099, climate change could cause approximately 6% loss in croplands and 7% in grasslands. In other regions of the world, climate change has been projected to interact with other drivers of land use change [e.g., socioeconomic variables such as wood extraction, domestic costs for land, labor and timber, price increase for cash crops, and agricultural and infrastructural expansions; soil erosion; topography; institutional factors related to neocolonial forest policies and poor forest governance; and other human pressures that correlate with population density] to substantially alter land use and land cover change in the long-term (Geist & Lambin, 2002, 2004; Hellwig et al., 2019). In order to provide accurate assessments of land cover change

dynamics within the Congo Basin, for decision making and planning purposes, the effects of climate change need to be considered in present and projected LULCC mapping scenarios.

Most studies in the Congo Basin have mapped and quantified forest cover and land use changes at relatively small geographical scales (e.g., country and landscape scales: Molinario et al., 2017; Potapov et al., 2012; Yuh et al., 2019), or over shorter time periods (e.g., 1 – 15 years: deWasseige et al., 2009; Ernst et al., 2013; Mayaux, 2004; Mayaux et al., 2002; Molinario et al., 2017; Potapov et al., 2012; Tyukavina et al., 2018; Yuh et al., 2019; Verhegghen et al., 2012). However, to date, to the best of our knowledge, no study has made comprehensive projections of future forest and land cover conditions that incorporate the predicted effects of socio-economic, demographic, and ecological impacts.

Many of the freely available forest cover and land use maps and data from various earth observation centers are limited to short time scales and/or provide inaccurate data for the Congo Basin. For example, the Copernicus Global Land Cover dataset and products from the European Land Monitoring Service contain data only for the 2015-2019 period (https://lcviewer.vito.be/download). Collections from the NASA Moderate Resolution Imaging Spectroradiometer (MODIS) Global Forest and Land Cover Scenes contain data only for the years 2010 and 2020, with several limitations identified as a result of inaccuracies with some LULC classes (Friedl & Sulla-Menashe, 2019).

Conventional data on forest cover, contributed by various nations, are available through the United Nations Food and Agricultural Organization (FAO, 2006, 2018, 2020). However, these datasets are either incomplete or lack consistency in geographic coverage and data collection approaches, making harmonization and synthesis difficult (Grainger, 2008; Matthews, 2003). Other global LULC datasets generated by prominent remote sensing researchers exist (Hansen et al., 2010, 2013; Potapov et al., 2021, 2022). However, these are

either limited to shorter time periods (e.g., 2000 or 2020), or to single LULC classes [e.g., global forest cover (Hansen et al., 2010, 2013)]; or to global built environments and croplands (Potapov et al., 2021, 2022).

Mapping tools and quantitative models can help describe and predict large-scale spatiotemporal changes, for present and future forest cover and land use patterns under corresponding climate change scenarios, as well as various representations in response to demographic and socioeconomic variables. This integrated approach can provide baseline information required for landscape conservation, management and planning for the Congo Basin, and can inform our overall understanding of global climate change and biodiversity loss.

In this study, therefore, we aimed to: 1) Generate accurate land cover maps for the Congo Basin for the period from 1990 to 2020, and quantitatively assess decadal changes in land cover patterns; 2) Model and project the 1990 – 2020 land cover maps to the year 2050, under various scenarios of socioeconomic effects, demographic factors, and climate change, to quantify the potential contributions of these aspects to LULCC. We hypothesize that large-scale changes in forest cover will have occurred over the past several decades, in relation to other land use types (e.g., croplands, grasslands, savannas, and built-up areas). We expect further that these changes to forests lands will have been influenced significantly by logging and clearing for agriculture, other human pressures related to increased population density, and climate change. We expect forest cover loss to continue for the year 2050 in response to both anticipated increases in population density, as well as increased global warming.

Materials and Methods

The study area

The study area comprises the entire Congo Basin (Figure 1), which lies between longitudes 4° N and 5° S, covering six Central African countries: Cameroon, Central African Republic, Gabon, Republic of Congo, Democratic Republic of Congo and Equatorial Guinea. This region covers a total surface area of approximately 4.2 million km^2 (Table 1), forming the World's second largest tropical forest (after the Amazon Forest of South America). Prominent flagship faunal species found in this area include central chimpanzees (*Pan troglodytes troglodytes*), western lowland gorillas (*Gorilla gorilla gorilla*), the African forest elephants (*Loxodanta cyclotis*), bonobos (*Pan paniscus*), and hyena (*Crocuta crocuta*). Prominent floral families include Bambusoideae, Araceae, Araliaceae, Flacourtiaceae, and Marantaceae. Annual rainfall ranges from 1500-2000mm and annual mean temperature ranges from 18-28°C across the region (CSC, 2013).

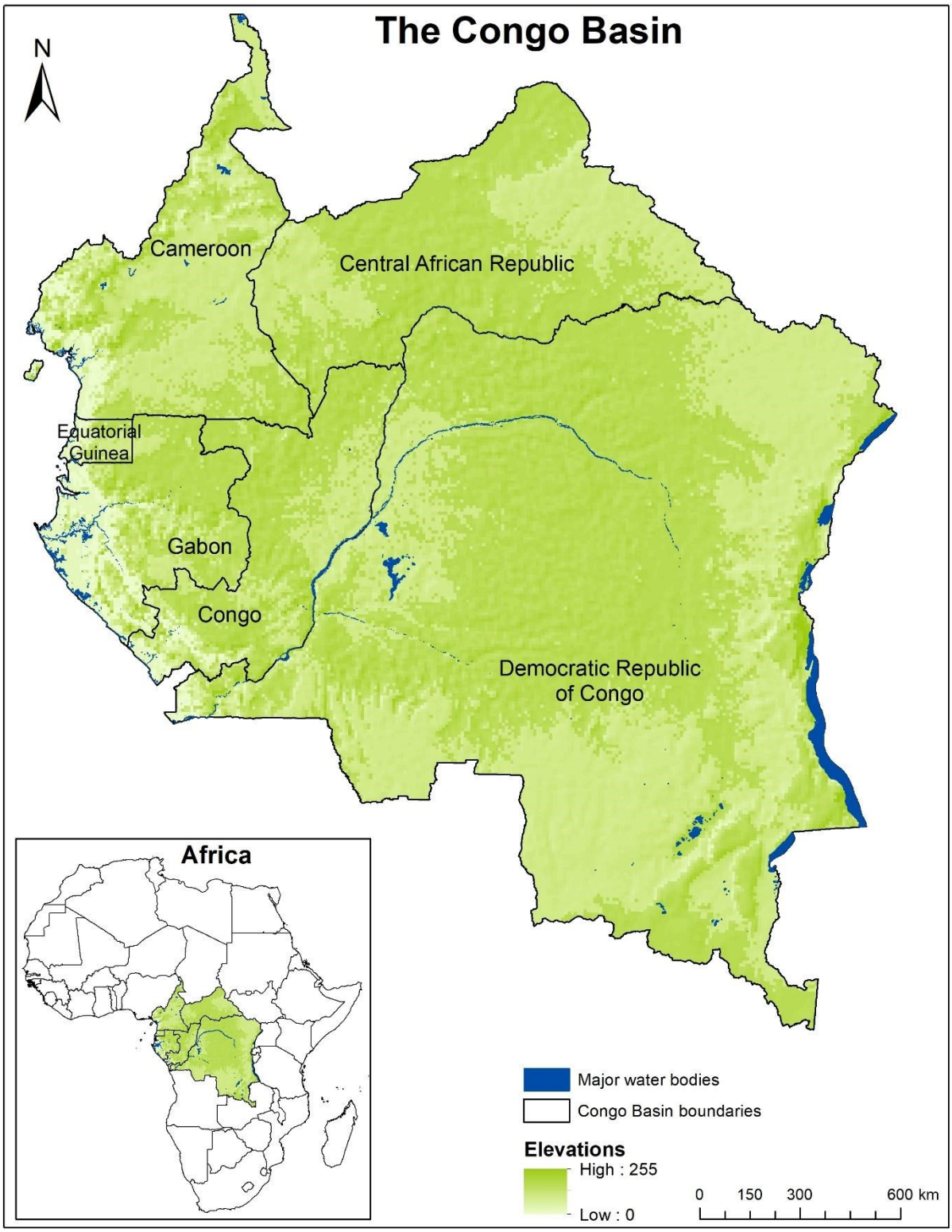

Figure 1. Map of the study area. Map shows the six Central African countries constituting the Congo Basin.

Table 1. Congo Basin countries and surface area covered

Country name	**Abbreviation**	**Total Area (km^2)**
Cameroon	CMR	468305
Central African Republic	CAR	647127.5
Congo	RC	345686.6
Equatorial Guinea	EG	26982.4
Gabon	GB	265267.8
Democratic Republic of Congo	DRC	2498343.5
Total Area		**4251712.8**

Land use and land cover mapping

To generate LULC maps for our study area for 1990-2020, we used the Google Earth Engine (GEE) cloud computing platform: a platform developed for dealing with big data challenges. Because our study area covers a total land surface area of approximately 4.2 million km^2, implying over 9 billion raster pixels to process, we applied the approach used by Midekisa et al., (2017) to map LULC. The approach involves using the GEE cloud computing platform to acquire, preprocess, train and classify satellite images using embedded image preprocessing and supervised classification algorithms.

Image acquisition and preprocessing

Using the GEE platform, we acquired Landsat collection 2 surface reflectance products from the NASA Earth Observation System, including Landsat 5 and 7 Thematic Mapper images for the years 1990, 2000 and 2010, and Landsat 8 Enhanced Thematic Mapper images for the year 2020 (Cook et al., 2014; Goward et al., 2021; Vermote et al., 2016; https://www.usgs.gov/landsat-missions/landsat-collection-2-surface-reflectance). We preprocessed the images through cloud cover removal with the quality assessment (QA) bands of the acquired Landsat images, using the GEE built-in cloud screening algorithm, and following the approach used by Midekisa et al., (2017). Because cloud removal generally

leads to loss in raster pixels in cloud dominated areas, we acquired Landsat images for three-year windows for each study period, and applied Midekisa and colleagues' (2017) approach to calculate the median of all cloud-free pixels for images acquired for each three-year window, to fill areas with missing pixels. For example, for the year 2010, we calculated the median of all cloud-free image pixels acquired between January 1st, 2009, and December 31st, 2011. This procedure was applied for the years 1990, 2000, and 2020, to generate cloud-free image composites with a complete number of pixels. Because cloud removal generally causes a drop in image quality, we normalized the image composites for each year of study by computing the median values of the Normalized Differential Vegetation Index (NDVI) and Normalized Differential Water Index (NDWI) for each three-year window (Midekisa et al., 2017). To ensure proper image visualization for sampling training data, the normalized images were calibrated with night-time light images from the National Oceanic and Atmospheric Administration (NOAA) center (Midekisa et al., 2017; Savory et al., 2017).

Image processing

(a) Sampling training data

In sampling training datasets, we first identified LULC categories suitable for the study area, following the criteria used in producing the 2010 and 2020 MODIS Global Land Cover Products by the National Aeronautics and Space Administration (NASA) agency (Friedl & Sulla-Menashe, 2019), as well as the approaches used in generating other single LULC classes, such as the 2000 and 2020 Global Forest Cover Data (Hansen et al., 2013; Potapov et al., 2021), and the 2000 and 2020 Global Croplands and Built-up Data (Potapov et al., 2021, 2022). We built on knowledge from these existing LULC products because they have been generated with high degrees of accuracy, and properly validated through

statistically significant correlations with ancillary datasets from the United Nations Food and Agricultural Organization (FAO), as well as with other global land cover products generated by the NASA Global Ecosystems Dynamics Investigation (GEDI) Service. We therefore used these datasets as references to conduct a stratified random sampling of pixel points for each suitable LULC class identified for the study area. We sampled a total of eight LULC classes, including dense forest, cropland, open savanna and bareland, woody savanna, grassland savanna, built-up areas, wetland, and water bodies, following sampling approaches applied in Yuh et al., (2023). When sampling forest (dense forest and woody savanna), for example, we defined forests as areas of land with trees ≥ 5m in height (Potapov et al., 2021), and a canopy cover ≥ 20% (FAO, 2000; Friedl & Sulla-Menashe, 2019). Dense forest and woody savanna were separately sampled based on the criteria of Friedl & Sulla-Menashe, (2019), that defined dense forests as having a > 60% canopy cover, and woody savannas as having a canopy cover of between 30% and 60%. In sampling cropland, we used the criteria of Friedl & Sulla-Menashe, (2019), that defined croplands as land use areas with at least 60% area cultivated with agricultural crops. In sampling built-up areas, we used the criteria established in Potapov et al., (2021), defining built-up areas as human-made landscapes associated with built environments such as commercial and residential infrastructures, urbanized areas, and roads. In sampling water bodies, we followed the criteria used in Friedl & Sulla-Menashe, (2019), defining water bodies as inland areas covered with at least 60% permanent water, and not obscured by objects above the surface such as buildings, tree canopies, and bridges. Approaches used for sampling all other proposed LULC classes are described in Table S1, and Yuh et al., (2023).

(b) Land use and land cover classification

To classify LULC for each year of our study, we first divided the sampled training datasets into 80% test and 20% validation subsets. For each of the test and validation data points, we extracted the Landsat spectral bands, NDVI, NDWI, and night-time light layers to be used as covariates in the mapping process. We then modeled and predicted LULC for each year of study by training the test data with the Random Forest decision tree classification algorithm (RF) embedded in the GEE platform. RF represents an ensemble of machine learning models that use bootstrap methods to build many single decision tree models (Breiman, 2001b; Mellor et al., 2013; Rodriguez-Galiano et al., 2012). The overall model uses a subset of explanatory variables (e.g. Landsat bands) to split observation datasets into a subset of homogenous samples used in building each decision tree (Mellor et al., 2013; Walton, 2008). The model has been successfully used in large-scale forest cover mapping (DeFries et al., 1997; Hansen et al., 2008, 2013), wetland mapping (Bwangoy et al., 2010; Midekisa et al., 2014), cropland mapping (Shelestov et al., 2017)), and land cover mapping (Gessner et al., 2015; Midekisa et al., 2017; Rodriguez-Galiano et al., 2012).

To validate the LULC classification accuracies for each year of study, we applied two different approaches. In the first approach, classification accuracies (the percentage of accurately classified pixels) were computed and compared with the test and validation datasets using a confusion or error matrix generated with a pivot table in Microsoft Excel (version 2016), following the approach of Yuh et al., (2019). An error matrix is a table used in quantifying the classification performance or accuracy of a machine learning algorithm using a set of test and validation datasets. In LULC mapping, the matrix clearly determines the error between two LULC classes i.e., identifies potentially mislabeled land use types. Three commonly used accuracies were computed: overall accuracy, producer's accuracy, and user's accuracy. An overall accuracy defines the percentage of correctly classified LULC

classes; a producer's accuracy defines the percentage accuracy of each LULC class in a LULC map; and a user's accuracy defines the percentage agreement between the classified data and ground observations (Olofsson et al., 2014; FAO, 2016). In the second approach, we applied the method used by Yuh et al. (2023); we employed a Pearson's correlation test to compute the correlation strength between the generated LULC products in our study and LULC products from already published studies, such as the Hansen et al., (2013) Global Forest Cover Data, the 2010 and 2020 MODIS global land cover products (Friedl & Sulla-Menashe, 2019), and the global built-up and cropland data published in Potapov et al., (2021), and Potapov et al., (2022).

Land use and land cover projections

(a) Acquisition of predictor variables

To project the 1990-2020 land cover data to the potential land cover in the year 2050, we used three predictor categories that have been proven to be important forest cover loss drivers in the Congo Basin, as well as LULCC drivers in other regions of the world. These include: the locations and areas of socioeconomic land use change factors such as industrial logging, small-scale clearing for agriculture, and large-scale agro-industrial clearing (Tyukavina et al., 2018); ecological or climate-driven factors such as landscape topography (slope and elevation), forest fires, and climatic variables (temperature and precipitation) (Geist & Lambin, 2002, 2004; Hellwig et al., 2019); and demographic factors, including human population density (Cafaro et al., 2022; Juárez-Orozco et al., 2017; Kleinschroth et al., 2019), which we used as a partial representation of anthropogenic influence. Although population density itself is not the primary driver of land use change, it is correlated with a number of aforementioned socioeconomic land use change drivers, as well as other

socioeconomic drivers (Steffen et al., 2015), such as those arising from issues with economic neocolonialism (e.g. forest resource exploitation in the region by higher income countries, increase agricultural productivity for export to higher income countries, and socioeconomic inequalities amongst and within nations) (Hughes et al., 2023). Datasets on socioeconomic factors were acquired from a recently published study by Tyukavina et al., (2018). To reduce variable redundancy, we grouped the logging and clearing datasets into a single composite indicator, defined in our model as "logging and forest clearing." Because developmental areas such as roads, bridges and buildings contribute in facilitating socioeconomic land use activities (Laurance, 2015; Laurance et al., 2009, 2012, 2014; Weinhold & Reis, 2008), as well as acting as important drivers of land use change (Geist & Lambin, 2002, 2004; Nuissl & Siedentop, 2021; Sang et al., 2022; Sarfo et al., 2022), we acquired datasets on the location and size of built-up areas (e.g. roads and buildings) from mapped datasets by Potapov et al., (2021), from which we created an auxiliary socioeconomic factor, "distance to built-up areas."

Datasets on human population density, consistent with both country-level population and gridded urban fractions, were acquired from the Veiko Lehsten climate and population projection data, archived in the Lund University database (https://dataguru.lu.se/app#worldpop). The datasets consist of human population density projections covering each year between 2010 and 2100, modeled under three shared socioeconomic pathways (SSP1, SSP2 and SSP5), through the Coupled Model Intercomparison Project 6 (CMIP6) of the Intergovernmental Panel on Climate Change (IPCC) (Olén & Lehsten, 2022). The datasets were mapped at a 1 km spatial resolution, and are consistent with both Shared Socioeconomic Pathways (SSP) and Representative Concentration Pathway (RCP) scenarios of the IPCC framework (Olén & Lehsten, 2022). We

therefore, acquired datasets for the periods between 2010 and 2050, corresponding to our LULC projection periods.

Biophysical factors, including landscape topography (slope and elevation) and the location, size and frequency of forest fires were calculated from digital elevation data acquired from the US geological survey database (http://srtm.usgs.gov/index.php), and from the 2000-2020 MODIS fire database (https://modis.gsfc.nasa.gov/data/dataprod/mod14.php) respectively.

Climatic datasets, including reanalyzed and projected temperature and precipitation (monthly maximum and minimum temperatures, and annual precipitation) datasets were acquired from the IPCC-AR6 ensemble climate projections of the CMIP6 project (Eyring et al., 2016; Thrasher et al., 2022), with future projections data acquired under three Shared Socioeconomic Pathways (SSP1, SSP2, and SSP5), consistent with the low, moderate and high greenhouse gas emission scenarios (RCP 2.6, 4.5, and 8.5) of the IPCC framework (SSP1-2.6, SSP2-4.5 and SSP5-8.5). The SSP1-2.6 climate change scenario represents conditions whereby societies move towards a more sustainable practice in energy and fossil fuel use and global carbon dioxide (CO2) emissions are cut to net zero and global temperatures peak during the second half of this century. The SSP2-4.5 represents conditions where CO2 emissions start falling as we approach the middle of the 21st century, but do not reach net zero by the end of the 21st century, leading to continued global temperature increases throughout the century. The SSP5-8.5 scenario represents a continued energy-intensive and fossil fuel-based economy, leading to larged increases in CO2 emissions and very substantial temperature increases by the end of the century. All datasets were projected at similar coordinate reference systems (WGS 1984, UTM zone 33N), and resampled at similar spatial resolutions (30m resolution) to ease the LULC modeling process. Table S2 provides a full description of these datasets and the available sources.

(b) The modeling process

The 1990-2020 land cover maps were projected to 2050 using the Idrissi Land Change Modeler (ILCM) from TerrSet (Eastman & Toledano, 2018; TerrSet, 2020), considered under various socioeconomic, demographic, biophysical and climatic change scenarios. The ILCM was developed by Clarks Lab (https://clarklabs.org/terrset/land-change-modeler/) as a stochastic and an ensemble model that simulates LULCC between two time steps (T1 and T2), following a set of transition rules assigned to each land cover type, and influenced by anthropogenic and natural disturbance factors (TerrSet, 2020). The model uses the Multi-Layer Perceptron Artificial Neural Network (MLP-ANN) (Atkinson & Tatnall, 1997) that applies a backpropagation modeling approach (i.e. backward transmission of errors from output nodes to input nodes) with a set of explanatory spatial variables to create transition potential maps (i.e., maps of transitions from a single land use class to other land use types) between two time steps (T1 and T2). The transition potential maps were then modeled in an ensemble approach with the Markov chain algorithm to generate LULC maps for a future time step (T3) (Gibson et al., 2018). The Markov chain algorithm is a stochastic modeling algorithm that, following a set of transition rules, models the probability that a system will remain stable in the future or will change from its previous or current state to a different future state (Gagniuc, 2017).

To project LULCC to the year 2050, we applied the approach of Gibson et al., (2018), which involves using the 2010 (T1) and 2020 (T2) LULC maps as baseline maps to: first, create transition potential maps with the MLP-ANN approach, and second, project the transition potential maps to the year 2050 (T3) using the Markov chain algorithm, and under three population change, and climate change scenarios (SSP1-2.6, SSP2-4.5 and SSP5-8.5).

In creating transition potential maps, we first identified all possible LULCC trajectories between the two current time steps (T1 and T2) (i.e., change from one LULC class in 2010 to another in 2020), following the approach of Yuh et al., (2019). Second, we created transition sub-models that included: grouping LULC transitions or trajectories with respect to the underlying drivers of change (Gibson et al., 2018; Pérez-Vega et al., 2012), quantified using an Ordinary Least Squared Regression (OLS) model (Tables S12-19). Table S3 shows the different transition sub-models that were created, including the identified underlying drivers of change, which were selected based on a ≥ 20% influence, following the approach used by Gibson et al., (2018). For each transition model, we evaluated the skill measure for each LULC transition [i.e., the percentage accuracy for a given LULC type to transition from one land use type to another between two time periods (T1 and T2), under a set of predictor variables]. We used the skill measure results to select the most accurate transitions and predictors to be modeled in an ensemble approach with the Markov chain algorithm of the ILCM.

To ensure accuracy in our future LULC projections, we first used the ILCM and the aforementioned predictors to model our 1990-2000 LULC maps to the years 2010 and 2020, using a Pearson's correlation test to cross validate the modeled outputs with our 2010 and 2020 LULC maps. Our modeled outputs for the years 2010 and 2020 strongly and significantly correlated with our 2010 and 2020 LULC maps (overall correlation strength; $R = 0.8$, $p < 0.05$ for both years 2010 and 2020) (Figure S1, Table S20a and b), suggesting the reliability of the ILCM in projecting LULCC. We therefore used the 2010 and 2020 LULC maps as baseline maps for projecting LULCC to the year 2050 under three climate and human population change scenarios (SSP1-2.6, SSP2-4.5 and SSP5-8.5). For future modeling, we used similar predictor datasets on logging, fire, and distance to built-up areas

acquired under current conditions, as projected future versions of these datasets were not available.

Land Use and Land Cover change detection

We quantified decadal changes (1990 – 2000, 2000 – 2010, and 2010 – 2020) in forest cover and land use patterns, using the ArcGIS geometry tool, following the approaches of Yuh et al., (2019) and Yuh et al., (2023). This approach involved: converting our classified LULC maps for each year of study from raster maps to vector shape files; intersecting the datasets on decadal basis with the ArcGIS intersect tool; creating a sub field "From-TO"; and performing change detection mapping and calculations (in km^2) from one LULC class to another between two time steps, using spatial statistics with the ArcGIS geometry tool. We further applied a similar approach for quantifying changes between current and projected future conditions (2020-2050) under all three climate change scenarios. We compared these changes at both regional and country scales.

Results

Model accuracy and LULC mapping

The current LULC maps (generated under four time scales: 1990, 2000, 2010 and 2020) are shown in Figure 2 (Figures S8a-13a show mapped outputs generated at country levels). Our RF model produced an overall classification accuracy of >90% in all four current conditions (Tables S4-S7). To further validate these accuracies, we correlated the generated LULC maps with existing land cover products, using a Pearson's correlation test, and following the approach of Yuh et al., (2023), and our results show strong and statistically significant correlations with map products published in Hansen et al., (2013), Friedl & Sulla-Menashe, (2019), Potapov et al., (2021), and Potapov et al., (2022). For example, our dense forest areas were strongly and significantly correlated with dense forest extracted from Potapov et al., (2021) and Hansen et al., (2013) ($R = 0.8$, $p < 0.05$ for the year 2020, and $R = 0.9$, $p < 0.05$ for the year 2010). Furthermore, we found strong and statistically significant correlations between our croplands and the croplands data published in Potapov et al., (2022) ($R = 0.9$, $p < 0.05$ for the years 2000 and 2020 respectively). We also found strong and significant correlations between our built-up data and datasets published in Potapov et al., (2021) ($R = 0.8$, $p < 0.05$ for the years 2000 and 2020 respectively). Correlation results for other LULC classes are shown in Tables S8-S10 and Figures S2-S3.

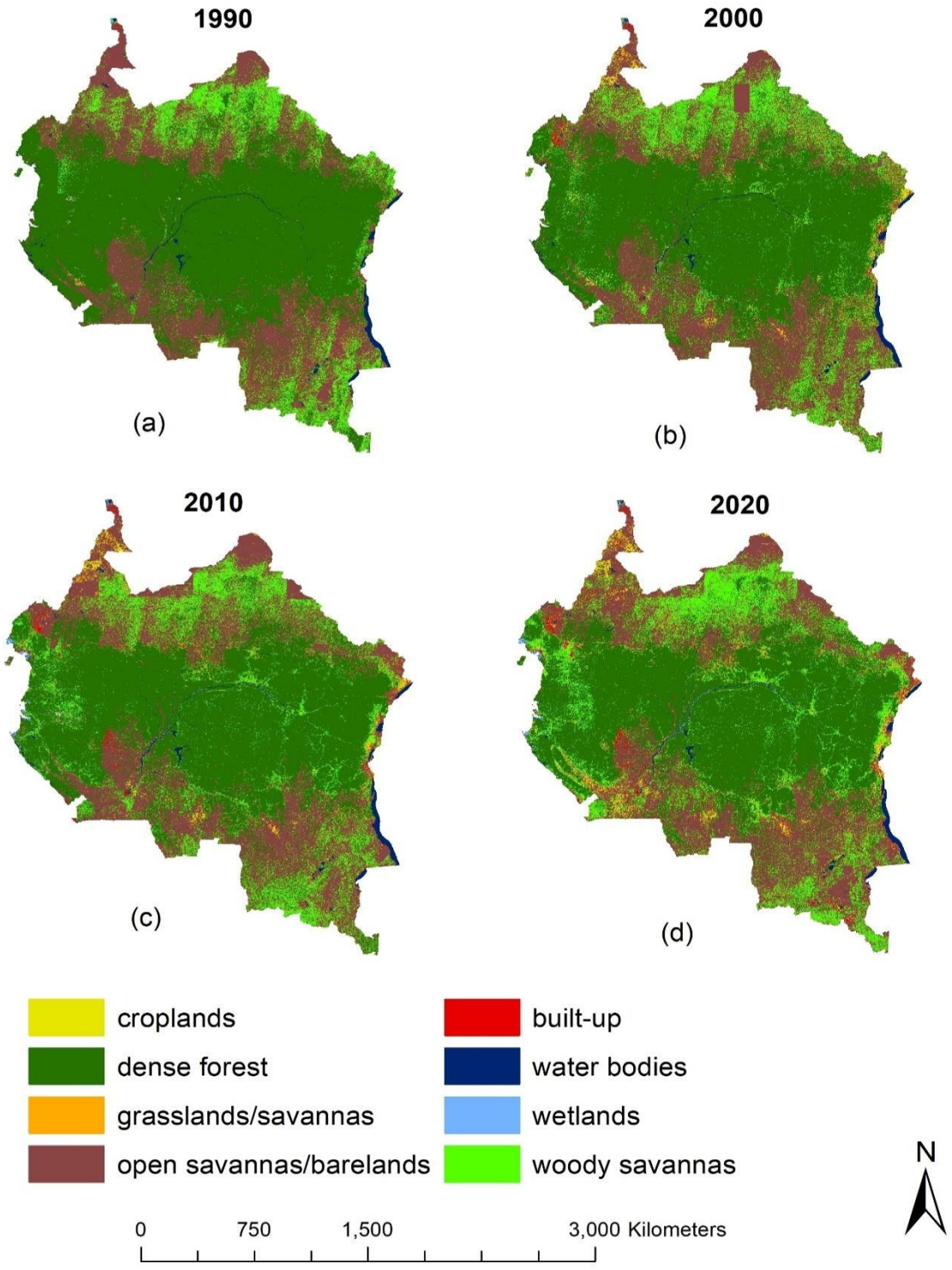

Figure 2. Land cover classification maps for the Congo Basin, for the years 1990, 2000, 2010, and 2020

Land cover projections

The LULC maps for the year 2050 (maps under all three population and climate change scenarios: SSP1-2.6, SSP2-4.5 and SSP5-8.5) are shown in Figure 3 (country-level results are shown in Figures S8b-13b). Table S11 shows the skill measure results (i.e., the % accuracy of each LULC category in transitioning from one given land use type to another between two time steps, under the influence of a given change driver). We show skill measure results only for the most accurate LULC transitions in each transition sub-model.

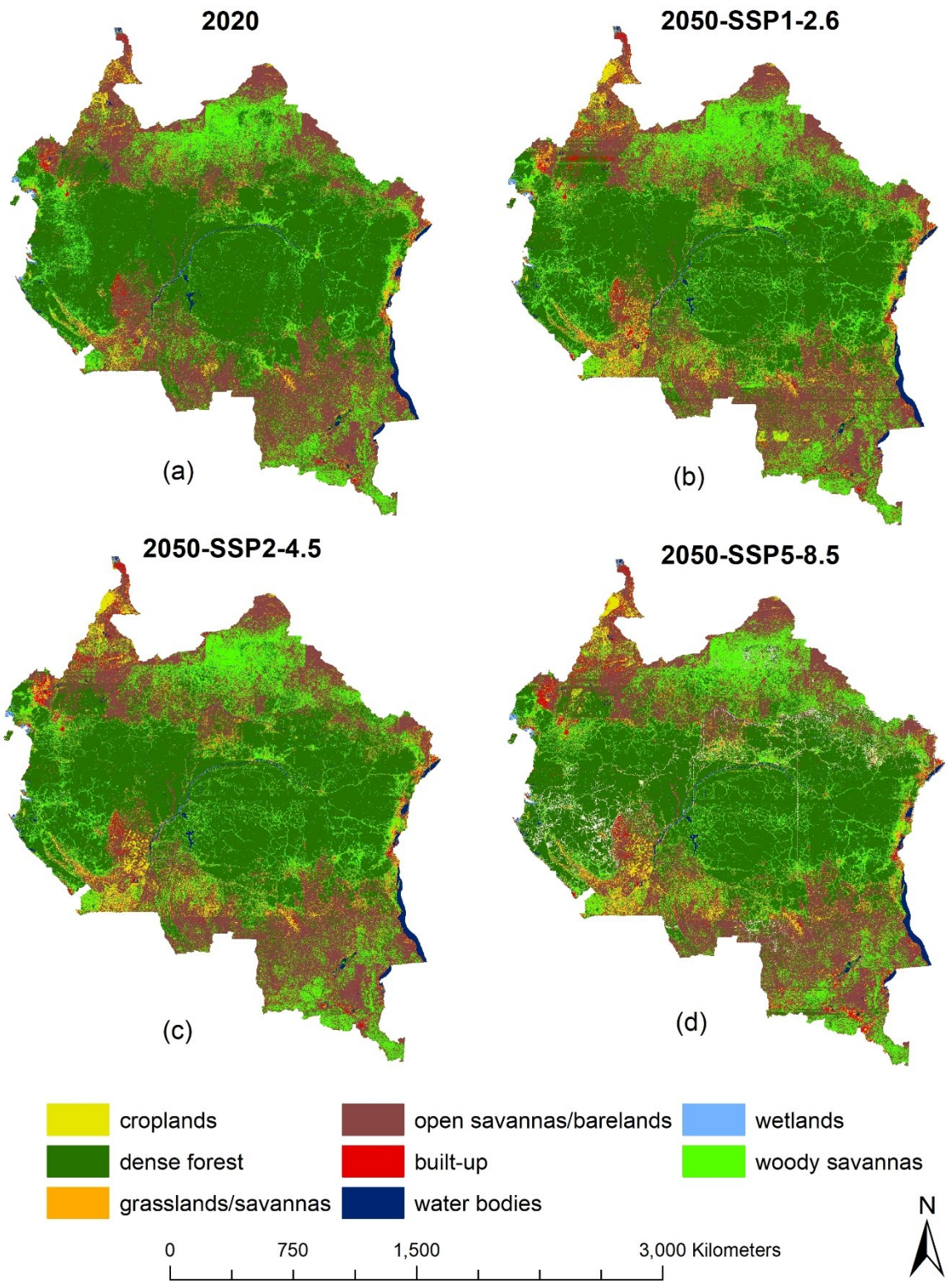

Figure 3. Projected LULC maps of the Congo Basin for the year 2050. Map shows projected results under all three climate change scenarios (SSP1-2.6, SSP2-4.5 and SSP5-8.5), with Figure 3a representing the baseline condition (for comparison purpose).

LULC quantification and contributions of predictor variables to LULCC

From our LULC maps, we provide estimates of the total area (in km^2) occupied by each LULC category in each year of study, as well as quantify detected change areas, i.e., changes from one land use type to another between two time steps, under decadal time scales. Quantified areas and detected changes between 1990-2000, 2000-2010, 2010-2020, and 2020-2050 (under all three climate change scenarios) are shown in Tables 2 and 3 (country-level information: Tables S21a-26a, and S21b-26b). We summarize results for four LULC types that predict significant changes to help inform land use planning. They include: Dense forest, woody savannas, built-up areas, and croplands. These LULC categories provide important spatial information that guides our understanding on trends in forest cover dynamics, agricultural land use dynamics, and changes in infrastructural development: information highly important for proper land use planning, and the sustainable management of forest ecosystems and forest resources. For these classes, we present quantified areas and hotspot maps of losses and gains (or expansions) in areas covered by each class for each change period.

Table 2. Area and proportion of land cover classes in each year of study in the Congo Basin

	1990		2000		2010		2020		2050					
									SSP1-2.6		SSP2-4.5		SSP5-8.5	
LULC class	**Area (km2)**	**% Area**	**Area (km2)**	**% Area**	**Area (km2)**	**% Area**	**Area (km2)**	**% Area**	Area (km2)	% Area	Area (km2)	% Area	Area (km2)	% Area
croplands	1834.3	0	32796.8	0.8	35335.9	0.9	86181	2.1	182107	4.4	177414.7	4.4	187798.5	4.7
dense forest	2342579.7	56.9	2126641.4	51.7	2076595.9	50.5	1989937.8	48.3	1815078.2	44.3	1790329.4	44.3	1785776.8	44.6
grassland/savannas	22806.6	0.6	50503.7	1.2	38129.5	0.9	52908	1.3	65855.4	1.6	58847	1.5	58891.3	1.5
open savannas/barelands	1224361.8	29.8	1244488.2	30.3	1277365.4	31.0	1205256.9	29.3	1114673.4	27.2	1123401.3	27.8	1110497.6	27.7
built-up areas	1407.9	0	19740.6	0.5	26814	0.7	46548.2	1.1	92837	2.3	93346.8	2.3	103189.2	2.6
water bodies	52710.2	1.3	62117.1	1.5	56215.8	1.4	57970.2	1.4	56714.9	1.4	56793.1	1.4	56782.4	1.4
wetlands	1283.4	0	4923.0	0.1	9311.3	0.2	12388	0.3	11684.3	0.3	11717.8	0.3	11676.5	0.3
woody savannas	468275.4	11.4	572513.9	13.9	595872.4	14.5	665461.9	16.2	758233.6	18.5	732603.5	18.1	691153.7	17.3
Total	4115259.3	100	4113724.7	100	4115640.2	100	4116652	100	4097183.7	100	4044453.6	100	4005766	100

Table 3. Quantified decadal changes in land cover patterns in the Congo Basin, between 1990-2020

	1990-2000		2000-2010		2010-2020		2020-2050					
							SSP1-2.6		SSP2-4.5		SSP5-8.5	
LULC classes	**Area (km2)**	**% Area**	**Area (km2)**	**% Area**	**Area (km2)**	**% Area**	**Area (km2)**	**% Area**	**Area (km2)**	**% Area**	**Area (km2)**	**% Area**
croplands	30962.4	0.8	2539.2	0.1	50845.1	1.2	95926.0	2.3	91233.7	2.3	101617.5	2.6
dense forest	-215938.3	-5.2	-50045.5	-1.2	-86658.2	-2.1	-174859.6	-4.0	-199608.4	-4.0	-204161.0	-3.7
grassland/savannas	27697.1	0.7	-12374.2	-0.3	14778.5	0.4	12947.4	0.3	5939.0	0.2	5983.3	0.2
open savannas/barelands	20126.4	0.5	32877.2	0.8	-72108.5	-1.8	-90583.5	-2.1	-81855.6	-1.5	-94759.3	-1.6
built-up areas	18332.7	0.4	7073.4	0.2	19734.3	0.5	46288.8	1.2	46798.6	1.2	56641.0	1.5
water bodies	9406.9	0.2	-5901.3	-0.1	1754.3	0.0	-1255.3	0.0	-1177.1	0.0	-1187.8	0.0
wetlands	3639.6	0.1	4388.3	0.1	3076.7	0.1	-703.7	0.0	-670.2	0.0	-711.5	0.0
woody savannas	104238.5	2.5	23358.5	0.6	69589.5	1.7	92771.7	2.3	67141.6	1.9	25691.8	1.1

Forest cover dynamics

(a) Dense forest cover

Our results (Tables 2-3 and Figure 4a) show that dense forest in the Congo Basin declined from 56.9% (2342580 km^2) in the year 1990 to 51.7% (2126641 km^2) in the year 2000, accounting for over 5.2 percentage points (pp) (215938 km^2) net loss in the Congo Basin's dense forest cover over the 10-year period. From 2000 – 2010, dense forest further declined by 1.2 pp (50046 km^2) – i.e., from 51.7% (2126641 km^2) in the year 2000 to 50.5% (2076596 km^2) in 2010. Between 2010 and 2020, a 2.1 pp (86658 km^2) loss in dense forest cover was further experienced in the region; dense forest declined from 50.5% (2076596 km^2) of land in the region in 2010 to 48.3% (1989938 km^2) in 2020. For the period 2020-2050, we modeled a 3.7-4 pp (174860- 204161 km^2) loss in dense forest cover under all three climate change scenarios. These results generally show that the Congo Basin has a net loss of over 8.6 pp (352642 km^2) of its entire dense forest cover over the last 30 years, with an anticipated 12.3 pp (556803 km^2) net loss over the full 60-year period of our study (1990-2050). Our findings further show that large areas of dense forest cover loss occurred in areas where dense forests have transitioned either to woody savannas, open savannas/barelands or grassland savannas, or were converted to croplands and built-up areas (Figure S10, Table S27). Key drivers of dense forest loss in this region include logging and forest clearing (R^2 = 0.67, $p < 0.05$), higher maximum and minimum temperatures ($R^2 = 0.66$, $p < 0.05$), wildland fires ($R^2 = 0.42$, $p < 0.05$), population density ($R^2 = 0.21$, $p < 0.05$), and proximity to built-up areas ($R^2 = 0.26$, $p < 0.05$) (Table S14). In terms of individual land use transitions, forest logging and clearing, human population density, and distance to built-up areas contribute to between 85% and 98% transition accuracy from dense forests to built-up areas and croplands, while wildland fires, maximum and minimum temperatures, and human population density

contribute to over 81-95% accuracy in the loss in dense forest cover to grasslands and woody savannas (Table S11).

At the country level, the largest share of dense forest loss is predicted for the DRC, which lost over 140834 km^2 of dense forest cover between 1990 and 2000, 4935 km^2 between 2000 and 2010, and 74030 km^2 between 2010 and 2020, with an anticipated loss of from 121832 to 125382 km^2 predicted for the period, 2020 – 2050 (Tables S23a and b). The loss in dense forest cover within the DRC is approximately 7 times greater than losses experienced within other individual Congo Basin countries under all four time scales (Tables S21b-S26b) and under all four change periods (Figures S8c-S13c).

Despite the overall loss in dense forest cover, there have also been some areas that have transitioned to dense forest cover from other LULC types, leading to a small gain in dense forest cover in some areas over the last 30 years, with much smaller gains predicted for the future (137966 km^2 between 1990 and 2000, 118584 km^2 between 2000 and 2010, 216654 km^2 between 2010 and 2020, and 95616 to 103877 km^2 from 2020 to 2050). The measured and projected gains are due to changes, actual and predicted, in other LULC types to dense forest cover over the study period (Table S27). For example, between 1990 and 2000, over 74176 km^2, 59119 km^2, and 3018 km^2 of open savannas/barelands, woody savannas and grassland savannas have been converted to dense forest cover respectively. Between 2000 and 2010, the respective conversions were 79181 km^2, 121462 km^2, and 10869 km^2, while between 2010 – 2020, they were 70060 km^2, 129135 km^2, and 6792 km^2. We estimate a conversion of approximately 65746 – 96644 km^2 of woody savannah areas to dense forests by the year 2050 (an area about 2-3 times the size of Belgium (https://statisticstimes.com/geography/countries-by-area.php), and our findings show that the main or key drivers of forest cover gain are precipitation and slope parameters, which contribute 69% and 59% influence respectively (Table S14). Figure 4b shows comparisons in

dense forest cover losses and gains within the Congo Basin, while Figure S4 shows hotspot maps of gains and losses (country-level comparisons: Figures S8d, e – S13d, e).

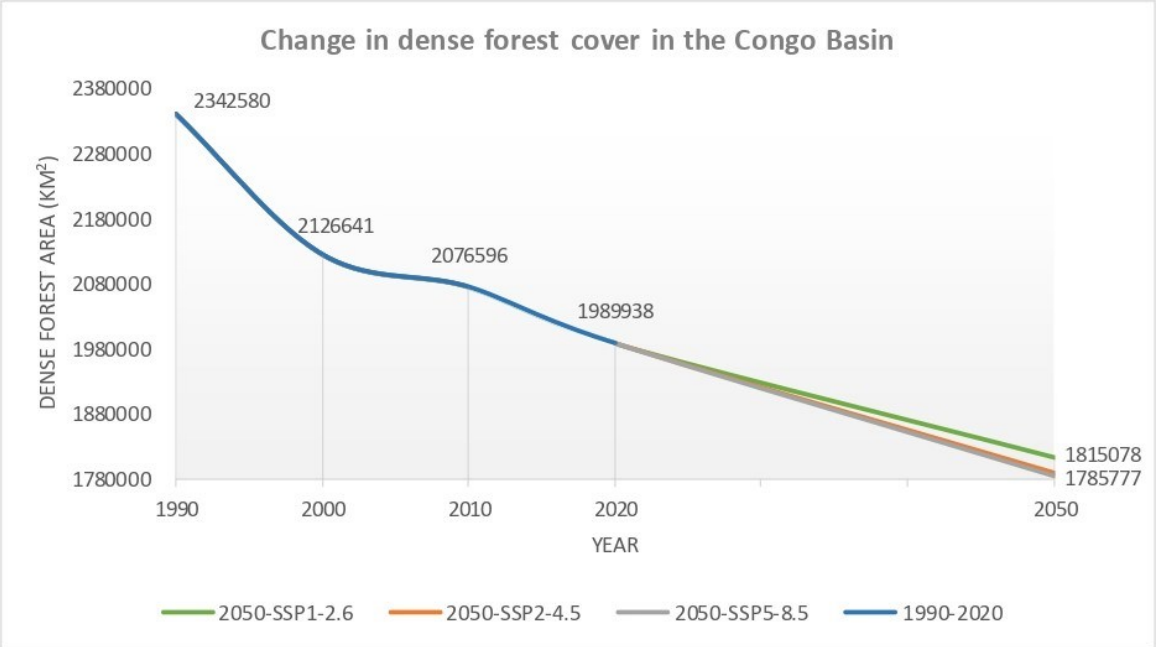

(a)

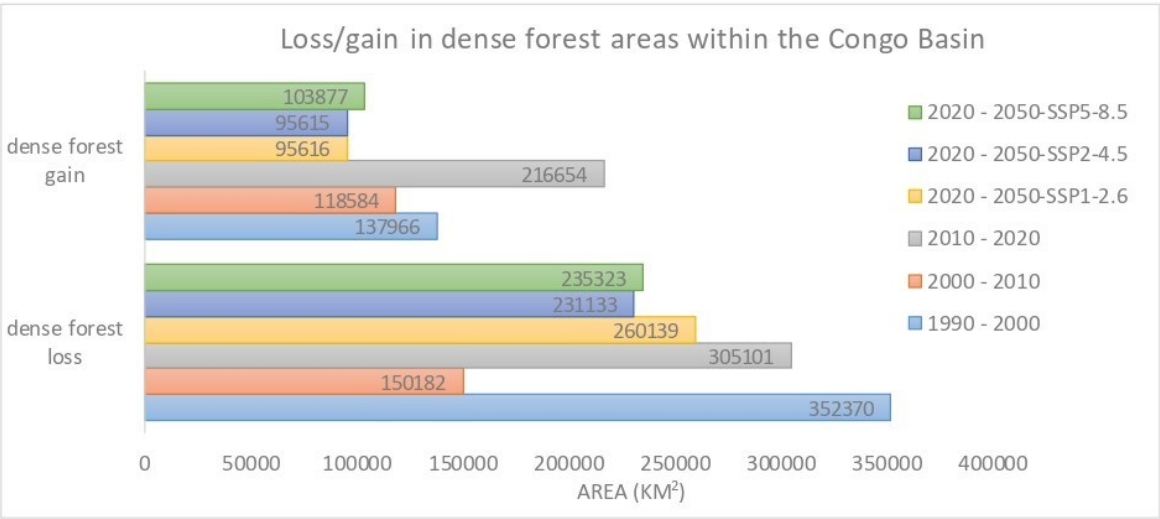

(b)

Figure 4. Dense forest cover dynamics: (a) Change in dense forest cover within the Congo Basin under all four change periods (1990-2000, 2000-2010, 2010-2020, and 2020-2050), under SSP1-2.6, SSP2-4.5, and SSP5-8.5 climate change scenarios; (b) Comparison in dense forest cover loss and gain in the Congo Basin, across all four change periods

(b) Woody savannas

Woody savanna areas increased from 11.4% (468275 km^2) in 1990 to 13.9% (572514 km^2) in the year 2000, accounting for over 2.5 pp (104239 km^2) increase in these areas within the Congo Basin (Table 2 and 3). Between 2000 and 2010, woody savanna areas further increased by 0.6% (23359 km^2), i.e., from 13.9% (572514 km^2) in the year 2000 to 14.5% (595872 km^2) in the year 2010. Finally, between the years 2010 to 2020, we found an additional 1.7 pp (3077 km2) increase in woody savanna areas ([increased from 14.5% (595872 km^2) in 2010 to 16.2% (665462 km^2) in 2020], with an anticipated 1-2.3 pp (25692 – 92772 km^2) gain in woody savanna areas modeled for the year 2050. Overall, there has been an increase in woody savanna areas in the Congo Basin of about 4.8 pp (197187 km^2) over the last 30 years, with a 5.9 pp (222878 km^2) increase projected over a 60-year period (1990-2050). Key drivers of woody savanna increase in this region include logging and forest clearing ($R^2 = 0.83$, $p < 0.05$), precipitation levels ($R^2 = 0.93$, $p < 0.05$), and slope of the land ($R^2 = 0.31$, $p < 0.05$) (Table S11). Figure 5a shows the change in woody savanna areas over all four change periods, while Figures 5b, and S5 show a comparison in woody savanna gains and losses, and hotspot maps of gains and losses respectively (country-level comparisons: Figures S8f, g, h to S13f, g, h).

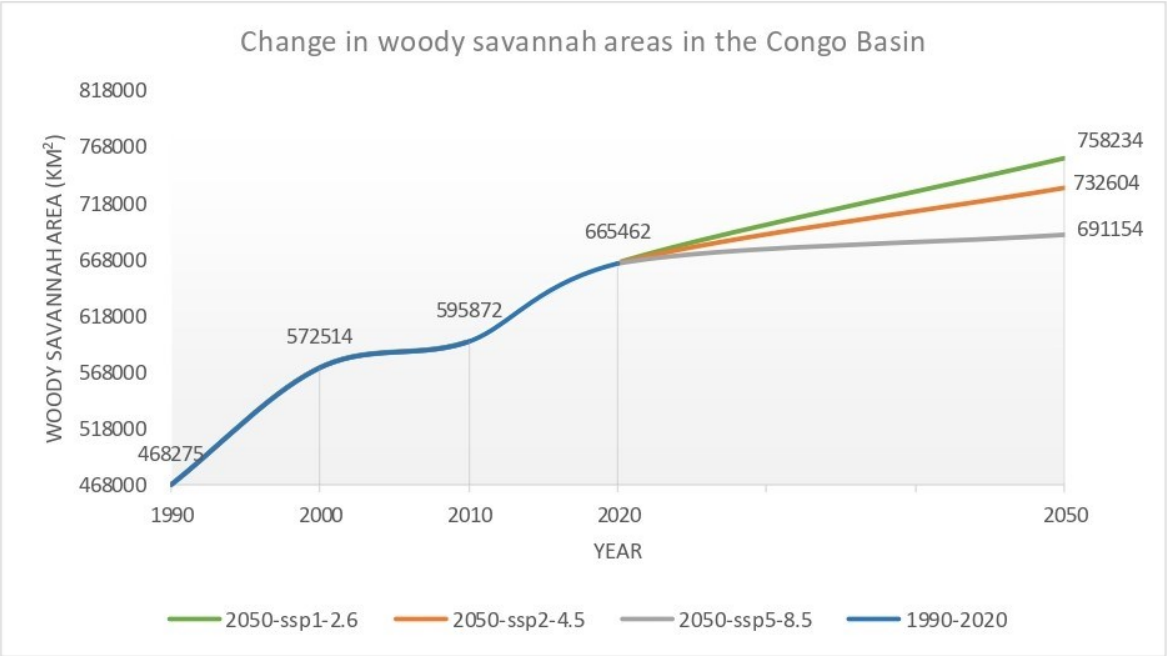

(a)

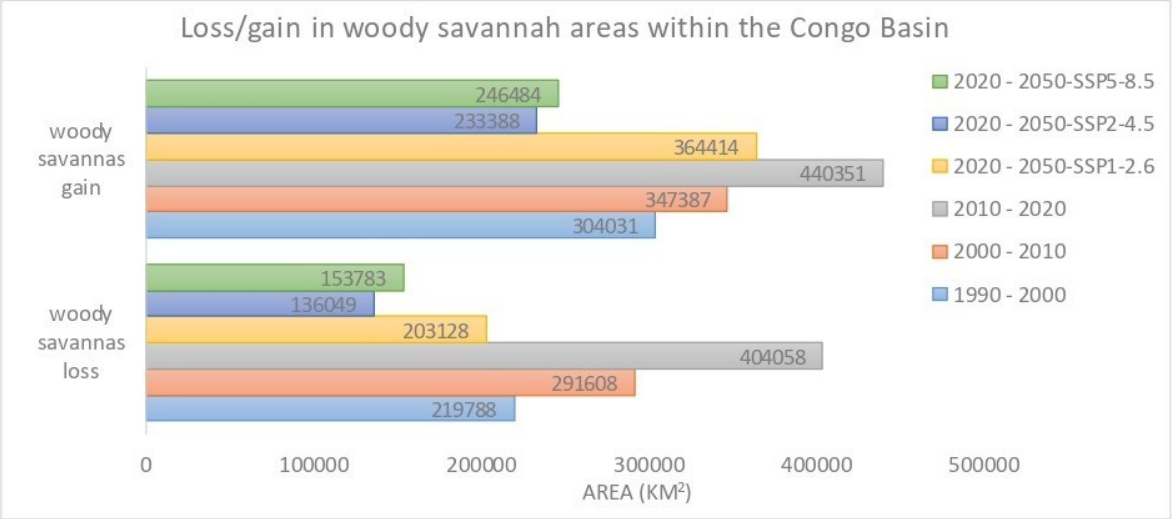

(b)

Figure 5. Woody savannah dynamics: (a) Change in woody savannah areas within the Congo Basin, under all four change periods (1990-2000, 2000-2010, 2010-2020, and 2020-2050-under SSP1-2.6, SSP2-4.5, and SSP5-8.5climate change scenarios); (b) Comparison in woody savannah loss and gain in the Congo Basin, under all four change periods.

Changes in built-up areas

Results from Figure 6a show a continuous expansion in built-up areas under the decadal change periods, with a two-fold expansion expected by the year 2050. Built-up areas increased from 1408 km^2 in the year 1990 to 19741 km^2 in the year 2000, accounting for over 18333 km^2 expansion within the Congo Basin. From 2000 to 2010, built-up areas further expanded by 7074 km^2 (from 19741 km^2 in the year 2000 to 26814 km^2 in 2010). For 2010 – 2020, a 19734 km^2 expansion in built-up areas was further experienced in the region; built-up areas increased from 26814 km^2 in the year 2010 to 46548 km^2 in the year 2020. For 2020 – 2050, we project an expansion of built-up areas between 46289 to 56641 km^2 under all three population and climate change scenarios. These results generally show that the Congo Basin has experienced a net expansion in built-up areas of about 45140 km^2 over the last 30 years, with an increase of approximately 101781 km^2 predicted over a 60-year period (1990 – 2050).

At the country level, the largest expansion in built-up areas is predicted for the DRC and Cameroon (Tables S23a, b, and S26a, b). The DRC has experienced an expansion in built-up areas of approximately 7698 km^2 between 1990 and 2000; 2358 km^2 between 2000 and 2010; and 10538 km^2 between 2010 and 2020, with an anticipated 21300 to 29548 km^2 expansion predicted for the period 2020 – 2050 (Figure S10i). Cameroon has experienced an expansion in built-up areas of approximately 7341 km^2 between 1990 and 2000; 715 km^2 between 2000 and 2010; and 5672 km^2 between 2010 and 2020, with an anticipated 14395 to 16330 km^2 expansion predicted for the period 2020 – 2050 (Figure S13i). Key drivers of built-up expansions (conversions from woody savannas, grasslands, and open savannas, as well as dense forests, to built-up areas include human population density ($R^2 = 0.3$, $p < 0.5$), and distance to built-up areas ($R^2 = 0.4$, $p < 0.5$) (Table S12).

Although the Congo Basin has experienced large expansions in built-up areas over the last 30 years, small proportions of built-up abandonment have also been recorded, with much smaller abandonments predicted for the period up to the year 2050. For example, between the years 1990 – 2000, approximately 3007 km^2 of built-up areas were abandoned and converted to other land use types. Between 2000 and 2010, over 1645 km^2 of built-up areas were abandoned, while between 2010 and 2020, over 3388 km^2 of built-up areas were abandoned. For the periods 2020 – 2050, we predict abandoned built-up areas of between 2703 to 2890 km^2 under all three population and climate change scenarios. Figure 6b shows a comparison in built-up area gain and loss within the Congo Basin between 1990 and 2050, while Figure S6 shows a hotspot map of built-up area gain and loss under all four change periods (country-level information: Figures S8j, k – S13j, k). Key drivers of built-up abandonment include slope of the land ($R^2 = 0.7$, $p < 0.5$), and distance to built-up ($R^2 = 0.4$, $p < 0.5$).

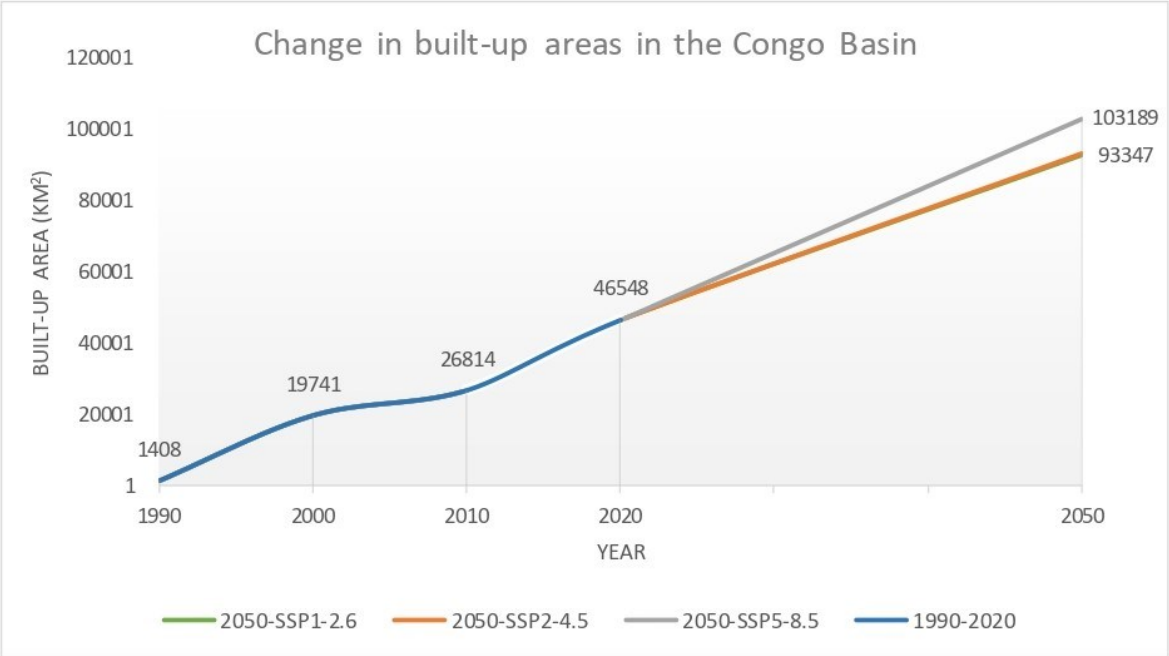

(a)

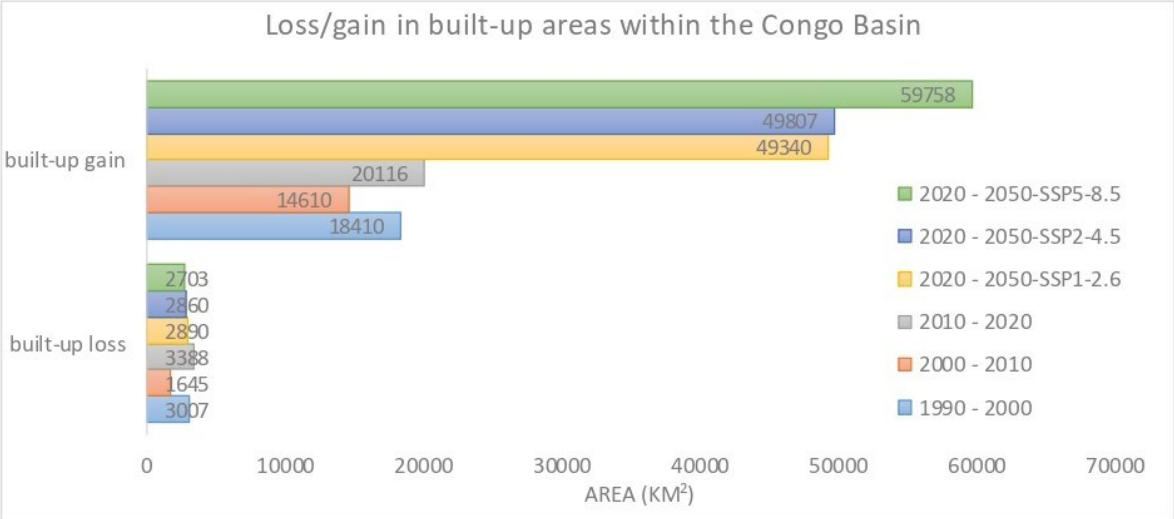

(b)

Figure 6. Built-up area dynamics: (a) Change in built-up areas within the Congo Basin under all four change periods (1990-2000, 2000-2010, 2010-2020, and 2020-2050 – under SSP1-2.6, SSP2-4.5, and SSP5-8.5 climate change scenarios); (b) Comparison in built-up area loss and gain in the Congo Basin, across all four change periods.

Croplands

Like built-up areas, our results shown in Tables 2 and 3 and in Figure 7a also reflect a consistent expansion in cropland areas over time, with a two-fold expansion expected by the year 2050. Cropland areas increased from 1834 km^2 in the year 1990 to 32797 km^2 in the year 2000, accounting for over 30962 km^2 expansion in cropland areas within the Congo Basin. Between 2000 and 2010, cropland areas further expanded by 2539 km^2 (from 32797 km^2 in the year 2000 to 35336 km^2 in 2010), and by the year 2020, a 50845 km^2 expansion in cropland areas occurred in the region (from 35336 km^2 in 2010 to 86181 km^2 in 2020). For the period 2020 – 2050, we have projected an increase of between 91234 and 101618 km^2 of cropland areas in the region under all three climate change scenarios.

At the country level, the largest expansions in cropland area occurred in the DRC and Cameroon (Tables 23a, b and 26a, b). The DRC experienced a cropland area expansion of approximately 14112 km^2 between 1990 and 2000. Between 2000 and 2010, over 3016 km^2 expansion occurred, while from 2010 to 2020, 27948 km^2 expansion occurred. We projected that cropland areas could increase by 47683 to 54759 km^2 in the DRC between the years 2020 and 2050 (Figure S10l). In Cameroon, over 11812 km^2 of cropland expansion occurred from 1990 to 2000. Between 2000 and 2010, there was approximately 4331 km^2 cropland expansion, while between 2010 and 2020, Cameroon experienced an expansion in cropland areas of about 6619 km^2. We projected an increase in cropland areas from 17804 to 21277 km^2 in Cameroon between the years 2020 and 2050 (Figure S13l). We found that the key driver of cropland expansion (i.e. the conversion of woody savannas, grasslands, and open savanna areas to croplands) was increased human population density ($R^2 = 0.2$, $p < 0.5$).

Though croplands generally expanded over time in our study area, we also observed abandonment of small cropland areas over the last 30 years, with much smaller

abandonments predicted for the future. For example, from 1990 to 2000, approximately 9154 km^2 of cropland areas were abandoned and converted to other land use types. Between 2000 and 2010, over 7385 km^2 of cropland areas were abandoned, while between 2010 and 2020, over 8680 km^2 were further lost to other land use types. For 2020 to 2050, we predict an abandonment in cropland areas of from 5852 to 6367 km^2 under all three population and climate change scenarios. Figure 7b shows a comparison in cropland area gain and loss within the Congo Basin between 1990 and 2050, while Figure S7 shows a hotspot map of cropland area gains and losses under all four change periods (country level information: Figures S8m, n – S13m, n). Key drivers of cropland loss include wildland fires ($R^2 = 0.36$, $p < 0.5$), and high maximum temperatures ($R^2 = 0.66$, $p < 0.5$).

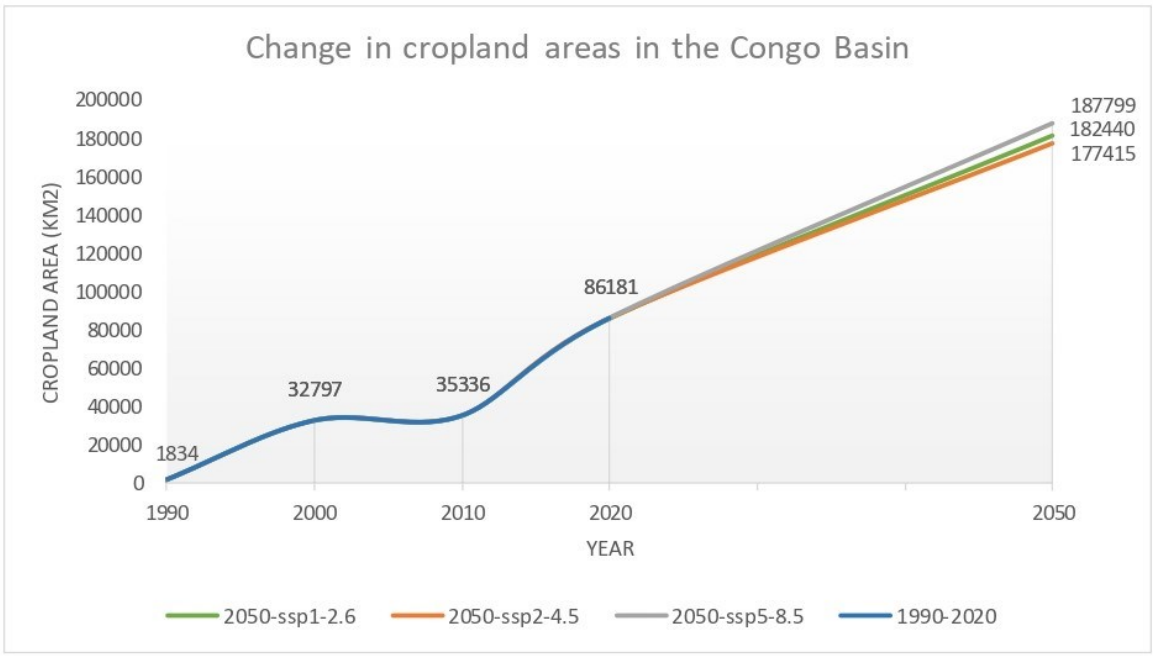

(a)

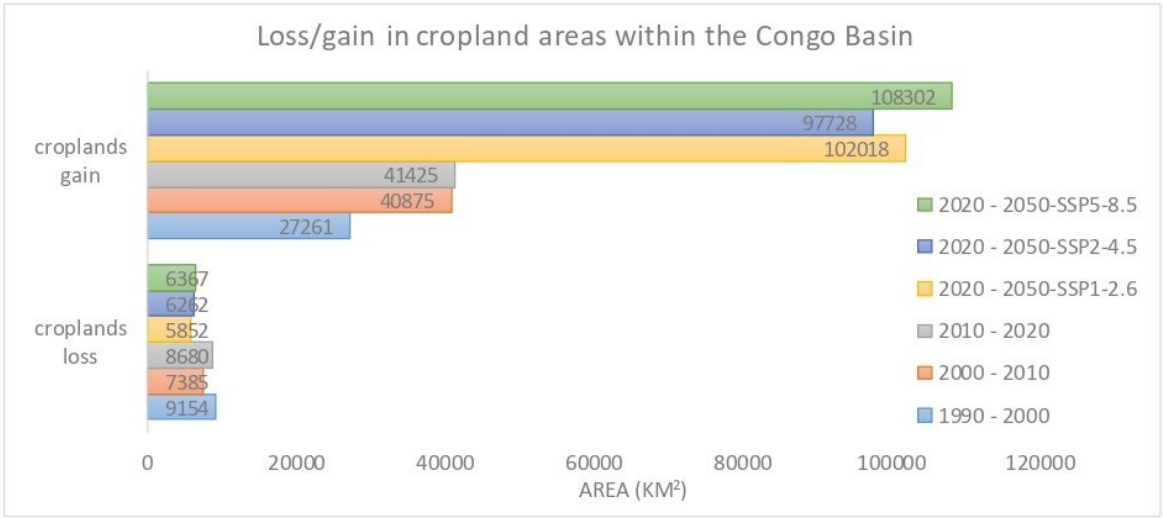

(b)

Figure 7. Cropland dynamics: (a) Change in cropland areas within the Congo Basin under all four change periods (1990-2000, 2000-2010, 2010-2020, and 2020-2050-under SSP1-2.6, SSP2-4.5, and SSP5-8.5 climate change scenarios); (b) Comparison in cropland area loss and gain in the Congo Basin, across all four change periods.

Discussion

We generated accurate LULC maps for the Congo Basin for the last 30 years (1990 – 2020), and modeled future changes (to 2050) under three climate change scenarios (SSP1-2.6, SSP2-4.5 and SSP5-8.5). We generated these datasets at a fine spatial resolution of 30m, and validated our current LULC maps through statistically significant correlations with existing map products [i.e., Friedl & Sulla-Menashe, (2019), Potapov et al., (2021), and Potapov et al., (2022)]. We mapped and quantified important LULCC trajectories under current and future change conditions, and as well, examined the contributions of socioeconomic, demographic, biophysical and climate change factors to LULCC within this region. We therefore provide novel, reliable and consistent spatial information that deals with the problem of data uncertainty and inconsistencies compiled by the FAO, as reported in Grainger, (2008) and Matthews, (2003). Our datasets provide baseline information required for landscape planning and management in this region.

Our results revealed dramatic changes in LULC within the Congo Basin, under increased socioeconomic disturbance and climate change conditions. First, we found that dense forests are declining at rates of approximately 0.3 pp (11700 km^2) per year, with over 8.6 pp (352642 km^2) loss in dense forest areas estimated for the last 30 years. A large proportion of dense forest areas have been converted to built-up areas, croplands, woody savannas, and open savannas (Table S27), and our findings show that the main drivers of these conversions are logging and forest clearing, wildland fires, proximity to built-up areas, other human pressures that correlate with population density, and higher maximum temperatures (Table S14). For example, we found that logging and clearing of forests, human population density, and proximity to built-up areas contributed to between 85-98% transition accuracy from dense forests to built-up areas and croplands, while wildland fires, maximum and minimum temperatures, and human population density contribute to over 81-95%

accuracy in the loss in dense forest cover to grasslands and woody savannas (Table S11). As human population continues to grow and the effects of global warming continue to persist (IPCC, 2014; Olén & Lehsten, 2022), we project a continuous loss in dense forest cover between the years 2020 – 2050, under all three population and climate change scenarios. Our findings on current forest cover loss conditions corroborate with those from Tyukavina et al., (2018) that have shown that the Congo Basin is losing approximately 1Mha (10000 km^2) of its forest cover per year as a result of industrial logging, and forest clearing. Our results also correspond to previous estimates reported at global scales by Kirilenko & Sedjo, (2007), that have indicated that primary (dense) forests are declining globally at rates of about 6Mha per annum, with over 4.9Mha loss recorded between Brazil and Indonesia, and approximately 1Mha loss recorded within Central Africa. The Brazilian Amazon forest has experienced a loss in forest cover of approximately 788300 km^2 between 1988 and 2018, accounting to over 14,500 km^2 loss in dense forest cover per year: results close to estimates reported in this study (Da Cruz et al., 2021). The Indonesian Bornean forest has experienced a total forest cover loss of approximately 168000 km^2 between 1973 and 2010, suggesting an annual loss of about 4500 km^2 (Gaveau et al., 2014) – results that are half the annual estimates that we report for the Congo Basin. In other regions of the world, such as in the Canadian and US boreal and temperate forests, similar findings have been reported. For example, a nationwide characterization of 25 years of forest disturbance within the Canadian boreal forest revealed that over 399,000 km^2 of forest cover were lost between 1985 and 2010 as a result of forest fires, suggesting an annual average loss of approximately 15900 km^2 (White et al., 2017). In the conterminous United States, Homer et al., (2020) have reported a net loss in forest cover of approximately 63000 km^2 between 2011 and 2016: results that are closer to the 50000 km^2 reported for the period 2000 – 2010 in our study.

Forest cover loss problems (particularly in tropical regions) have been closely linked to issues with socioeconomic land use (Tyukavina et al., 2018), arising from increases in human population density (Juárez-Orozco et al., 2017; Kleinschroth et al., 2019; Cafaro et al., 2022), which interacts with many drivers of anthropogenic environmental change and pressures, and reflects many factors associated with economic neocolonialism (Hughes et al., 2023). In Central Africa, anthropogenic needs for resources are increasing with increased human population density. According to a 2022 report from the United Nations Population Department, the population of this region has increased from approximately 70 million people in the year 1990 to over 181 million people in the year 2020 (United Nations Department of Economic and Social Affairs Population Division, 2022). Over 50-70% of the entire population in this region lives in rural areas and in close proximity to forests, with the livelihoods of most rural people dependent on shifting cultivation for subsistence, firewood and charcoal production, and the use of non-timber forest products as food sources and health products (FAO, 2004). A 2016 report by Mosnier et al., (2016) has shown that large-scale deforestation in the Congo Basin is attributable to increases in agricultural land use, with a case study from the DRC revealing that over 12-27% of forest areas were converted to croplands. In addition to subsistence farming, much of this conversion arises from the cultivation of high demand cash crops such as palm oil, corn, cassava, beans, groundnut, sweet potatoes, rice and millet, by a growing rural population (Mosnier et al., 2016), as well as to support urban populations, and international markets that push cash crop production and buy cash crops for export. As with the DRC, we found that Cameroon is also experiencing large-scale expansion of cropland areas, due to increases in local population density and associated need for subsistence, and also as a result of demand for large-scale cash crop exports to neighboring countries such as Gabon, Equatorial Guinea, and the CAR, that depend on Cameroon for many food products (Achancho, 2013). Cameroon is particularly

well known for its large-scale conversion of forest areas to oil palm plantations, banana plantations, and to cassava, cocoyam, plantain and cocoa farms. For example, oil palm expansion has been reported to contribute to over 67% of the loss in forest cover within Southwest Cameroon (Ordway et al., 2019). Large-scale expansion of cocoa farms within forest habitats has also been reported for several western African countries, including Cameroon (Sassen et al., 2022). These findings are in line with our projections for the region.

As with croplands, we found that the Congo Basin is experiencing large-scale expansions in built-up areas, with a two-fold increase expected by the year 2050. Several infrastructural development projects are ongoing within Congo Basin countries, with such projects potentially contributing to the built-up expansions mapped and projected in this study. For example, Cameroon and the Republic of Congo are completing a $235 million Ketta-Djoum Road project to link the capitals of the two countries. A 285-km road linking Ndende in Gabon and Dolisie in the Republic of Congo is currently under construction. A 500 km project that links Kribi in Cameroon to the Nabeba and iron-ore deposits in the Republic of Congo is also currently underway (Rainforest Foundation, 2021). Such infrastructural developments contribute to the increases in built-up areas within the Congo Basin by facilitating movement from one urban area to another (Rainforest Foundation, 2021). The development of infrastructure depends on timber; most wood production companies in the Congo Basin carry out industrial logging, with over 7-20% timber products extracted per hectare within timber producing landscapes (Durrieu de Madron et al., 2000; Ruiz Pérez et al., 2005), and our results suggest that such logging practices contribute significantly to forest cover loss in this region. For example, it is reported that over 2-3 million m^3 of timber are harvested in Cameroon per year (Cerutti & Tacconi, 2006; Eba'a Atyi, 1998). In the DRC, over 3-4 million m^3 of timber extraction has been reported (Lescuyer et al., 2014). If timber exploitation and agricultural land conversions continue to

increase, all our projections suggest that the Congo Basin will increasingly experience extensive loss in its dense forest cover to croplands and built-up areas by the year 2050 (Table S27).

We also found significant climatic drivers of LULCC in this region. Limited information is available in the scientific literature on the contributions of climate change to forest cover and land use change in the Congo Basin, although some studies are reporting conversions from grassland savannas to woody savannas in western and central Sahel regions, as a result of increased rainfall and recovery from droughts (Anchang et al., 2019; Brandt et al., 2019), as well as the exacerbation of climate-driven vegetation change as a result of socioeconomic land use activities (Aleman et al., 2017). In this study, however, we provided a focused analysis that presents evidence that climate change is a significant and direct contributor to LULC change in this region. We found that higher maximum temperatures contributed significantly to the loss in dense forest cover with associated land cover change to grassland and woody savannas (Table S11 and S14). We also found that higher precipitation contributed significantly to the increase in size and frequency of waterbody and wetlands in our study area (Table S11 and S17-18).

Under future climate change scenarios, we modeled a continued loss in forest cover and expansion of croplands, and concluded that these land cover change patterns were influenced in our models by changing temperature conditions. Climatic changes have been reported to contribute significantly to forest cover and land use change in several regions of the world. For example, in Canada and USA, rising and extreme high temperatures have been shown to ignite forest fires, which burn large patches of forested areas yearly, thereby converting them to Tundra forests, grasslands or woody savannas, at least temporarily (Kolden & Abatzoglou, 2012; Stralberg et al., 2018). Model projections for future scenarios

of climate change show shifts in forest cover to other land use types within parts of these regions by the end of the 21st century (Ameray et al., 2023). Similar scenarios are reported for some tropical regions of the world, such as in the South American Amazon forest (Cox et al., 2004; López et al., 2022), and the Indian forests (Chaturvedi et al., 2011; Upgupta et al., 2015). Our model projections for the Congo Basin align with results reported in these case studies, as well as in studies conducted at global scales (Beaumont & Duursma, 2012; Chen et al., 2020; Hurtt et al., 2011).

The productivity of croplands is also expected to suffer from extreme temperature conditions, where significant proportions of cropland areas are expected to be abandoned and converted to either grasslands, woody savannas, or open savannas, over time. Although we project more expansions than loss in croplands, some studies have shown that climate change will pose serious threats to food production in many regions of the world, with rural Africa expected to be highly vulnerable (Gomez-Zavaglia et al., 2020; IPCC, 2014; Mangaza et al., 2021), including the Congo Basin (Dove et al., 2021; Sonwa et al., 2012). With the current practices and prospects of Climate-Smart Agriculture (Karume et al., 2022), however, there is evidence that cropland areas will expand in the future to meet the needs of the local human population, and especially driven by the demand from the Global North for export cash crops such as cocoa, tea and palm oil (Megevand et al., 2013). Our model projects such expansion under all three climate change scenarios. Climate-Smart Agriculture, defined here as climate resilient approaches to agriculture that recognize and integrate challenges associated with food soverenty and security and climate change is becoming increasingly important for fostering agricultural adaptation in many regions across Africa; suggesting higher prospects for increased crop productivity in the long run (reviewed in Abegunde & Obi, 2022; Ariom et al., 2022; Ogunyiola et al., 2022). For example, in Ghana, Nigeria, Senegal, and Burkina Faso, the planting of drought-resistant crops as a Climate-Smart Agricultural approach has

been shown to be successful in dealing with climate change impact problems (Ngigi, 2009). Crop diversification has been implemented as a Climate-Smart Agricultural approach in solving climate impact problems in South Africa (Ziervogel et al., 2008). Mixed crop planting, agroforestry, and soil treatments with the use of fertilizers have been respectively applied as Climate-Smart Agricultural approaches in many other regions across Africa (Mendelsohn et al., 2000; Lema & Majule, 2009). These, and more, suggest increase potential for future expansions in croplands many African regions, including the Congo Basin.

Limitations of the study

Although our study provides novel and accurately validated LULC maps for the last 30 years (1990 – 2020), as well as projected maps for the future (2050), several limitations exist. First, we validated our land cover maps by correlating them with existing datasets from the MODIS global land cover products (Friedl & Sulla-Menashe, 2019), as well as with single land use products (global forest cover, croplands, and built-up data) generated by Hansen et al., (2013), and Potapov et al., (2021), Potapov et al., (2022). Although this approach is robust, a much better approach would have been to cross validate our mapped outputs by correlating them with ground-truthed data or datasets classified at a local level. However, these datasets are unavailable for our study area, considering its extremely large geographic extent. To deal with this limitation, we applied the approach of Yuh et al., (2023), that utilized a standardized protocol developed for mapping the MODIS global land cover products, as well as the Hansen et al., (2013), and Potapov et al., (2021), Potapov et al., (2022) global forest cover, croplands and built-up datasets respectively. The Hansen and Potapov datasets have been mapped with high levels of accuracy, and properly validated

through comparison with more conventional datasets from the United Nations Food and Agricultural Organization (FAO), as well as with other global LULC products generated by the NASA Global Ecosystems Dynamics Investigation (GEDI) service. However, for results validated with the MODIS global land cover products, we apply some caution in interpreting them, as the MODIS global land cover data has several limitations due to misclassification of some land cover features (Friedl & Sulla-Menashe, 2019).

Second, it is well known that there is limited availability of Landsat clear-sky data for many regions of the world, with parts of the Congo Basin encountering these limitations. Our acquired Landsat products for the years 1990, 2000, 2010, and 2020 had extensive cloud cover in over 40% of the study area, which might have reduced our pixel resolutions and pixel numbers during cloud removal. Our attempts to fill areas of missing raster pixels with Landsat data for three-year windows for each study period could have led to overestimation of some LULC classes, and could account for the minor discrepancies between the total LULC estimated for each study period (Table 2, and S21a-26a). Though our LULC products produced high degrees of accuracy in all four years of study (Tables S4-S10), we again interpret our quantified land cover and change detection results with some caution, owing to the effects of pixels overfitting and class overestimation.

Third, our projected LULC products possess some limitations in the methodological approach. Datasets on logging and forest clearing, fires and distance to built-up areas are unavailable for the future; in projecting future LULC, we therefore used predictor variables of changing human population density and climatic projections, but held distributions of logging, fire, and distance to built-up areas constant at current values. This could result in future changes attributed to population density changes that were driven historically by other changing human pressures. Furthermore, population density is not in itself the driver of anthropogenic pressures in the Congo Basin, although population growth in the Global South

is often erroniously treated as such (Hughes et al., 2023). We used population density as a partial indicator of human pressures on the local environment, as it was an available quantitative measure that is correlated with many socioeconomic drivers of environmental change (Steffen et al., 2015). However, we recognize that population density at best provides a partial representation of the set of anthropogenic factors that cause LULC and other environmental changes.

Conclusion and management recommendations

Our study represents a novel effort to map and quantify decadal changes in forest cover and land use patterns within the Congo Basin, as well as to model and project specific future LULC changes in the region under IPCC climate change scenarios. We generated accurate LULC maps for the Congo Basin for the years 1990, 2000, 2010, 2020 and projected these LULCC to the year 2050, under three climate change scenarios (SSP1-2.6, SSP2-4.5 and SSP5-8.5). We found that large areas of dense forest cover have been lost to woody savannas, croplands, built-up areas, and open savannas in this region between 1990 and 2020, with continued loss projected for the period 2020-2050 under each of three defined climate change scenarios. We found that historical loss in dense forest cover in the Congo Basic was highly and significantly influenced by human population density, distance to built-up areas, forest clearing and logging, wildland fires, and high maximum temperatures. In particular, croplands and built-up areas have both shown rapid expansion over the historical period, with two-fold expansions projected between 2020-2050. We found that historical expansions were strongly associated with human population density, and distance to built-up areas. Over the last 30 years, human population density has doubled within Congo Basin countries, with more than 50% of the population living in rural areas, and seriously lacking in economic and

social support systems. There is, therefore, an urgent need to provide economic and social support to these rural areas, to enable people in these areas to live sustainably, and to support the maintenance of important ecosystem services (Abernethy et al., 2016). Moreover, several infrastructural development projects are on-going in this region (as described previously), aiming to meet the needs of the future population, and our model projects a two-fold expansion in built-up areas over the next 30 years compared to the historical period.

For other LULC trajectories (e.g. losses and gains in water bodies and wetlands, as well as losses and gains in woody and grassland savannas), we found that climatic factors, including higher maximum temperatures and greater precipitation are significant contributors of these change trajectories, suggesting the importance of climate change in predicting LULC changes within the Congo Basin. Our results thus fill a critical gap in knowledge about the current state of forests and land use in this region and on the potential impacts of human activities, changes in population density and climate change. Results from our analysis are also particularly relevant to initiatives such as the United Nations Framework Convention on Climate Change (UNFCCC) REDD+ (Reduce Emissions from Deforestation and Forest Degradation) program, as they could assist in designing a long-term regional strategy and action plan for monitoring deforestation, and urban expansion within Congo Basin countries. Our current forest cover loss data could be used to estimate the amount of carbon that has been emitted from the Congo Basin through deforestation activities over the last 30 years, while datasets for the year 2050 could serve in predicting future emissions, thereby contributing to the important work of the UNFCCC REDD+ program.

Chapter 4: Recent decline in suitable large mammal habitats within the Dzanga Sangha Protected Areas, Central African Republic

Published as:

Yuh, Y. G., N'Goran, K. P., Beukou, G. B., Wendefeuer, J., Neba, T. F., Ndotar, A. M., NdombaA, D. L., Ndadet, A. C. J., Herbinger, I., Matthews, H. D., & Turner, S. E. (2023). Recent decline in suitable large mammal habitats within the Dzanga Sangha Protected Areas, Central African Republic. *Global Ecology and Conservation*, 42, e02404. https://doi.org/10.1016/j.gecco.2023.e02404

Abstract

The forests of the Congo Basin are an important home to some of the world's most critically endangered species, including the central chimpanzee (*Pan troglodytes troglodytes*), the western lowland gorilla (*Gorilla gorilla gorilla*) and the forest elephant (*Loxodanta cyclotis*). To contribute to the long-term sustainability of these species and their habitats within the Dzanga Sangha Protected Areas (DSPA) in the Central African Republic, the World Wide Fund for Nature (WWF) developed an ecological monitoring program to assess the spatial drivers of species' habitat changes. Here, we assess and quantify chimpanzee, gorilla and elephant habitat suitability within the DSPA using data from two survey years (2015 and 2020), to identify priority habitat areas and recommend conservation measures to mitigate ongoing habitat changes. We found that priority chimpanzee habitats covered about 1383 km2 (30 %) of the entire DSPA in the year 2015, while priority gorilla and elephant habitats covered approximately 2569 km2 (56 %) and 3075 km2 (67 %) respectively. Priority habitat area for the three species declined by 4, 4.5 % and 9.8 % points respectively between 2015 and 2020, mostly due to increased human pressures. We further provide evidence that the Dzanga National Park represents a region of higher priority habitat for all three species owing to the reduced human pressure that has resulted from higher eco-guard patrol efforts. Based on our analysis, we recommend maintaining a nonviolent patrol presence to mitigate human pressures within remaining priority habitat areas, recognizing also the importance of collaboration with local communities to support long-term conservation goals.

Key words: Ensemble models, Eco-guard patrols, Elephants, Great Apes (chimpanzees and gorillas), Priority habitats, Dzanga Sangha Protected Areas (DSPA).

Introduction

Mammal habitats, especially those suitable for large fauna, are declining at rapid rates across tropical Africa. Flagship species that have been identified as likely to suffer the most dramatic population declines associated with habitat loss and degradation include great apes (Junker et al., 2012; Stokes et al., 2010; Strindberg et al., 2018) and elephants (Blake et al., 2008; Blake & Hedges, 2004; Maisels et al., 2013; Poulsen et al., 2017, 2018; Rood et al., 2010; Stokes et al., 2010). Several factors have been shown to influence the distribution of these species and the suitability of their habitat across their ranges. We define habitat suitability as the attributes of a habitat that allow it to support a viable population of a given species, or groups of species, over an ecological time scale of decades to centuries (Kellner et al., 1992). Ecological characteristics are fundamental determinants of habitat quality and can include: climatic factors (e.g. temperature (Hill, 2006; Kosheleff & Anderson, 2009; Pruetz et al., 2002; Thomas & Bacher, 2018) and precipitation (Reed & Fleagle, 1995)); landscape factors such as topography (Fitzgerald et al., 2018) and presence and distribution of water bodies (Plumptre, 2010); and the type of land cover (dense forests, swampy forests, grasslands) (Strindberg et al., 2018, Yuh et al., 2019, Morgan et al., 2019, Ginath-Yuh et al., 2020). In addition to ecological habitat characteristics, human activities can also influence the suitability of habitat for particular species. Prominent examples include the presence of human disturbance factors such as hunting (Araújo et al., 2004; Chase et al., 2016; Ginath Yuh et al., 2020; Humle et al., 2016; Kyale et al., 2011; Maingi et al., 2012; Peres & Lake, 2003; Wittemyer et al., 2014), human population density (Strindberg et al., 2018; Zhao et al., 2018), anthropogenic deforestation (Estrada, 2013; Humle et al., 2016; Isabirye-Basuta & Lwanga, 2008; Sá, 2012; Yuh et al., 2019) and anthropogenic habitat fragmentation (e.g. caused by permanent land use change and road construction) (Fotang et al., 2021; Wittemyer et al., 2014); and the enforcement of laws associated with conservation and protection, such

as those enforced with the presence of eco-guard patrols (Kablan et al., 2019; Morgan et al., 2018; N'Goran et al., 2012). These factors interact to determine habitat suitability for most species (Heinicke et al., 2019; Junker et al., 2012; Stokes et al., 2010; Strindberg et al., 2018a); results from modeling and mapping these factors on landscapes can be used to identify priority habitats for long term conservation (Ginath Yuh et al., 2020; Watson et al., 2011; Groves & Game, 2016).

Despite evidence that the above-listed factors contribute to species distribution and habitat suitability, some important factors relevant to western gorilla, chimpanzee, and forest elephant distribution and conservation remain poorly documented. First, while several studies have mapped and documented the spatial variability in ape and elephant habitat suitability across their ranges (Junker et al., 2012; Plumptre, 2010; Stokes et al., 2010; Strindberg et al., 2018; Wittemyer et al., 2014), little is known about the short or long-term changes in suitability of these species' habitats, particularly within protected areas (PAs) where gorillas, chimpanzees and forest elephants can occur sympatrically. In particular, there is an urgent need to quantify the spatial relationship between habitats for different priority species across protected areas, so as to identify the priority habitats that best support several species. Mapping and quantifying the short and long-term changes in habitat suitability can therefore show where suitable habitat areas are declining.

Second, eco-guard patrols to deter and prevent poaching activities, are part of the law enforcement strategy in this region, and were established as a strategic conservation action to protect wildlife species and their habitats (Kablan et al., 2019). However, the effectiveness of these eco guard patrols has received little attention, and here we provide a measure of their role in supporting the maintenance and conservation of suitable species habitats.

Third, habitat fragmentation, the breakdown of large and continuous areas of forest into a number of smaller and spatially distinct forest patches, isolated from each other by a matrix of other habitat and land use types (Didham et al., 2012; Vogt et al., 2007) is increasing rapidly in this region and must be examined in relation to large mammal conservation. Habitat fragmentation variables including, the size and shape of core forests, patch forests and perforated forests, and the density of the forest edge (Vogt et al., 2007) are both predictors of great ape movements and indicators of disturbed forests (Fotang et al., 2021). However, the influence of habitat fragmentation on species distribution has not been fully documented, nor has the potential for mapping these variables been fully explored. Core forests in this context, represent intact and continuous forest fragments with sizes greater than 200 ha. Patch forests are isolated forest fragments smaller than 200 ha. Perforated forests are core forest areas with relatively small perforations or clearings that produce edge effects, while edge density is a measure of the effect of the forest edge between two or more isolated forest patches (Parent, 2009; Rahman et al., 2016; Vogt et al., 2007).

The sustainable management of mammal habitats poses a major challenge to most conservation practitioners across Africa, especially in the Congo Basin where species habitat loss is largely associated with increased anthropogenic pressure resulting from the combination of growth in the human population and the need for resources for sustenance and socio-economic development (Wittemyer et al., 2008). The six countries surrounding the Congo Basin (Republic of Cameroon, Central African Republic, the Democratic Republic of Congo (DRC), Equatorial Guinea, Gabon, and Republic of the Congo) established a number of transboundary conservation landscapes in the year 2000 based on the Commission for the Forests of Central Africa (COMIFAC) agreement. Among these landscapes, the Sangha Tri-National Landscape (TNS) established between the Republic of Congo, the Republic of

Cameroon and the Central African Republic (CAR), was identified as one of the key areas requiring urgent management intervention.

To assess conservation efforts and effectively measure conservation impacts on wildlife and suitable habitats for wildlife species within this landscape, the World Wide Fund for Nature (WWF, also known in some countries as World Wildlife Fund) developed an ecological monitoring program (N'Goran et al., 2014) as part of the Green Heart of Africa (GHoA) monitoring & evaluation framework. The objectives of the WWF ecological monitoring program are to operationalize an adequate system for the monitoring and evaluation of conservation activities, support the adaptive management of priority landscapes, and demonstrate conservation impacts in the Congo basin (N'Goran et al., 2017). As part of its conservation strategy, the WWF ecological monitoring program focuses on medium and large size mammals (in particular, but not limited to, the forest elephants and great apes (chimpanzees, gorillas, and bonobos).

Great Apes (specifically chimpanzees and gorillas) and forest elephants are facing increasing threats within the Dzanga Sangha Protected Areas (DSPA) in the CAR segment of the TNS (TNS-CAR) (N'Goran et al., 2014, 2017). According to consultations conducted by the International Union for the Conservation of Nature (IUCN) and the United Nations Educational, Scientific and Cultural Organization (UNESCO), these large mammal species are losing the suitable habitats required for their survival, and therefore their conservation requires urgent management intervention (UNESCO, 2015, 2017, 2019; UNESCO/IUCN, 2016). WWF and partners require reliable evidence in order to identify priority species habitats, and document areas of suitable habitat and changes in habitat suitability for establishing long-term conservation plans and meeting the objectives of the DSPA conservation initiatives, yet this information is largely absent in the scientific literature. Moreover, eco-guard patrols have been adopted as a key measure to protect the DSPA

(N'Goran et al., 2016; Tranquilli et al., 2014; UNESCO, 2015, 2017, 2019), yet, to our knowledge no study has evaluated the potential impacts of these patrol activities on species distribution and survival. In addition, the impacts of human pressure (e.g., hunting, road constructions and deforestation), climatic variability, topography and landscape fragmentation have not been fully investigated within these PAs. These factors have been identified as having important potential impacts on species distribution and survival across several geographic ranges (Junker et al., 2012; Strindberg et al., 2018; Yuh et al., 2019). Mapping the spatial variability and short and long-term changes in ape and elephant habitat suitability under the combined influence of these factors can help identify priority habitats as well as document the decline of suitable habitats within the DSPA. Quantifying the effects of these factors on species distribution will provide information on the key factors and priority areas for management interventions within this landscape.

Several studies have used nest count data, which indicate the distribution of great ape species sleeping sites, to map the spatial variability in suitable great ape habitats across their range (Ginath Yuh et al., 2020; Heinicke et al., 2019; Junker et al., 2012; Strindberg et al., 2018). However, other types of data associated with the occurrence of great apes (e.g., direct sightings, dung, hair, vocalization, feeding signs, and footprints) could be used to measure presence of great apes and habitat suitability and contribute to species-specific habitat suitability mapping. Such occurrence signs have been used in quantifying species-specific population abundance and declines (Arandjelovic et al., 2011; Devos et al., 2008). Thus, comparing species suitability mapping between nest count data and a combination of nesting data and other signs provides a more detailed understanding of species distribution, which is necessary to support conservation activities.

In this study, we aim to: (1) produce spatially explicit species distribution models to map the spatial variability and changes in ape and elephant habitat suitability within the

DSPA between two survey years (2015 and 2020), using spatial datasets of eco-guard patrol activities, habitat fragmentation, land cover, human pressure, topography, and climatic variability, as model predictors; (2) identify priority habitats, as well as key factors affecting species distribution; (3) quantify priority habitat loss/gain, and evaluate the contributions of key factors to these changes; (4) compare species suitability mapping between nest count data and a combination of nesting data and other signs; and (5) evaluate the relationship between suitable habitats among species, and identify overlapping priority habitats for conservation.

In the context of these objectives, we investigate the following hypotheses: (1) that predicting ape habitat suitability with nest count data, as compared to a combination of nesting data and other signs (e.g., direct sightings, dung, hair, vocalization, feeding signs, and footprints) will produce similar spatial estimates of habitat suitability; (2) that the suitable habitat areas for great apes and elephants have declined spatially within the DSPA over the five-year study period as a result of increased human pressure, with larger declines occurring outside existing National Parks (NPs); and (3) that species habitat areas overlap spatially within the entire DSPA, with large proportions of overlapping priority habitats predicted to occur within NPs, and in areas with increased presence of eco-guard patrols.

Materials and Methods

The study area

Our study area covers the Dzanga Sangha Protected Areas (DSPA) located in the Central African Republic (CAR) segment of the Sangha Tri-National (TNS) landscape (Figure 1). The TNS is a transboundary landscape between the Republic of Congo, CAR and Cameroon. It comprises three National Parks (NP), including the Lobéké NP in Cameroon, the Dzanga-Ndoki NP in CAR, and the Nouabalé-Ndoki NP in Republic of Congo (Figure 1b).

The DSPA (Figure 1a) encompasses a Special Reserve of dense forests that include the Community Hunting Zone (ZCC), Kambi, Plateau Bilolo, Libwe, and Yobe Lidjombo sectors; and the Dzanga-Ndoki NP comprises the Dzanga and Ndoki sectors. All sectors were defined for conservation purposes under the COMIFAC agreement. The Special Reserve and the Dzanga-Ndoki NP were officially established in 1990 as part of the WWF conservation program. The term DSPA was officially defined in the year 2007, and as part of the TNS landscape, it was listed as a UNESCO World Heritage Site in 2012. Since 2019, there has been a co-management agreement in place between WWF and the CAR government (see https://dzanga-sangha.org/facts-infos/). Two logging concessions for SINFOCAM (Société Industrielle des Forêts Centrafricaines et d'Aménagement) and STBC (Société de Transformation de Bois en Afrique Central) companies were created in 2014; the STBC concession overlaps the Plateau Bilolo and Kambi sectors while the SINFOCAM concession overlaps the Libwe and Yobe Lidjombo sectors; exploitation activities were stopped in 2019.

The DSPA covers a total area of approximately 4596 km^2 (Table 1). The landscape is surrounded by four categories of habitats: dense and semi deciduous evergreen forests, swampy forests, open forests, and wetlands (Balinga et al., 2006). Prominent fauna species

supported by these habitats include the central chimpanzee (*Pan troglodytes troglodytes*), the western lowland gorilla (*Gorilla gorilla gorilla*), the forest elephant (*Loxodanta cyclotis*), the forest buffalo (*Syncerus caffer nanus*), and the bongo, an African forest antelope (*Tragelaphus euryceros*) (Blom, 2000). Prominent floral taxa include bamboo, Araceae, Araliaceae, Flacourtiaceae, and Marantaceae. Annual rainfall ranges from 1500 to 2000 mm, annual mean temperatures range from 24 to 28 °C, and altitudes range from 340 to 700 m above sea level (Shutt, 2014).

A number of ongoing human activities represent direct and indirect threats for wildlife species and their habitats in the DSPA. Prominent examples include poaching, which arises from both international demand for ivory and local subsistence needs (UNESCO, 2019), and the indirect effects of local armed conflicts such as increased availability of weapons and more human presence in the forests and use of forest resources and wild game for food (State Parties of Cameroon, 2019). Other examples include the expansion of roads for logging, illegal mining, and small-scale subsistence agriculture around villages.

Table 1. Protected Areas within the study area

	Protected Areas (Pas)	Total surface area (km^2)
National Parks	Ndoki	750.3
	Dzangha	495.2
DSPA Special Reserves	ZCC	584.3
	Libwe	683.7
	Yobe-Lidjombo	752.4
	Kambi	397.3
	Plateau Bilolo	933.2
Total		4596.4

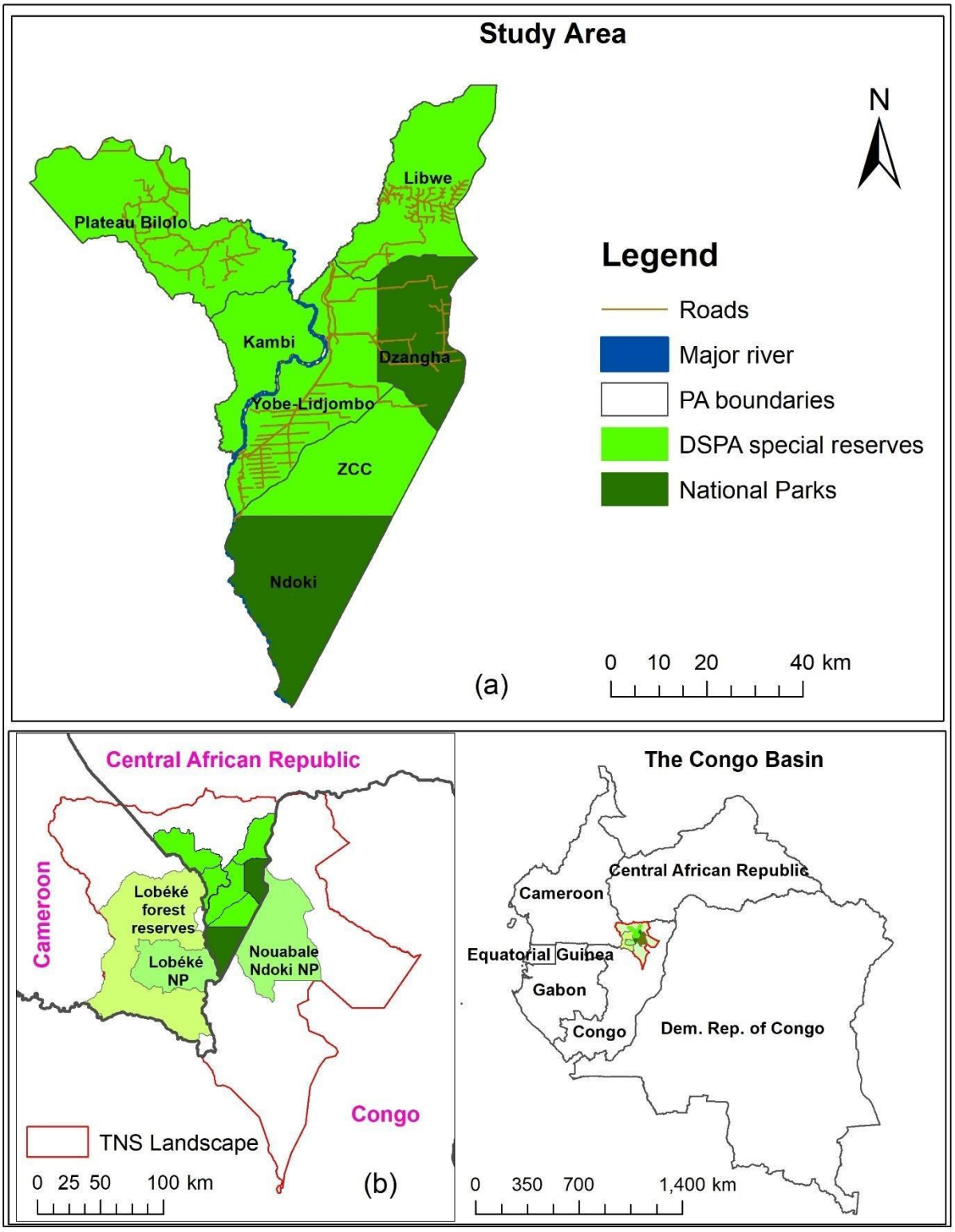

Figure 1. Map of the study area. Map shows (a) protected areas of the Sangha Tri-National (TNS) landscape, and (b) location of the DSPA within the CAR segment of the TNS.

Acquisition and preparation of great ape and elephant data

We obtained observations of great ape (chimpanzee and gorilla) and elephant distributions within the DSPA from the 2015–2020 wildlife survey data (Figure 2). Data were collected by a team of WWF biomonitoring experts, using distance sampling methods with line transects (Buckland et al., 2001; Thomas et al., 2010) and following the IUCN best practice guidelines for the survey of great apes (Kühl et al., 2008). For the great apes, observations included footprints, nests, dung, feeding signs, vocalizations and direct sightings; for elephants, observations included footprints, carcasses, dung, mud stamps on trees, tracks, audible vocalization and direct sightings (Figure 2).

Field sampling was conducted by a team of 4 members; it consisted of detecting all signs for the presence of each species and recording them with associated GPS coordinates when walking transects at 0.5 km/h in the DSPA. The sampling design consisted of 172 transects of 2 km each in 2015, with 319 km completed, and 184 transects of 2 km each in 2020, with 335 km completed. In order to avoid double counting in all transects surveyed in both years of study, transects were separated from one another by a minimum distance of 5 km.

During data collection, special emphasis was placed on chimpanzee and gorilla nests, as nesting data have been successfully used to estimate species population size and abundance (Kühl et al., 2008; Moore & Vigilant, 2014; Pruetz et al., 2002; Strindberg et al., 2018), as well as to map species habitat suitability across their ranges (Fitzgerald et al., 2018; Ginath Yuh et al., 2020; Junker et al., 2012; Plumptre, 2010; Strindberg et al., 2018).

For each survey year (2015 and 2020), we merged all surveyed points in ArcGIS, created 1 km × 1 km sampling grids within the entire study area and spatially rarefied the survey points (presence data) at minimum distances of 10 m between each point in order to

eliminate duplicated points, avoid over-clustering and reduce sampling bias (Araújo et al., 2004; Barratt et al., 2021; Ginath Yuh et al., 2020; Merow et al., 2013, 2014). From the merged data for each survey year, we separately extracted all chimpanzee observations (N = 182 for the year 2015 and N = 157 for the year 2020) from gorilla and elephant observations (N = 551 and N = 2829 for the year 2015; N = 597 and N = 2547 for the year 2020 respectively). For chimpanzee and gorilla observations, we performed two types of analysis for each survey year by categorizing datasets into nest data alone (N = 165 for chimpanzees and N = 234 for gorillas for the year 2015; N = 121 and N = 200 for the year 2020, model 1) and the full data (nest + other observations, including dung, feeding signs, audible vocalization and direct sightings) (N = 182 for chimpanzees and N = 551 for gorillas for the year 2015; N = 157 and N = 597 for the year 2020, model 2). Our objective was to compare spatial variability and changes in ape habitat suitability between the two models as basis for improving ape species distribution mapping, considering that most studies have focused on nest data alone for mapping ape species distribution (Fitzgerald et al., 2018; Ginath Yuh et al., 2020; Heinicke et al., 2019; Junker et al., 2012; Moore & Vigilant, 2014; Strindberg et al., 2018). For elephants, we carried out a single analysis for each year with all observation data (footprints, carcasses, dung, mud stamps on trees, tracks and vocalizations).

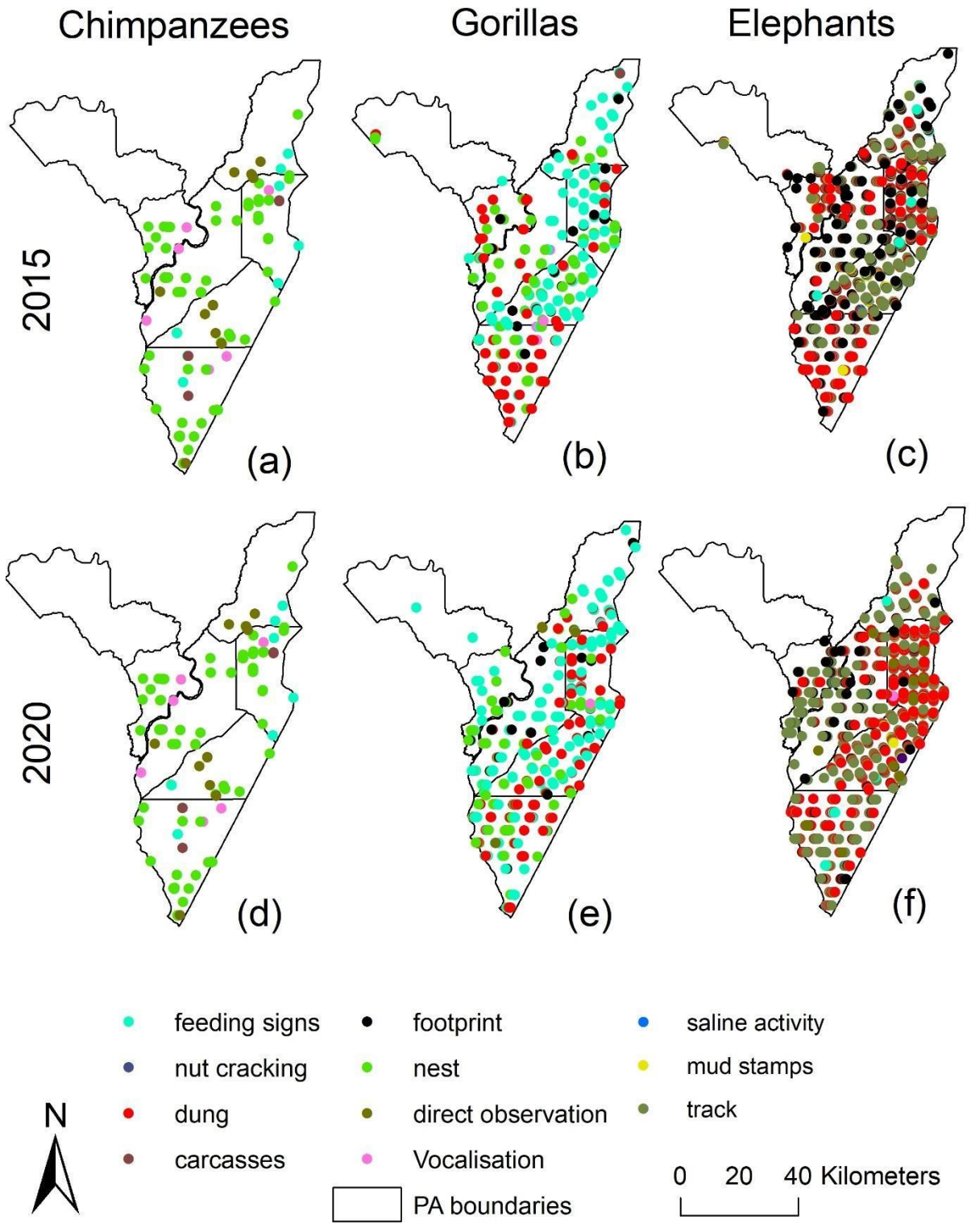

Figure 2. Ape and elephant occurrence points: a – c represent chimpanzee, gorilla and elephant observation points for the year 2015 while d – e represent chimpanzee, gorilla and elephant observation points for the year 2020.

Acquisition and preparation of predictor variables

To attain our research objectives, we acquired data on six categories of predictor variables, including human pressure data, eco-guard patrols, climatic and topographic data, land cover and forest disturbance datasets (Table S3).

(a) Human pressure data

Datasets on hunting signs (e.g. arms, gunshots heard, presence of hunters, hunting trails, empty cartridges, hunting camps, wildlife traps, and dead animals), logging, mining and farming signs (e.g. cleared areas, croplands, presence of farmers, miners and loggers, logging roads, related camps, and logging and mining sites), presence of humans through direct observations, and presence of villages and roads were recorded in the field during the 2015 and 2020 wildlife surveys, and categorized into human pressure data. Table S4 presents the encounter rates of human activity signs in the DSPA.

Density estimates of large mammals through line transect sampling have revealed that mammals inhabiting the DSPA are under threat as a result of hunting, forest degradation and deforestation caused by artisanal mining, logging and farming (N'Goran et al., 2016, 2017). Moreover, several villages and temporary camps in the DSPA are home to thousands of people, including hunters, farmers, loggers and miners (Figure S3). To select the best human pressure indices and reduce the effects of redundancy in our models, we conducted a principal component analysis (PCA) and used the first principal component (PCA1 – which explained the highest percentage of overall variance (79 %)) to select variables that had the highest percent performance as measures of human pressure. Because human presence, hunting, presence of villages and roads explained more than 50 % of the total variance (59 %, 52 %, 54 % and 55 % respectively), we combined these variables into a single composite indicator to form our human pressure predictor variable (Figure 3b).

The density of large mammals has been reported to be strongly related to the distance from roads and villages, as a result of the effect of roads and villages on hunting activities (Blom et al., 2005). To measure how proximity to roads, villages and camps could influence ape and elephant distribution within the DSPA, we created three additional variables associated with human pressure, including distance from each study area pixel to roads, camps and villages. We tested for correlations between these variables using a Pearson's correlation test (which tests for collinearity between variables), as well as a variance inflation factor (VIF – which tests for both collinearity and multi-collinearity between variables), and as such, eliminated distance to villages due to a strong correlation with distance to roads, and a higher VIF than distance to roads (Table S5a).

(b) Eco-guard patrols

Over the last 10 years, eco-guard patrols, herewith defined as anti-poaching patrolling activities or nonviolent paramilitary operations aimed at deterring and preventing wildlife poaching, have been successfully implemented within the DSPA to try to better protect endangered large mammals and their habitats (N'Goran et al., 2016, 2017). To evaluate the impacts of these efforts on large mammal species distribution, we obtained eco-guards patrol data from the WWF Spatial Monitoring and Reporting Tool (SMART). The database contains data collected in the field by 21 patrol teams from November 2017 to December 2020 (Table S6a and b), with 30 % of all patrols conducted on foot, 35 % conducted with speedboats, and another 35 % conducted with vehicles. We used patrol points representing the presence of guards to create a density map of eco-guard patrol efforts (Figure 3a).

(c) Land cover, fragmentation and forest disturbance variables

Land cover variables such as dense or primary forests, secondary forests, swampy forests and herbaceous vegetation provide suitable environmental conditions for the distribution of large mammals (Ginath Yuh et al., 2020; Junker et al., 2012; Strindberg et al., 2018). More than 90 % of the DSPA is covered with dense and closed forest habitats (Figure S2), and being part of the TNS, dense forest habitats may be important predictors of suitable mammal habitats, as has been previously reported with the great apes of the Lobéké National Park and its surrounding management units (Ginath Yuh et al., 2020). We thus obtained data on closed forests for the years 2015 and 2019 from the Copernicus Global Land Service (https://land.copernicus.eu/global/products/) (Buchhorn et al., 2020). Because herbaceous and swampy vegetation types are reported to be highly suitable for gorilla distribution, especially in other protected areas of the TNS (Yuh et al., 2019, Ginath Yuh et al., 2020), we derived a second land cover variable (herbaceous wetlands) as a measure of swampy vegetation, however, we later eliminated this variable from our analysis due to its relatively low spatial extent (i.e., has a total land cover area of less than 3 km2). We also used the presence of rivers as a third land cover variable as studies by Ayres & Clutton-Brock, (1992) have shown that primate distribution is highly influenced by the presence of rivers. To measure the influence of rivers, we created a distance to rivers variable following the approach of N'Goran et al., (2012). Because distance to rivers strongly correlated with road distance, as well as had a similar VIF to distance to roads (Table S5a), we performed a principal component analysis and retained distance to roads for our modeling analysis, as it explained 56 % of the variance as compared to 44 % for distance to rivers.

Disturbed forests have been found to negatively impact the distribution of great apes in some parts of the TNS (e.g., within the Lobéké protected areas) (Yuh et al., 2019), and evidence from this study shows that forest disturbance could be an important predictor of

large mammal distribution within the DSPA. To obtain a measure of forest disturbance, we used a combination of habitat fragmentation and open forest (habitat areas with very few trees, mostly comprising a low overstory density) data from the 2015–2019 Copernicus Global Land Service land cover datasets. Fragmentation indices, including isolated forest patches, perforated forests and edge densities were calculated from the Copernicus land cover datasets using the ArcGIS landscape fragmentation tool, following the approach of Vogt et al., (2007). Because all four patterns (open forests, perforated forests, patch isolation and edge densities) were highly correlated (Table S5a), we performed a PCA to select variables that explained high percentages of variance. We retained open forests and edge densities as they had greater than 50 % performance in our first PCA (59 % and 57 % respectively) as compared to patch isolation (47 %) and perforated forest (30 %). We therefore combined open forests and edge densities into a single composite indicator, herewith referred to as our forest disturbance predictor variable (Figure 3g).

(d) Climate and topographic data

Historical climate measurements (temperature and precipitation) have been used to predict past forest refugia for great apes across Africa (Barratt et al., 2021), suggesting that climatic variables could be important predictors of suitable large mammal habitats. Our study area has a high spatial variability in annual mean temperature and precipitation; we thus obtained climatic datasets (maximum and minimum temperatures, and annual precipitation) for the years 2015 and 2020 from the monthly TerraClimate datasets embedded in the Google Earth Climate Engine (https://app.climateengine.org/climateEngine), and generated at a 4 km spatial resolution. Because of high spatial correlation and VIF values between maximum and minimum temperatures (Table S5a), we performed a PCA and retained only maximum

temperatures for our modeling analysis, as it explained 51 % of the variance as compared to 49 % for minimum temperatures.

Topographic parameters such as slopes have also been shown to be important landscape factors influencing ape species distribution within parts of the TNS (e.g., TNS-Cameroon) (Ginath-Yuh et al., 2020). To obtain datasets on landscape topography, we used ArcGIS to extract slope and elevation data from the 2010 global multi-resolution digital terrain data created by the US Geological Survey (https://earthexplorer.usgs.gov/). Because elevations were strongly correlated with precipitation (Table S5a), we performed a PCA and retained elevation for our modeling analysis, as it explained 53 % of the variance as compared to 47 % for precipitation. Precipitation also had a higher VIF value than elevation in our correlation tests, suggesting redundancy amongst our predictor variables.

From our correlation tests and PCA, we ended up with a total of nine spatially independent predictors generated from all six predictor categories, including human pressure data, eco-guard patrols, climatic (maximum temperature), topographic (elevation and slope), land cover (dense forest) and forest disturbance datasets, and distance to roads and distance to camps (Figure 3). To ensure complete variables independence in our retained variables, we again tested for the effects of collinearity and multi-collinearity using a VIF. Our test results showed no correlations between variables (Table S5b). All datasets were projected to a similar coordinate reference system (WGS 84, UTM zone 33N), and sampled at spatial resolutions of 30 m in order to facilitate modeling in R (R Core Team, 2022).

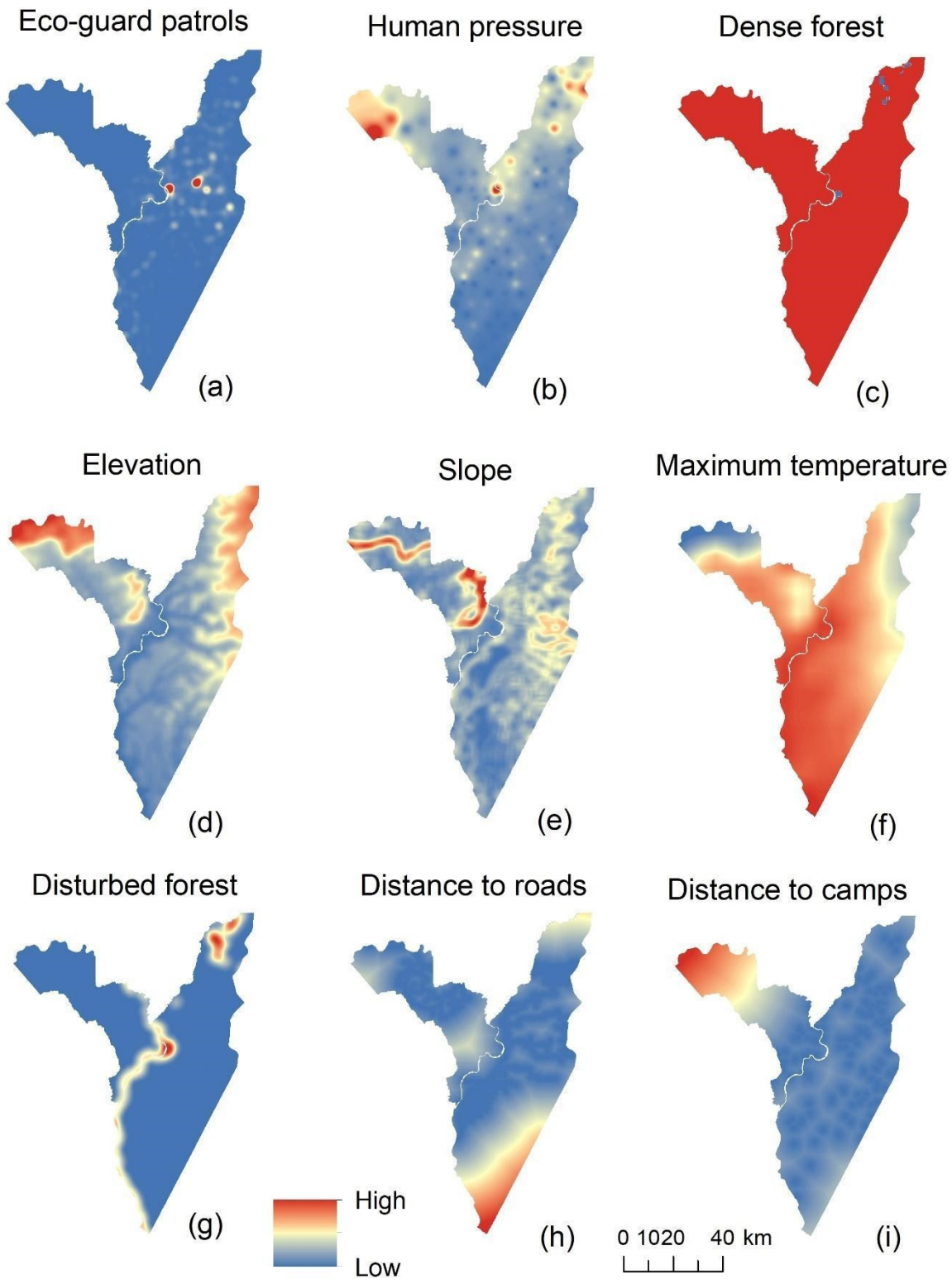

Figure 3. Sample preparation of predictor variables.

Data analysis

To map species distribution for both years of study, we modeled occurrence data for each species (chimpanzees, gorillas, and elephants) using our set of nine spatially independent predictors by cross validating an ensemble of two species distribution models (SDMs) (GAMs and GLMs) in R, following the approach of Barratt et al., (2021). We used five cross validated replicates for each of the two modeling algorithms available in the R sdm package version 1.0–46 (Naimi & Araújo, 2016). We used the ensemble approach because ensemble models have been shown to generate more accurate results than single models due to their combined power (Forester et al., 2013; Moore & Vigilant, 2014). Because not all variables are important in species distribution mapping, we applied the "getVarImp" function in the R "sdm" package to measure the permutation importance of each predictor variable, thereby identifying the most important or key factors affecting species distribution.

For chimpanzees and gorillas, we ran two separate models under two experimental treatments for each model in each year of study. The treatments involved modeling nest data alone as a response variable, and modeling a combination of nest data with other ape signs (feedings signs, vocalizations, footprints, dung and direct sightings). We conducted the models in this way in order to test if suitable habitats for nests (sleeping) differed from suitable habitats for the broad ecological niche of the species. For elephants, we conducted a single model using all observation signs as response variables for each year. This resulted in five treatments for each year of study (two for chimpanzees, two for gorillas and one for elephants). For each model, we applied 10,000 background points, and ran 500 iterations of the model, using 80 % of the datasets as training, and 20 % as validation. We validated model performances using AUC values determined by the receiver operator characteristics (ROC) (Phillips et al., 2006). In the validation process, we used an AUC threshold value of ≥ 0.7, as this threshold has been reported to be acceptable for measuring model performances in

various studies (Duan et al., 2014; Mandrekar, 2010; Swets, 1988) by providing a ≥ 70 % chance that the predicted occurrence of species will be closer to the the true observations.

Quantifying species habitat suitability and changes over time

We used the model-predicted species distribution maps to define habitat suitability classes for each species and for each year of study. Here, we define habitat suitability as a function of both ecosystem characteristics (e.g. land cover type and climate) and human factors (e.g. human pressures or eco-guard patrol activities), such that a higher model-predicted species occurrence is taken to reflect a higher habitat suitability for that species. We classified the modeled species distribution maps into four classes in ArcGIS, following the approach of Ginath Yuh et al., (2020): unsuitable (with reclassified values of 0–0.2); low suitability (with reclassified values of 0.2–0.4); moderate suitability (with reclassified values of 0.4–0.6) and high suitability (with values ≥ 0.6). We then converted the reclassified maps to vector polygons from which we calculated and compared the total area of suitable and unsuitable habitats occupied by each species in each year of study. We present the changes in habitat areas between 2015 and 2020 in units of percentage points (pp) which represent the difference in the percentage coverage of a particular habitat suitability category between the two years. We also tested the relationship between suitable species habitats using Pearson's correlation tests as well as paired sample t tests. We further used a combination of suitable and moderately suitable habitats for each species in each year of study to generate maps of priority species habitats, and finally, applied the ArcGIS intersect tool to map and quantify areas of priority habitat loss and gain (change) between both years. To evaluate the contributions of key factors to these changes, we used a stepwise Ordinary Least Squares

(OLS) linear regression approach in R to separately model changes in priority species habitats as a function of key factors contributing to species distribution.

Results

Mapping, quantifying and comparing species habitat suitability

We generated five habitat suitability (HS) maps for each year of study (two for chimpanzees, two for gorillas and one for elephants) (Figures 4 and 5) based on high model performances after repeated cross validations (See Table S7a and b for details on model performances). We found that there is strong and statistically significant relationship between ape species distribution maps (SDMs) produced with nest data alone and a combination of nest data and other signs (Figure 6), suggesting that ape SDMs can be produced with a high degree of accuracy using either nest data alone or a combination of nest data and other occurrence signs. By testing the relationship between all three species habitats, we also found that there is a significant and overlapping relationship between all three species' habitats within the study area (Fig. 7), with the most suitable and moderately suitable overlapping areas distributed spatially within the ZCC, Dzanga and Ndoki sectors (Figure S4, Table S1).

By quantifying species habitat suitability (Table 2, see Methods for suitability classification), we found that for 2015, suitable and moderately suitable chimpanzee habitats covered approximately 483 km^2 (10.5 %) and 899 km^2 (19.5 %) of the entire DSPA, while low and unsuitable areas covered about 1206 km^2 (26.1 %) and 2034.9 km^2 (44 %) respectively. For the year 2020, suitable and moderately suitable chimpanzee habitats covered 387 km^2 (8.4 %) and 814 km^2 (17.6 %) respectively, while low and unsuitable areas covered about 1783 km^2 (39 %) and 1638 km^2 (35 %) respectively. These results show that highly suitable chimpanzee habitats have declined by approximately 2.1 % point (pp) (143 km^2), accounting for approximately 20 % loss in suitable species habitats over the five years of study (2015–2020). Our results were similar for nest sites, with suitable nest sites reduced from 8.9pp in 2015–5.8pp in 2020, accounting for approximately 35 % loss in

suitable nesting habitats over the five years of study. We calculate percentage change in species habitat suitability as ((2020 area − 2015 area)/2015 area) * 100.

For gorillas, our results show that for the year 2015, suitable and moderately suitable habitats covered about 1373 km^2 (29.7 %) and 1196 km^2 (25.9 %) of the entire DSPA, while low and unsuitable areas covered 982 km^2 (21.2 %) and 1073 km^2 (23.2 %) respectively. For the year 2020, suitable habitats declined to 739 km^2 (14.6 %), suggesting a 46 % (13.7 pp) loss of suitable habitat, while moderate, low, and unsuitable habitats increased to 35.1 %, 21.6 % and 27.3 % respectively. Our results were similar for gorilla nest sites, where suitable nest habitats have declined by approximately 69.8 % (16.4 pp) over the last 5 years i.e., decreased from 1086 km^2 (23%) in 2015 to 308 km^2 (6.7 %) in 2020.

For elephants, we found that for 2015, suitable and moderately suitable habitats covered about 1895 km^2 (41 %) and 1179 km^2 (25.5 %) of the entire DSPA, while low and unsuitable areas covered 523 km^2 (11.3 %) and 1026 km^2 (22.2 %) respectively. For 2020, suitable and moderately suitable species habitats covered approximately 1205 km^2 (263.1 %) and 1414 km^2 (30.6 %) respectively, while low and unsuitable areas covered about 936 km^2 (20.3 %) and 1068 km^2 (23.1 %) respectively. These results show that suitable elephant habitats declined by 37% (15 pp) over the last 5 years.

Overall, our findings show that great apes (chimpanzees + gorillas), occupied a total of approximately 1523 km^2 (33 %) of all suitable habitat areas in the entire DSPA in 2015, with these habitat areas declining to approximately 905 km^2 (20 %) in 2020 (Figure 8, Table 3). Therefore, between 2015 and 2020, great apes have lost about 13 pp of the entire suitable habitat required for their survival. Our results also show that all three mammal species together occupied about 2424 km^2 (52 %) of all suitable habitat in the year 2015, with these

habitat areas declining to about 1682 km^2 (36 %) in 2020 (Figure 8, Table 3), suggesting a 16 pp loss over the study period.

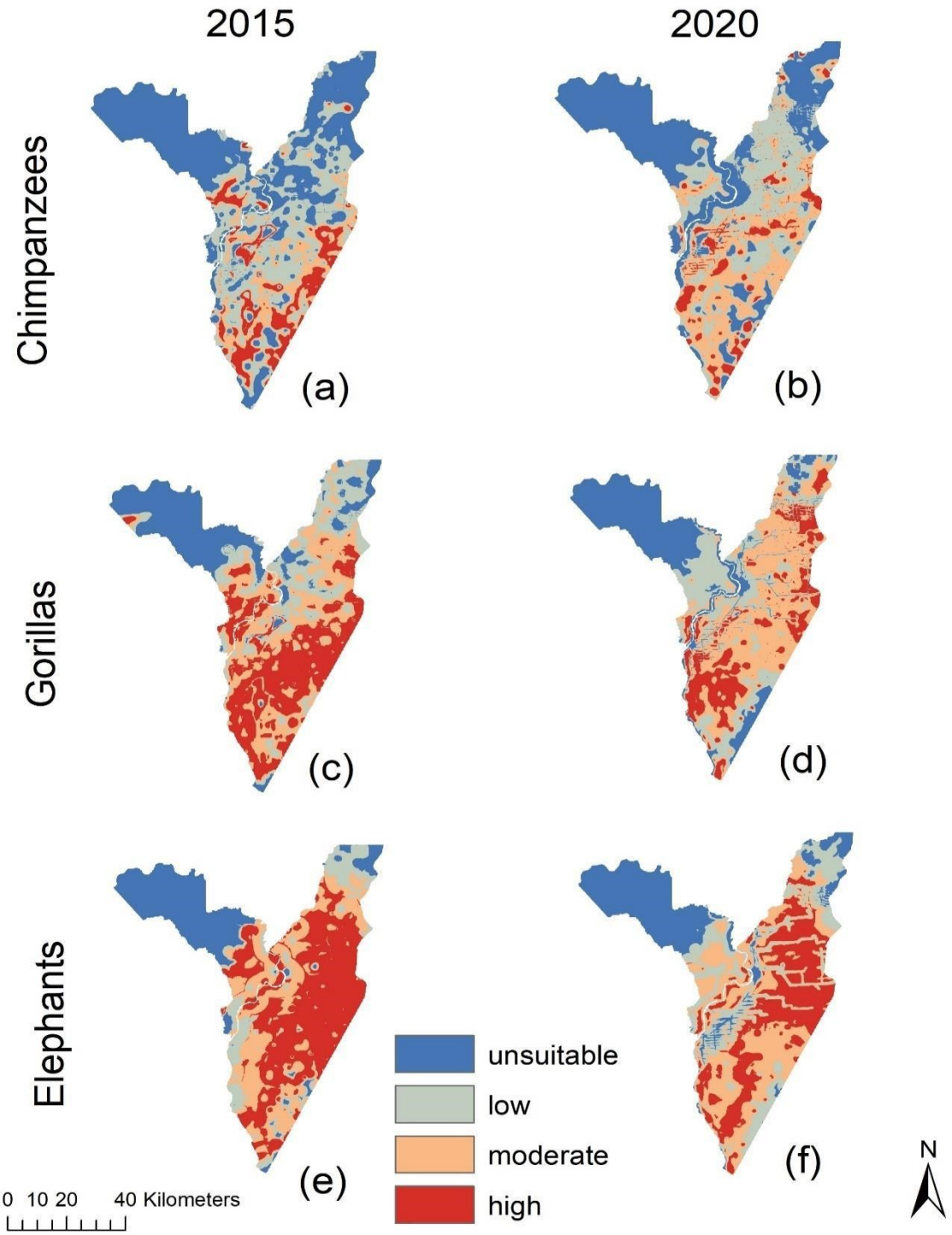

Figure 4. Comparison of ape and elephant habitat suitability for the DSPA between 2015 and 2020, using all observational signs of species presence.

.

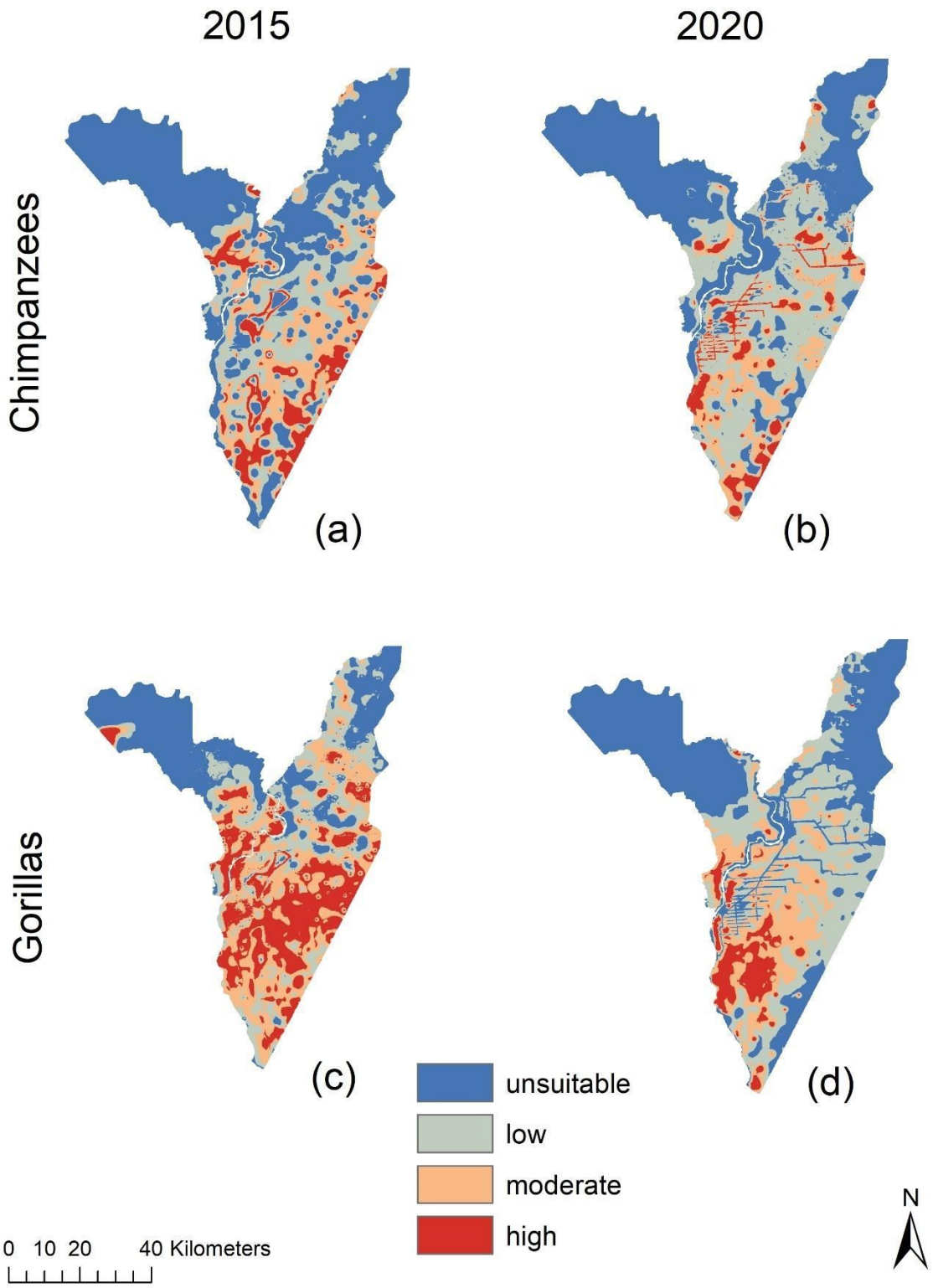

Figure 5. Comparison of suitable chimpanzee and gorilla habitats within the DSPA, between 2015 and 2020, using only nest presence data.

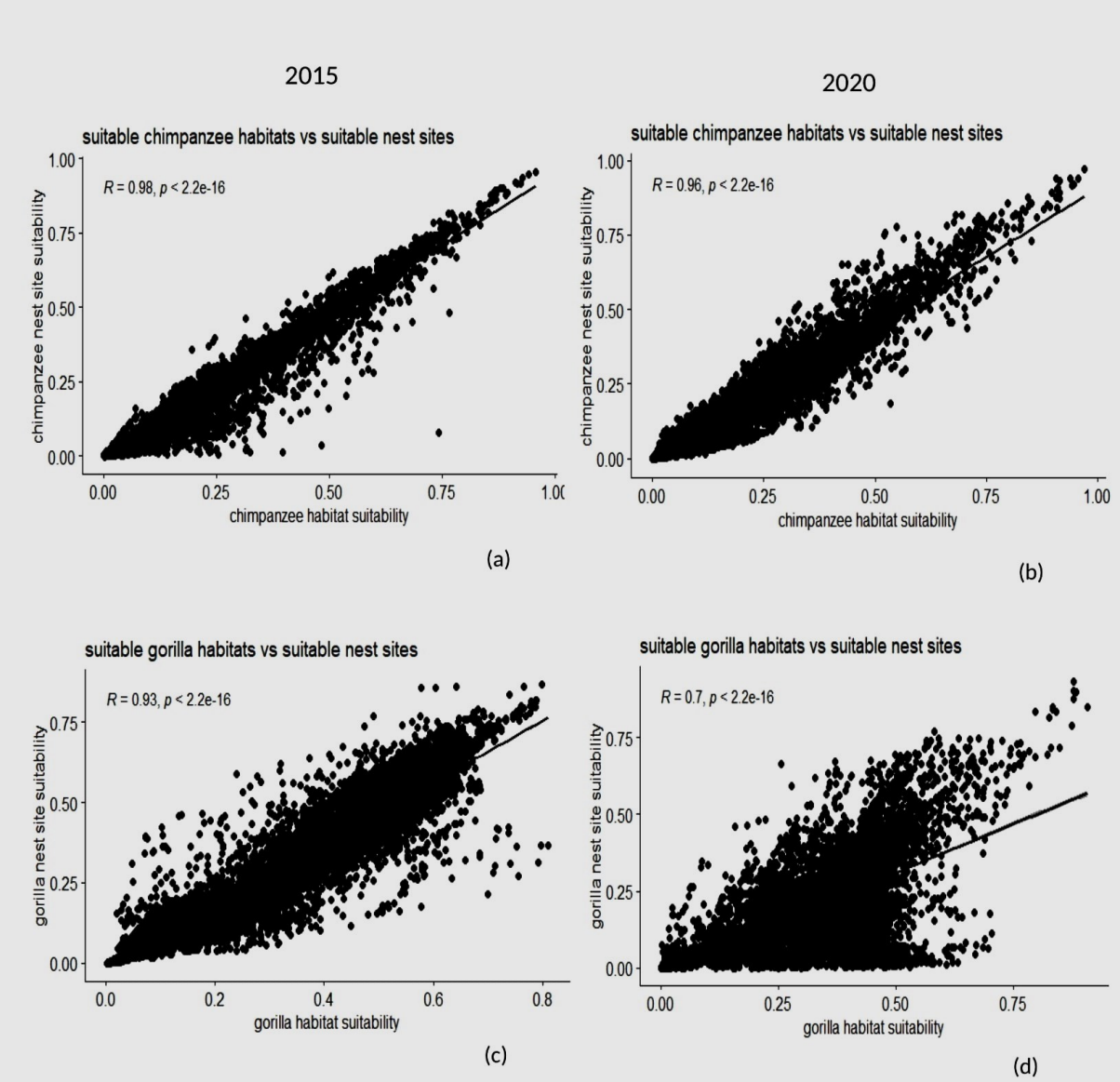

Figure 6. Relationship between ape habitats and nest site suitability within the DSPA for 2015 and 2020.

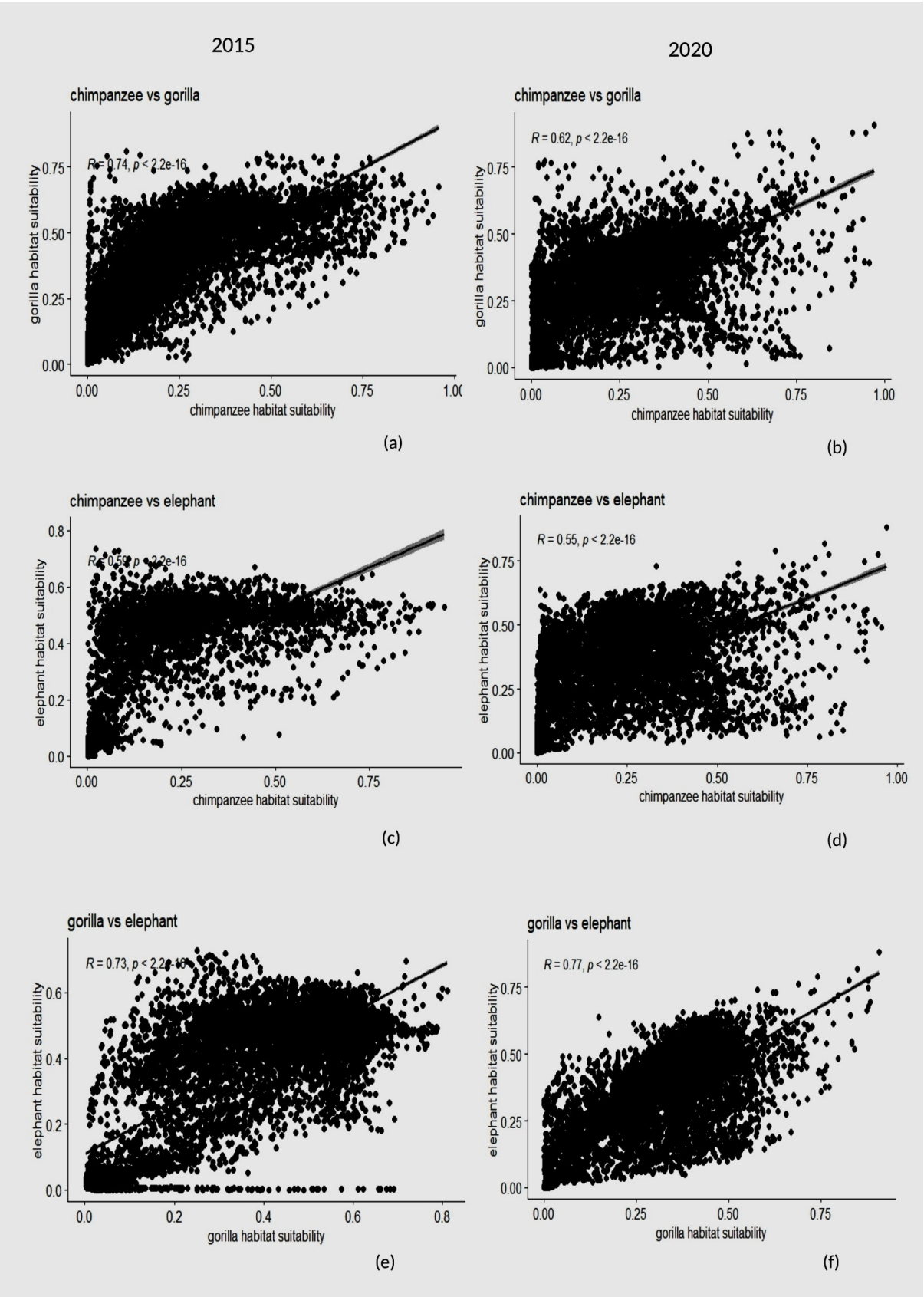

Figure 7. Relationship between ape and elephant habitats within the DSPA for 2015 and 2020.

Table 2. Quantified changes in ape and elephant habitat suitability between 2015 and 2020

Chimpanzees												
	Year 2015				Year 2020				Change (2020 – 2015)			
	All habitats		Nesting habitats		All habitats		Nesting habitats		All habitats		Nesting habitats	
Suitability	Area (km^2)	% Area	Area (km^2)	% Area	Area (km^2)	% Area	Area (km^2)	% Area	Area (km^2)	% Area	Area (km^2)	% Area
Unsuitable	2034.9	44	2313.2	50	1638.3	40	2063.9	44.6	-396.6	-4	-249.3	-5.4
Low	1206	26.1	1061.8	23	1783.5	38.6	1630	35.3	577.5	12.5	568.2	10.7
Moderate	899.3	19.5	838.4	18.1	814.5	17.6	621.5	13.4	-84.8	-1.9	-216.9	-4.7
High	483.4	10.5	410.3	8.9	387.4	8.4	266.9	5.8	-96	-2.1	-143.4	-3.1
Gorillas												
Unsuitable	1072.9	23.2	1357.7	29.4	1263.3	27.3	2053.6	44.4	190.4	4.1	566.3	12.2
Low	981.8	21.2	959.5	20.8	997	21.6	1392.7	30.1	15.2	0.4	433.2	9.3
Moderate	1196.1	25.9	1220.2	26.4	1624.2	35.1	850.3	18.4	428.1	9.2	-369.9	-8
High	1372.9	29.7	1086.3	23.5	739.2	16	308.3	6.7	-633.7	-13.7	-759.1	-16.4
Elephants												
Unsuitable	1025.9	22.2			1068.4	23.1			42.5	0.9		
Low	523.3	11.3			936.4	20.3			413.1	9		
Moderate	1179.4	25.5			1413.9	30.6			234.5	5.1		
High	1895.2	41			1205.1	26.1			-690.1	-14.9		

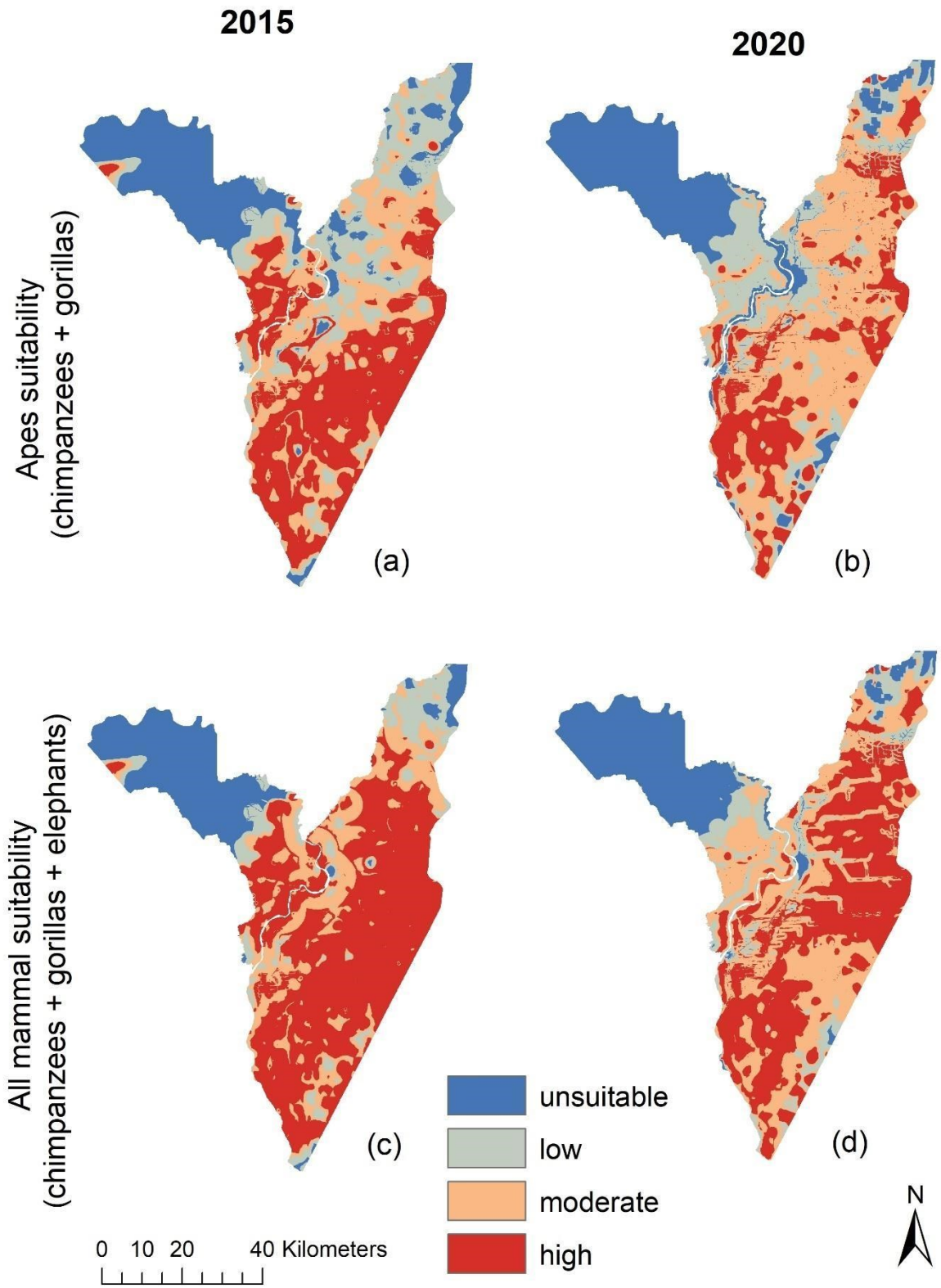

Figure 8. Combined mammal habitat suitability for 2015 and 2020 observation years: a and b represent the combined suitability of ape habitats (chimpanzees + gorillas) for each respective year of study, while c and d represent the combined habitat suitability for all three mammal species (chimpanzees + gorillas + elephants) for each respective year of study.

Table 3. Quantified changes in combined mammal and ape habitat suitability between 2015 and 2020

Great Apes (Chimpanzees + Gorillas)						
	Year 2015		**Year 2020**		**Change (2020 – 2015)**	
Suitability	Area (km^2)	% Area	Area (km^2)	% Area	Area (km^2)	% Area
Unsuitable	1018.5	22	1131.7	24.5	113.2	2.5
Low	975.1	21.1	836.1	18.1	-139	-3
Moderate	1107.6	24	1751.4	37.9	643.8	13.9
High	1523.3	32.9	905.5	19.6	-617.8	-13.3
All mammals Gchimpanzees + Gorillas + Elephants)						
Unsuitable	854.4	18.5	940.1	20.3	85.7	1.8
Low	442	9.6	511.5	11.1	69.5	1.5
Moderate	904.3	19.6	1490.1	32.2	585	12.6
High	2424.8	52.4	1682.3	36.4	-742.5	-16

Contributions of predictor variables to species habitat suitability

By predicting variable importance in our ensemble models (Table 4), our findings showed that the most important factors that predicted chimpanzee habitat suitability in 2015 were the extent of human pressure (31.3 %), the presence of eco-guard patrols (26.1 %), slopes (19.5 %), and distance to roads (11.2 %). For 2020, the most important predictors were human pressure (40.5 %), eco-guard patrols (39.5 %), and distance to roads (12.7 %). For gorillas, the most important factors that predicted species habitat suitability for both 2015 and 2020 were eco-guard patrols (42.4 % and 22.3 % respectively) and human pressure (24.5 % and 36.8 % respectively). With elephants, for 2015, eco-guard patrols were the most important predictor (73.3 %) while for 2020, the most important factors were eco-guard patrols (45.4 %), human pressure (20.2 %) and distance to roads (17.2 %). Eco-guard patrols and human pressures were therefore key predictors of habitat suitability for all three species, as they were the only variables that contributed significantly to predicting suitable species' habitats in all five treatments conducted for both years of study. Because distance to roads also performed well for chimpanzees (in both years of study), and for elephants for 2020, we also considered distance to roads as a key predictor of suitable habitat.

Table 4. Contributions of each predictor variable in predicting ape and elephant habitat suitability.

Variables	% Contribution for chimpanzees		% Contribution for gorillas		% Contribution for elephants		Directionality
	2015	2020	2015	2020	2015	2020	
Eco-guard patrols	26.1	35.9	42.4	22.3	73.3	45.4	Positive: higher patrol presence increased suitability for all three species
Human pressure	31.3	40.5	24.5	36.8	3.5	20.2	Negative: Increased human pressures decreased suitability for all three species
Distance to roads	11.2	12.7	5.3	10.8	4.4	17.2	Positive: Increased road distance increased suitability for all three species
slope	19.5	2.9	9.4	1.1	1.8	1.4	Positive: steeper slopes increased suitability for all three mammal species
Maximum temperature	2.4	0.2	5.4	4.7	1.3	3.3	Positive: high temperatures increased suitability for all three mammal species
Distance to camps	3.3	2	6.4	6.3	1.9	3.5	Positive: Increased camp distance increased suitability for all three species
Dense forest	1.3	0.8	0.2	14.6	0.7	5.9	Positive: Increased forest density increased suitability for all three species
Disturbed forest	1.7	3.4	3.1	2.6	8.8	2.3	Negative: Increased forest disturbance decreased suitability for all three species
Elevation	3.1	1.6	3.3	0.9	4.3	0.8	Negative: higher elevations decreased suitability for all three species

Identifying priority species habitats and quantifying the effects of key predictors

Based on our species' habitat suitability maps, we argued that all moderate and high suitability habitats should be considered as priority areas for long-term species sustainability (Figure 9) and report results for each protected area within the DSPA (Table 5 – 7). We found that the largest distribution of priority habitats for elephants for 2015 fell within the community hunting zones – ZCC (99.8 % of this sector), followed by the Dzanga sector

(98.9 % of this area), and the Yobe-Lidjombo and Ndoki sectors (85.3 % and 80 % respectively). These priority habitats have declined to 91.6 % for the Dzanga sector, accounting for a 7.3 pp (7.5 %) habitat loss; 97.8 % for the ZCC sector, accounting for a 2 pp (2 %) habitat loss; 59.6 % for the Yobe-Lidjombo sector, accounting for a 25.7 pp (30 %) habitat loss; and 79.8 % for the Ndoki sector, accounting for approximately 0.2 pp (0.2 %) habitat loss.

For chimpanzees, the largest distribution of priority habitats for 2015 fell within the ZCC and Ndoki sectors (65.3 % and 63.1 % of these sectors respectively) followed by the Kambi (40.5 %), Dzanga (36.6 %) and Yobe-Lidjombo sector (20.3 %). These priority habitats have declined to 53 % for the Ndoki NP in 2020, accounting for a 10 pp (15.8 %) priority habitat loss; 52.5 % for the ZCC sector, accounting for a 12.8 pp (19.6 %) priority habitat loss; and 8.9 % for the Kambi sector, accounting for a 31.6 pp (78 %) priority habitat loss. For the Yobe-Lidjombo sector, species priority habitats have increased to 29.1 %, accounting for a 9.2 pp (45 %) habitat gain.

For gorillas, the largest distribution of priority habitats for 2015 fell within the ZCC sector (99.4 % of this area) followed by the Ndoki NP (89.6 %), Dzanga NP (80.4 %), Kambi (75.4 %) and Yobe-Lidjombo sector (56.4 %). These priority habitats declined to 91.8 % for the ZCC in the year 2020, accounting for a 7.6 pp (7.6%) priority habitat loss; 57.2 % for the Ndoki NP, accounting for a 32.4 pp (36%) priority habitat loss; and 15.8 % for the Kambi sector, accounting for a 59.6 pp (79 %) priority habitat loss. For the Dzanga and Yobe-Lidjombo sectors, species priority habitats have increased to 91.6 % and 61.3 % respectively, accounting for a 11.2 pp (13.9 %) habitat gain for the Dzanga sector, and 4.9 pp (8.7 %) habitat gain for the Yobe-Lidjombo sector.

Following this analysis, we found that over 276 km^2, 547 km^2 and 413 km^2 of all chimpanzee, gorilla and elephant priority habitats have been converted to non-priority areas over the last five years (Figure 10 and Table 5 – 7), with declining areas highly and significantly influenced by increase human pressures ($R^2 = 0.54$, $p < 0.05$ for chimpanzees; $R^2 = 0.58$, $p < 0.05$ for gorillas; and $R^2 = 0.47$, $p < 0.05$ for elephants) (Tables 8 and 9). These findings mostly correspond to the Ndoki, Kambi and ZCC special reserves (Table 5 – 7) where there have been a relatively low number of eco-guard patrol activities implemented within these sectors over the last five years (Tables S6a and b). We also show that over 92 km^2 and 343 km^2 of priority chimpanzee and gorilla habitats have been gained over the last five years (Figure 10 and Table 5 – 7), with habitat stability and gained areas highly and significantly influenced by increased eco-guard patrols ($R^2 = 0.44$, $p < 0.05$ for chimpanzees; and $R^2 = 0.75$, $p < 0.05$ for gorillas) (Tables 8 and 9). For elephants however, the role of eco-guards only contributed ~ 14 % to species priority habitat stability and gains ($R^2 = 0.14$, $p = 0.008$). These findings primarily correspond to the Dzanga, Libwe and Yobe-Lidjombo sectors where cumulative eco-guard patrol efforts were relatively high over the last five years (Tables S6a and b). Our findings also show that distance to roads also contributed positively towards all three species' priority habitat gain ($R^2 = 0.14$, $p < 0.05$ for chimpanzees; $R^2 = 0.41$, $p < 0.05$ for gorillas; and $R^2 = 0.15$, $p < 0.05$ for elephants), with species finding much suitable habitats in roadless areas.

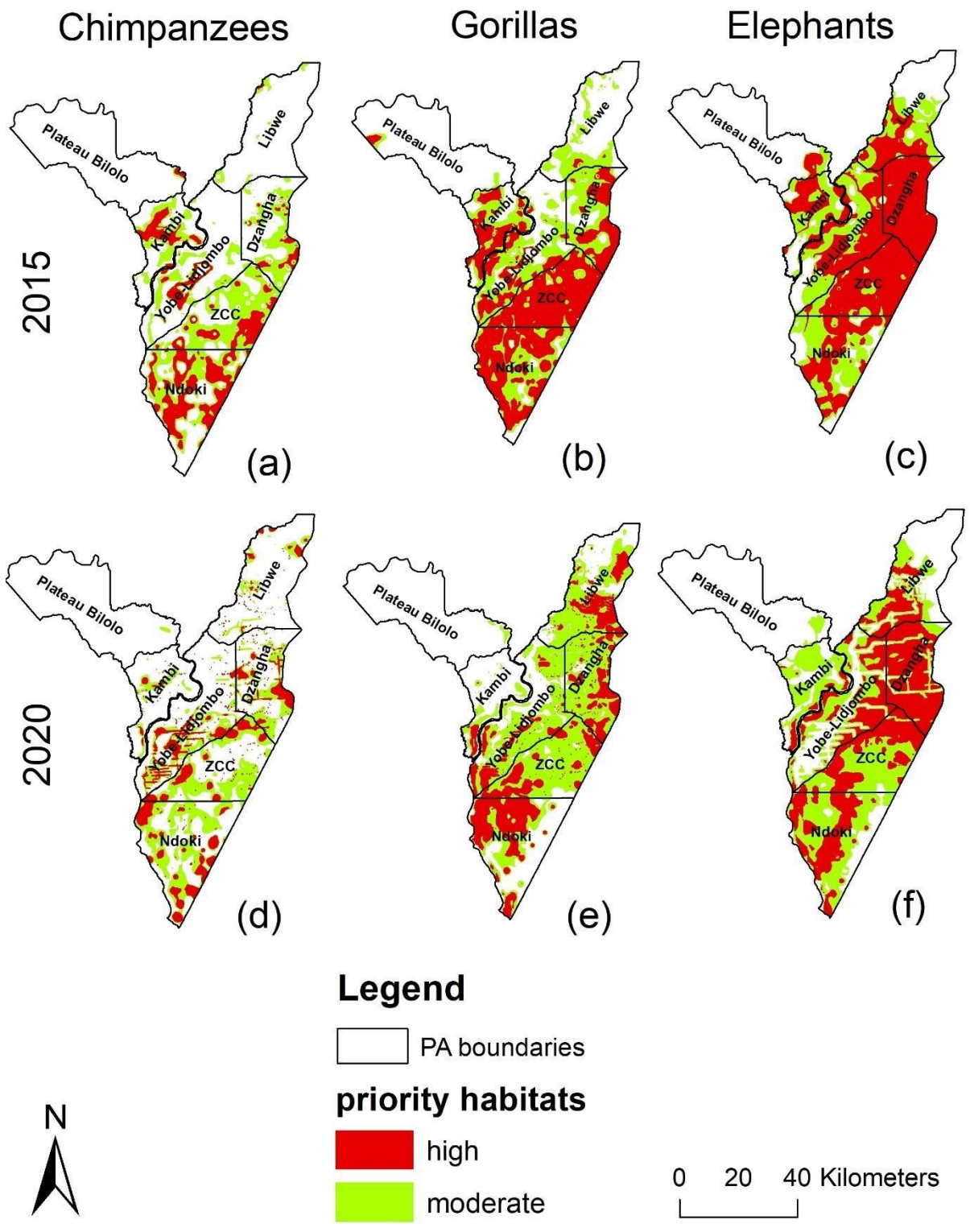

Figure 9. Comparison in priority ape and elephant habitats between 2015 and 2020

Table 5. Proportion of priority and non-priority habitats for chimpanzees within the DSPA

National Park												
	Year 2015				**Year 2020**				**Change (Year 2020 - Year 2015)**			
	Habitat category				*Habitat category*				*Habitat category*			
Sectors	*priority*		*Non-priority*		*priority*		*Non-priority*		*Priority*		*Non-priority*	
	Area (km^2)	% Area	Area (km^2)	% Area	Area (km^2)	% Area	Area (km^2)	% Area	Area (km^2)	% Area	Area (km^2)	% Area
Dzanga	181.1	36.6	314.4	63.4	183.8	37	313.4	63	2.7	0.4	-63	-2.7
Ndoki	473.6	63.1	276.7	36.9	400	53.1	354	46.9	-73.6	-10	73.6	10
Special Reserve												
Plateau Bilolo	8.6	0.9	924.6	99.1	4.1	0.4	931.3	99.6	-4.5	-0.5	4.5	0.5
Libwe	22.2	3.2	661.5	96.8	48.7	7.1	637.4	92.9	26.5	3.9	-26.5	-3.9
Kambi	161.1	40.5	236.2	59.5	35.6	8.9	363.3	91.1	-125.5	-31.6	125.5	31.6
Yobe-Lidjobo	152.7	20.3	599.7	79.7	215.7	29.1	541.7	70.9	63	9.2	-63	-9.2
ZCC	381.5	65.3	202.8	34.7	308.5	52.5	278.9	47.5	-73	-12.8	73	12.8

Table 6. Proportion of priority and non-priority habitats for gorillas within the DSPA

National Park												
	Year 2015				**Year 2020**				**Change (Year 2020 - Year 2015)**			
	Habitat category				*Habitat category*				*Habitat category*			
Sectors	*priority*		*Non-priority*		*priority*		*Non-priority*		*Priority*		*Non-priority*	
	Area (km^2)	% Area	Area (km^2)	% Area	Area (km^2)	% Area	Area (km^2)	% Area	Area (km^2)	% Area	Area (km^2)	% Area
Dzanga	398.1	80.4	97.1	19.6	453.6	91.6	42.3	8.4	55.2	11.2	-55.2	-11.2
Ndoki	672	89.6	78.3	10.4	429.4	57.2	324.1	42.8	-242.6	-32.4	242.6	32.4
Special Reserve												
Plateau Bilolo	30.1	5.2	905.1	96.8	6.5	0.7	928.8	99.3	-23.6	-4.5	23.6	4.5
Libwe	160.2	23.4	526	76.6	411.5	60.2	274.6	39.8	251.3	36.8	-251.3	-36.8
Kambi	299.5	75.4	99.3	24.6	62.9	15.8	335.8	84.2	-236.6	-59.6	236.6	59.6
Yobe-Lidjobo	424	56.4	331.8	43.6	461	61.3	294.8	38.7	37	4.9	-37	-4.9
ZCC	580.8	99.4	6.4	0.6	536.4	91.8	50.8	8.2	-44.4	-7.6	44.4	7.6

Table 7. Proportion of priority and non-priority habitats for elephants within the DSPA

National Park												
	Year 2015				**Year 2020**				**Change (Year 2020 - Year 2015)**			
	Habitat category				*Habitat category*				*Habitat category*			
Sectors	*priority*		*Non-priority*		*priority*		*Non-priority*		*Priority*		*Non-priority*	
	Area (km^2)	% Area	Area (km^2)	% Area	Area (km^2)	% Area	Area (km^2)	% Area	Area (km^2)	% Area	Area (km^2)	% Area
Dzanga	489.6	98.9	1.1	1.6	453.5	91.6	43.8	8.4	-36.1	-7.3	36.1	7.3
Ndoki	599.6	80	153.9	20	598.6	79.8	155	20.2	-1	-0.2	1	0.2
Special Reserve												
Plateau Bilolo	63.7	6.8	871.1	93.2	93.1	10	842.3	90	29	3.2	-29	-3.2
Libwe	387.5	56.7	198.6	43.3	283	41.4	403.1	48.6	-104.5	-15.3	104.5	15.3
Kambi	304	76.5	94.7	23.5	237.9	59.9	159.1	40.1	-66.1	-16.6	66.1	16.6
Yobe-Lidjobo	642.1	85.3	113.3	14.7	448.5	59.6	307.3	40.4	-193.6	-25.7	193.6	25.7
ZCC	582.9	99.8	4.3	0.2	571.5	97.8	15.7	2.2	-11.4	-2	11.4	2

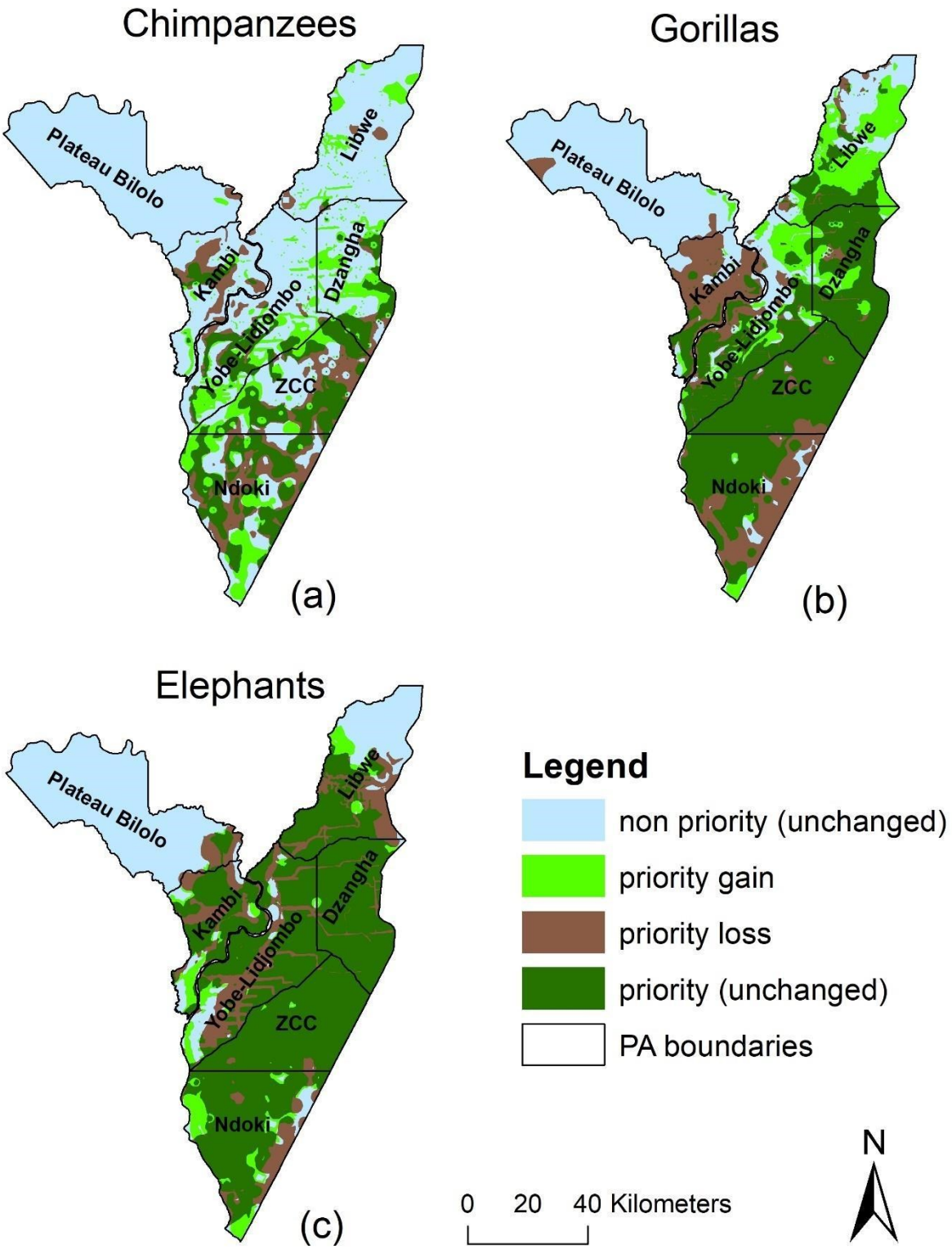

Figure 10. Change (Loss and gain) in priority species habitats between 2015 – 2020: a represents changes in priority chimpanzee habitats; b represents changes in priority gorilla habitats; and c represents changes in elephant habitats.

Table 8. Effects of key predictors to species priority habitat decline

Chimanzees			
Predictor	*R-squared*	*Adjusted R-squared*	*p-value*
Human pressure	0.54	0.54	2.2e-16
Eco-guard patrols	0.015	0.01	0.1841
Distance to roads	0.02	0.02	2.2e-16
Gorillas			
Human pressure	0.58	0.58	2.2e-16
Eco-guard patrols	0.03	0.02	4.163e-08
Distance to roads	0.09	0.08	2.2e-16
Elephants			
Human pressure	0.47	0.46	2.2e-16
Eco-guard patrols	0.017	0.01	0.4149
Distance to roads	0.04	0.04	6.731e-07

Table 9. Effects of key predictors to species priority habitat gain

Chimanzees			
Predictor	*R-squared*	*Adjusted R-squared*	*p-value*
Human pressure	0.028	0.012	0.1807
Eco-guard patrols	0.44	0.42	8.605e-05
Distance to roads	0.14	0.14	2.2e-16
Gorillas			
Human pressure	0.04	0.04	0.0003165
Eco-guard patrols	0.75	0.74	2.655e-05
Distance to roads	0.41	0.4	2.2e-16
Elephants			
Human pressure	0.01	0.01	0.2489
Eco-guard patrols	0.14	0.12	0.008206
Distance to roads	0.15	0.14	2.2e-16

Discussion

Mapping suitable ape and elephant habitats and quantifying changes

We generated five species distribution maps for each year of study: two chimpanzee suitability maps (one with nest data alone and another with all observation signs), two gorilla suitability maps (one with nest data alone and another with all observation signs) and one elephant suitability map (Figures 4 and 5). Chimpanzee and gorilla nesting habitats were strongly and significantly correlated with habitats mapped with all species signs (Figure 6). Moreover, all three species' habitats (chimpanzees, gorillas and elephants) were significantly correlated with each other (Figure 7), suggesting that species' habitats overlap spatially within the DSPA (Figure S4, Table S1). Highly suitable overlapping areas were mostly distributed within the Dzanga, Ndoki and ZCC sectors. By reclassifying habitat suitability into unsuitable, low, moderate and high suitability, we found that all three species' habitats have declined considerably between 2015 and 2020 (Table 2). For example, about 96 km^2 (2.1 % of the total area of the DSPA) of all suitable chimpanzee habitat has been converted to moderate, low and unsuitable areas over the last five years. Gorillas have lost over 634 km^2 of their suitable habitat (13.7 pp of the DSPA), while elephants have lost over 690 km^2 of suitable habitat (about 15 pp of the DSPA). By combining the spatial patterns of 1) both species of great ape and 2) of all three mammals, our findings suggest that great apes in general, have lost over 13 % of the suitable habitat required for their survival, while all three mammals have together lost a total of 16 % over the last five years (Table 3). Such losses are due to continuous increases of human activities in the DSPA based on the 2015 (N'Goran et al., 2016) and 2020 wildlife surveys data (Table S4).

We argue that all moderate and high suitability habitats should be considered as priority areas for long-term species sustainability (Figure 9). Our findings show that highest

priority ape and elephant habitats were spatially distributed within the ZCC, Ndoki, Yobe Lidjombo and Dzanga sectors in 2015 (Figure 9). These results match previous patterns of ape and elephant population abundance estimates documented by N'Goran et al., (2016), N'Goran et al., (2017). These findings also provide evidence that in addition to national parks, some special reserves like the ZCC and Yobe Lidjombo sectors previously served as suitable zones for the survival of large mammals within the DSPA. These results confirm documented evidence from other parts of Central Africa, such as in the Dja Biosphere Reserve (Tudge et al., 2021), and the Lobéké forest management units (Ginath Yuh et al., 2021) of Cameroon. Moreover, the high spatial variability in priority habitats within these sectors could be associated with high variability in the presence of eco-guard patrols and consequently a lower increase in hunting pressures, particularly within the Dzanga-Ndoki NP (Table S4 & Table S6a and b). Large mammals have been previously reported to occur at high densities within landscapes with high levels of eco-guard patrol activity and reduced human pressures (Kablan et al., 2019; Morgan et al., 2019), suggesting that these areas are important for species distribution and survival.

Indeed, between 2015 and 2020, our findings show that priority chimpanzee habitats declined by about 73 km^2 within the community hunting zones (ZCC), 63 km^2 within the Yobe-Lidjombo sector and over 74 km^2 within the Ndoki sector, however they increased by approximately 3 km^2 with the Dzanga sector. In addition, species have also lost over 130 km^2 of all priority habitats within the Kambi and Plateau Bilolo sectors, suggesting that chimpanzees are facing significant threats within these two sectors alongside the ZCC and Yobe-Lidjombo sectors. Gorillas have lost about 44 km^2 of their priority habitats within the ZCC, 260 km^2 within the Kambi and Plateau Bilolo sectors, and about 243 km^2 within the Ndoki sector. However, gorillas gained about 55 km^2 within the Dzanga sector. Elephants have lost about 11 km^2 of their priority habitat within the ZCC, 194 km^2 within Yobe-

Lidjombo, 36 km^2 within the Dzanga sector, 1 km^2 within the Ndoki sector, and about 171 km^2 within the Kambi and Libwe sectors. Our findings with the Dzanga National Park correspond with those of previous studies by Yuh et al., (2019) and Ginath Yuh et al., (2020) that have shown that national parks are highly suitable for the survival of chimpanzees and gorillas, especially when strict hunting regulations are enforced. The gain in priority habitats for both species within this national park therefore suggest that the national park is better managed and is thus valuable for the survival of these large mammals and correspond with reports from N'Goran et al., (2016), N'Goran et al., (2017) and findings from other regions (Ayres & Clutton-Brock, 1992). Species therefore seem to experience lower hunting pressure within this sector (Table S4), leading to higher habitat suitability within these areas, and supporting higher densities in the population abundance estimates conducted by N'Goran et al., (2016), N'Goran et al., (2017). For the Ndoki NP, as well as certain special reserves where species priority habitats have declined considerably over last five years (e.g., ZCC), our findings show that there is still a large spatial variability in the remnants of priority habitats within these sectors (Figure 9), suggesting that they still constitute zones of high conservation importance.

Contributions of predictor variables to species distribution and priority habitat change

Our findings show that the key factors that affect great ape and elephant distribution within the DSPA are eco-guard patrols and human pressure. These two variables together contributed more than 50 % prediction performance in all five model treatments for both years of study, with species finding much suitable habitats under increased eco-guard patrols, and less suitable habitats under increased human pressures (Table 4). We therefore quantified the effects of both variables to species priority habitat change (loss /gain) between both years

of study, and we found that increased human pressure is the primary cause of priority habitat decline for all three species within parts of the DSPA (Tables 8 and 9). We related these findings mostly to the Ndoki NP, as well as the Kambi, Plateau Bilolo and ZCC sectors (Table 2) where results from cumulative eco-guard patrol efforts have shown a relatively low number of eco-guard patrol activities implemented within these sectors over the last five years (Table S6a and b). Several hunting and logging camps, as well as villages, roads and hunting activities occur at high densities within the DSPA (Figure S3). These activities led to increased human pressure within certain sectors, thereby threatening the habitats and survival of large mammals. The high encounter rates with hunting activities in particular (Table S4), suggest that the local population inhabiting the DSPA depends mostly on subsistence and commercial hunting for their livelihoods. Hunting activities are therefore an important driver of increasing human pressure in our study area, aligning with previous findings documented for the Congo Basin (Nasi et al., 2011; Ziegler et al., 2016). Commercial hunting is highly linked to increased demand for bush meat in nearby cities, as well as increased access to roads (Fa et al., 2019; Ziegler et al., 2016). Roads also constitute an important additional indicator of human pressure within the DSPA, and our findings suggest that they play a significant role in contributing to ape and elephant distribution, with species gaining and maintaining priority habitat stability in landscape areas further from roads (Table 8). These results are supported by other studies from the Congo Basin, where large mammals have been reported to find suitable habitats in areas far from roads (Heinicke et al., 2019; Morgan et al., 2018). With the increased construction of roads in several parts of this region, hunters have gained access to protected areas, as well as increased the commercialization of hunting activities. These factors have triggered a more than 60 % loss in large mammal populations (Maisels et al., 2013; Wasser et al., 2004), as well as the reductions in suitable habitats that we reported here.

For areas where there was gain in priority habitats, we found that eco-guard patrols were the main contributors to this stability and improvement. These findings were significant for chimpanzees and gorillas. For elephants however, the role of eco-guards only contributed about 14 % to their priority habitat stability. These findings were particularly relevant to the Dzanga NP, as well as the Libwe and Yobe-Lidjombo special reserves where cumulative eco-guard patrol efforts were relatively high within these sectors over the last five years (Table S6a and b). With the launch of a harmonized approach to wildlife monitoring within priority landscapes in the Congo Basin (N'Goran et al., 2014; N'Goran, 2015), WWF in partnership with ministries of Forestry and Wildlife within Central Africa developed anti-poaching patrol strategies (eco-guard patrols) for safeguarding wildlife and habitats within this region. Since 2017, patrol efforts have increased substantially, especially within some sectors of the DSPA, contributing positively towards habitat and population stability of large mammals, particularly the great apes (N'Goran et al., 2017). In the Dzanga NP for example, eco-guard patrol activities are highly prioritized, providing increased stability in chimpanzee and gorilla priority habitats, and supporting the findings of higher densities in previous population abundance estimates conducted by N'Goran et al., (2016), N'Goran et al., (2017).

In general, anti-poaching patrols have been found to be effective in protecting large mammals within several landscapes across Africa (Critchlow et al., 2015, 2017; Gandiwa et al., 2013; Jachmann, 2008a; Jachmann, 2008b; Junker et al., 2012; Kablan et al., 2019; Morgan et al., 2019; Ngene et al., 2009; Tranquilli et al., 2014), and our results also suggest their effectiveness within parts of the DSPA. However, our results also show continued and substantial declines in suitable habitat areas between 2015 and 2020, suggesting that the increased presence of eco-guard patrols has not succeeded in preventing human pressures from negatively affecting large mammal populations over this period.

Anti-poaching patrolling activities are very often implemented as a joint effort of conservation organizations (e.g., WWF and WCS (Wildlife Conservation Society)) and forestry agents or eco-guards, regulated by certain ministerial Decrees, such as Decree No. 86/230 of 13 March 1986 of the Ministry of Forestry and Wildlife in Cameroon. As a result of the increased presence of eco-guard activities, several protected areas and landscapes of conservation value are gaining protection (Kablan et al., 2019; Morgan et al., 2019), with species population and suitable habitats maintaining stability. Despite this conservation strength, poaching still remains a big problem across several landscapes (Nzooh Dongmo et al., 2016a; Nzooh Dongmo et al., 2016b), with effects likely due to limited resources (e.g., access to funding to support patrolling activities, as well as access equipment such as vehicles and motorbikes), insufficient numbers of patrol staffs, lack of knowledge of conservation laws by local communities, and poverty (Patrice Dkamela & Nguiffo, 2022; Ramutsindela et al., 2022). The intractability of the problem of poaching and bushmeat or wild game hunting in particular has led some authors to suggest that re-establishing local tenure and land rights may be more effective than current practices of exclusionary conservation (Mavah et al., 2022). Furthermore, among the 23 Targets of the Kunming-Montreal Global Biodiversity Framework, ratified at COP15, the UN biodiversity meetings in Montreal, Canada, Target 3 states that: "by 2030 at least 30 % of terrestrial, inland water, and coastal and marine areas are effectively conserved and managed, recognizing and respecting also the rights of indigenous peoples and local communities including over their traditional territories" (Convention on Biological Diversity (CBD)). International agreements and practical conservation applications both support the need to recognize traditional ecological knowledge and work with local communities as partners in conservation. Our results clearly highlight the need for continuous conservation action within the NPs and special reserves of the DSPA, and it is likely that a combination of both existing and community-based conservation

approaches and initiatives will be required to sustain the DSPA as an important hotspot of mammal diversity within Central Africa.

Our model predictions show that disturbed forests, dense forests, temperature variability and topography provide very little to no influence on all three species distribution within the DSPA. Quantified results from land cover datasets generated by the Copernicus Global Land Monitoring Service (Figure S3, Table S2) provide evidence that there has been no substantial change in forest cover within the DSPA over the last five years, hence very little to no forest disturbance. Over 99 % of the entire forest cover is intact, and our models found that the decline in habitat areas suitable for all three mammal distributions were the result of increased human pressure, mostly arising from hunting and road developments. Sloped and high elevation areas are mostly confined to the Plateau Bilolo sector and results from the 2015 to 2020 mammal survey show low to no indications of mammal species occurrence within this sector, hence relatively low prediction performance in our models (Figure 2). With temperature, the low prediction performance perhaps suggests that all three mammal species were less sensitive to climatic variables, probably due to forest shading, but also likely because other factors had such strong influence on habitat suitability.

Conclusions and management recommendations

In this paper, we mapped and quantified changes in ape and elephant habitat suitability between two survey years (2015 and 2020), and identified priority habitats as a contribution to conservation planning in the DSPA. Our results provide an accurate, recent representation of the sizes and locations of suitable species' habitats, and changes in those habitats over this 5-year period. We provide evidence that priority chimpanzee habitats covered about 1383 km^2 (30 %) of the entire DSPA in 2015, while priority gorilla and

elephant habitats covered approximately 2569 km^2 (56 %) and 3075 km^2 (67 %) respectively, with all three species, priority habitats declining by 4, 4.5 and 9.8 pp respectively between 2015 and 2020. We found that these declines were primarily due to increases in human pressure. We further provide evidence that the species' habitats overlapped significantly, and were distributed spatially within the Dzanga National Park where there were high rates of eco-guard patrols and reduced human pressure. We also showed that all three species' habitats were distributed spatially within the Ndoki and ZCC sectors despite evidence of priority habitat decline within these sectors. Finally, we provided evidence that the presence of eco-guard patrols and the distribution of human pressure constituted the most important factors influencing all three species' distribution within the DSPA.

Our results suggest that great apes are seriously threatened within the ZCC, Kambi and Ndoki sectors, while elephants are seriously threatened within the entire DSPA. We therefore recommend that increased efforts are needed to decrease negative human pressures on these species within priority habitat areas. One strategy could be to increase eco-guard patrol efforts within these sectors, though other approaches that focus on the empowerment of local people through increased local land tenure and rights could also be effective at enhancing conservation outcomes (Mavah et al., 2022). We emphasize that any effective conservation efforts should be implemented in consultation with local communities and alongside developing a long-term strategy of education and co-management with local people. Protection measures that allow for the sustainability of endangered species and their habitats along with improved living conditions of Indigenous peoples and local communities need to be at the center of the DSPA management efforts. Conservation and management planning therefore needs to take into careful consideration where and why suitable habitat losses appear in DSPA in order to identify possible mitigation measures. We suggest that managers review zoning and use regulations of each sector within the DSPA in consultation

with Indigenous and local populations, as well as with the private sector that exploits parts of the reserve for logging purposes, in order to facilitate social and ecological sustainability and conservation of endangered species.

Chapter 5: General conclusions and management recommendations

My thesis documents and models new data and findings on present and projected future changes in forest cover and land use patterns as a result of climate change and socioeconomic impacts in the Congo Basin. It was my aim with this work to help fill a critical knowledge gap about the current state of forests in this region and on potential impacts of human activities and climate change. My results also contribute to our understanding of great ape conservation biology, and provide tools and data to help secure their future within the DSPA. Our closest animal relatives, the great apes, are in imminent danger of extinction, especially within several protected areas and forest management units within the Congo Basin; the extinction of great apes would be an incalculable loss for the diversity of life on Earth, and for our understanding of the human story. There is therefore an urgent need to identify the suitable environmental conditions required for planning species conservation in this part of the world, and my dissertation work provide such baseline information within the DSPA, suggesting the importance of implementing our approach within nearby protected Areas of high conservation importance in the long run.

I provided a novel first application and comparison of four statistical and ML models (kNN, ANN, RF and SVM) as potentially robust means of monitoring changes in LULC using coarse resolution satellite images within a tropical African biome; used the most performant ML algorithm for a large scale forest cover and land use change mapping within the Congo Basin under various scenarios of climate change and socioeconomic impacts; and finally, documented the impacts of human activities, land use change, and climatic factors on large mammal species distributions within a UNESCO world heritage Protected Area of the Congo Basin, the DSPA. The results of this thesis are highlighted in three manuscript-based chapters.

In Chapter 2, I compared the aforementioned statistical and ML models with cloud free Landsat images from the northern section of the Mayo Rey department of northern Cameroon. We showed that all four classification algorithms provided significant and relatively high degrees of accuracy in LULC classification (i.e. all models had > 80% OA), supporting similar findings from other regions of the world. However, the RF model outperformed the kNN, SVM and ANN models, and produced highly accurate LULC maps, which produced statistically significant correlations when validated against other existing global LULC products. We therefore, generated a methodological approach that could help foster the advancement of knowledge in the application of ML algorithms for LULC monitoring within tropical rain forest regions across Africa, especially with the use of coarse-resolution Landsat images. We recommend that these mapping approaches be tested further in forested areas across other African regions that remain underrepresented in the remote sensing literature.

In Chapter 3, we used the most performant ML model (RF) identified in Chapter 2 to map decadal changes in forest cover and land use patterns in the Congo Basin for the period 1990 – 2020. We further projected these changes to the year 2050 using the M-ANN and Markov chain algorithms of the ILCM, under various scenarios of human population density and climate change. Following this integrated modeling approach, we generate highly accurate LULC maps for the Congo Basin for the years 1990, 2000, 2010, and 2020 and projected our detected change maps to the year 2050-under three climate change scenarios, after cross validating our current LULC products with existing global land use products. We summarized the results for four LULC types that predict significant changes to help inform land use planning in this region (dense forest, woody savannas, built-up areas, and croplands), and showed that the Congo Basin is losing approximately 0.3 pp (11700 km^2) of its entire forest cover per year, corresponding to findings documented by Tyukavina et al.,

(2018) and Kirilenko & Sedjo, (2007). We further showed that a large proportion of dense forest areas have been converted to built-up areas, croplands, woody savannas, and open savannas, and we expect loss of forest areas to continue for the next several decades (i.e. under all three climate change scenarios). According to our models, key drivers to historical conversions were human population density, logging and forest clearing, wildland fires, distance to built-up areas, and maximum temperatures. We also found that croplands and built-up areas have expanded significantly over the 1990 – 2020 study period, with more expansions expected by the year 2050, owing to the expected growth in human population, and associated needs for food, resources and farmlands, as well as expected increases in infrastructural development projects.

Although population density and logging and forest clearing play the largest role in driving forest cover and land use change within the Congo Basin, our results also provide new evidence that climate change is also a significant driver of LULC changes in this region. Our results align with evidence documented in other regions of the world, e.g. in the Amazon Basin of South America (López et al., 2022), in the North American boreal and temperate forest (Mu et al., 2017; Ameray et al., 2023; Kolden & Abatzoglou, 2012; Stralberg et al., 2018), in the Indian forests (Chaturvedi et al., 2011; Upgupta et al., 2015), in European landscapes (Carozzi et al., 2022), and at global scales (Beaumont & Duursma, 2012; Chen et al., 2020; Hurtt et al., 2011) . Because climate change contributes to LULC changes and the loss in forest cover contributes to climate change problems, we recommend including our results in the UNFCCC REDD+ program. Deforestation monitoring, carbon emissions estimations, and the implementation of nature-based solution plans under the UNFCCC REDD+ framework could be achieved for the long-term, using the LULCC and projected datasets generated in this study. This could foster the implementation of our approach within

East, West, North, and Southern African regions, where nature-based solutions to climate change problems are of also high need.

In chapter four, we applied an ensemble of two species distribution models in R (GLM and GAM) to map the habitat suitability of great apes and elephants within the DSPA, as well as quantify changes between two survey years (2015 and 2020). Through this modeling approach, we generated five species distribution maps for each year of study: two chimpanzee suitability maps (one with nest data alone and another with all observation signs), two gorilla suitability maps (one with nest data alone and another with all observation signs) and one elephant suitability map, as well as mapped and identified priority habitats as a contribution to conservation planning. By quantifying our mapped outputs, we showed that for a total habitat suitability area of 4624 km^2, priority habitat areas for chimpanzees, gorillas and elephants covered approximately 1383 km^2 (30%), 2569 km^2 (56%) and 3075 km^2 (67%) of the entire DSPA for the year 2015. These habitat areas declined considerably by approximately 4, 4.5 and 9.8 pp respectively over the 5-year survey period, suggesting an average priority habitat loss of approximately 9.2 pp for all three large mammal species. We predicted that the loss in priority habitats were mostly due to increased human pressures. We further provided evidence that the National Parks of the DSPA represent regions of higher priority habitat for all three species owing to the reduced human pressures that had resulted from higher eco-guard patrol efforts, and our findings corresponded to results documented within other PAs of the Congo Basin (Morgan et al., 2019; Kablan et al., 2019). Based on our analysis, we recommended maintaining a nonviolent patrol presence to mitigate human pressures within remaining priority habitat areas, recognizing also the importance of collaboration with local communities to support long-term conservation goals.

My dissertation research therefore, provides a novel focused analysis that compares the classification performance of multiple Machine Learning classifiers in large-scale LULC

mapping within afro-tropical forest settings, thereby providing basis for selecting the appropriate modeling algorithms required for projecting future changes under IPCC climate change scenarios. I also produced spatially explicit species distribution models to map and identify areas of priority habitats required for planning the long-term conservation of large mammal species within the DSPA; a region reported by the IUCN and UNESCO as facing increasing threats from human activities (logging and poaching), and where anti-poaching patrol activities that were established for limiting these threats have not been fully assessed. With this integrated modeling approaches, I have generated deliverables, including land cover change maps, quantified changes, species distribution and change maps, and the contributions of socioeconomic, climate-driven, and law enforcement factors, that are consistent with outputs generated in several regional and global studies. For example, the 30-year land cover maps generated in my dissertation research are consistent with global land cover products generated by Potapov et al., (2021), Potapov et al., (2022), Hansen et al., (2013), and Friedl & Sulla-Menashe, (2019), as well as with quantified regional-scale results reported for the Central African region (Tyukavina et al., 2018), the Brazilian Amazon Basin (López et al., 2022; da Cruz et al., 2021), the Indonesian Bornean forest (Gaveau et al., 2014), and the Canadian boreal forest (White et al., 2017). The large mammal habitat suitability mapping results generated in my dissertation are consistent with results reported for the whole of Africa (Junker et al., 2012), Central Africa (Srindberg et al., 2018), and West Africa (Heinicke et al., 2019). Together, these studies show that biodiversity loss is a serious global issue, and land use activities and climate change are significant contributors. The Congo Basin is one such area of the world where these threats are highly alarming, especially as issues with socioeconomic neocolonial pressures, poverty, poor governance, and the inadequate participation of indigenous local communities in sustainable forest management keep increasing.

Although I provide novel and useful results that deal with LULC classification uncertainties within African tropical biomes (Chapter 2), as well as select the most performant algorithm for large-scale LULC mapping (chapter 3), I highlight some limitations to my methodological approaches. First, my approach for chapter 2 was tested within a sub-Saharan tropical region that is highly dominated by woody savannas relative to dense forests areas. I focused on this region because it constitutes part of the Congo Basin, where I intended to apply the most peformant algorithm for large-scale LULCC mapping to support landscape planning, as well as make important recommendations for other tropical rain forest regions across Africa. I therefore, generated highly accurate results for the selected study area in chapter 2, although a much better approach would have been to compare the performance of my algorithms within denser tropical forest areas. I however, limited my study to this sub-Saharan tropical region due to its potential for acquiring cloud free satellite images as compared to denser forest areas. Cloud free images minimize classification uncertainties and biased predictions of LULC categories using ML models, an issue that could have been encountered from processing cloud dominated images from denser forest areas. I however, recommend testing my approach within other tropical rain forest areas across East and West Africa. Second, although the RF model outperformed other ML algorithms in Chapter 2, as well as selected as the best modeling approach for large-scale land cover mapping in chapter 3, its performance relative to the other ML models would have been best validated through smaller-scale mapping of denser tropical forest areas. However, its efficiency was fully validated in relation to similar studies that have documented its high computational power relative to other ML models when applied in other tropical regions across the globe (Belgiu & Drăguţ, 2016; Pelletier et al., 2016; Rodriguez-Galiano et al., 2012).

Appendices

Appendix 1. Supplementary Materials for Chapter 2, Yuh et al. (2023)

Table S1. Description of R packages used in the LULC analysis

Package	Description
Raster	This package executes an important *raster()* function for importing (reading) single raster layers. It equally executes a *brick()* function for reading multiple raster layers for a multi-layer GeoTIFF file, as well as a *stack()* function for combining multiple raster files.
rgdal	This package provide possibilities for importing and exporting spatial data in various raster and vector formats (shapefiles, GeoTIFF, img etc)
RStoolbox	This package provides numerous functions for satellite data analysis such as image preprocessing (e.g. radiometric correction) and image processing (e.g. supervised and unsupervised classification, spectral indices analysis etc.).
randomForest	The *"randomForest"* package was used for implementing the random forest classification algorithm
caret	The caret package was used for classification and regression training, as well as for pre-processing, data splitting and evaluation of machine learning algorithms
kknn	The *"kknn"* package was used for generating weighted k nearest neigbours for classification, regression and clustering
rpart	The *"rpart"* package was used for partitioning classifications and regressions
e1071 and *kernlab*	These packages provided functions for support vector machines (SVM)
nnet	The *"nnet"* package was used for implementing the artificial neural network algorithm following the MLP approach
sp	The *"sp"* package was used for projecting, managing, querying and analyzing spatial datasets such as points, polygons, pixels etc.
NeuralNetTools	The "*NeuralNetTools*" package was used for visualizing and interpreting neural network models.
ggplot	The *"ggplot2"* package was used for plotting graphics

Table S2. Identified land use and land cover classes for the Mayo-Rey department of Northern Cameroon. Classes were identified following definitions and approaches used for the MODIS global land cover mapping (Friedl and Sulla-Menashe 2019), and land use/cover maps generated by Potapov et al., (2020, 2021, 2022)

Name	Code	Description
Croplands	1	Land use areas with at least 60% area cultivated as croplands (Friedl & Sulla-Menashe, 2019).
Dense forest	2	Areas of land with trees ≥ 5m in height (Potapov et al. 2021, 2022), and a canopy cover > 60% (FAO, 2002; Friedl & Sulla-Menashe, 2019).
Grasslands/savannas	3	Land use areas dominated by herbaceous vegetation or grasslands
Open savannas/barelands	4	Land use areas that are non-vegetated or contain less than 10% vegetation (Friedl & Sulla-Menashe, 2019)
Built-up areas	5	man-made land surfaces associated with built-up lands such as commercial and residential infrastructures, and roads (Potapov et al., 2022)
Water bodies	6	inland areas covered with at least 60% permanent water, and not obscured by objects above the surface such as buildings, tree canopies, and bridges (Potapov et al., 2022)
Wetlands	7	Vegetated and non-vegetated lands inundated with between 30-60% water (Friedl & Sulla-Menashe, 2019), and usually forming swampy or peatlands
Woody savannas	8	Areas of land a canopy cover of between 10 - 60% (FAO 2002; Friedl & Sulla-Menashe, 2019).

Table S3. Model parameterization settings and description

Modeling algorithm	Package name	Number of tuning parameters/iterations	Tuning method and description
kNN	"kknn"	5	Repeat (5): The model parametrization processes were repeated five times for each model, so as to ensure a fivefold cross validation of model parameters in each model. However, the number of iterations varied per model. For example, the kNN and SVM models were ran under 5 iterations; the MLP ANN model was ran under 100 iterations considering the number of hidden nodes; while the RF was ran under 500 iterations, with 500 trees generated after using default settings.
MLP ANN	"nnet"	100	
SVM	"kernlab" and "svmRadial"	5	
RF	"randomForest"	500	

Table S4. Land cover change detection from one cover class in the year 2000 to another in the year 2020

Land cover change from_to	Change area (ha)	% change
Croplands (unchanged)	47913.7	8.141
Croplands -> grasslands/savannas	1046.4	0.178
Croplands -> open savannas/barelands	98.1	0.017
Croplands -> built-up areas	653	0.111
Croplands -> wetlands	3.8	0.001
Croplands -> woody savannas	383.5	0.065
Dense forests -> croplands	218.1	0.037
Dense forests -> grasslands/savannas	52.4	0.009
Dense forests -> open savannas/barelands	0.4	0.000
Dense forests -> built-up areas	0.7	0.000
Dense forests -> woody savannas	19.3	0.003
grasslands/savannas -> croplands	542.9	0.092
grasslands/savannas (unchanged)	173.1	0.029
grasslands/savannas -> open savannas/barelands	0.5	0.000
grasslands/savannas -> built-up areas	12.3	0.002
grasslands/savannas -> wetlands	0	0.000
grasslands/savannas -> woody savannas	27.2	0.005
open savannas/barelands -> croplands	71266.4	12.108
open savannas/barelands -> dense forest	0.1	0.000
open savannas/barelands -> grasslands/savannas	91372.6	15.525
open savannas/barelands (unchanged)	1205.7	0.205
open savannas/barelands -> built-up areas	2981.9	0.507
open savannas/barelands -> water bodies	0	0.000
open savannas/barelands -> wetlands	67.1	0.011
open savannas/barelands -> woody savannas	18894.8	3.210
built-up areas ->croplands	162.5	0.028
built-up areas -> grasslands/savannas	14.8	0.003
grasslands/savannas -> open savannas/barelands	0.7	0.000
open savannas/barelands (unchanged)	1289	0.219
open savannas/barelands ->wetlands	1	0.000
open savannas/barelands ->woody savannas	279.7	0.048
Water bodies -> croplands	7604.9	1.292
Water bodies -> dense forest	9	0.002
Water bodies -> grasslands/savannas	5063.8	0.860
Water bodies -> open savannas/barelands	328.9	0.056
Water bodies -> built-up areas	31	0.005
Water bodies (unchanged)	24091.4	4.093
Water bodies -> wetlands	5371	0.913
Water bodies -> woody savannas	307.1	0.052
Wetlands -> croplands	1635.6	0.278
Wetlands -> dense forest	0	0.000
Wetlands -> grasslands/savannas	388	0.066
Wetlands -> open savannas/barelands	0.7	0.000

Wetlands -> built-up areas	4.7	0.001
Wetlands -> water bodies	0	0.000
Wetlands (unchanged)	8.1	0.001
Wetlands -> woody savannas	97	0.016
Woody savannas -> croplands	41900	7.119
Woody savannas -> dense forest	0	0.000
Woody savannas -> grasslands/savannas	28610	4.861
Woody savannas -> open savannas/barelands	805.2	0.137
Woody savannas -> built-up areas	310.8	0.053
Woody savannas -> wetlands	7.6	0.001
Woody savannas (unchanged)	233312.3	39.641

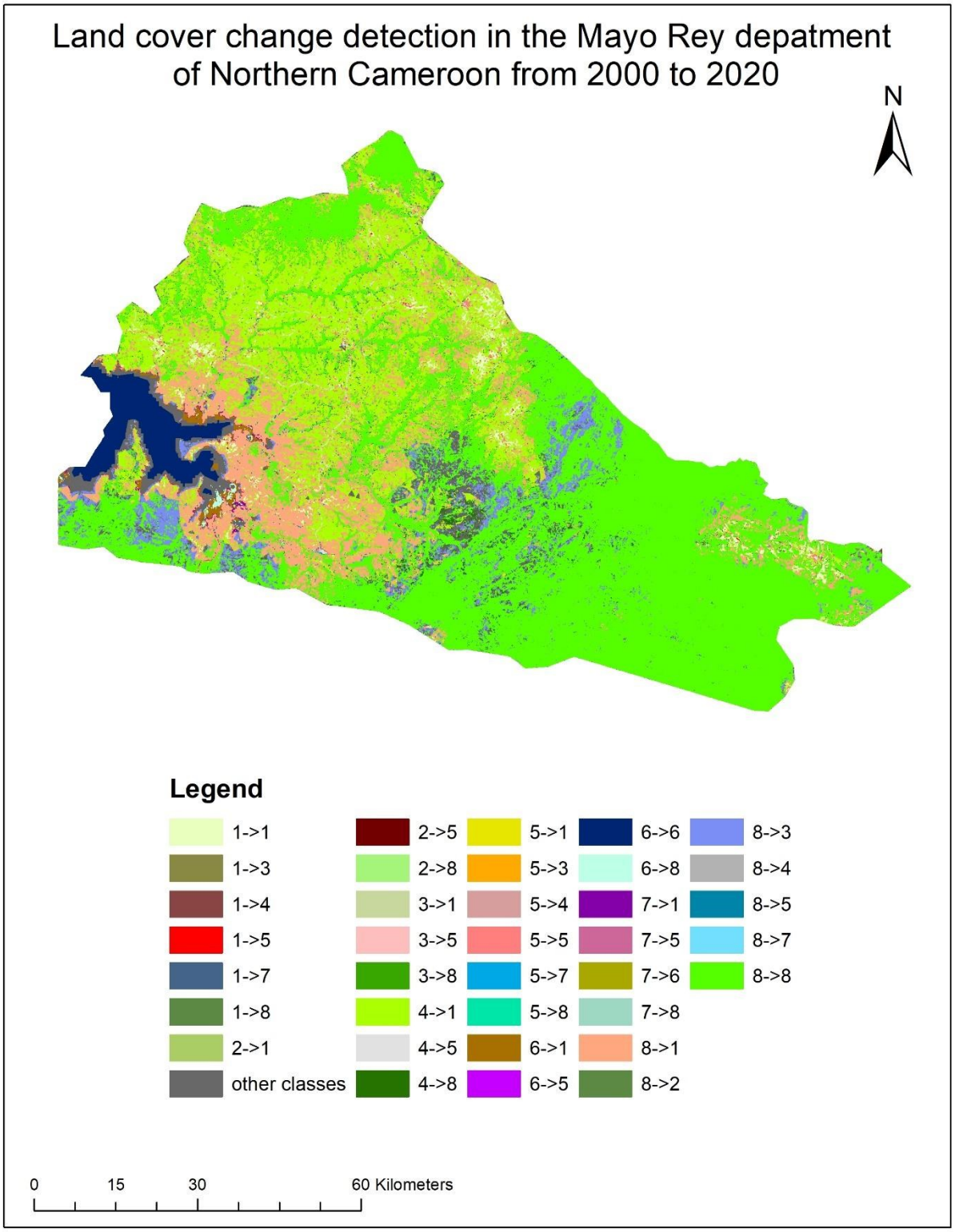

Figure S1. LULC change detection. Map shows changes from one land cover class to another (From-To). 1 = croplands, 2 = dense forest, 3 = grasslands/savannas; 4 = open savannas/barelands; 5 = built-up areas; 6 = water bodies; 7 = wetlands; 8 = woody savannas. A full list of all possible transitions is available in Table S3.

Appendix 2. Supplementary Materials for Chapter 3

Table S1. Examples of LULC class descriptions, and their importance in global land cover mapping (Hansen et al., 2013; Friedl & Sulla-Menashe, 2019; Potapov et al., 2020, 2021)

Name	Description
Croplands	Lands with at least 60% of the area cultivated as croplands (Friedl & Sulla-Menashe, 2019).
Dense forest	Areas of land with trees ≥ 5m in height (Potapov et al., 2021, 2022), and a canopy cover > 60% (FAO, 2002; Friedl & Sulla-Menashe, 2019)
Grasslands/savannas	Land use areas dominated by herbaceous vegetation or grasslands
Open savannas/barelands	Land use areas that are non-vegetated or contain less than 10% vegetation (Friedl & Sulla-Menashe, 2019)
Built-up areas	Man-made land surfaces associated with built-up lands such as commercial and residential infrastructures, and roads (Potapov et al., 2022)
Water bodies	inland areas covered with atleast 60% permanent water, and not obscured by objects above the surface such as buildings, tree canopies, and bridges (Potapov et al., 2022)
Wetlands	Vegetated and non-vegetated lands inundated with between 30-60% water (Friedl & Sulla-Menashe, 2019), and usually forming swampy or peatlands
Woody savannas	Areas of land with a canopy cover of between 10 - 60% (FAO, 2002; Friedl & Sulla-Menashe, 2019).

Table S2. Sample datasets used as predictors in the land use/cover change projections.

Data category	Data type	Source	Data years/ projections	Description
Climate-related	Annual temperatures (maximum and minimum temperatures), and annual precipitations	IPCC-AR6 ensemble climate projections of the CMIP6 project (Eyring et al., 2016; Thrasher et al., 2021; 2022)	1990-2020, 2050	Gridded climatic data for the Congo Basin, obtained from the IPCC-AR6 ensemble climate projections of the CMIP6 project.
	Forest fires	MODIS fire products: (https://modis.gsfc.nasa.gov/data/dataprod/mod14.php	2000-2020	Daily fire data recorded at 1km spatial resolution
Socioeconomic	Industrial selective logging, small scale clearing for agriculture, large scale agro-industrial clearing, mining, roads, settlements	Tyukavina et al., (2018) Potapov et al., (2020)	2000-2018	Mapped socioeconomic data for the Congo Basin. Data available only for current conditions. Roads and settlement data calculated as distance to built-up areas, using the Euclidean distance tool in ArcGIS.
Biophysical	Landscape topography (slope Elevation)	http://srtm.usgs.gov/index.php	Not applicable	Digital elevation models were acquired for the Congo Basin, from which slope data was extracted.
Demographic data	Population density	https://dataguru.lu.se/app#worldpop	2010-2020, 2050	Current and projected population density data acquired from the Veiko Lehsten climate and population projection data, and modeled under three three shared socioeconomic pathways (SSP1, SSP2 and SSP3), through the Coupled Model Intercomparison Project 6 (CMIP6) of the IPCC, at a 1 km spatial resolution

Table S3. Transition sub-models to be included in the MLP-ANN of the TerrSet ILCM. Table was designed, following the approach used in Gibson et al., (2018), and with drivers of change selected from Tables S4-S11.

LULC transitions or change	Transition sub-model and label	Description	Drivers of change
Dense forest to Croplands; Dense forest to Built-up areas; Dense forest to Open savannas/Barelands; Dense forest to Grassland savannas; Dense forest to Wetlands; Dense forest to Water bodies; and Dense forest to Woody savannas	Deforestation (D)	Conversion or change from forest cover to other LULC types	Wildland fires; Population density; Maximum temperatures; Minimum Temperatures; Logging and forest clearing; and Distance to built-up areas
Croplands to Forest; Open savannas/Barelands to Forest; Grasslands savannas to Forest; Wetlands to Forest; Water bodies to Forest; and Woody savannas to Forest	Afforestation (A)	Conversion or change from other land use types to forest	Precipitation; Slope;
Dense forest to Croplands; Open savannas/Barelands to Croplands; Grassland savannas to croplands; Built-up areas to Croplands Wetlands to croplands; Water bodies to croplands; and Woody savannas to Croplands	Croplands Intensification (CI)	Conversion or change from other land use types to croplands	Population density
Croplands to Dense forest; Croplands to open savannas/Barelands; Croplands to Grassland savannas; Croplands to Built-up areas; Croplands to Water bodies; Croplands to Wetlands; and Croplands to Woody savannas	Croplands Abandonment (CA)	Conversion or change from croplands to other land use types	Population density, and Maximum temperatures
Dense forest to Built-up areas; Croplands to Built-up areas; Open savannas/Barelands to Built-up areas; Grassland savannas to Built-up areas; Water bodies to Built-up areas; Wetlands to Built-up areas; and Woody savannas to Built-up areas	Built-up areas Intensification (BUI)	Conversion or change from other LULC types to built-up areas	Population density; and distance to built-up areas
Built-up to Dense forest; Built-up areas to Grassland savannas; Built-up areas to Open savannas/Barelands; Built-up areas to Water bodies; Built-up areas to Wetlands; and Built-up areas to Woody savannas	Built-up areas Abandonment (BUA)	Conversion or change from built-up areas to other LULC types	Distance to built-up areas; and slope
Woody savannas to Dense forest; Woody savannas to Croplands;	Woody savannah Area loss (WAL)	Conversion or change from woody savannas	Wildland fires, maximum

Woody savannas to Built-up areas; Woody savannas to open savannas/Barelands; Woody savannas to Grassland savannas; Woody savannas to Water bodies; and Woody savannas to Wetlands		areas to other LULC types	temperatures, population density, and logging and forest clearing
Dense forest to Woody savannas; Croplands to Woody savannas; Built-up to Woody savannas; Open savannas/Barelands to Woody savannas; Grassland savannas to Woody savannas; Water bodies to Woody savannas; and Wetlands to Woody savannas	Woody savannah Area Increase (WAI)	Conversion or change from other LULC types to woody savannas	Precipitation; maximum and minimum temperatures; slope, and logging and forest clearing
Open savannas/Barelands to Woody savannas; Open savannas/Barelands to Built-up areas; Open savannas/Barelands to Grassland savannas; Open savannas/Barelands to Water bodies; Open savannas/Barelands to Wetlands to Woody savannas; Open savannas/Barelands to Croplands; and Open savannas/Barelands to Dense forest	Open savannas/Barelands Depletion (OBD)	Conversion or change from other LULC types to open savannas/barelands	Population density, distance to built-up areas, precipitation, minimum temperatures, elevation and slope
Woody savannas to Open savannas/Barelands; Built-up areas to Open savannas/Barelands; Dense forest to Open savannas/Barelands; Croplands to Open savannas/Barelands; Water bodies to Open savannas/Barelands; Wetlands to Open savannas/Barelands; and Grassland savannas to Open savannas/Barelands	Open savannas/Barelands Area Increase (OBAI)	Conversion or change from open savannas/barelands to other LULC types	Logging and forest clearing, distance to built-up areas, population density, wildland fires, and elevation
Woody savannas to Grassland savannas; Built-up areas to Grassland savannas; Dense forest to Grassland savannas; Croplands to Grassland savannas; Water bodies to Grassland savannas; Wetlands to Grassland savannas; and Open savannas/Barelands to Grassland savannas	Grassland savannah Area Increase (GSAI)	Conversion or change from other LULC types to grassland savannas	Elevation, slope, maximum and minimum temperatures, distance to built-up areas, population density, and logging and forest clearing
Grassland savannas to Open savannas/Barelands; Grassland savannas to Croplands; Grassland savannas to Built-up areas; Grassland savannas to Dense	Grassland savannah Area Decline (GSAD)	Conversion or change from grassland savannas to other LULC types	Population density, wildland fires, distance to built-up areas, and maximum temperatures

forest; Grassland savannas to Woody savannas; Grassland savannas to Water bodies; and Grassland savannas to Wetlands			
Water bodies to Open savannas/Barelands; Water bodies to Croplands; Water bodies to Built-up areas; Water bodies to Dense forest; Water bodies to Woody savannas; Water bodies to Grassland savannas; and Water bodies to Wetlands	Water body Loss (WL)	Conversion or change from water bodies to other LULC types	Maximum temperatures; and slope
Open savannas/Barelands to Water bodies; Croplands to Water bodies; Built-up areas to Water bodies; Dense forest to Water bodies; Woody savannas to Water bodies; Grassland savannas to Water bodies; and Wetlands to Water bodies	Water body Increase (WI)	Conversion or change from other LULC types to water bodies	Precipitation; and logging and forest clearing
Open savannas/Barelands to Wetlands; Croplands to Wetlands; Built-up to Wetlands; Dense forest to Wetlands; Woody savannas to Wetlands; Grassland savannas to Wetlands; and Water bodies to Wetlands	Wetland Increase (WI)	Conversion or change from other LULC types to wetlands	Precipitation
Wetlands to Open savannas/Barelands; Wetlands to Croplands; Wetlands to Built-up areas; Wetlands to Dense forest; Wetlands to Woody savannas; Wetlands to Grassland savannas; and Wetlands to Water bodies	Wetlands Loss (WetL)	Conversion or change from wetlands to other LULC types	Maximum temperatures, wildland fires and slope

Table S4. Accuracy assessment for the year 1990

LULC class	Croplands	Dense forest	Grassland savanna	Open savanna/ barelands	Built-up areas	Water bodies	Wetlands	Woody savanna	**Overall User's accuracy**
Croplands	85	3	0	24	0	0	0	1	75.2
Dense forest	0	1310	0	19	0	0	0	33	96.2
Grassland savanna	0	17	178	24	0	0	0	18	75.1
Open savanna/barelands	1	22	3	1082	2	0	0	32	94.9
Built-up areas	0	3	0	23	67	0	0	1	71.3
Water bodies	0	1	0	3	0	150	0	0	97.4
Wetlands	0	2	0	13	0	0	57	7	72.2
Woody savanna	0	63	0	63	0	0	0	616	83
Total	**86**	**1421**	**181**	**1261**	**69**	**150**	**57**	**708**	**83%**
Overall producer's accuracy (%)	**98.8**	**92.2**	**98.3**	**85.8**	**97.1**	**100**	**100**	**87**	
Overall accuracy = 94.9%									

Table S5. Accuracy assessment for the year 2000

LULC class	Croplands	Dense forest	Grassland savanna	Open savanna/ barelands	Built-up areas	Water bodies	Wetlands	Woody savanna	**Overall User's accuracy**
Croplands	96	1	0	28	2	0	0	3	76.8
Dense forest	2	1334	1	14	0	0	0	37	96.1
Grassland savanna	1	11	173	36	0	0	0	16	73
Open savanna/barelands	1	20	1	1074	1	1	0	44	94
Built-up areas	3	1	0	21	67	0	0	2	71.3
Water bodies	0	2	0	4	0	154	0	0	96.3
Wetlands	0	1	0	22	0	0	53	3	67.1
Woody savanna	0	69	0	63	0	0	0	610	82.2
Total	**103**	**1439**	**175**	**1262**	**70**	**155**	**53**	**715**	**82.1%**
Overall producer's accuracy (%)	**93.2**	**92.7**	**98.9**	**85.1**	**95.7**	**99.4**	**100**	**85.3**	
Overall accuracy = 93.8%									

Table S6. Accuracy assessment for the year 2010

LULC class	Croplands	Dense forest	Grassland savanna	Open savanna/ barelands	Built-up areas	Water bodies	Wetlands	Woody savanna	**Overall User's accuracy**
Croplands	95	0	0	32	0	0	0	3	73.1
Dense forest	1	1329	1	9	0	0	0	48	95.7
Grassland savanna	0	9	175	33	0	0	0	20	73.3
Open savanna/barelands	1	17	1	1089	2	0	1	31	95.4
Built-up areas	1	0	0	22	68	0	0	3	72.3
Water bodies	0	3	0	4	0	153	0	0	95.6
Wetlands	0	1	0	19	0	0	55	4	69.6
Woody savanna	2	16	3	20	0	0	0	701	94.5
Total	**100**	**1375**	**180**	**1228**	**70**	**153**	**56**	**810**	**83.7**
Overall producer's accuracy (%)	**95**	**96.7**	**97.2**	**88.7**	**97.2**	**100**	**98.2**	**86.5**	
Overall accuracy = 95%									

Table S7. Accuracy assessment for the year 2020

LULC class	Croplands	Dense forest	Grassland savanna	Open savanna/ barelands	Built-up areas	Water bodies	Wetlands	Woody savanna	**Overall User's accuracy**
Croplands	101	1	2	20	3	0	0	3	77.7
Dense forest	0	1345	1	11	1	0	0	30	96.9
Grassland savanna	0	7	179	29	0	0	0	22	75.5
Open savanna/barelands	2	17	1	1090	3	0	0	29	95.4
Built-up areas	2	0	0	6	85	0	1	0	90.4
Water bodies	0	2	0	4	0	154	0	0	96.3
Wetlands	0	1	0	7	0	1	67	3	84.8
Woody savanna	0	23	1	22	0	0	0	696	93.9
Total	**105**	**1396**	**184**	**1206**	**92**	**155**	**68**	**783**	**88.9**
Overall producer's accuracy (%)	**96.2**	**96.3**	**97.3**	**90.4**	**92.4**	**99.4**	**98.5**	**88.9**	
Overall accuracy = 94.9%									

Table S8. Validation of our LULC data for the year 2020. We validate our results through statistically significant correlations with datasets from other published studies. We report correlation strengths only for datasets that are available from the cited studies, and following the approach used in Yuh et al., (2023).

Land cover class	Modis global land cover products		Global forest cover data		Global croplands data		Global built-up data	
	Data available ?	Correlation strength	Data available ?	Correlation strength	Data available ?	Correlation strength	Data available ?	Correlation strength
Croplands	Yes	0.3	No	NA	Yes	0.9	No	NA
Dense forest	Yes	0.8	Yes	0.8	No	NA	No	NA
Grassland savanna	Yes	0.4	No	NA	No	NA	No	NA
Open savanna/ barelands	Yes	0.5	No	NA	No	NA	No	NA
Built-up areas	Yes	0.3	No	NA	No	NA	Yes	0.8
Water bodies	Yes	0.9	No	NA	No	NA	No	NA
Wetlands	Yes	0.9	No	NA	No	NA	No	NA
Woody savanna	Yes	NS	Yes	NS	No	NA	No	NA
Overall correlation		**0.6**		**0.8**		**0.9**		**0.8**

* Modis global land cover products (Friedl & Sulla-Menashe, 2019; Global forest cover data (Hansen et al., 2020; Potapovet al., 2020); Global croplands data (Potapovet al., 2021); Global built-up data (Potapovet al., 2020); NA = Not Applicable; NS = Non-significant

Table S9. Validation of our LULC data for the year 2010. We validate our results through statistically significant correlations with datasets from other published studies. We report correlation strengths only for datasets that are available from the cited studies, and following the approach used in Yuh et al., (2023).

Land cover class	Modis global land cover products		Global forest cover data		Global croplands data		Global built-up data	
	Data available ?	Correlation strength	Data available ?	Correlation strength	Data available ?	Correlation strength	Data available ?	Correlation strength
Croplands	Yes	0.4	No	NA	No	NA	No	NA
Dense forest	Yes	0.9	Yes	0.8	No	NA	No	NA
Grassland savanna	Yes	0.2	No	NA	No	NA	No	NA
Open savanna/ barelands	Yes	0.5	No	NA	No	NA	No	NA
Built-up areas	Yes	0.2	No	NA	No	NA	No	NA
Water bodies	Yes	0.8	No	NA	No	NA	No	NA
Wetlands	Yes	0.7	No	NA	No	NA	No	NA
Woody savanna	Yes	0.7	Yes	0.8	No	NA	No	NA
Overall correlation		**0.6**		**0.8**		**NA**		**NA**

* Modis global land cover products (Friedl & Sulla-Menashe, 2019; Global forest cover data (Hansen et al., 2013); Global croplands data (Potapovet al., 2021); Global built-up data (Potapovet al., 2020); NA = Not Applicale; NS = Non-significant

Table S10. Validation of our LULC data for the year 2000. We validate our results through statistically significant correlations with datasets from other published studies. We report correlation strengths only for datasets that are available from the cited studies, and following the approach used in Yuh et al., (2023).

Land cover class	Global forest cover data		Global croplands data		Global built-up data	
	Data available ?	Correlation strength	Data available ?	Correlation strength	Data available ?	Correlation strength
Croplands	No	NA	Yes	0.9	No	NA
Dense forest	Yes	0.9	No	NA	No	NA
Grassland savanna	No	NA	No	NA	No	NA
Open savanna/ barelands	No	NA	No	NA	No	NA
Built-up areas	No	NA	No	NA	Yes	0.8
Water bodies	No	NA	No	NA	No	NA
Wetlands	No	NA	No	NA	No	NA
Woody savanna	Yes	0.7	No	NA	No	NA
Overall correlation		**0.8**		**0.9**		**0.8**

* Global forest cover data (Hansen et al., 2010); Global croplands data (Potapov et al., 2021); Global built-up data (Potapov et al., 2020); NA = Not Applicable; NS = Non-significant

Table S11. Skill measure results for the most accurate LULC transitions

LULC transition	% transition accuracy/ skill measure	Key drivers
Dense forest to built-up	98	Distance to built-up areas and population density
Dense forest to croplands	85	Distance to built-up areas, logging and forest clearing, and population density
Dense forest to grassland savannas	95	Logging and forest clearing, maximum temperatures, wildland fires, and population density
Dense forest to woody savannas	81	Maximum temperatures, minimum temperatures, and logging and forest clearing
Dense forest to open savannas/barelands	96	Distance to built-up areas, population density, wildland fires, and logging and forest clearing
Grassland savannas to dense forest	82	slope
Open savannas/barelands to dense forest	70	slope
Woody savannas to dense forest	79	Slope and minimum temperatures
Grassland savannas to croplands	93	Population density
Woody savannas to croplands	80	Population density
Croplands to built-up areas	94	population density
Grassland savannas to built-up areas	88	Distance to built-up areas and population density
Open savannas/barelands to built-up areas	93	Distance to built-up areas and population density
Woody savannas to built-up	96	Distance to built-up areas and population density
Grassland savannas to woody savannas	71	Precipitation, and slope
Grassland savannas to water bodies	78	Precipitation and slope
Grassland savannas to wetlands	70	Precipitation
Grassland savannas to woody savannas	80	Minimum temperature, slope and elevation
Open savannas/barelands to grassland savannas	76	Precipitation, elevation, and slope
Open savannas/barelands to water bodies	87	Precipitation and slope
Open savannas/barelands to wetlands	81	Precipitation, minimum temperatures, and slope
Water bodies to wetlands	97	Maximum temperatures, and slope
Wetlands to water bodies	78	Precipitation
Woody savannas to grassland savannas	82	Population density, logging and forest clearing, and maximum and minimum temperatures

Table S12. Model results showing the influence of each land use change driver on the Built-up Abandonment and Intensification transition sub-models

Target variables	Built-up area Intensification			Built-up area Abandonment		
Predictor variables	**R^2**	**Adjusted R^2**	**p-value**	**R^2**	**Adjusted R^2**	**p-value**
Logging and forest clearing	0.03	-0.01	0.4088	0.003	-0.001	0.4088
Distance to built-up areas	0.4	0.4	2.2e-16	0.4	0.4	2.2e-16
Elevation	0.08	-0.03	0.6679	0.009	-0.004	0.6679
Slope	0.07	0.03	0.2064	0.7	0.6	0.00206
Wildland fires	0.02	-0.02	0.5024	0.002	-0.002	0.5024
Population density	0.3	0.2	0.0006	0.002	-0.003	0.6104
precipitation	0.05	-0.04	0.9165	0.005	-0.004	0.9165
Maximum temperature	0.01	0.01	0.1088	0.01	0.007	0.1088
Minimum temperature	0.02	0.01	0.05392	0.02	0.01	0.05392

Table S13. Model results showing the influence of each land use change driver on the Croplands Abandonment and Intensification transition sub-models

Target variables	Croplands Intensification			Croplands Abandonment		
Predictor variables	**R^2**	**Adjusted R^2**	**p-value**	**R^2**	**Adjusted R^2**	**p-value**
Logging and forest clearing	0.001	-0.001	0.5492	0.002	-0.001	0.4385
Distance to built-up areas	0.09	0.06	0.0601	0.004	-0.003	0.9704
Elevation	0.05	0.02	0.182	0.05	0.02	0.1768
Slope	0.03	0.09	0.2451	0.007	-0.003	0.8739
Wildland fires	0.04	0.02	0.1718	0.36	0.31	0.00714
Population density	0.2	0.2	0.04246	0.002	-0.002	0.7663
precipitation	0.005	-0.002	0.6663	0.02	-0.02	0.7651
Maximum temperature	0.09	-0.02	0.5343	0.66	0.63	0.00119
Minimum temperature	0.08	-0.02	0.561	0.001	-0.001	0.489

Table S14. Model results showing the influence of each land use change driver on the Deforestation and Afforestation transition sub-models

Target variables	Afforestation			Deforestation		
Predictor variables	**R^2**	**Adjusted R^2**	**p-value**	**R^2**	**Adjusted R^2**	**p-value**
Logging and forest clearing	0.01	0.01	1.07e-14	0.67	0.65	0.00071
Distance to built-up areas	0.12	0.12	2.2e-16	0.26	0.26	2.2e-16
Elevation	0.16	0.16	2.2e-16	0.2	0.2	2.2e-16
Slope	0.69	0.67	6.86e-08	0.14	0.13	2.2e-16
Wildland fires	0.08	0.08	2.2e-16	0.42	0.42	2.2e-16
Population density	0.03	0.03	2.2e-16	0.21	0.19	0.00139
precipitation	0.59	0.58	0.00091	0.02	0.02	0.001266
Maximum temperature	0.05	0.03	0.00118	0.66	0.22	0.00922
Minimum temperature	0.07	0.06	0.053	0.22	0.64	0.00077

Table S15. Model results showing the influence of each land use change driver on the Grassland Savannah Area Increase and Decline transition sub-models

Target variables	**Grassland savanna area increase**			**Grassland savanna area decline**		
Predictor variables	**R^2**	**Adjusted R^2**	**p-value**	**R^2**	**Adjusted R^2**	**p-value**
Logging and forest clearing	0.16	0.15	0.04997	0.001	-0.007	0.6942
Distance to built-up areas	0.45	0.36	0.02351	0.16	0.11	0.01698
Elevation	0.48	0.41	0.01855	0.07	-0.08	0.7743
Slope	0.96	0.84	0.00297	0.04	-0.04	0.5003
Wildland fires	0.11	0.1	0.00038	0.44	0.36	0.0018
Population density	0.18	0.11	0.1546	0.24	0.2	0.00962
precipitation	0.1	0.1	0.01945	0.07	-0.02	0.3794
Maximum temperature	0.19	0.19	4.43e-05	0.22	0.21	0.01117
Minimum temperature	0.17	0.17	0.000171	0.12	0.12	8.5e-05

Table S16. Model results showing the influence of each land use change driver on the Open savannas/Barelands Area Increase and Depletion transition sub-models

Target variables	Open savannas/Barelands Area Increase			Open savannas/Barelands Area Depletion		
Predictor variables	R^2	Adjusted R^2	p-value	R^2	Adjusted R^2	p-value
Logging and forest clearing	0.31	0.29	0.00021	0.003	0.002	0.00019
Distance to built-up areas	0.3	0.3	0.01367	0.18	0.13	0.01367
Elevation	0.28	0.25	0.00040	0.28	0.25	0.00040
Slope	0.02	0.02	0.00059	0.26	0.24	0.00062
Wildland fires	0.17	0.17	0.03361	0.002	-0.002	0.3361
Population density	0.41	0.41	0.04632	0.21	0.21	0.04632
precipitation	0.01	0.01	6.4e-12	0.19	0.19	6.45e-12
Maximum temperature	0.00	0.00	0.9	0.002	-0.002	0.9231
Minimum temperature	0.02	0.02	2.2e-16	0.15	0.15	2.2e-16

Table S17. Model results showing the influence of each land use change driver on water bodies increase and loss transition sub-models

Target variables	**Water body increase**			**Water body loss**		
Predictor variables	**R^2**	**Adjusted R^2**	**p-value**	**R^2**	**Adjusted R^2**	**p-value**
Logging and forest clearing	0.47	0.37	0.02723	0.05	0.04	0.02723
Distance to built-up areas	0.002	-0.009	0.967	0.002	-0.009	0.967
Elevation	0.004	-0.005	0.5026	0.004	-0.005	0.5026
Slope	0.08	0.08	0.00196	0.91	0.82	0.0023
Wildland fires	0.04	0.03	0.03466	0.04	0.03	0.03466
Population density	0.007	-0.009	0.5276	0.007	-0.009	0.5276
precipitation	0.44	0.43	0.00832	0.004	-0.009	0.8527
Maximum temperature	0.18	0.17	0.004601	0.7	0.7	0.0056
Minimum temperature	0.16	0.11	0.1949	0.02	0.01	0.29

Table S18. Model results showing the influence of each land use change driver on wetlands Increase and loss transition sub-models

Target variables	**Wetland gain**			**Wetland loss**		
Predictor variables	**R^2**	**Adjusted R^2**	**p-value**	**R^2**	**Adjusted R^2**	**p-value**
Logging and forest clearing	0.02	0.004	0.2546	0.008	-0.004	0.4177
Distance to built-up areas	0.02	0.008	0.2174	0.03	0.02	0.1319
Elevation	0.05	0.04	0.05686	0.11	0.1	0.00249
Slope	0.05	0.04	0.07496	0.24	0.21	0.01671
Wildland fires	0.02	0.02	3.9e-06	0.29	0.28	2.6e-07
Population density	0.004	-0.02	0.6649	0.01	-0.001	0.3426
precipitation	0.94	0.81	0.01074	0.11	0.11	0.00208
Maximum temperature	0.002	-0.01	0.9149	0.2	0.2	0.00208
Minimum temperature	0.07	0.06	0.02538	0.13	0.12	0.00122

Table S19. Model results showing the influence of each land use change driver on woody savannah Area Increase and loss transition sub-models

Target variables	**Woody savanna gain**			**Woody savanna loss**		
Predictor variables	**R^2**	**Adjusted R^2**	**p-value**	**R^2**	**Adjusted R^2**	**p-value**
Logging and forest clearing	0.83	0.79	5.4e-05	0.35	0.31	0.008273
Distance to built-up areas	0.01	0.01	0.0661	0.04	0.04	0.003014
Elevation	0.12	0.11	1.2e-06	0.01	0.01	7.28e-08
Slope	0.31	0.26	0.01368	0.03	0.02	0.01529
Wildland fires	0.14	0.14	6.9e-08	0.23	0.22	1.25e-11
Population density	0.002	-0.002	0.5017	0.77	0.76	0.002195
precipitation	0.93	0.88	2.0e-05	0.15	0.11	0.08551
Maximum temperature	0.28	0.23	0.0183	0.41	0.36	0.004641
Minimum temperature	0.22	0.21	6.3e-11	0.13	0.13	2.84e-07

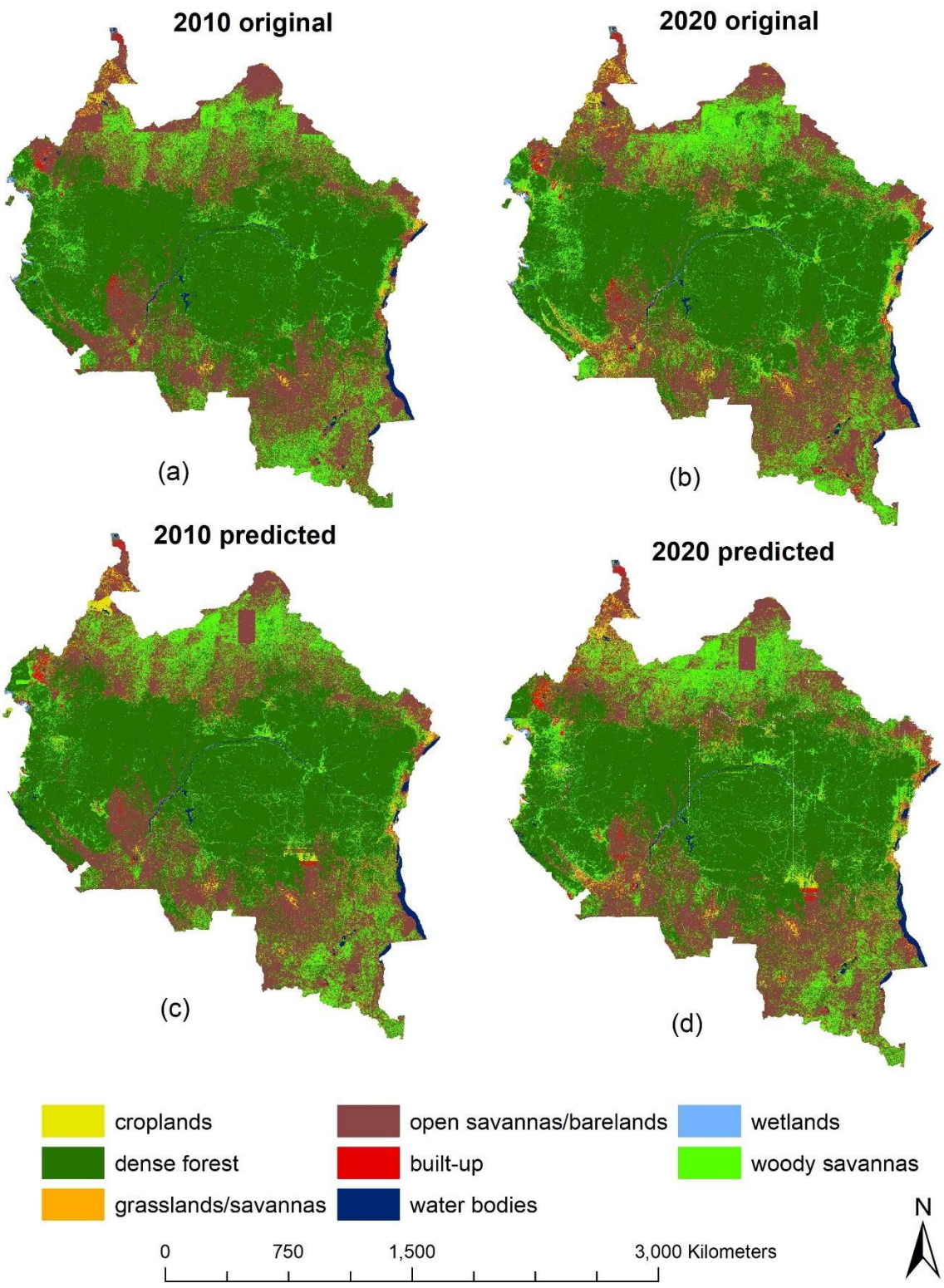

Figure S1. Comparison between our mapped (original) and predicted LULC products between the years 2010 and 2020. Map products show strong correlations between the original and predicted datasets as quantified in Table S12a and b, suggesting the reliability of the ILCM in predicting LULCC.

Table S20a. Accuracy validation for our predicted LULC datasets for the year 2010. Table shows Correlation strengths between our mapped LULC data for the year 2010, and datasets predicted for the year 2010 by the TerrSet Idrissi Land Change Modeler.

LULC classes	Croplands predicted 2010	Dense forest predicted 2010	Grassland savanna predicted 2010	Open savannas/ barelands predicted 2010	Built-up area predicted 2010	Water bodies predicted 2010	Wetlands predicted 2010	Woody savanna predicted 2010
Croplands	0.7							
Dense forest		0.9						
Grassland savanna			0.6					
Open savannas/ barelands				0.8				
Built-up areas					0.8			
Water bodies						0.8		
Wetlands							0.8	
Woody savanna								0.7

Overall correlation strength = 0.8

Table S20b. Accuracy validation for our predicted LULC datasets for the year 2020. Table shows Correlation strengths between our mapped LULC data for the year 2020, and datasets predicted for the year 2020 by the TerrSet Idrissi Land Change Modeler.

LULC classes	Croplands predicted 2020	Dense forest predicted 2020	Grassland savanna predicted 2020	Open savannas/ barelands predicted 2020	Built-up area predicted 2020	Water bodies predicted 2020	Wetlands predicted 2020	Woody savanna predicted 2020
Croplands	0.8							
Dense forest		0.9						
Grassland savanna			0.5					
Open savannas/ barelands				0.8				
Built-up areas					0.8			
Water bodies						0.9		
Wetlands							0.8	
Woody savanna								0.7

Overall correlation strength = 0.8

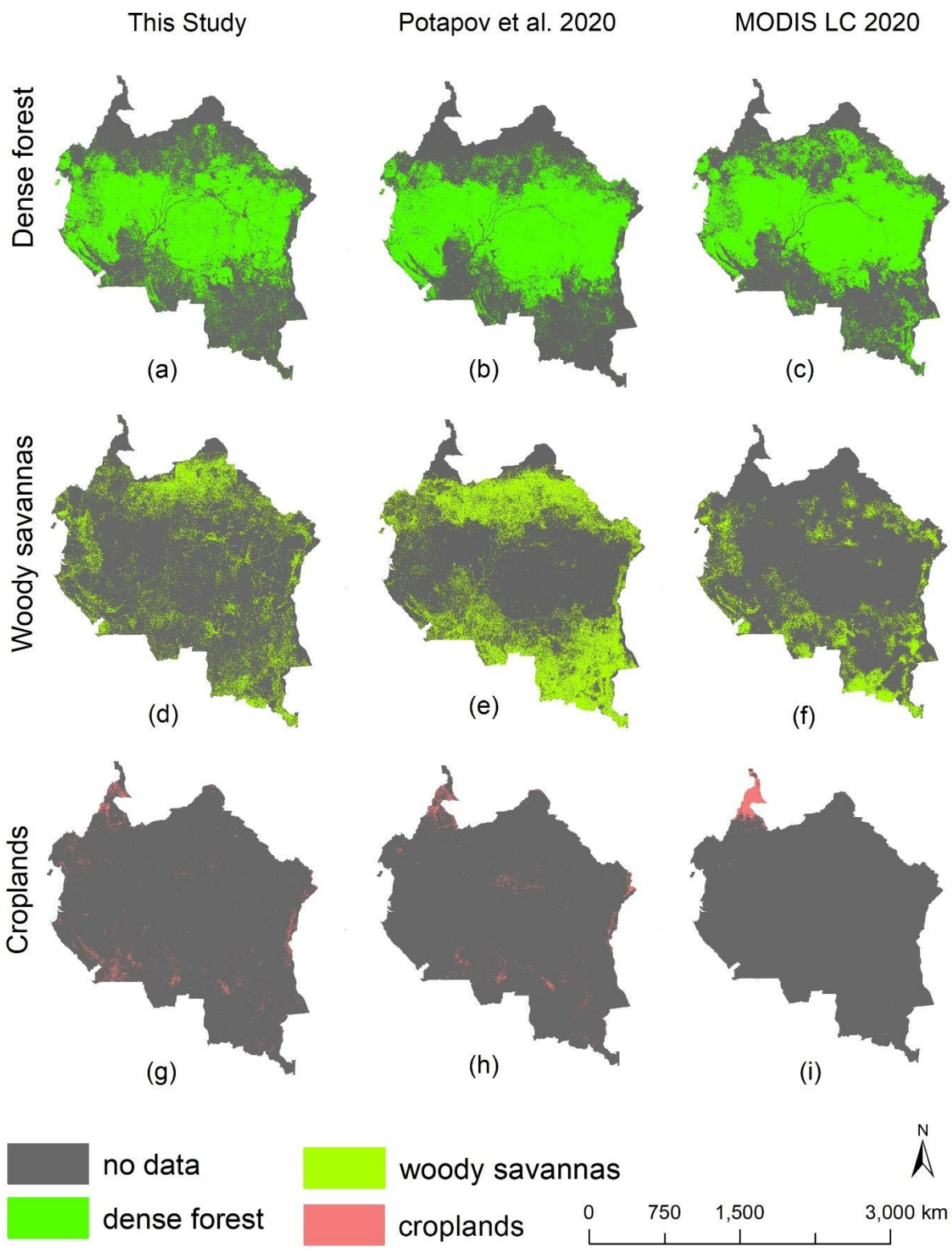

Figure S2. Maps showing comparison between our LULC classes and LULC data extracted from the MODIS global land cover products (Friedl & Sulla-Menashe, 2019), as well as products published by Potapov et al., (2020, 2021). Map comparisons are for the year 2020, and represent a comparison between dense forest (a-c), woody savanna (d-f) and croplands (g-i).

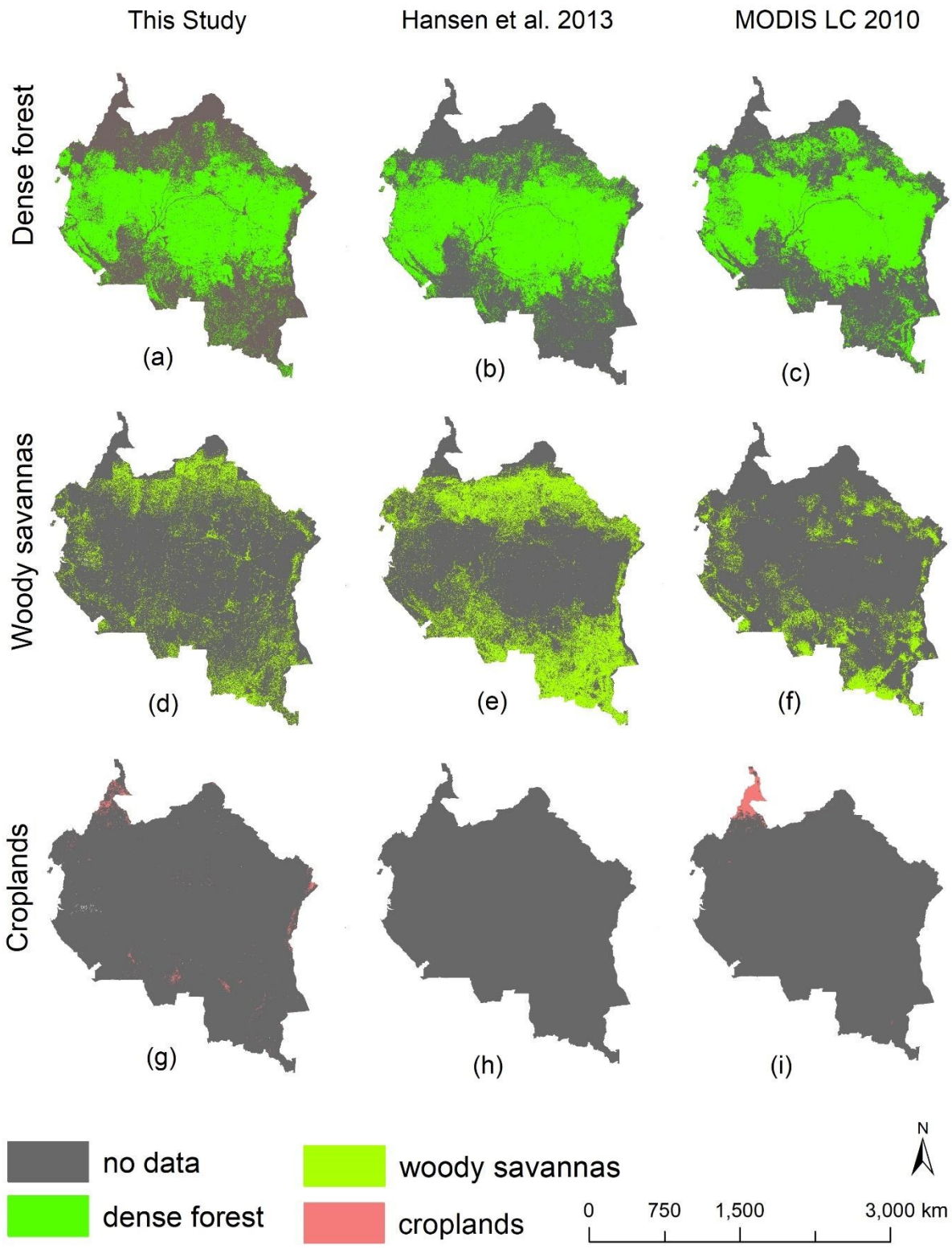

Figure S3. Maps showing comparison between our LULC classes and LULC data extracted from the MODIS global land cover products (Friedl & Sulla-Menashe, 2019), as well as products published by Hansen et al., (2013), Potapov et al., (2021). Map comparisons are for the year 2010, and represent a comparison between dense forest (a-c), woody savanna (d-f) and croplands (g-i).

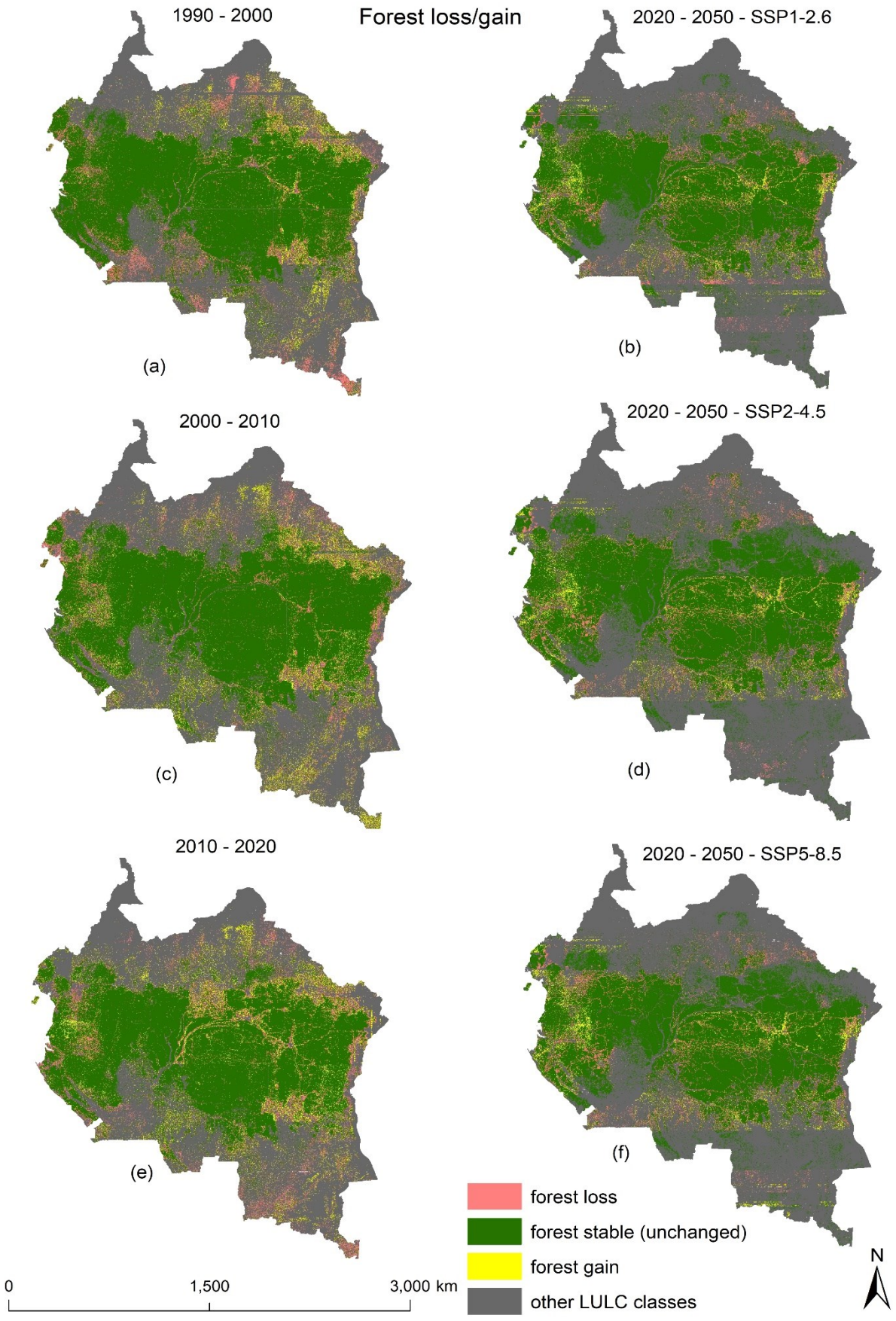

Figure S4. Map of forest cover loss and gain in the Congo Basin, under all four change periods

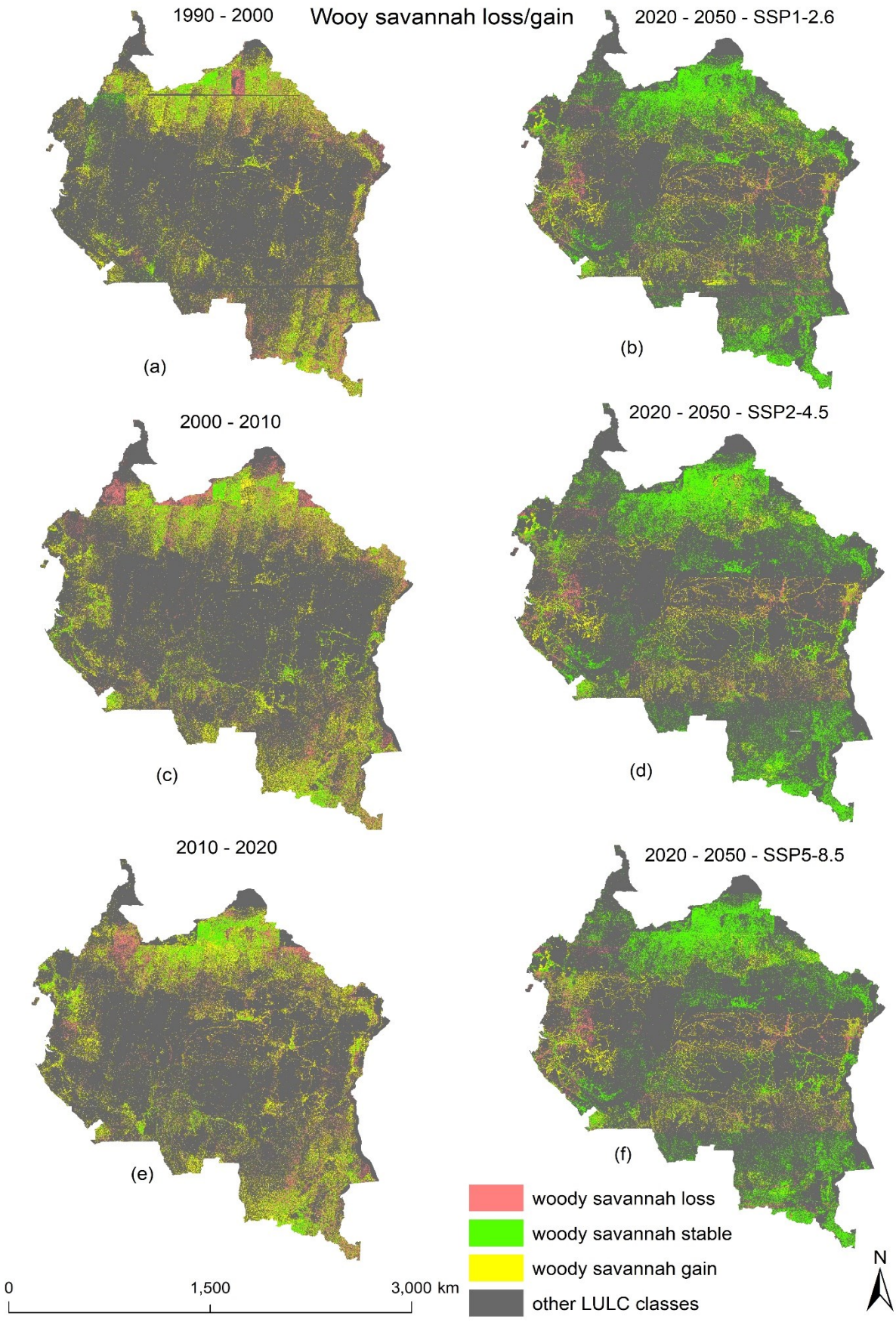

Figure S5. Map of woody savannah loss and gain in the Congo Basin, under all four change periods

Figure S6. Map showing loss and gains in built-up areas within the Congo Basin under all four change periods.

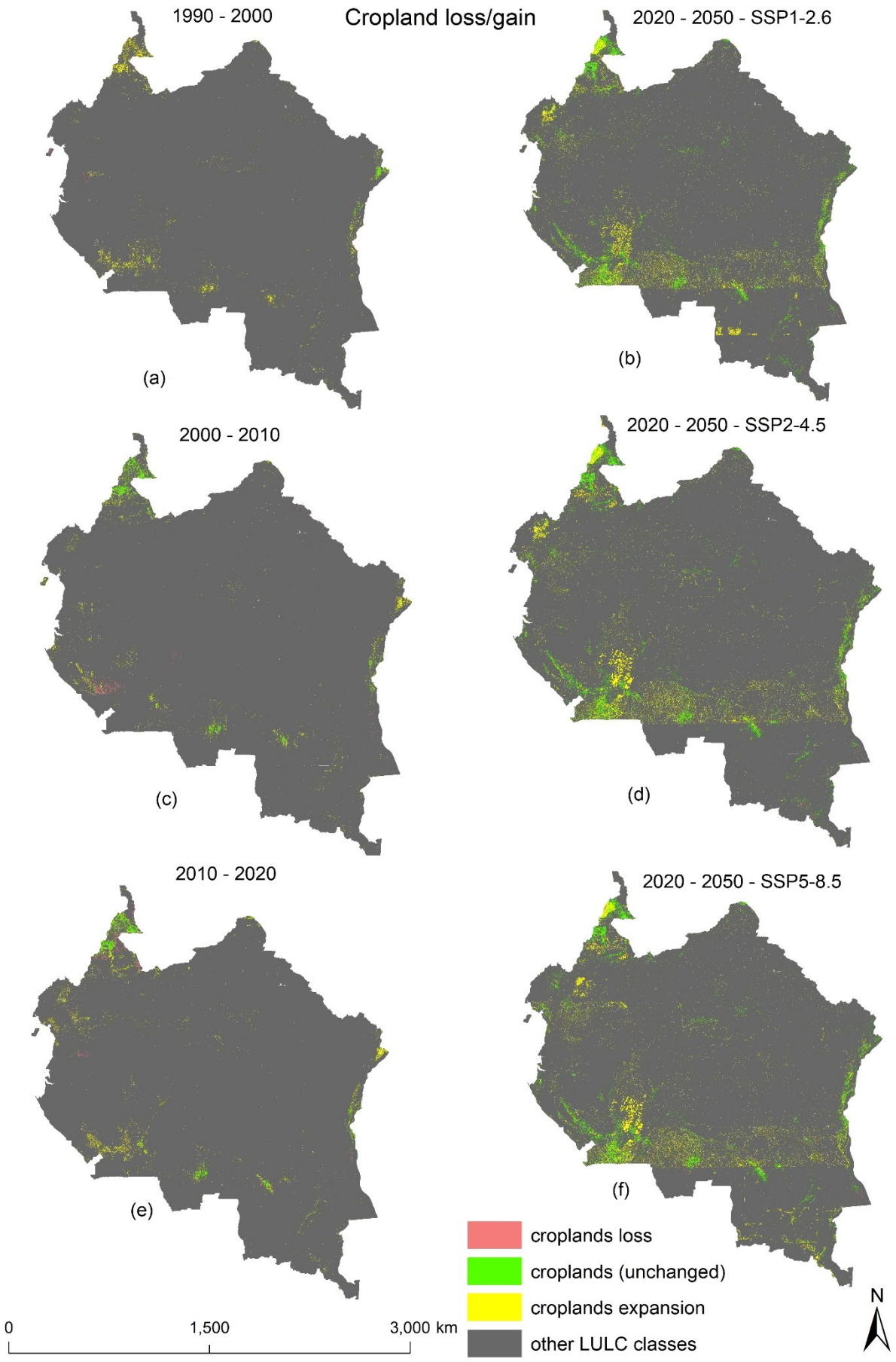

Figure S7. Map of croplands gains/losses in the Congo Basin, under all four change periods

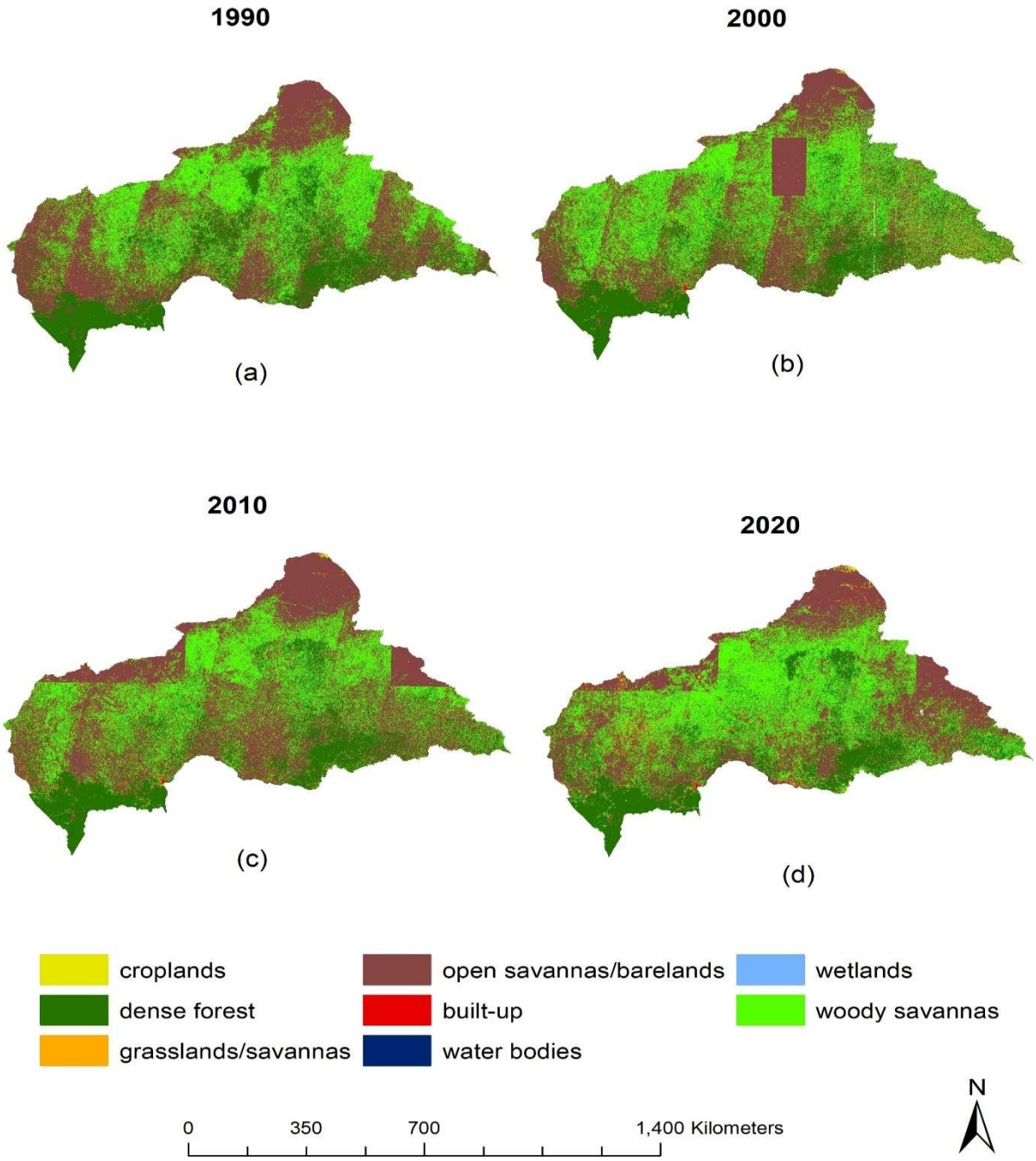

Figure S8a. Land cover classification maps for the Central African Republic (CAR), for the years 1990, 2000, 2010, and 2020.

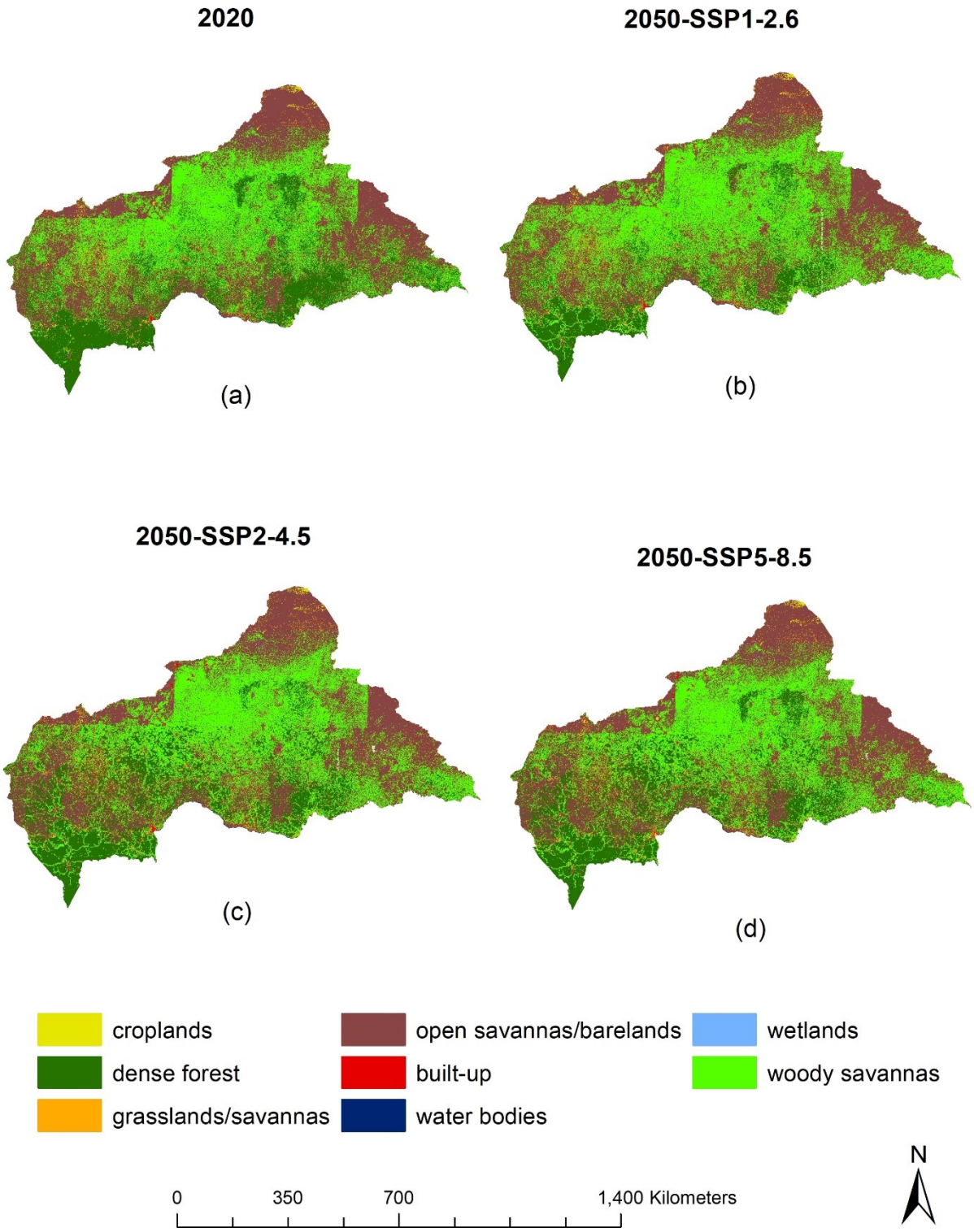

Figure S8b. Projected LULC maps of the CAR for the year 2050. Map shows projected results under all three climate change scenarios (SSP1-2.6, SSP2-4.5 and SSP5-8.5), with the year 2020 representing the baseline condition (for comparison purpose).

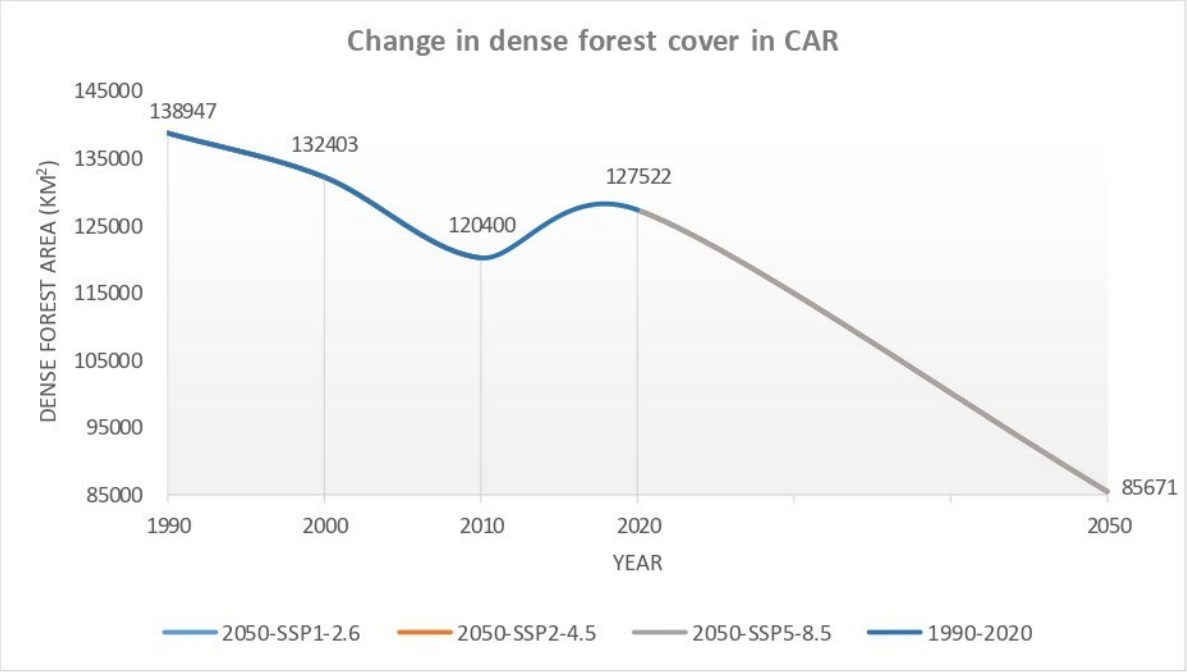

Figure S8c. Change in dense forest cover within the CAR under all four change periods (1990-2000, 2000-2010, 2010-2020, and 2020-2050-under SSP1-2.6, SSP2-4.5, and SSP5-8.5 climate change scenarios).

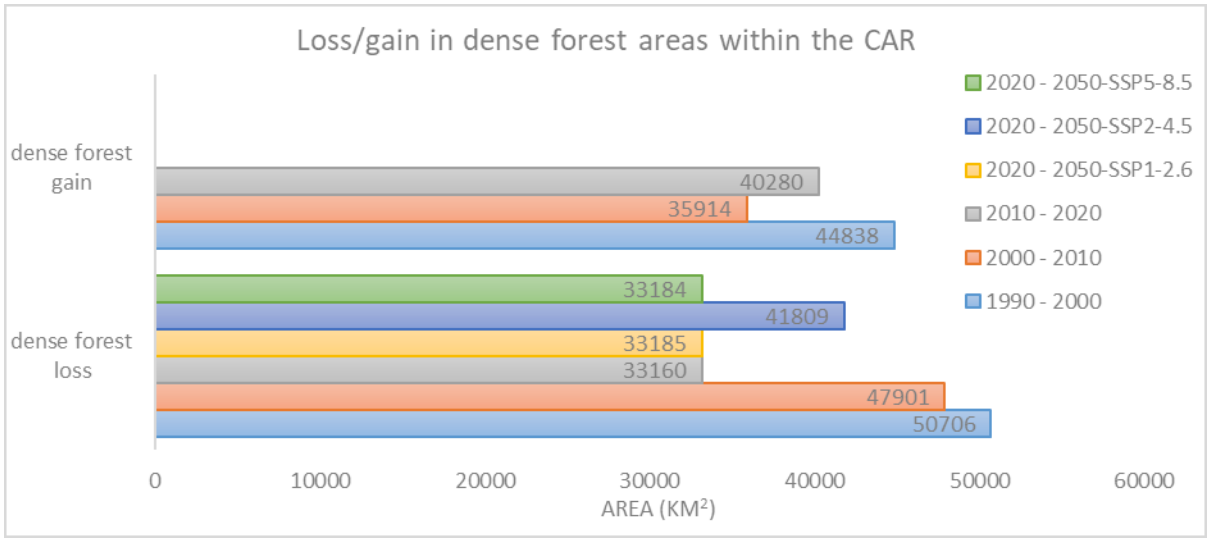

Figure S8d. Comparison in dense forest cover loss and gain in the Central African Republic, across all four change periods

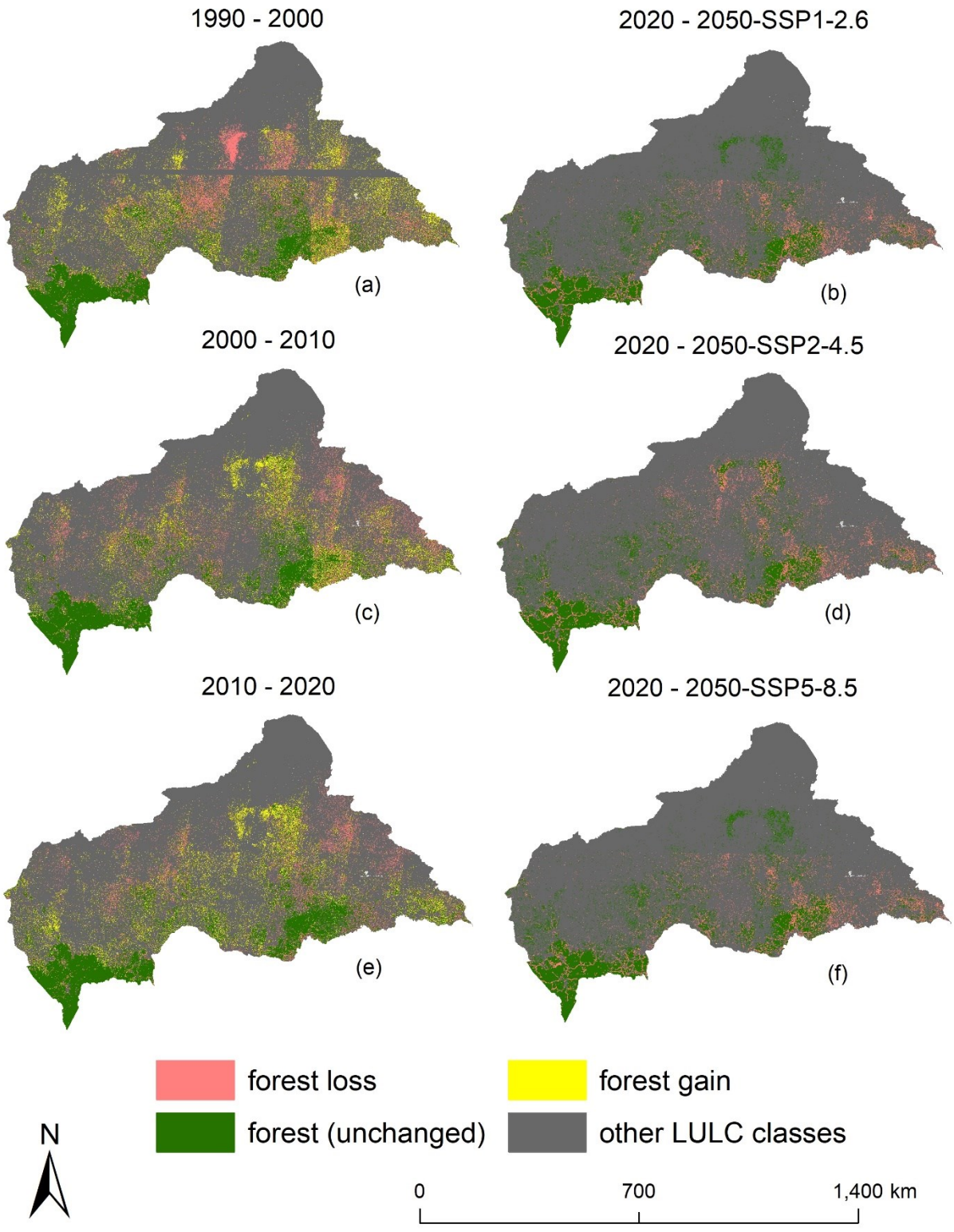

Figure S8e. Map of forest cover loss and gain in the CAR, under all four change periods

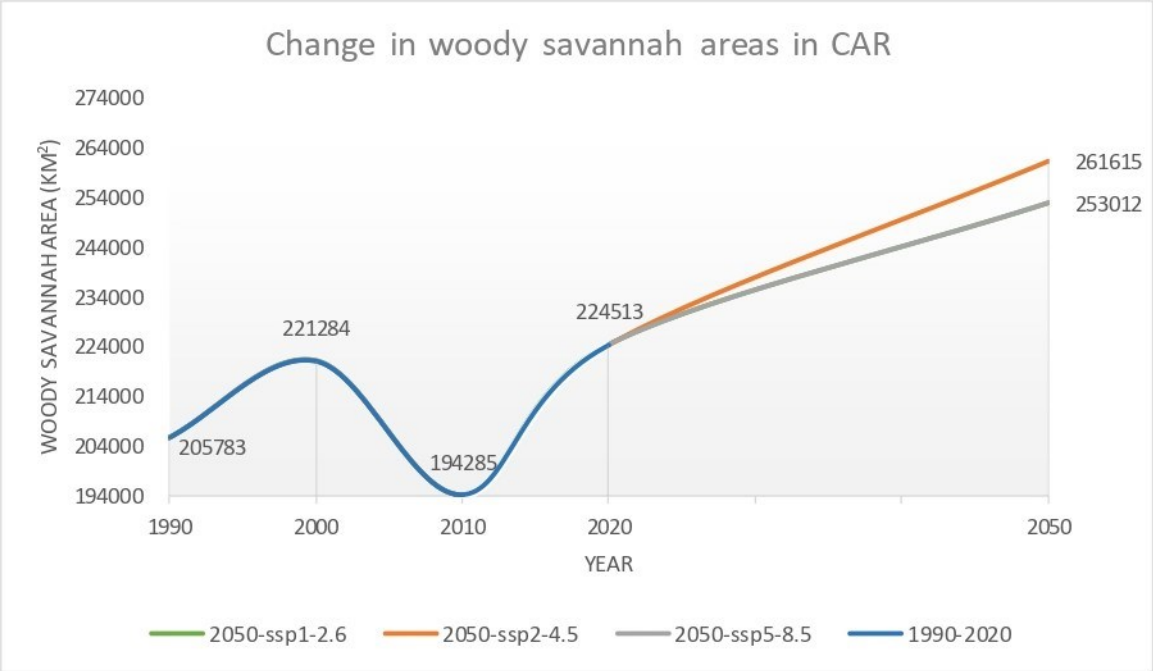

Figure S8f. Change in woody savannah areas within the CAR, under all four change periods

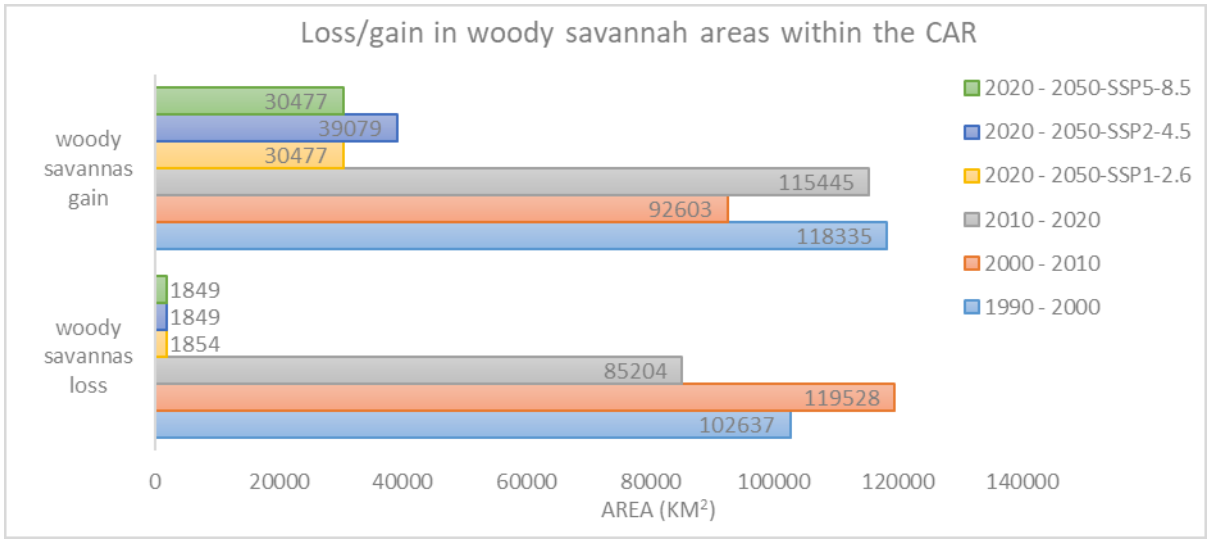

Figure S8g. Comparison in woody savannah loss and gain in the CAR, across all four change periods

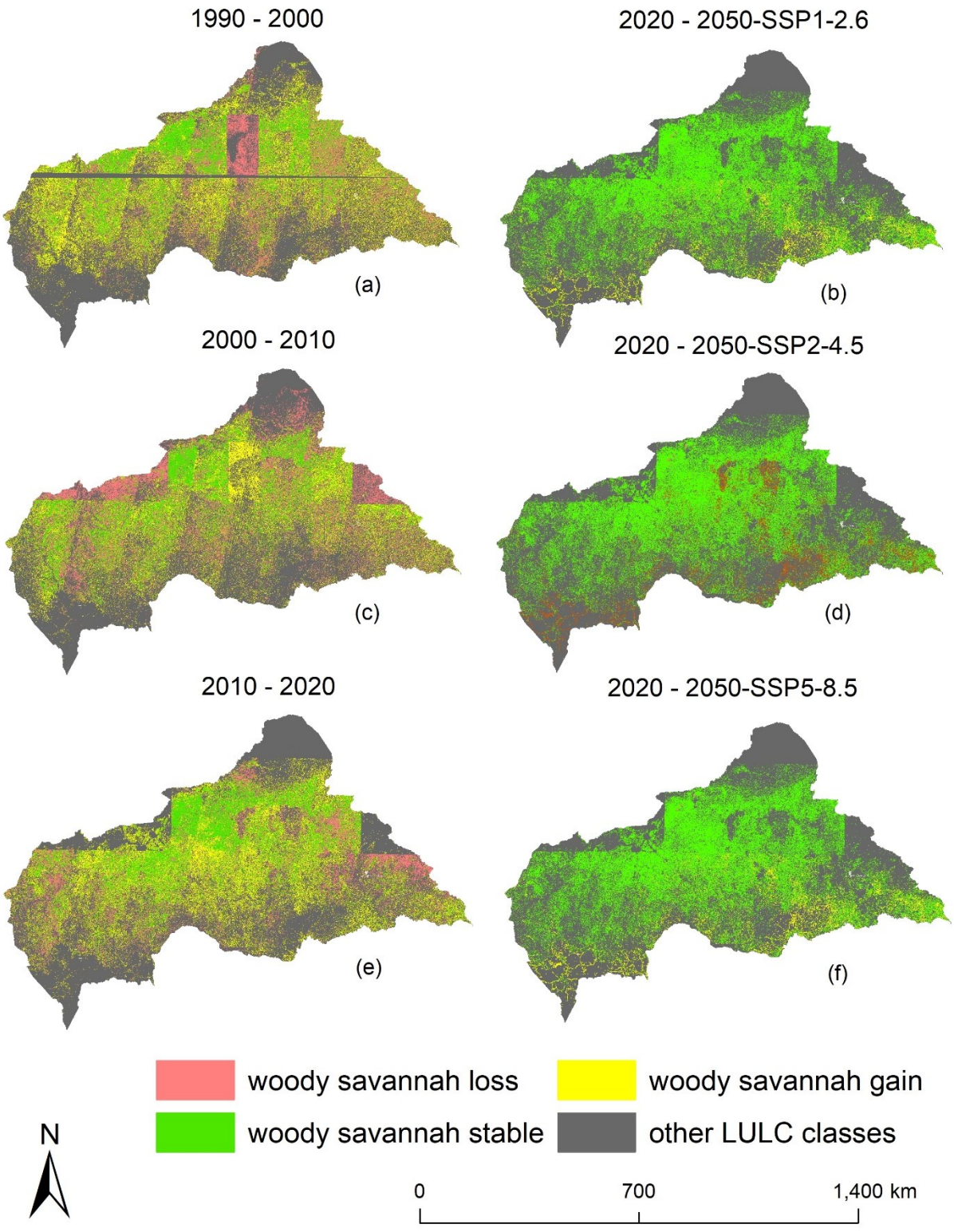

Figure S8h. Map of woody savannah loss and gain in the CAR, under all four change periods

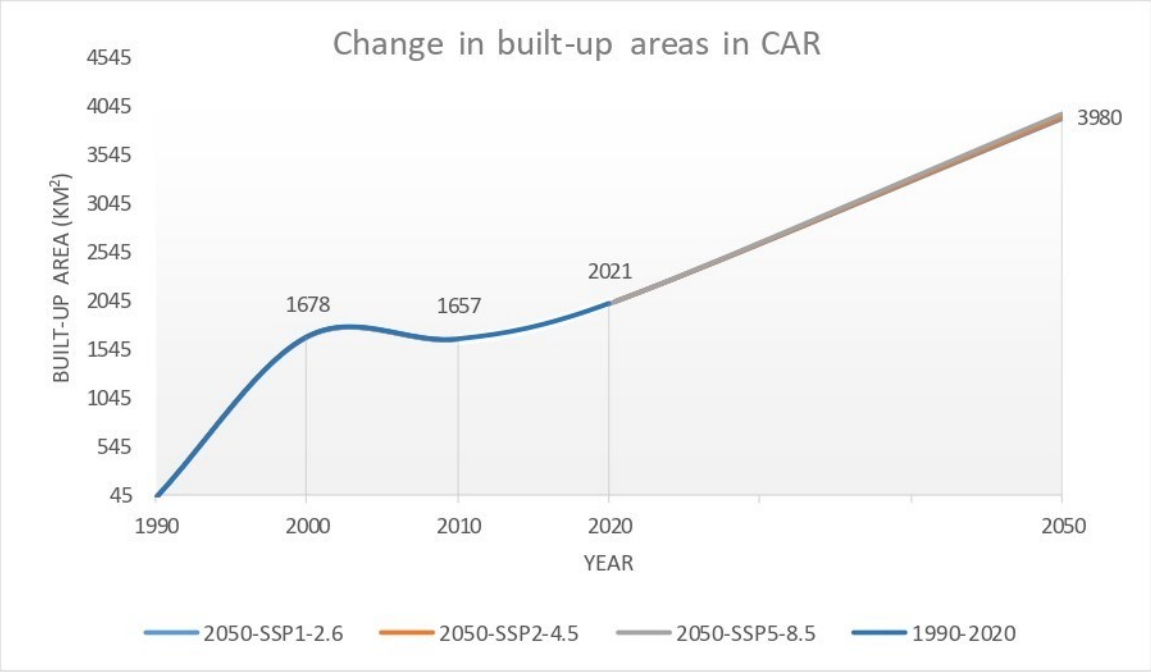

Figure S8i. Change in built-up areas within the CAR under all four change periods

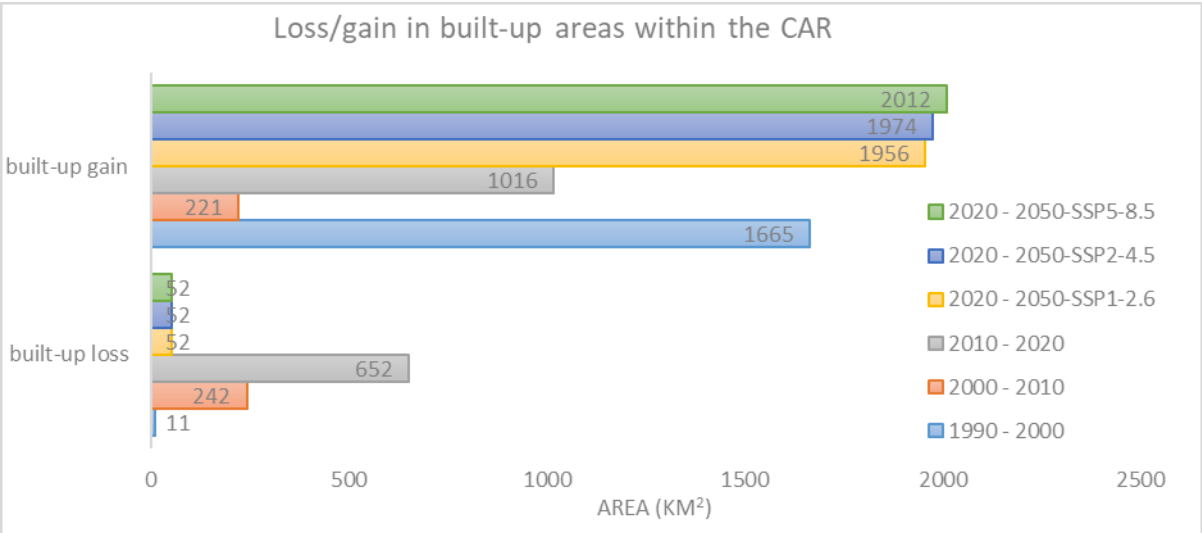

Figure S8j. Comparison in built-up area loss and gain in the CAR, across all four change periods

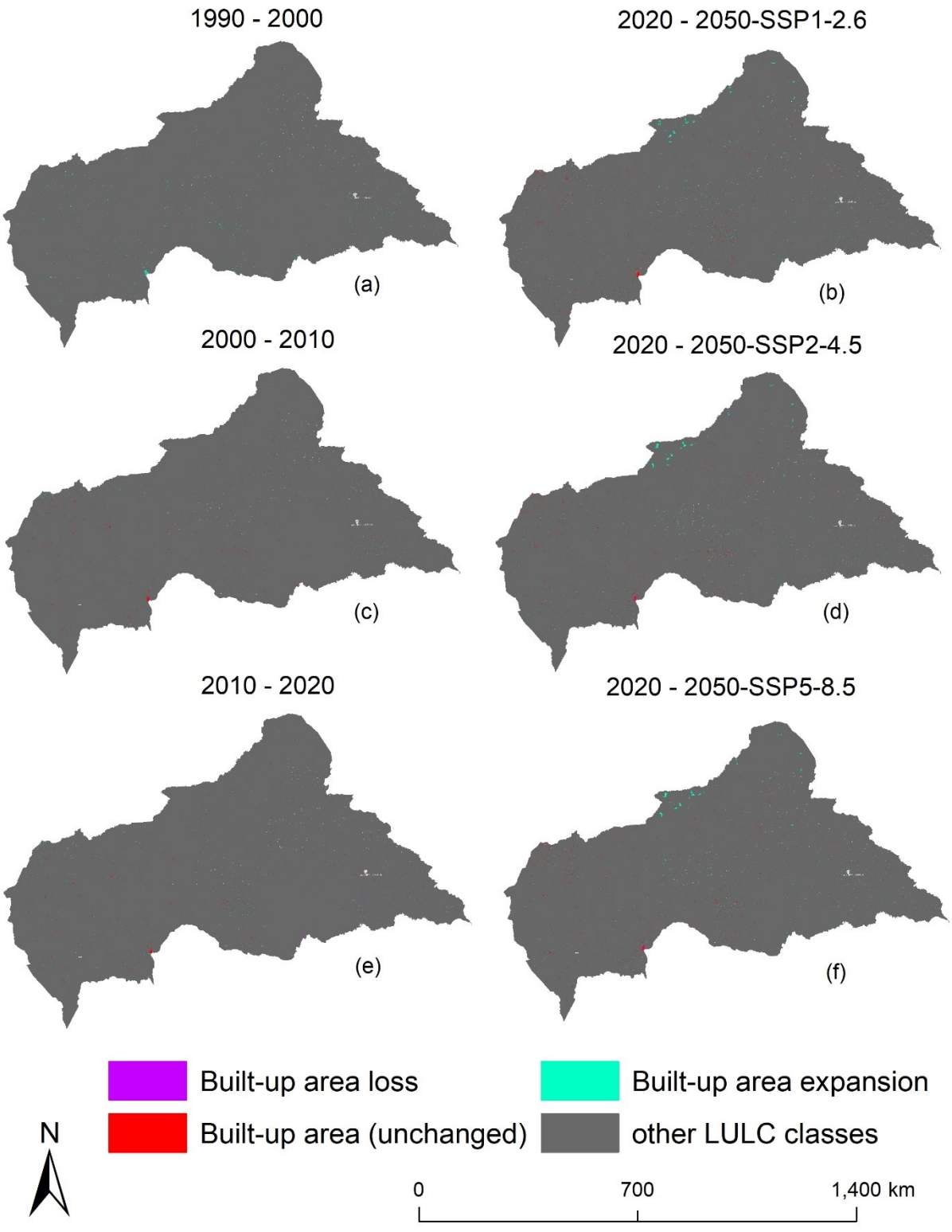

Figure S8k. Map showing loss and gains in built-up areas within the CAR, under all four change periods

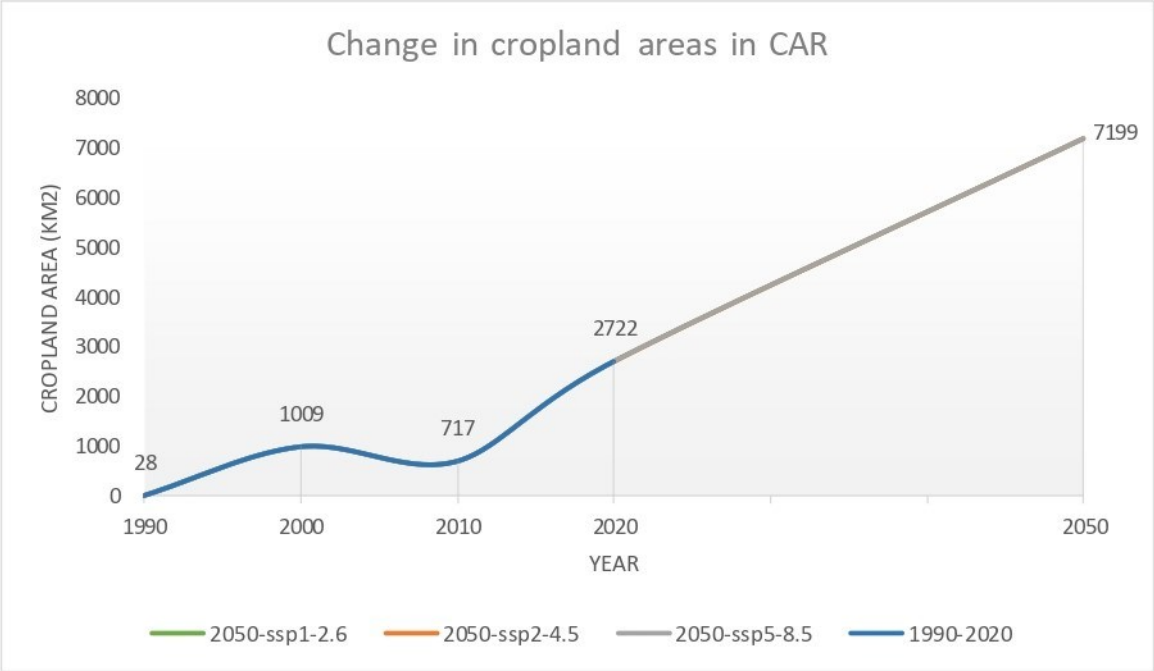

Figure S8l. Change in cropland areas within the CAR, under all four change periods

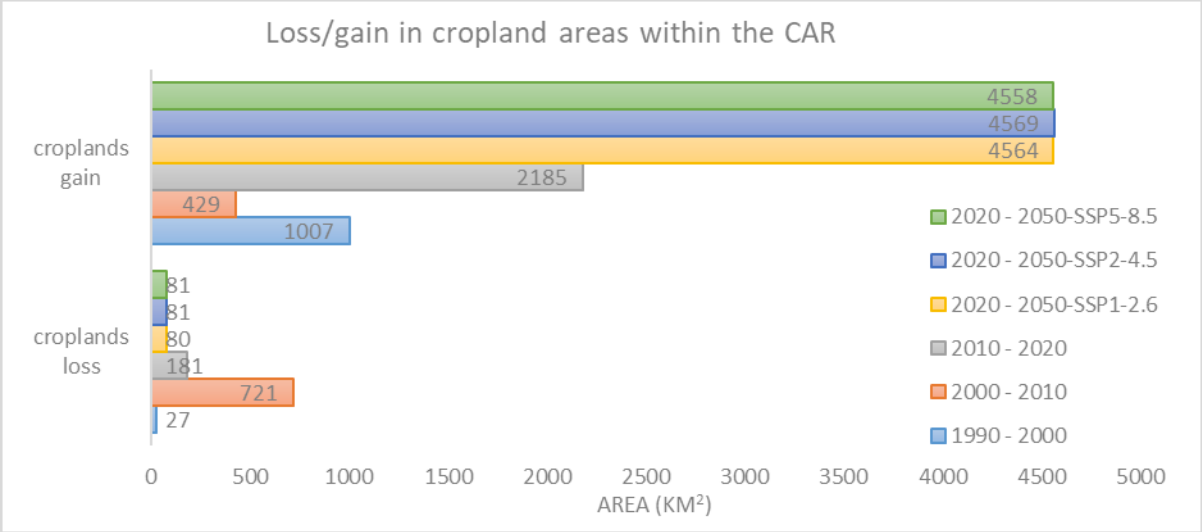

Figure S8m. Comparison in cropland area loss and gain in the CAR, across all four change periods

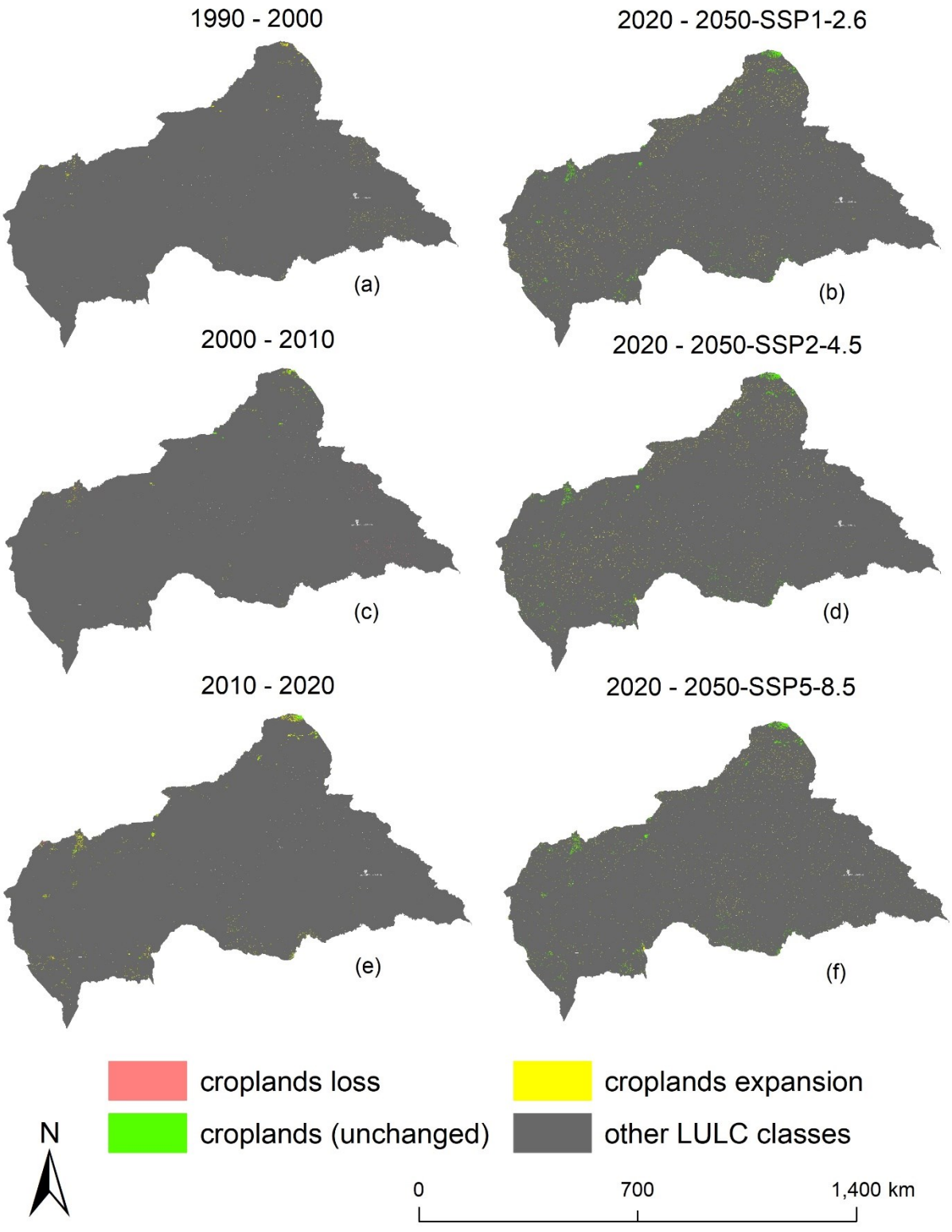

Figure S8n. Map of croplands gain/loss in the CAR, under all four change periods

Table S21a. Area and proportion of land cover classes in each year of study in CAR

	1990		2000		2010		2020		2050					
									SSP1-2.6		SSP2-4.5		SSP5-8.5	
LULC class	**Area (km2)**	**% Area**	**Area (km2)**	**% Area**	**Area (km2)**	**% Area**	**Area (km2)**	**% Area**	Area (km2)	% Area	Area (km2)	% Area	Area (km2)	% Area
croplands	28	0	1008.5	0.2	717.3	0.1	2721.5	0.4	7204.3	1.2	7209.7	1.2	7198.5	1.2
dense forest	138947.1	22.2	132402.5	21.1	120399.7	19.2	127521.6	20.4	85670.7	13.9	85671.2	13.7	85671.2	13.9
grassland/savannas	3697.5	0.6	12930.1	2.1	8323.3	1.3	11215.7	1.8	12902.5	2.1	12950.4	2.1	12902.5	2.1
open savannas/barelands	277273.3	44.2	252308	40.3	299309	47.8	256369.9	41	252769.5	41	252713.7	40.4	252713.7	40.9
built-up areas	23.3	0	1677.6	0.3	1657	0.3	2020.2	0.3	3924.5	0.6	3942.6	0.6	3980.1	0.6
water bodies	1055.5	0.2	2576.6	0.4	1169.5	0.2	1046	0.2	1029.7	0.2	1030.5	0.2	1029.7	0.2
wetlands	83.5	0	2190.3	0.3	360.9	0.1	636.9	0.1	627.1	0.1	627	0.1	627	0.1
woody savannas	205782.8	32.8	221284.2	35.3	194285.4	31	224512.5	35.9	253006.8	41	261614.7	41.8	253012.2	41
Total	626891.1	100	626377.8	100	626222	100	626044.3	100	617135.1	100	625759.9	100	617135.1	100

Table S21b. Quantified decadal changes in land cover patterns in CAR, between 1990-2020

	1990-2000		2000-2010		2010-2020		2020-2050					
							SSP1-2.6		SSP2-4.5		SSP5-8.5	
LULC classes	**Area (km2)**	**% Area**	**Area (km2)**	**% Area**	**Area (km2)**	**% Area**	**Area (km2)**	**% Area**	**Area (km2)**	**% Area**	**Area (km2)**	**% Area**
croplands	980.4	0.2	-291.1	0	2004.2	0.3	4482.8	0.8	4488.2	0.8	4477	0.8
dense forest	-6544.7	-1	-12002.8	-1.9	7121.9	1.1	-41850.9	-6.5	-41850.4	-6.7	-41850.4	-6.5
grassland/savannas	9232.6	1.5	-4606.8	-0.7	2892.4	0.5	1686.8	0.3	1734.7	0.3	1686.8	0.3
open savannas/barelands	-24965.3	-3.9	47001	7.5	-42939.1	-6.8	-3600.4	0.0	-3656.2	-0.6	-3656.2	-0.1
built-up areas	1654.3	0.3	-20.6	0	363.2	0.1	1904.3	0.3	1922.4	0.3	1959.9	0.3
water bodies	1521.1	0.2	-1407.1	-0.2	-123.5	0	-16.3	0.0	-15.5	0.0	-16.3	0.0
wetlands	2106.9	0.3	-1829.4	-0.3	276	0	-9.8	0.0	-9.9	0.0	-9.9	0.0
woody savannas	15501.4	2.5	-26998.8	-4.3	30227.1	4.8	28494.3	5.1	37102.2	5.9	28499.7	5.1

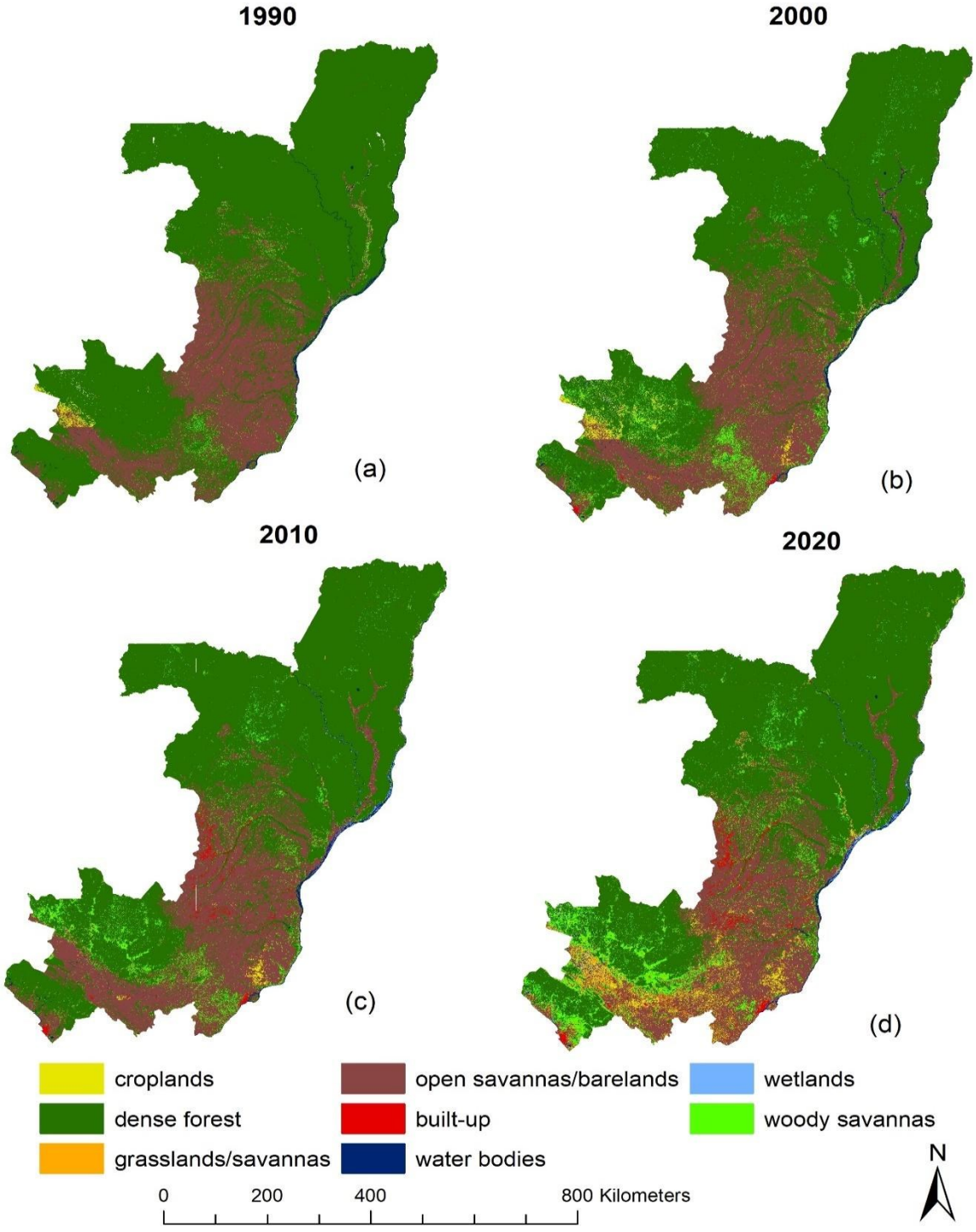

Figure S9a. Land cover classification maps for the Republic of Congo, for the years 1990, 2000, 2010, and 2020.

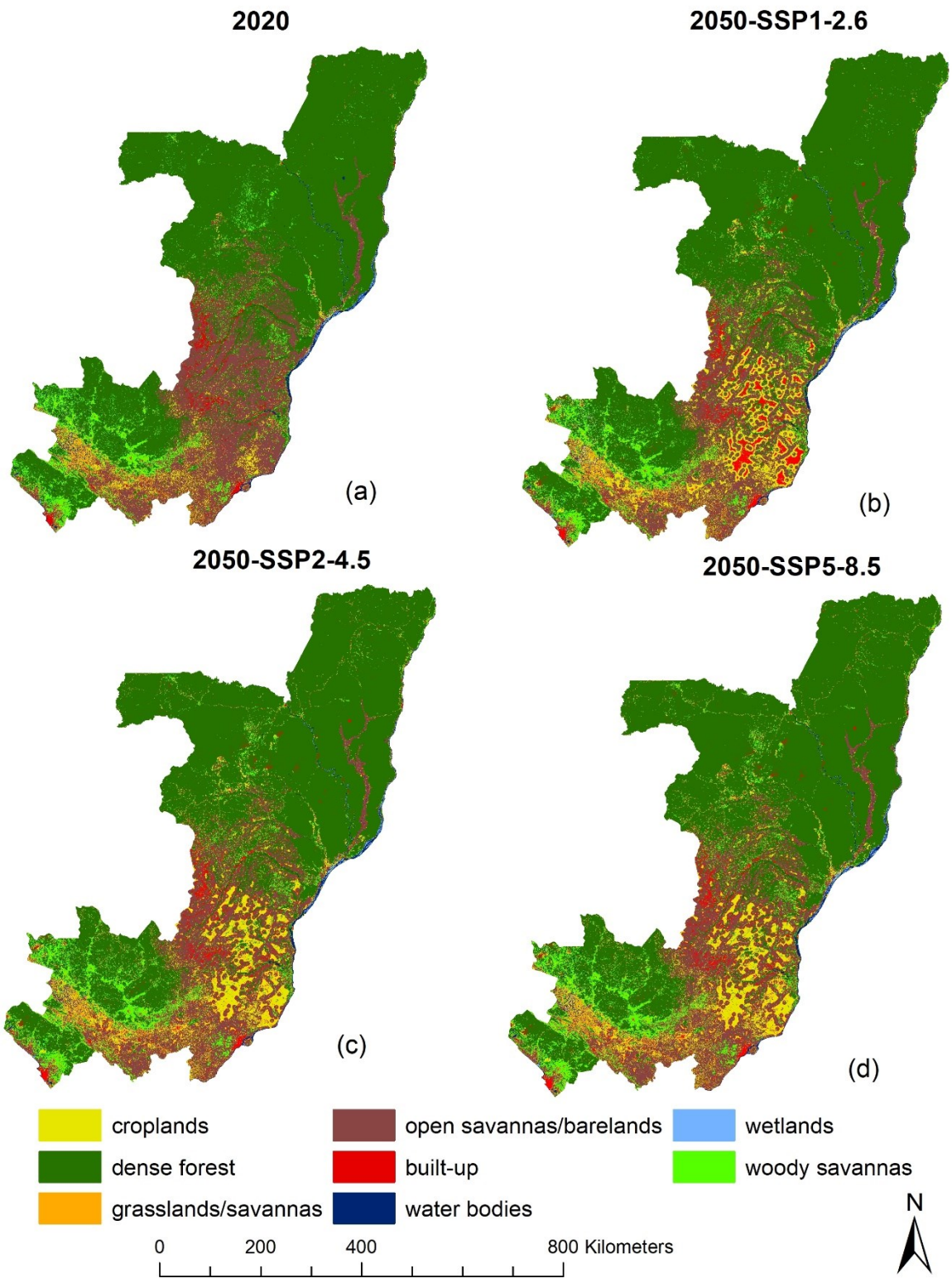

Figure S9b. Projected LULC maps of the Republic of Congo for the year 2050. Map shows projected results under all three climate change scenarios (SSP1-2.6, SSP2-4.5 and SSP5-8.5), with the year 2020 representing the baseline condition (for comparison purpose).

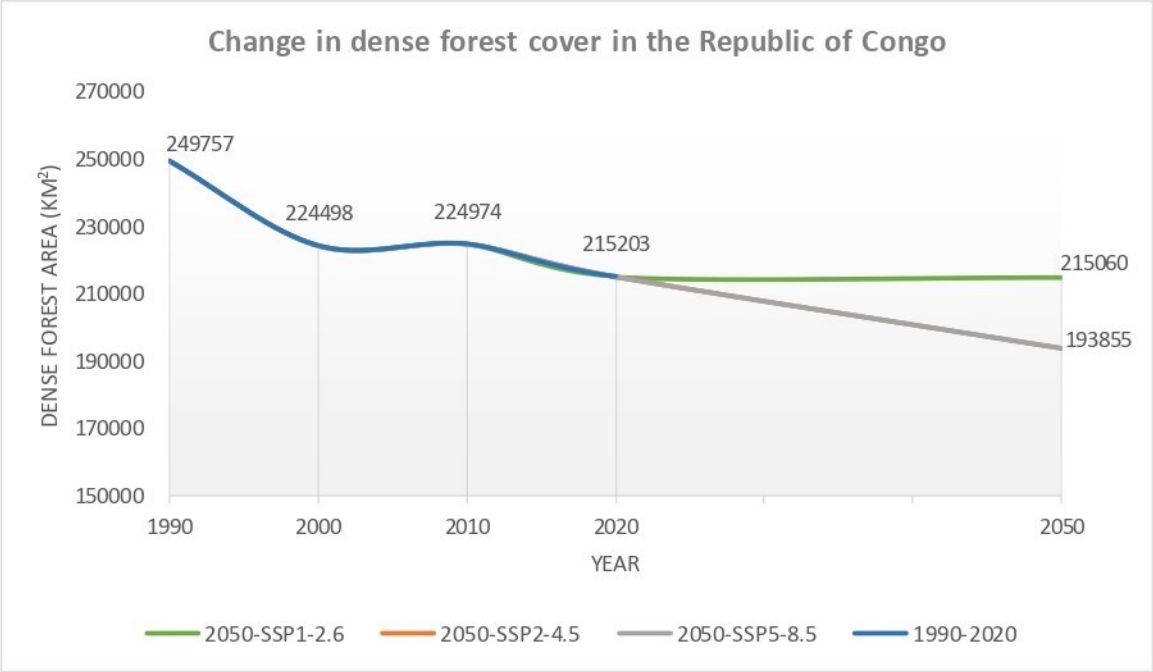

Figure S9c. Change in dense forest cover within the Republic of Congo, under all four change periods

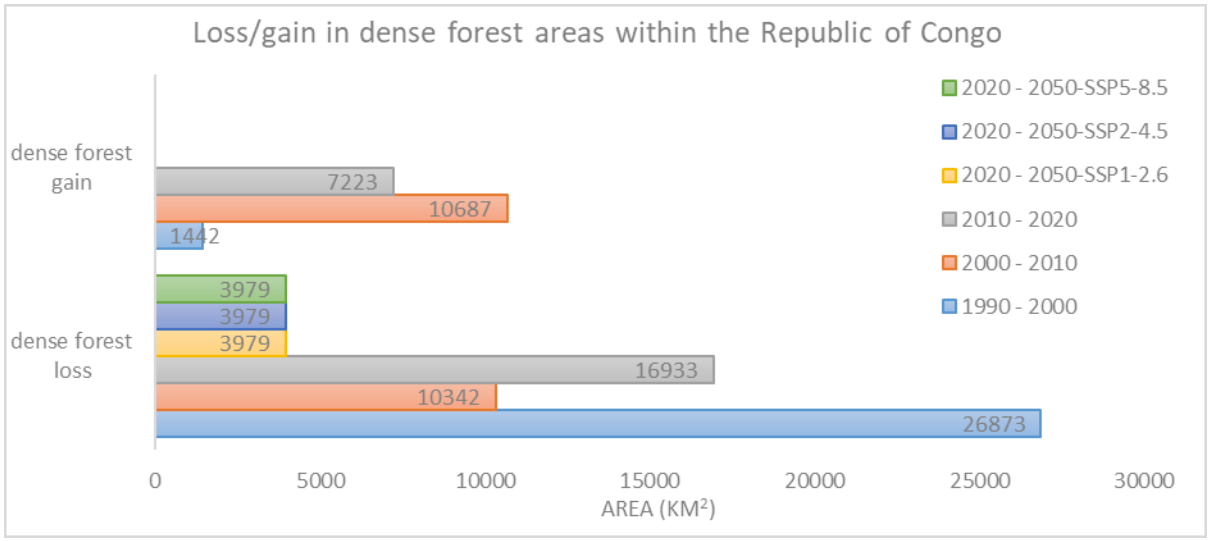

Figure S9d. Comparison in dense forest cover loss and gain in the Republic of Congo, across all four change periods

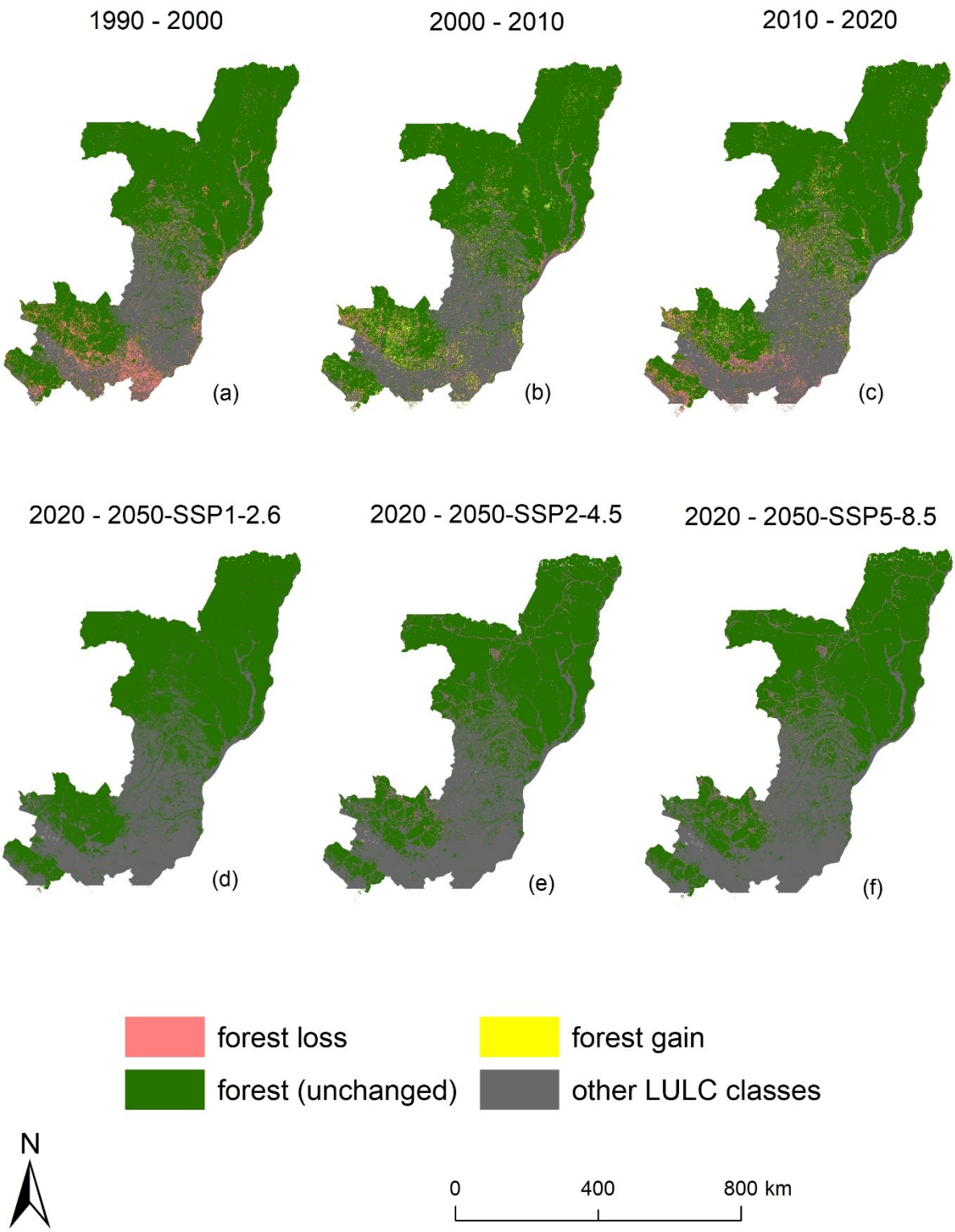

Figure S9e. Map of forest cover loss and gain in the Republic of Congo, under all four change periods

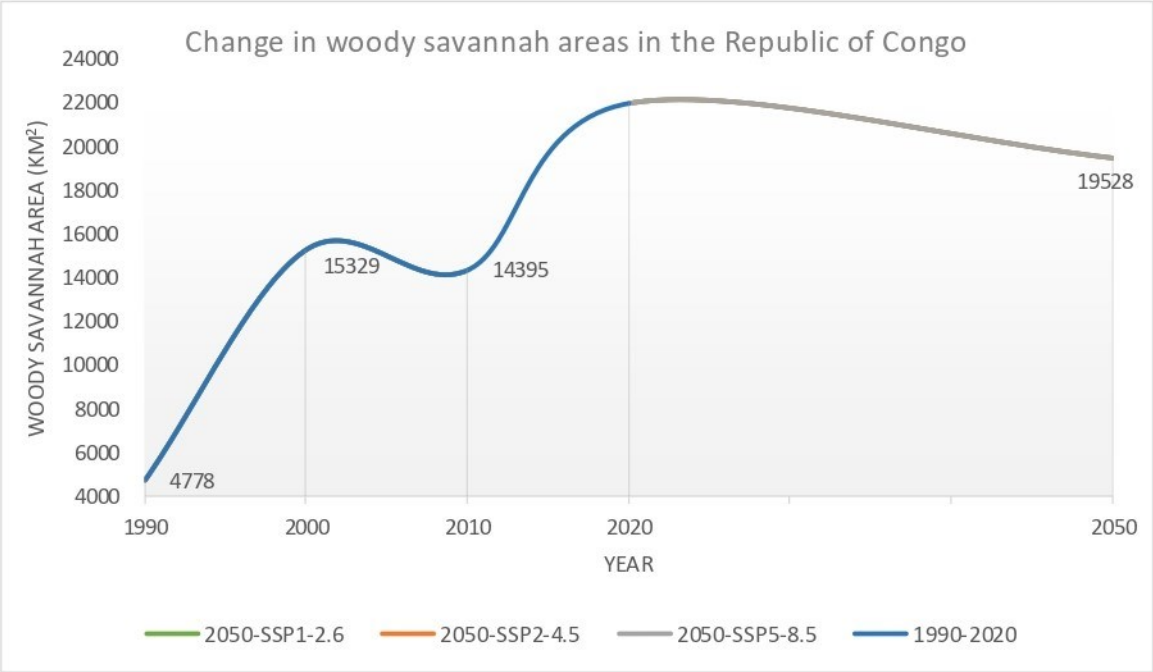

Figure S9f. Change in woody savannah areas within the Republic of Congo, under all four change periods

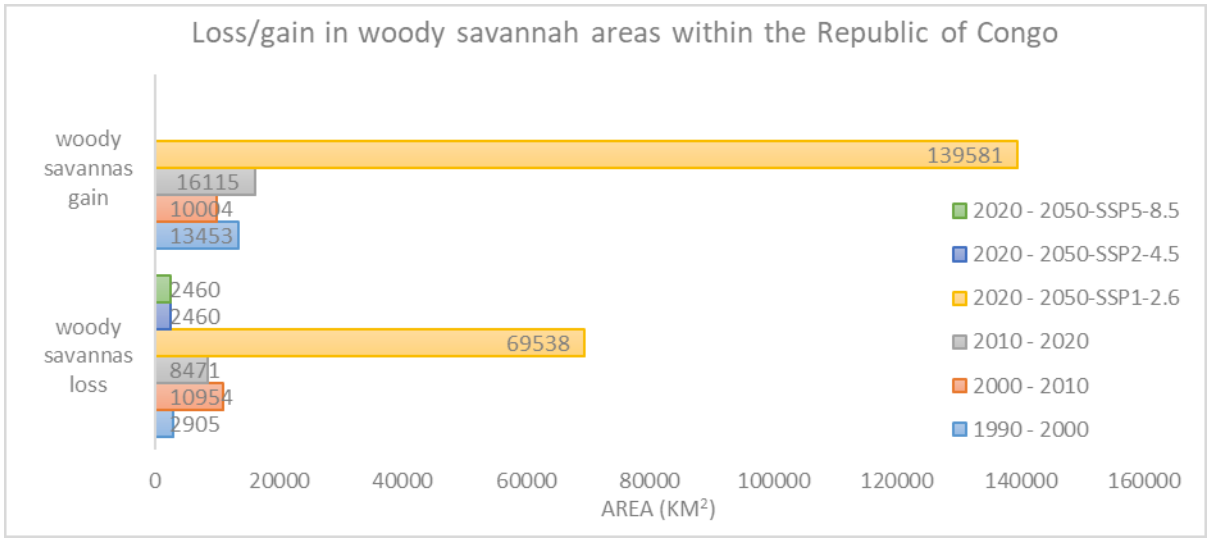

Figure S9g. Comparison in woody savannah loss and gain in the Republic of Congo, across all four change periods

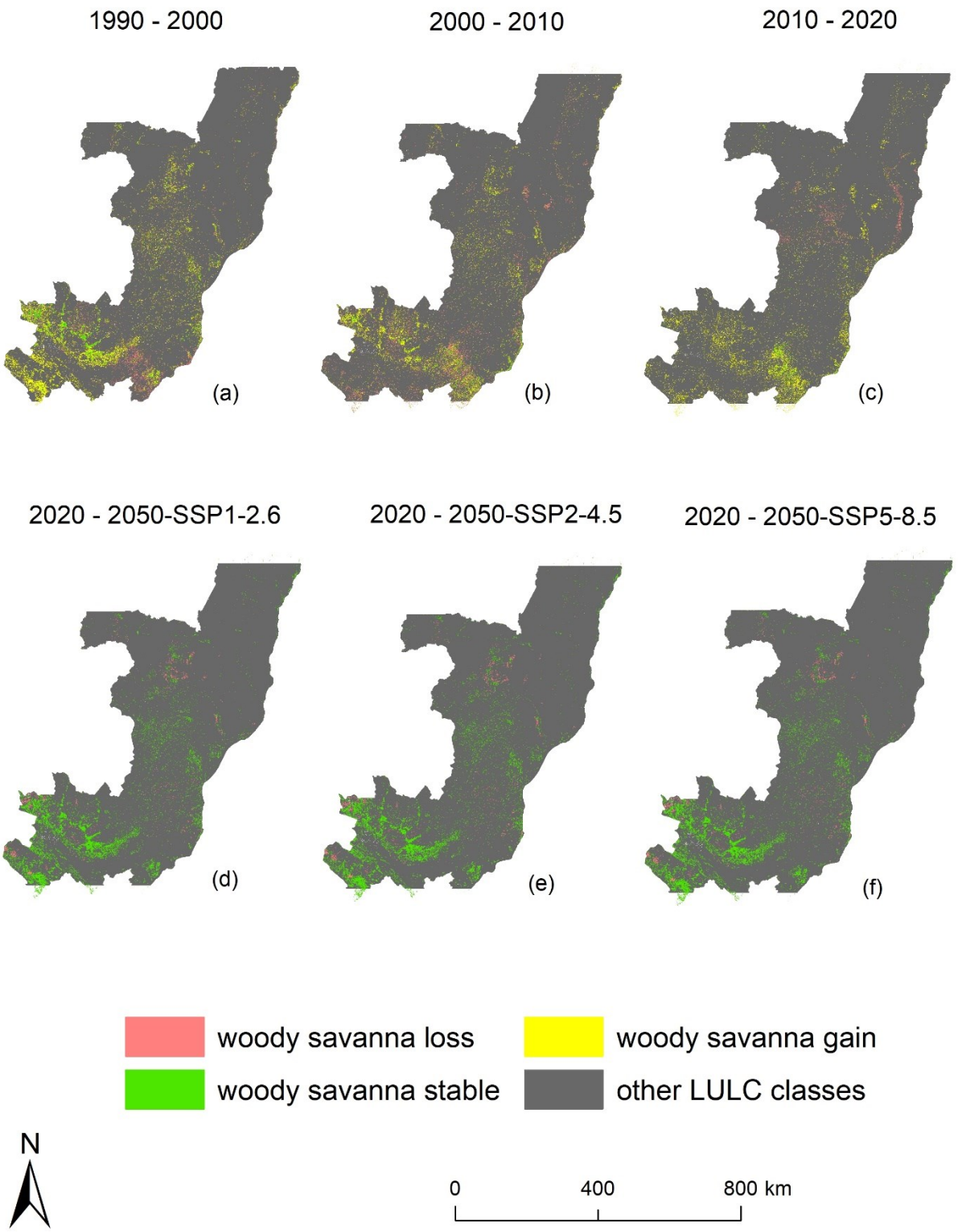

Figure S9h. Map of woody savannah loss and gain in the Republic of Congo, under all four change periods

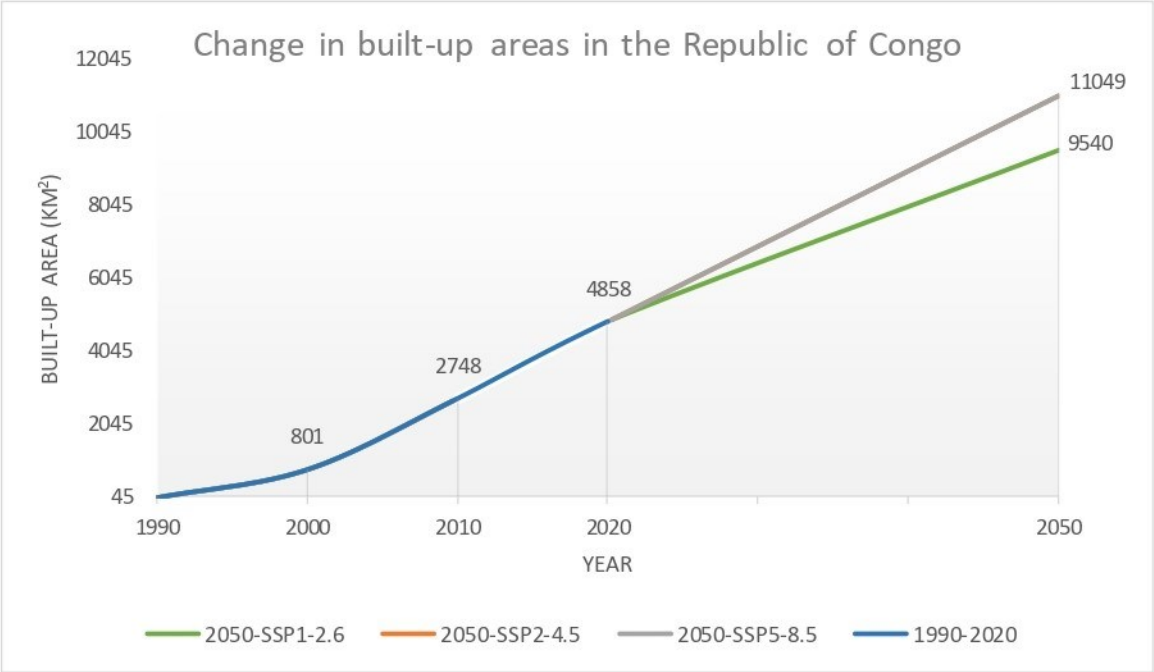

Figure S9i. Change in built-up areas within the Republic of Congo, under all four change periods

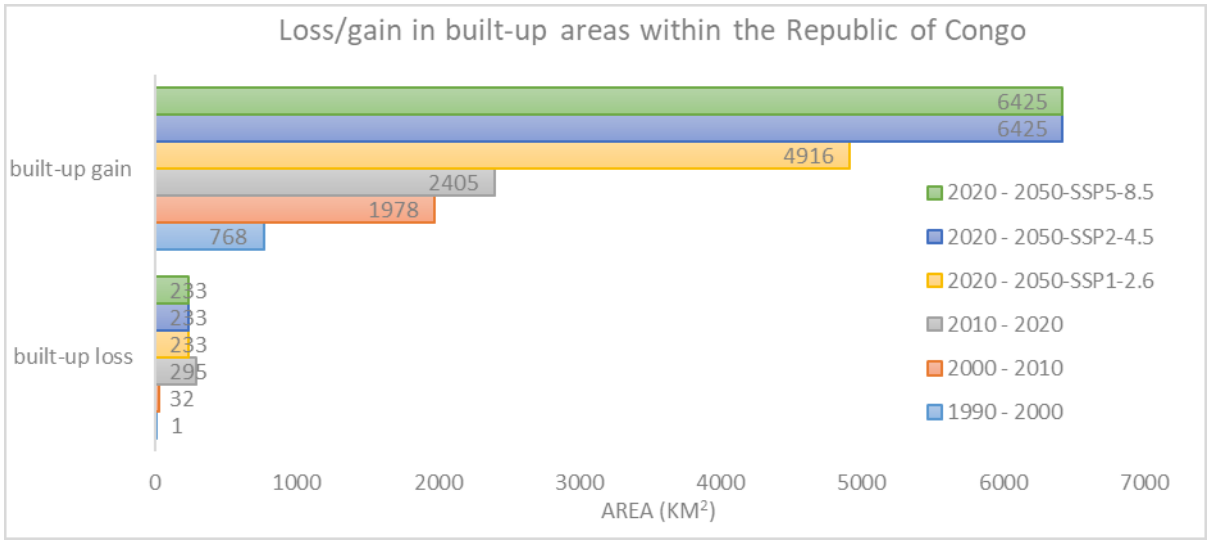

Figure S9j. Comparison in built-up area loss and gain in the Republic of Congo, across all four change periods

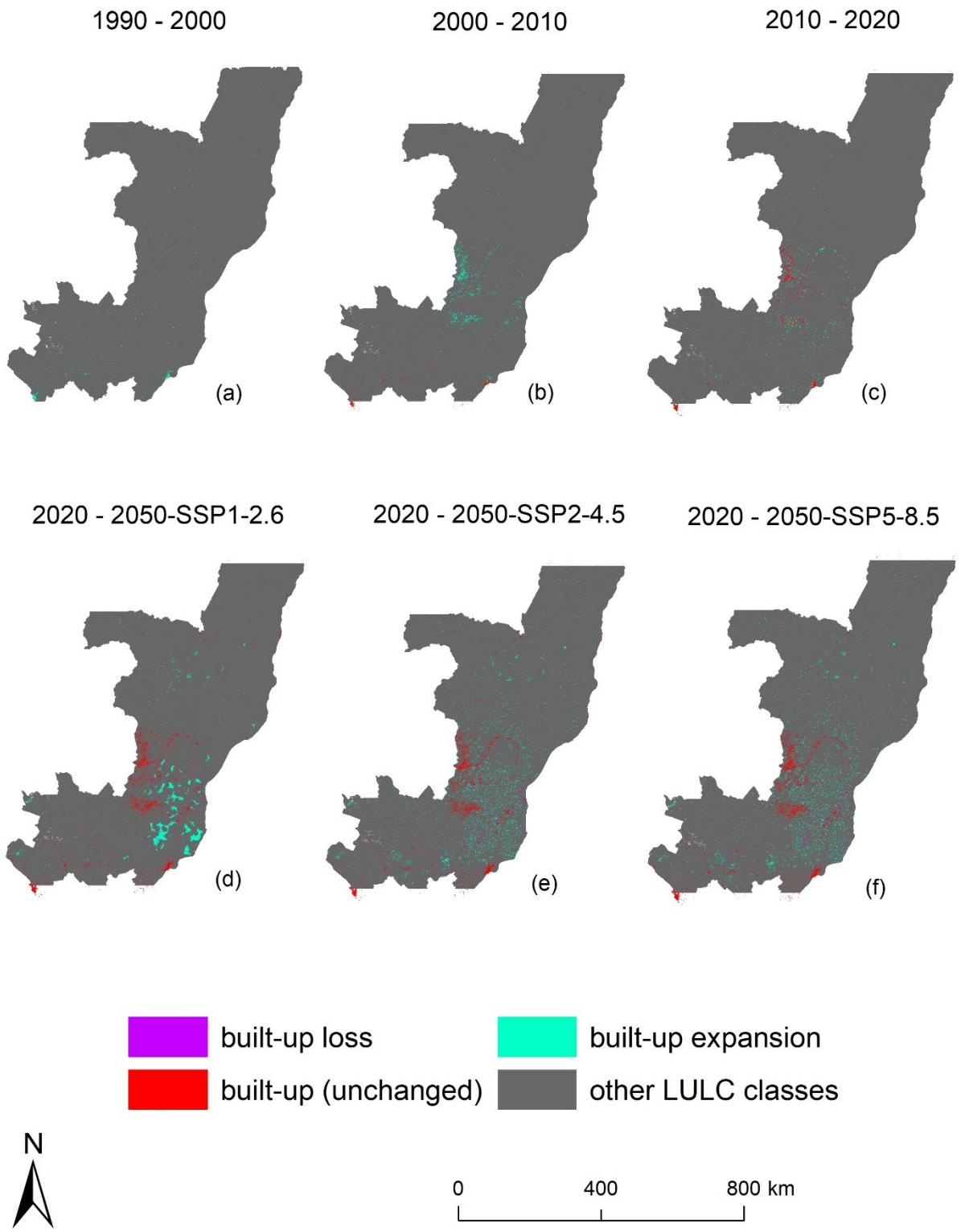

Figure S9k. Map showing loss and gains in built-up areas within the Republic of Congo, under all four change periods

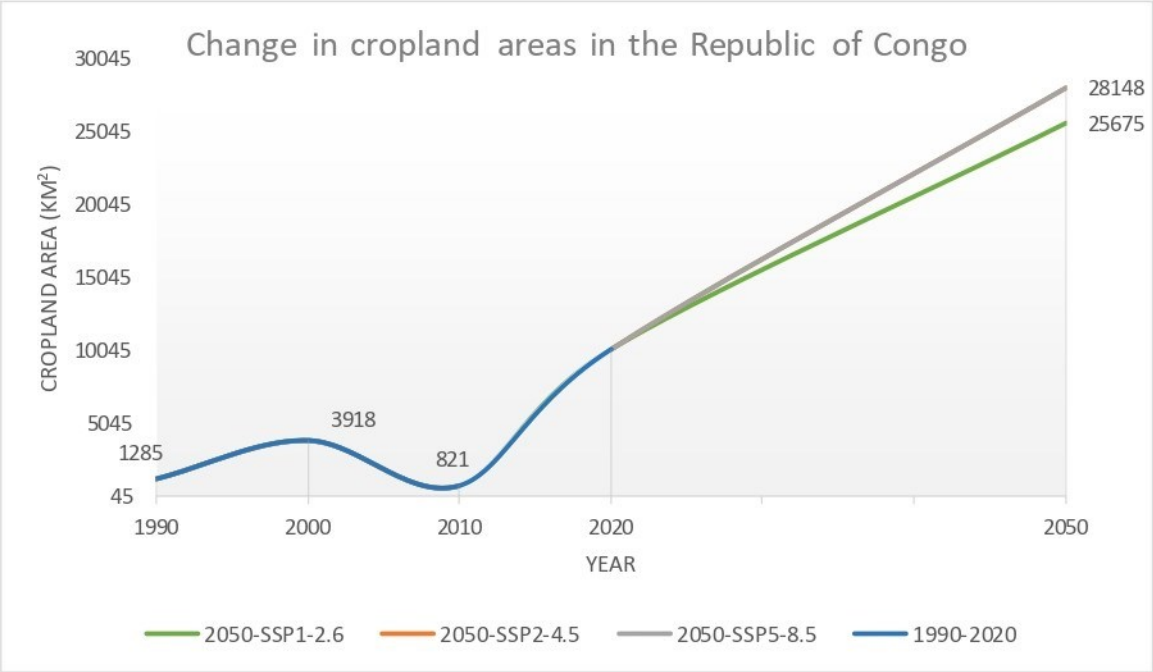

Figure S9l. Change in cropland areas within the Republic of Congo, under all four change periods

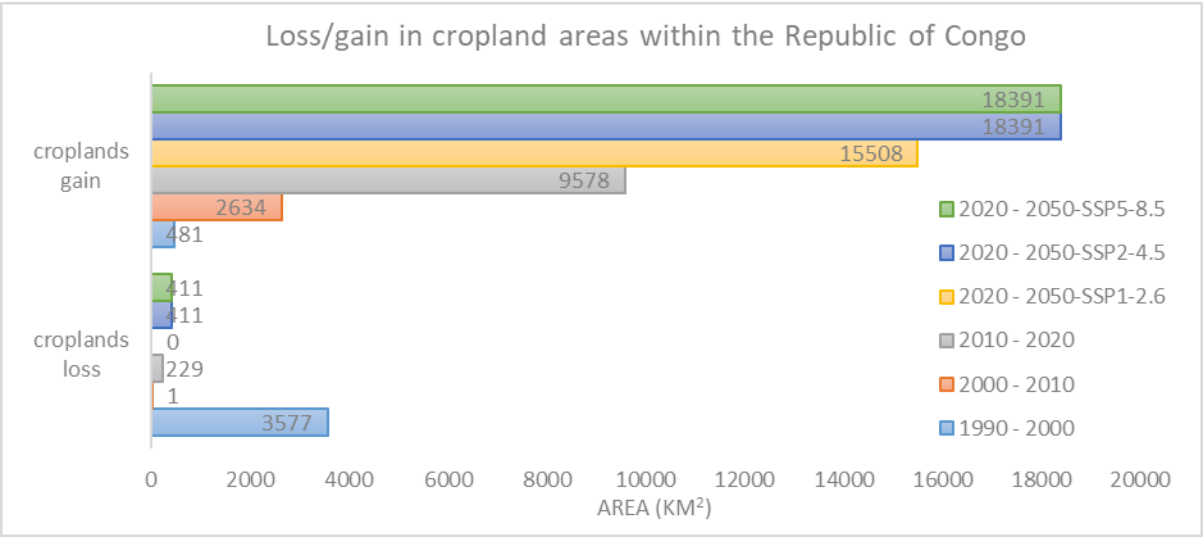

Figure S9m. Comparison in cropland area loss and gain in the Republic of Congo, across all four change periods

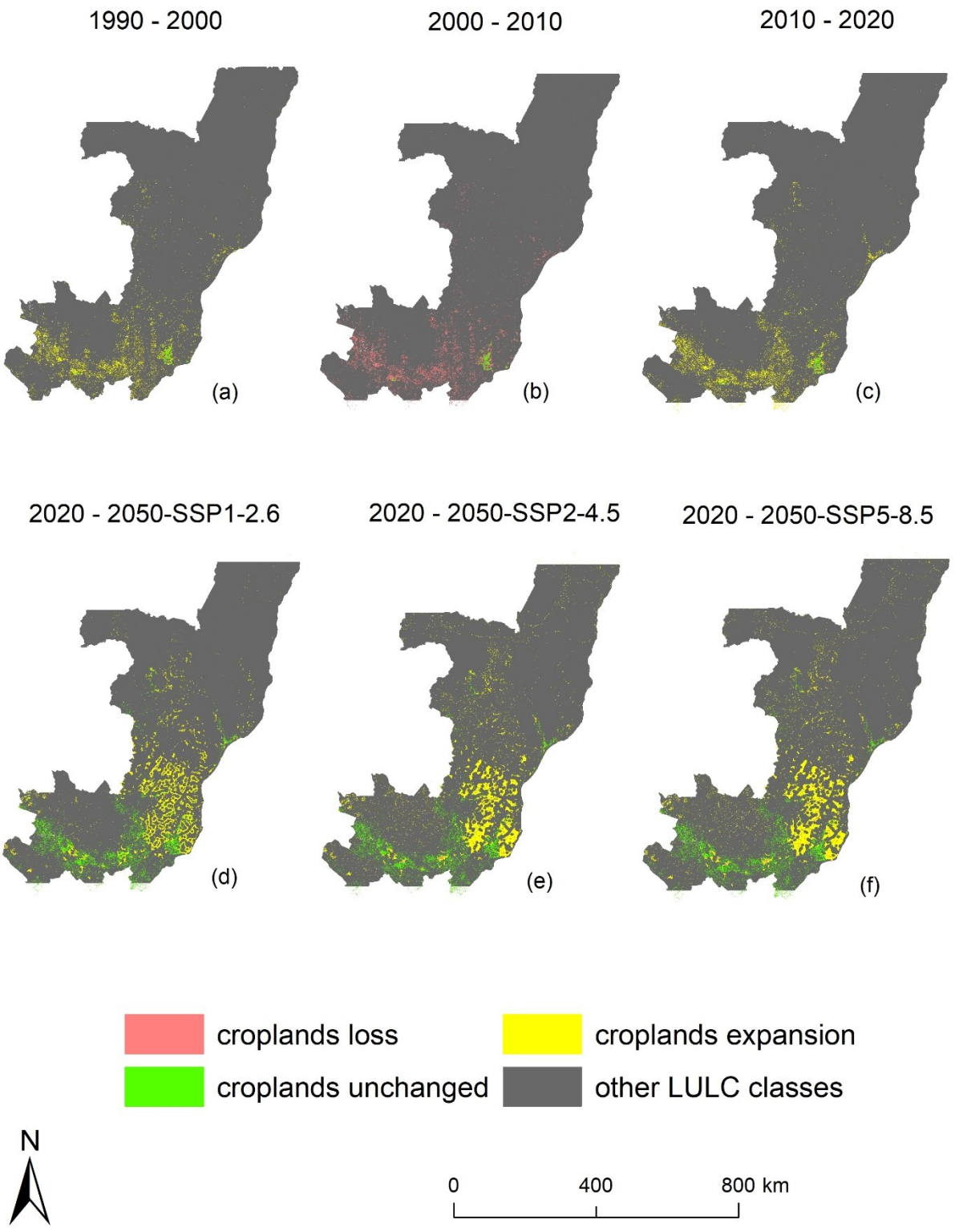

Figure S9n. Map of croplands gain/loss in the Republic of Congo, under all four change periods

Table S22a. Area and proportion of land cover classes in each year of study in the Republic of Congo

	1990		2000		2010		2020		2050					
									SSP1-2.6		SSP2-4.5		SSP5-8.5	
LULC class	**Area (km2)**	**% Area**	**Area (km2)**	**% Area**	**Area (km2)**	**% Area**	**Area (km2)**	**% Area**	Area (km2)	% Area	Area (km2)	% Area	Area (km2)	% Area
croplands	1284.9	0.4	3917.7	1.1	821	0.2	10170.9	3	25675	7.5	28147.8	8.7	28147.8	8.7
dense forest	249757.2	73.2	224498.4	65.8	224974	65.9	215203.1	63	215060.2	63	193855.3	59.8	193855.3	59.8
grassland/savannas	422.5	0.1	618.8	0.2	394	0.1	3519.6	1	3518.5	1	3518.5	1.1	3518.5	1.1
open savannas/barelands	81643.3	23.9	91908.8	26.9	93961.5	27.5	80364.2	23.5	62917.2	18.4	62914.6	19.4	62914.6	19.4
built-up areas	33.1	0	800.8	0.2	2747.5	0.8	4857.6	1.4	9539.9	2.8	11048.9	3.4	11048.9	3.4
water bodies	3258.8	1	4264.7	1.2	3437.4	1	4111.7	1.2	3879	1.1	3878.7	1.2	3878.7	1.2
wetlands	33.8	0	60.1	0	822.1	0.2	1138.9	0.3	1061.9	0.3	1062	0.3	1062	0.3
woody savannas	4778.4	1.4	15329.3	4.5	14395.1	4.2	22029	6.5	19527.7	5.7	19527.3	6	19527.3	6
Total	341211.9	100	341398.7	100	341552.6	100	341395	100	341179.5	100	323953.1	100	323953.1	100

Table S22b. Quantified decadal changes in land cover patterns in the Republic of Congo, between 1990-2020

	1990-2000		2000-2010		2010-2020		2020-2050					
							SSP1-2.6		SSP2-4.5		SSP5-8.5	
LULC classes	**Area (km2)**	**% Area**	**Area (km2)**	**% Area**	**Area (km2)**	**% Area**	**Area (km2)**	**% Area**	**Area (km2)**	**% Area**	**Area (km2)**	**% Area**
croplands	2632.8	0.8	-3096.6	-0.9	9349.9	2.7	21757.3	6.4	24230.1	7.6	24230.1	7.6
dense forest	-25258.8	-7.4	475.6	0.1	-9770.9	-2.8	-9438.2	-2.8	-30643.1	-6.0	-30643.1	-6.0
grassland/savannas	196.3	0.1	-224.8	-0.1	3125.5	0.9	2899.7	0.8	2899.7	0.9	2899.7	0.9
open savannas/barelands	10265.5	3	2052.7	0.6	-13597.3	-4	-28991.6	-8.5	-28994.2	-7.5	-28994.2	-7.5
built-up areas	767.7	0.2	1946.7	0.6	2110.1	0.6	8739.1	2.6	10248.1	3.2	10248.1	3.2
water bodies	1006	0.3	-827.3	-0.2	674.3	0.2	-385.7	-0.1	-386.0	0.0	-386.0	0.0
wetlands	26.3	0.0	762.0	0.2	316.8	0.1	1001.8	0.3	1001.9	0.3	1001.9	0.3
woody savannas	10550.9	3.1	-934.3	-0.3	7634	2.2	4198.4	1.2	4198.0	1.5	4198.0	1.5

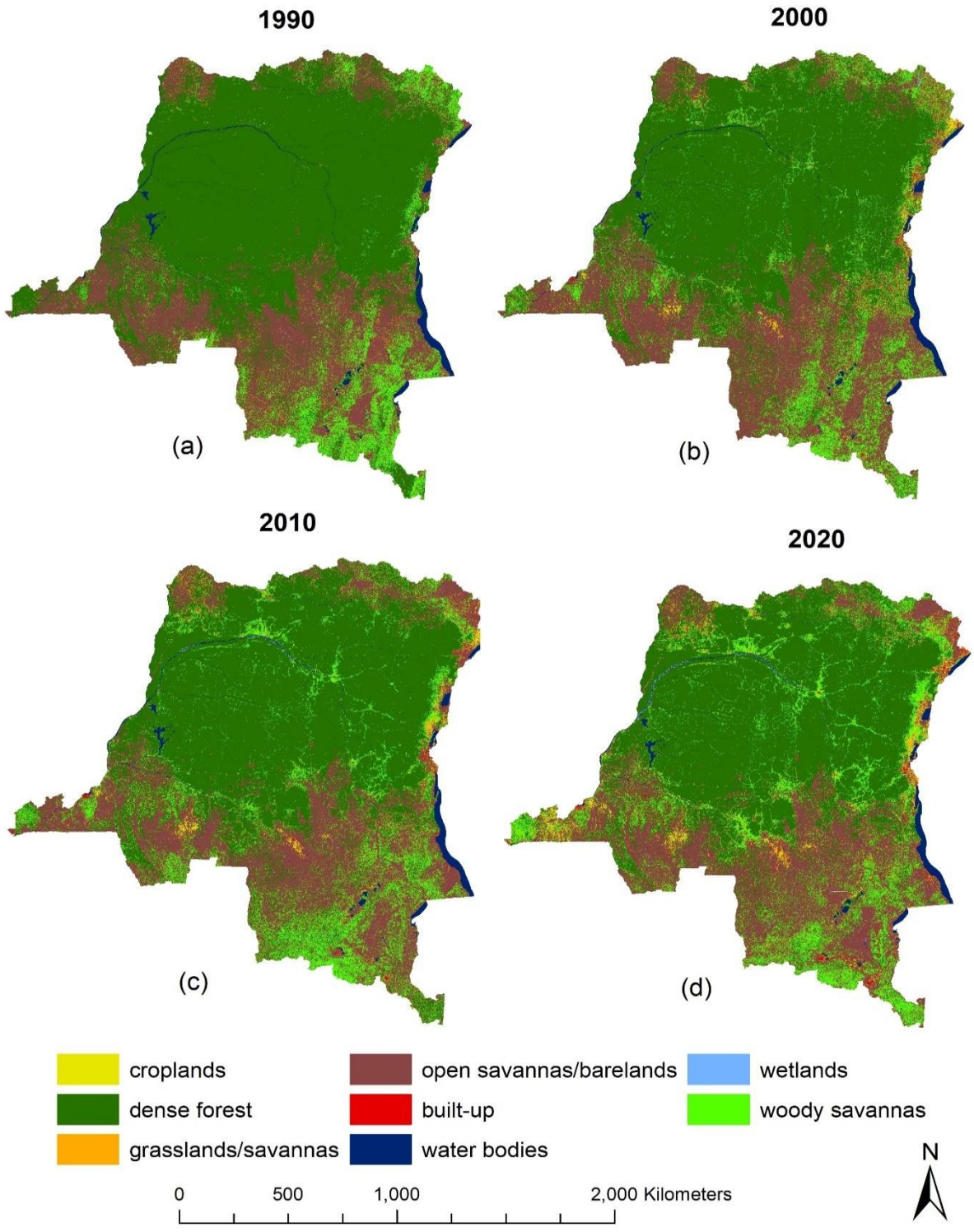

Figure S10a. Land cover classification maps for the Democratic Republic of Congo (DRC), for the years 1990, 2000, 2010, and 2020.

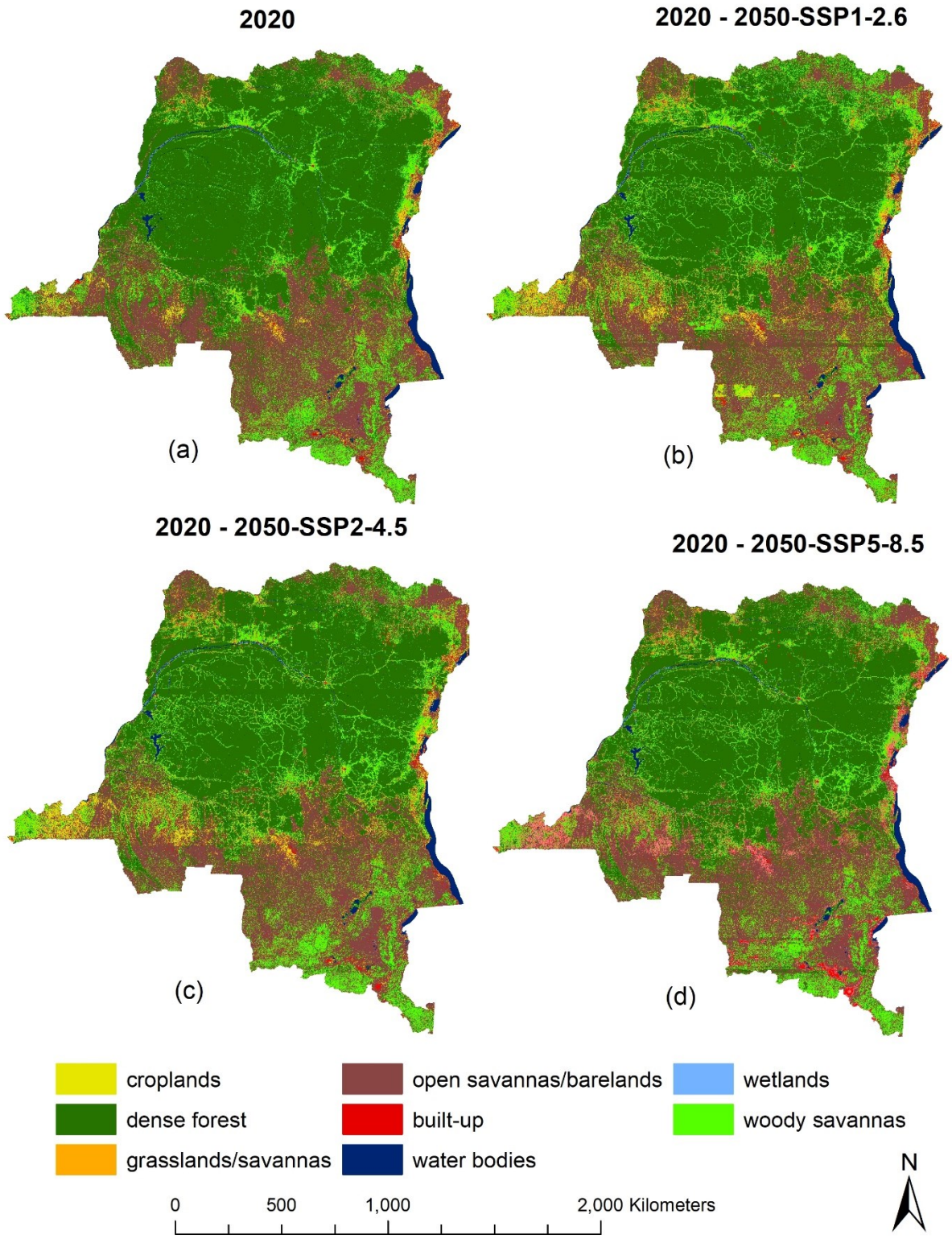

Figure S10b. Projected LULC maps of the DRC for the year 2050. Map shows projected results under all three climate change scenarios (SSP1, SSP2 and SSP5; Figures 5b-c), with the year 2020 representing the baseline condition (for comparison purpose).

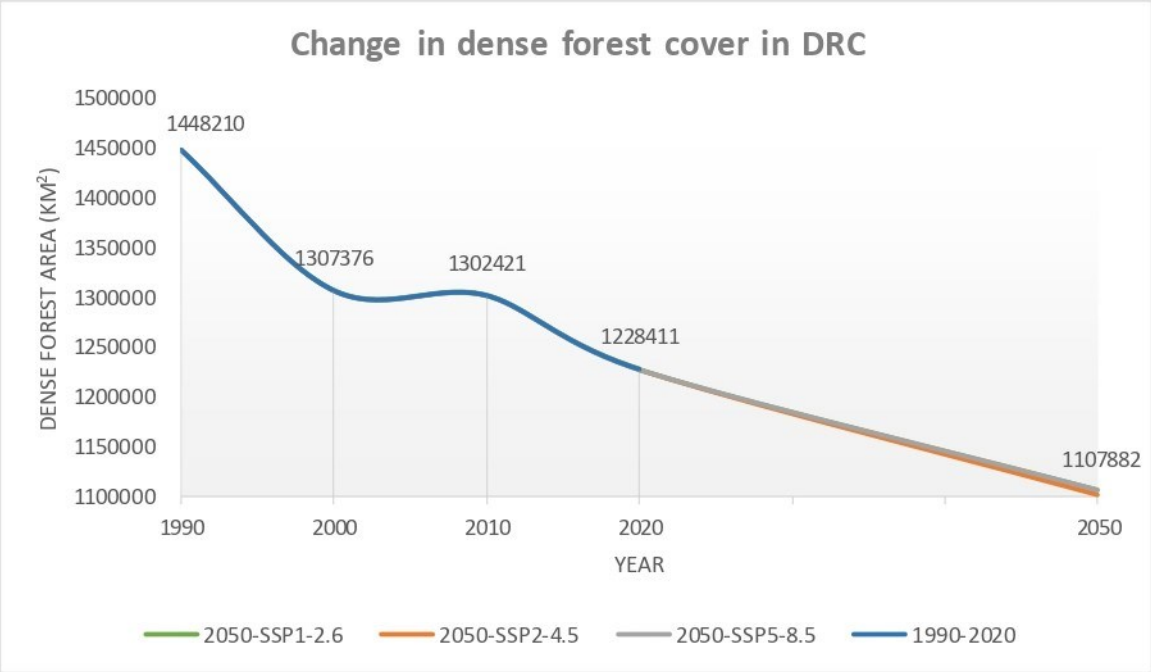

Figure S10c. Change in dense forest cover within the DRC, under all four change periods (1990-2000, 2000-2010, 2010-2020, and 2020-2050-under SSP1-2.6, SSP2-4.5, and SSP5-8.5 climate change scenarios).

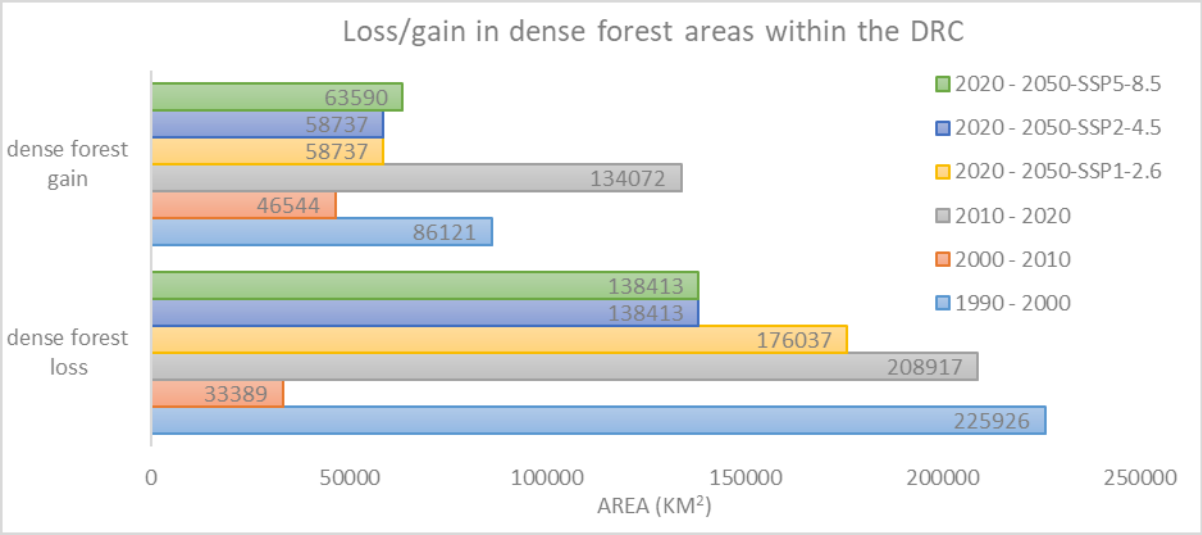

Figure S10d. Comparison in dense forest cover loss and gain in the DRC, across all four change periods

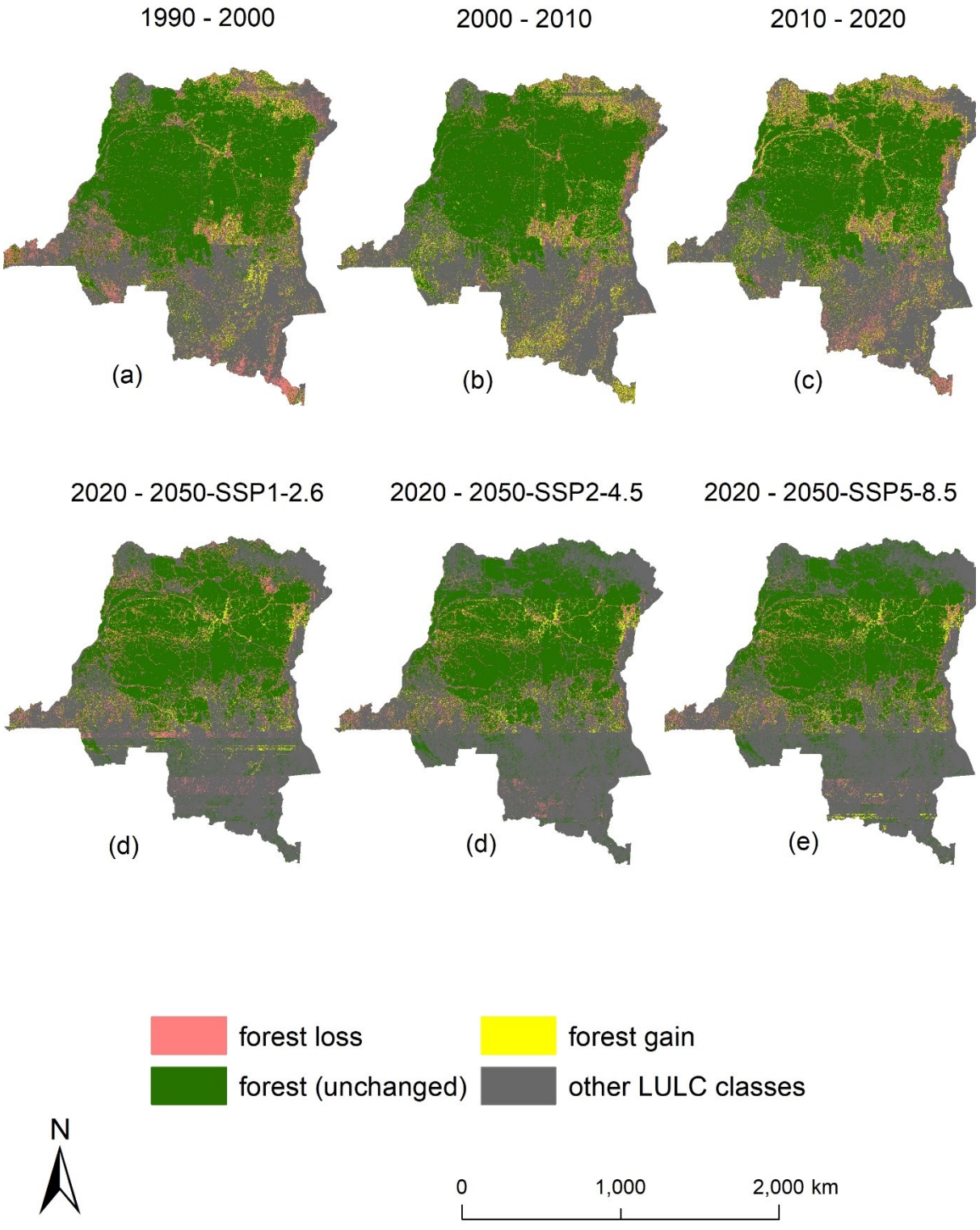

Figure S10e. Map of forest cover loss and gain in the DRC, under all four change periods

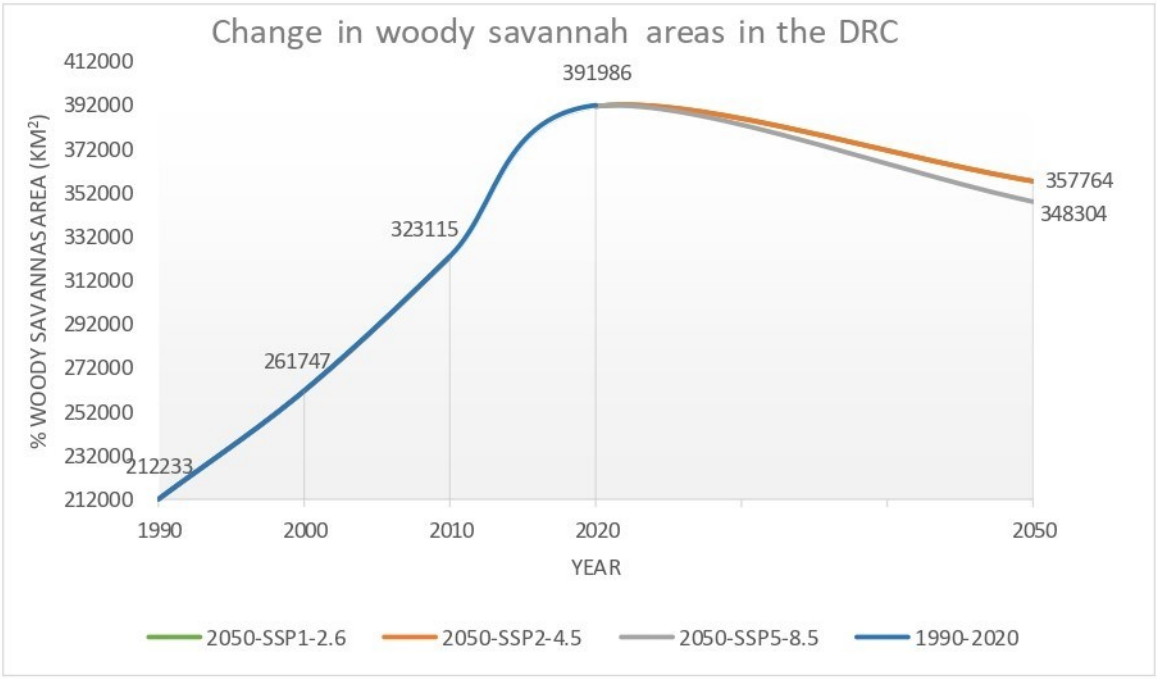

Figure S10f. Change in woody savannah areas within the DRC, under all four change periods

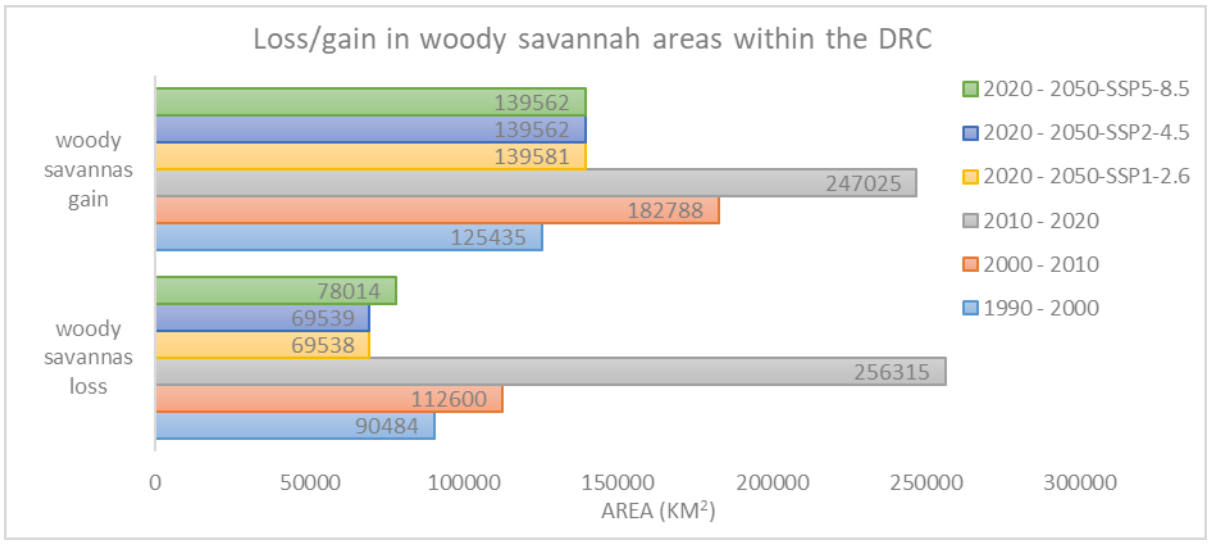

Figure S10g. Comparison in woody savannah loss and gain in the DRC, across all four change periods

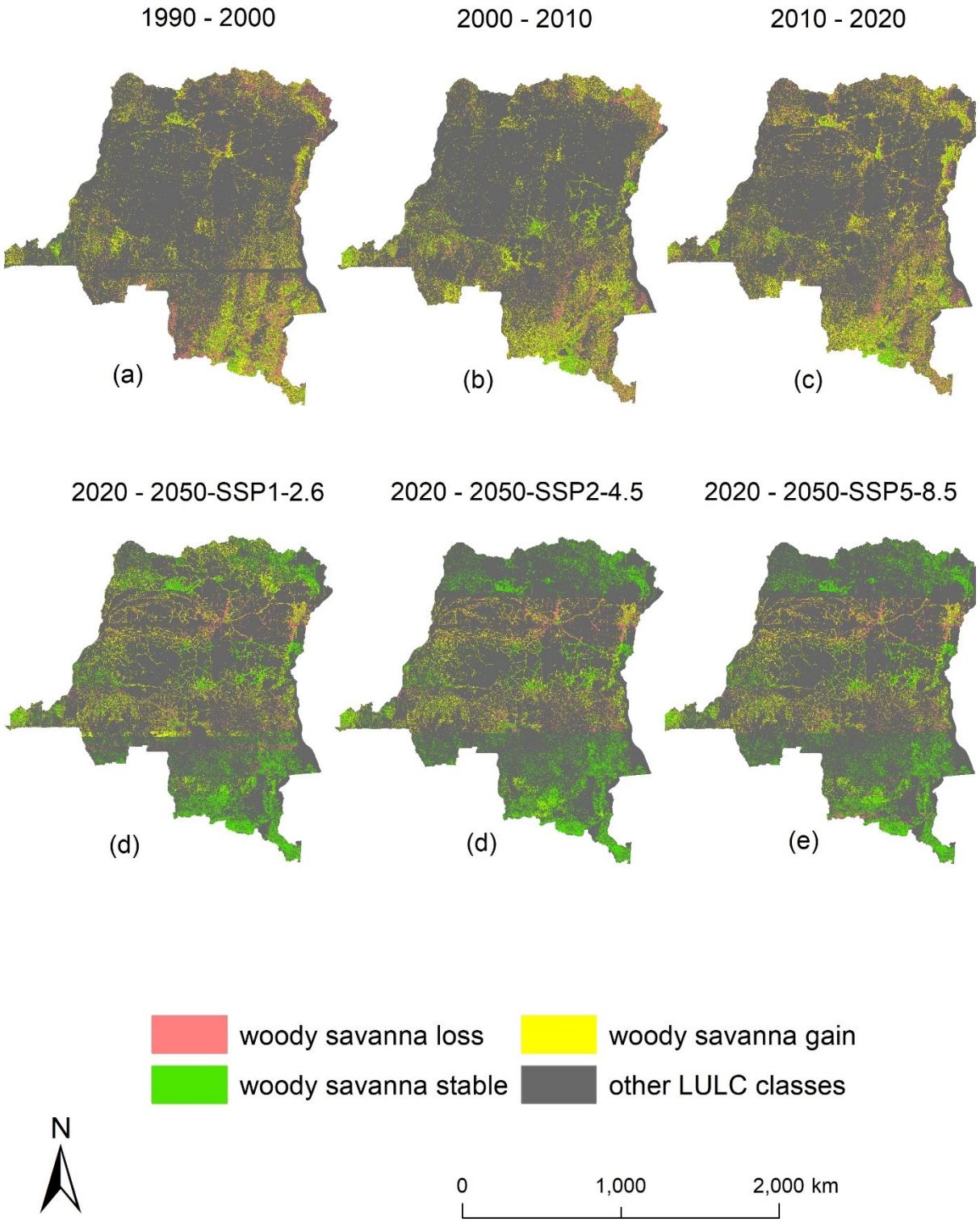

Figure S10h. Map of woody savannah loss and gain in the DRC, under all four change periods

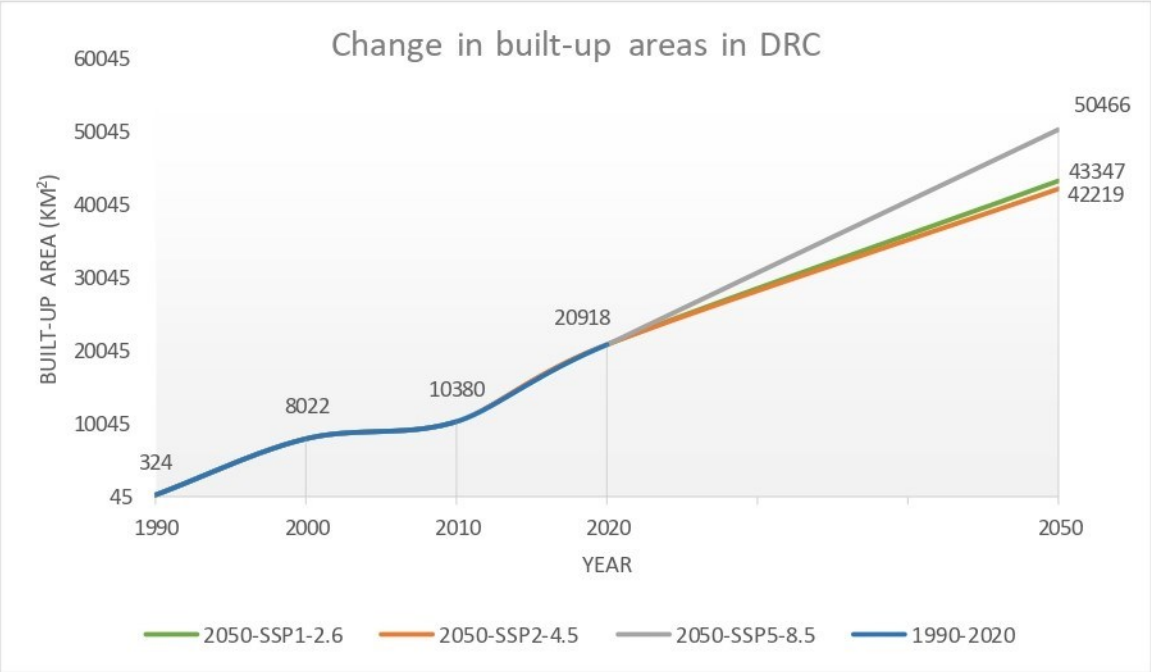

Figure S10i. Change in built-up areas within the DRC, under all four change periods

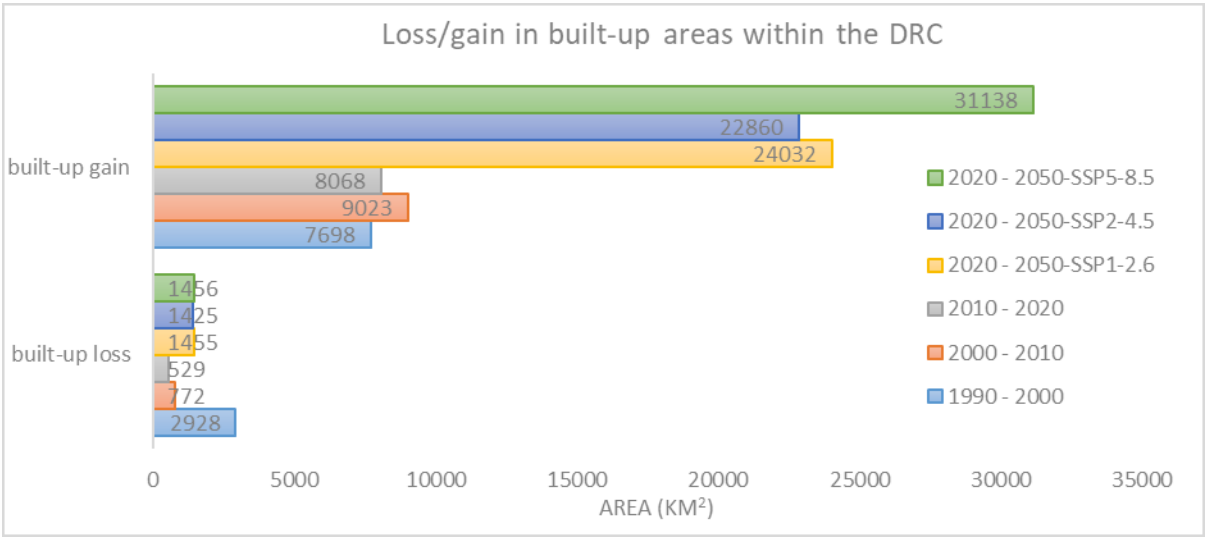

Figure S10j. Comparison in built-up area loss and gain in the DRC, across all four change periods

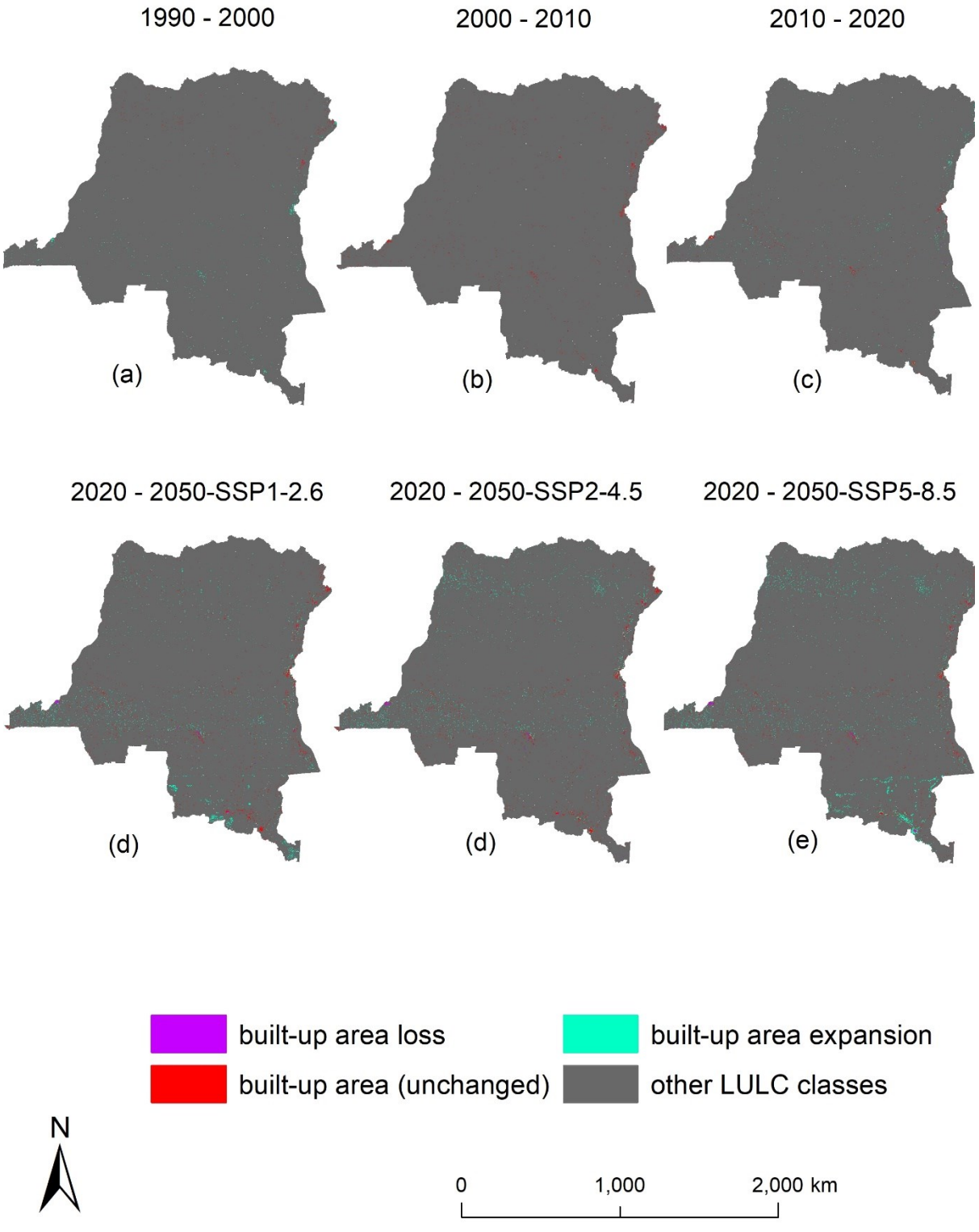

Figure S10k. Map showing loss and gains in built-up areas within the DRC, under all four change periods

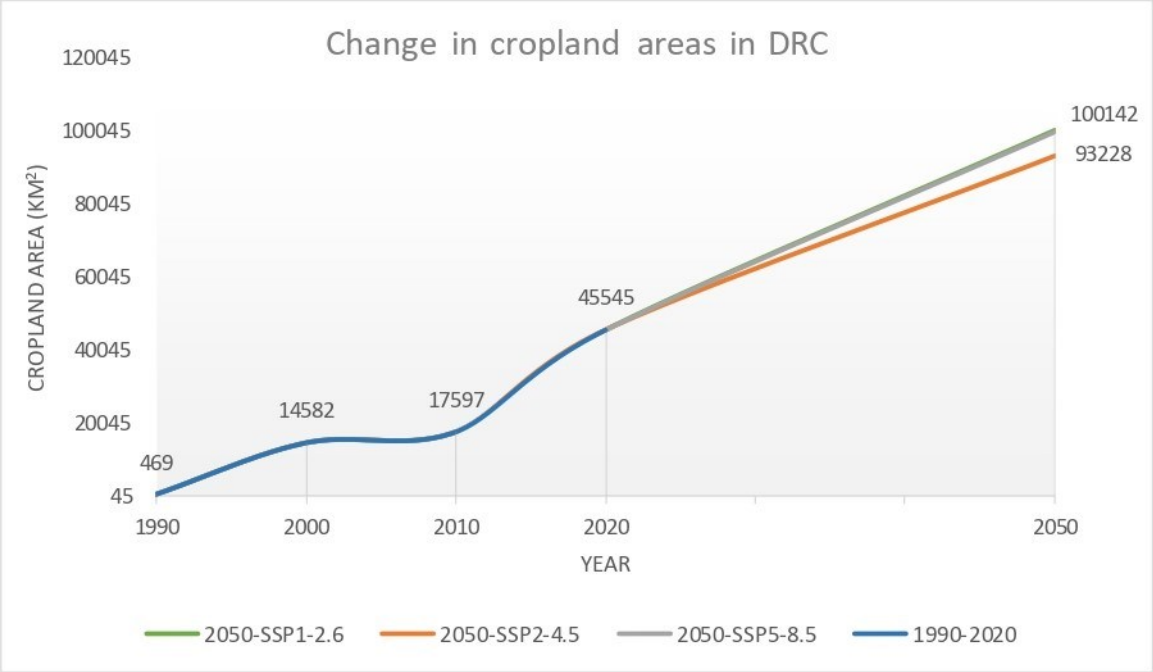

Figure S10l. Change in cropland areas within the DRC, under all four change periods

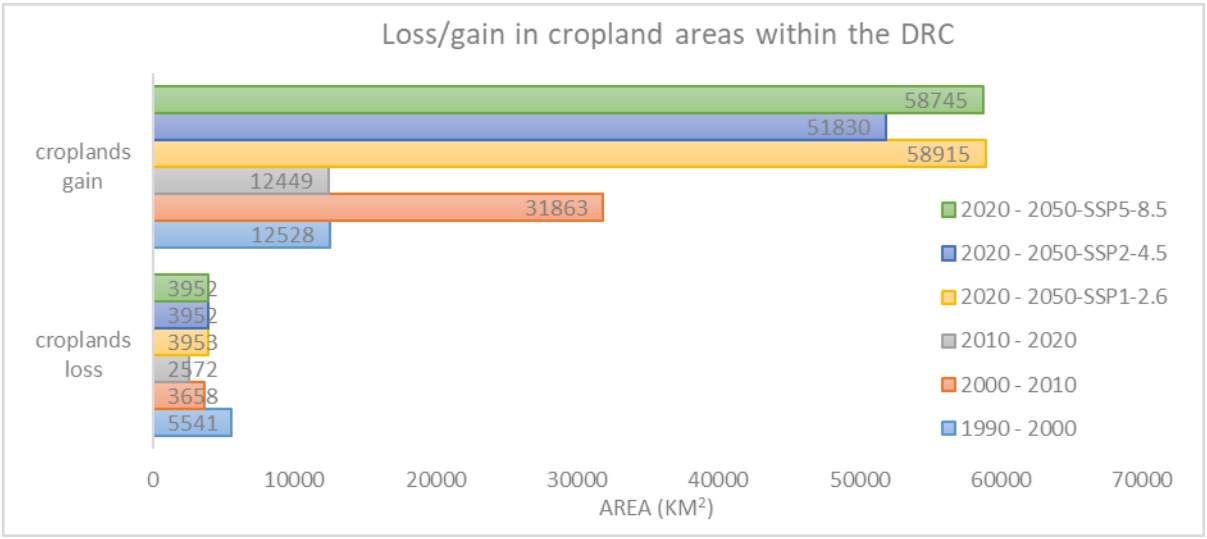

Figure S10m. Comparison in cropland area loss and gain in the DRC, across all four change periods

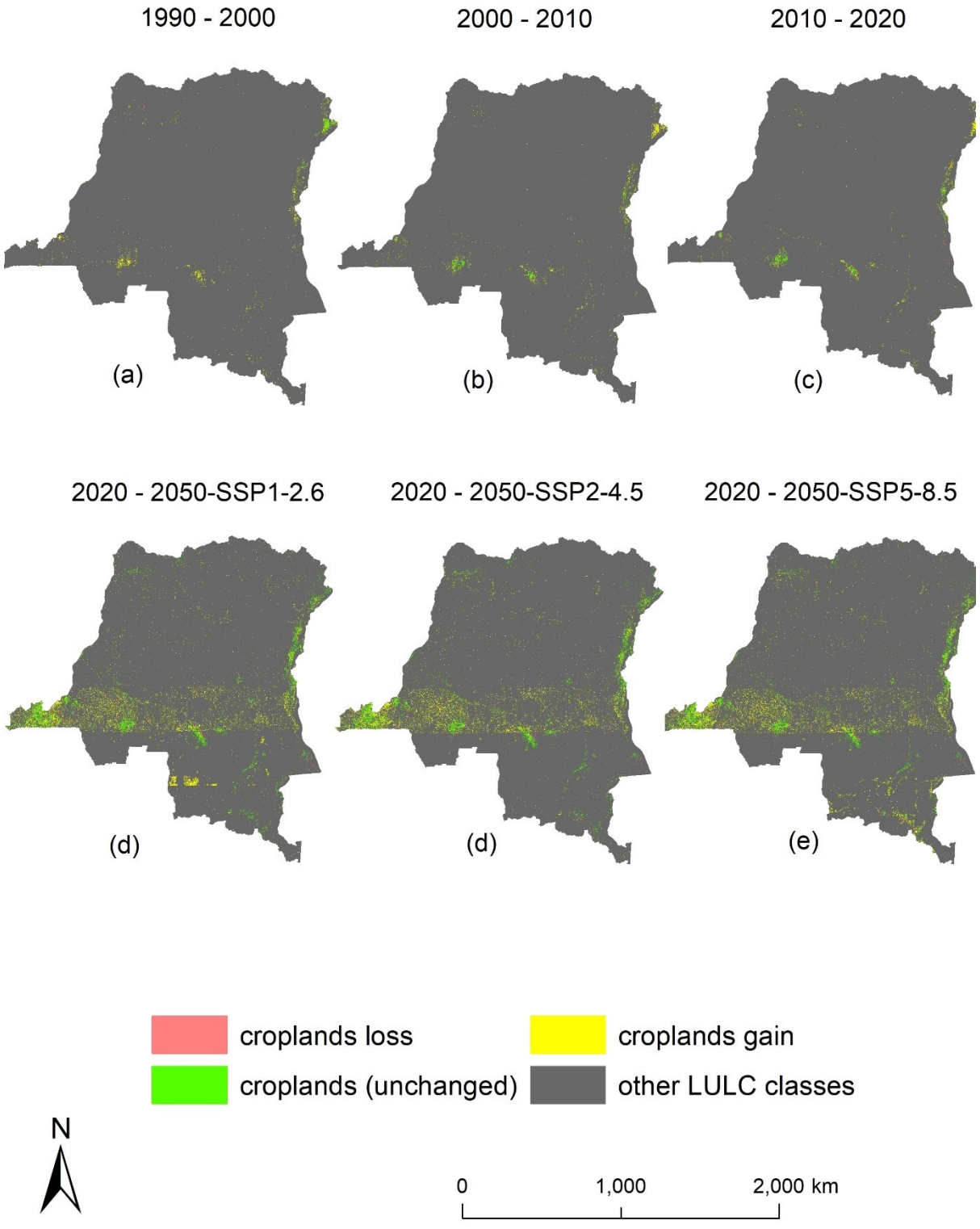

Figure S10n. Map of croplands gain/loss in the DRC, under all four change periods

Table S23a. Area and proportion of land cover classes in each year of study in the DRC

	1990.0		2000.0		2010.0		2020.0		2050					
									SSP1-2.6		SSP2-4.5		SSP5-8.5	
LULC class	**Area (km2)**	**% Area**	**Area (km2)**	**% Area**	**Area (km2)**	**% Area**	**Area (km2)**	**% Area**	**Area (km2)**	**% Area**	**Area (km2)**	**% Area**	**Area (km2)**	**% Area**
croplands	469.3	0	14581.6	0.6	17597.1	0.7	45544.8	1.9	100303	4.2	93227.7	4	100141.7	4.3
dense forest	1448210	60.6	1307375.7	54.7	1302441	54.5	1228411.1	51.4	1106579	46.5	1103029.5	47.2	1107882.2	47.4
grassland/savannas	16833.5	0.7	34191.9	1.4	25847.4	1.1	33424.2	1.4	45150.4	1.9	38094.7	1.6	38094.7	1.6
open savannas/ barelands	668915.2	28.0	714160.5	29.9	689246.5	28.8	690630.4	28.9	646924.2	27.2	655715.8	28.1	645227.8	27.6
built-up areas	324	0	8022.1	0.3	10380	0.4	20917.9	0.9	43347.3	1.8	42218.5	1.8	50466	2.2
water bodies	41992.5	1.8	46023.7	1.9	43404.1	1.8	43787.5	1.8	43044.9	1.8	43122.6	1.8	43067.1	1.8
wetlands	451.6	0	2116.3	0.1	2149.3	0.1	4513.8	0.2	4375.1	0.2	4408.6	0.2	4398	0.2
woody savannas	212233.1	8.9	261746.7	11	299426.9	12.5	323115.1	13.5	391985.5	16.5	357764.1	15.3	348304	14.9
Total	2389429.2	100	2388218.5	100	2390492.1	100	2390344.8	100	2381710	100	2337581	100	2337581	100

Table S23b. Quantified decadal changes in land cover patterns in the DRC, between 1990-2020

	1990-2000		2000-2010		2010-2020		2020-2050					
							SSP1-2.6		SSP2-4.5		SSP5-8.5	
LULC classes	**Area (km2)**	**% Area**	**Area (km2)**	**% Area**	**Area (km2)**	**% Area**	**Area (km2)**	**% Area**	**Area (km2)**	**% Area**	**Area (km2)**	**% Area**
croplands	14112.3	0.6	3015.5	0.1	27947.7	1.2	54758.5	2.3	47682.9	2.1	54596.9	2.4
dense forest	-140834.3	-5.9	-4934.7	-0.3	-74029.9	-3.1	-121831.7	-4.9	-125381.6	-4.2	-120528.9	-4.0
grassland/savannas	17358.4	0.7	-8344.5	-0.4	7576.9	0.3	11726.2	0.5	4670.5	0.2	4670.5	0.2
open savannas/barelands	45245.3	1.9	-24914	-1.1	1383.9	0.1	-43706.2	-1.7	-34914.6	-0.8	-45402.6	-1.3
built-up areas	7698.1	0.3	2357.9	0.1	10538	0.4	22429.4	0.9	21300.6	0.9	29548.1	1.3
water bodies	4031.2	0.2	-2619.6	-0.1	383.4	0	-742.6	0.0	-664.9	0.0	-720.4	0.0
wetlands	1664.7	0.1	32.9	0	2364.5	0.1	-138.7	0.0	-105.2	0.0	-115.8	0.0
woody savannas	49513.6	2.1	37680.3	1.6	23688.2	1	68870.4	3.0	34649.0	1.8	25188.9	1.4

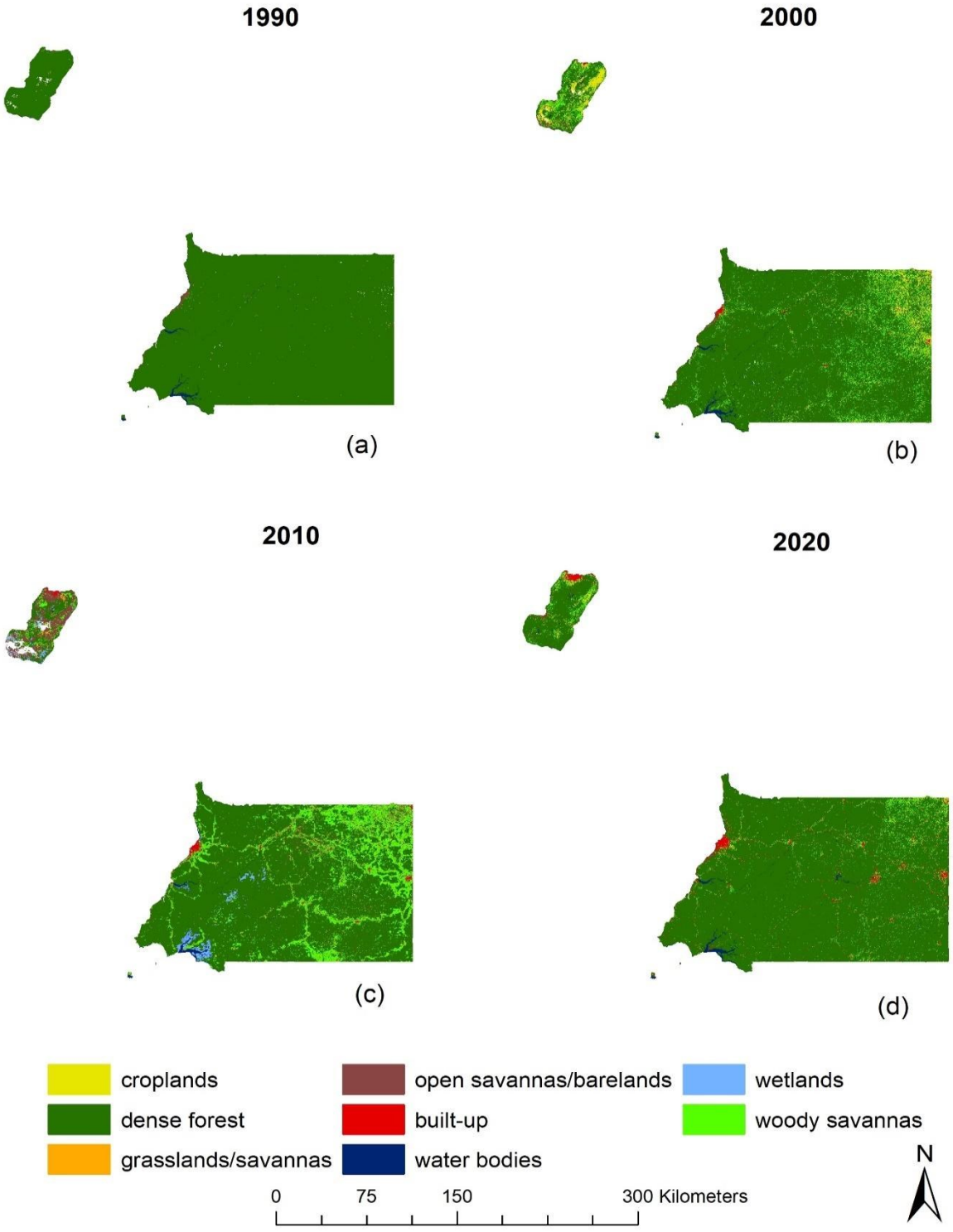

Figure S11a. Land cover classification maps for Equatorial Guinea (EG), for the years 1990, 2000, 2010, and 2020.

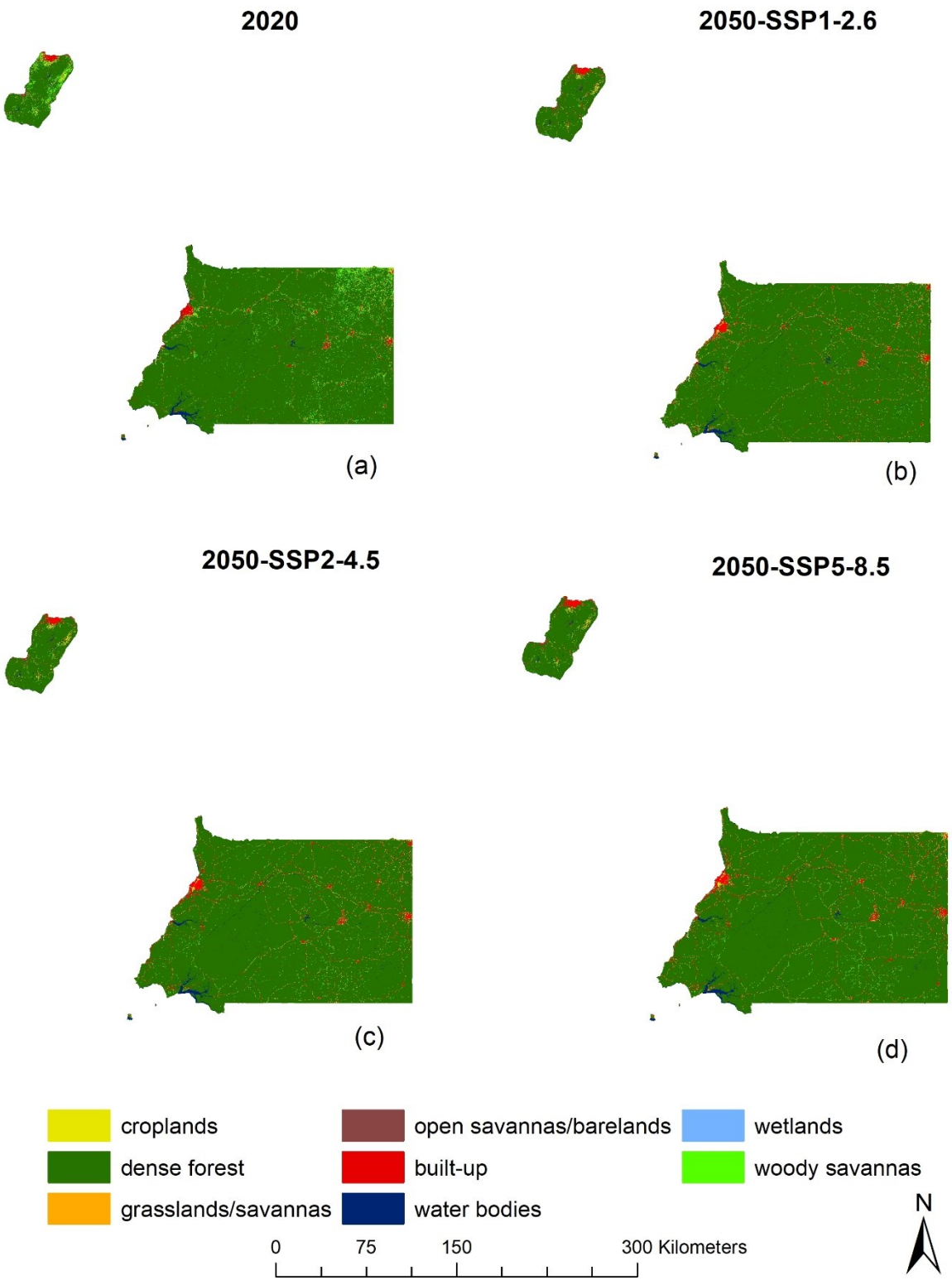

Figure S11b. Projected LULC maps of Equatorial Guinea for the year 2050. Map shows projected results under all three climate change scenarios (SSP1-2.6, SSP2-4.5 and SSP5-8.5), with the year 2020 representing the baseline condition (for comparison purpose).

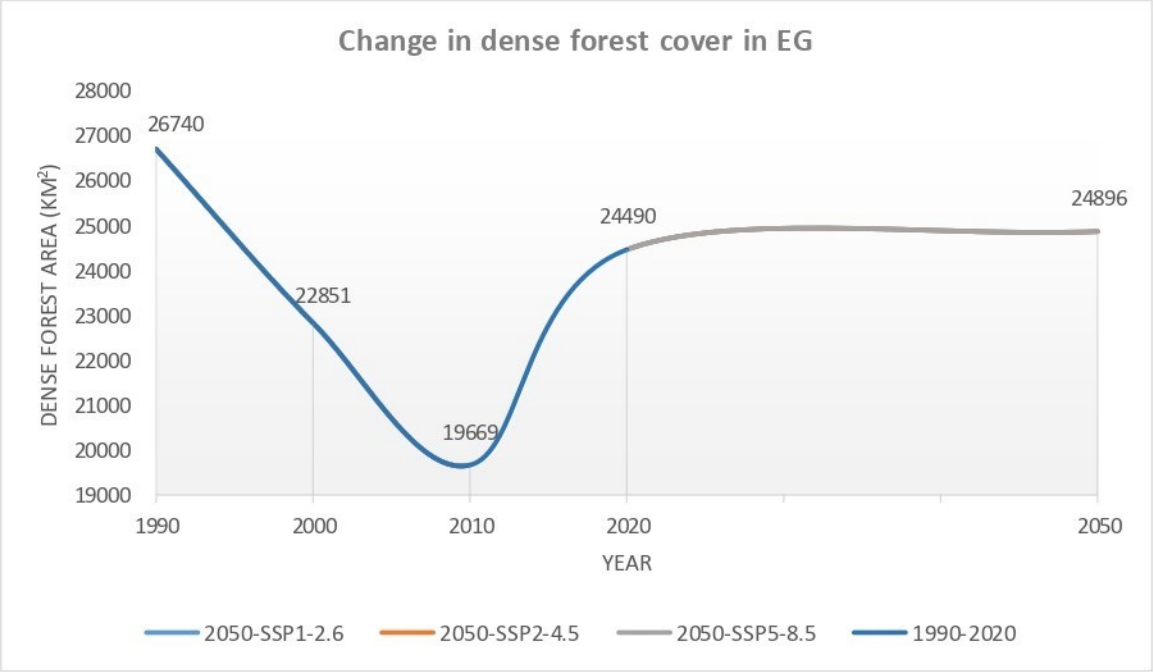

Figure S11c. Change in dense forest cover within Equatorial Guinea, under all four change periods

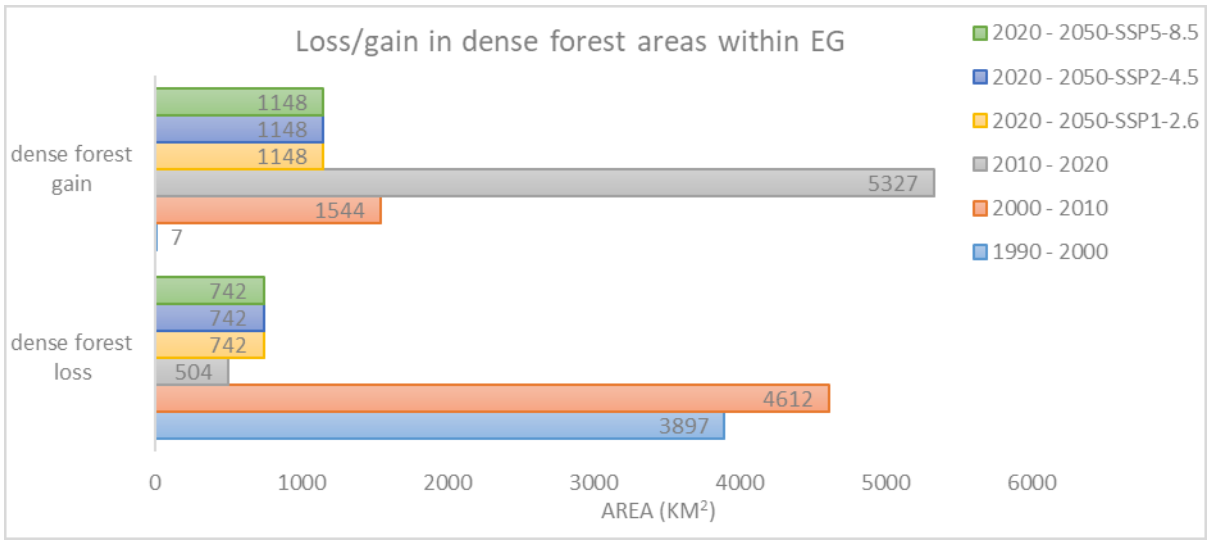

Figure S11d. Comparison in dense forest cover loss and gain in Equatorial Guinea, across all four change periods

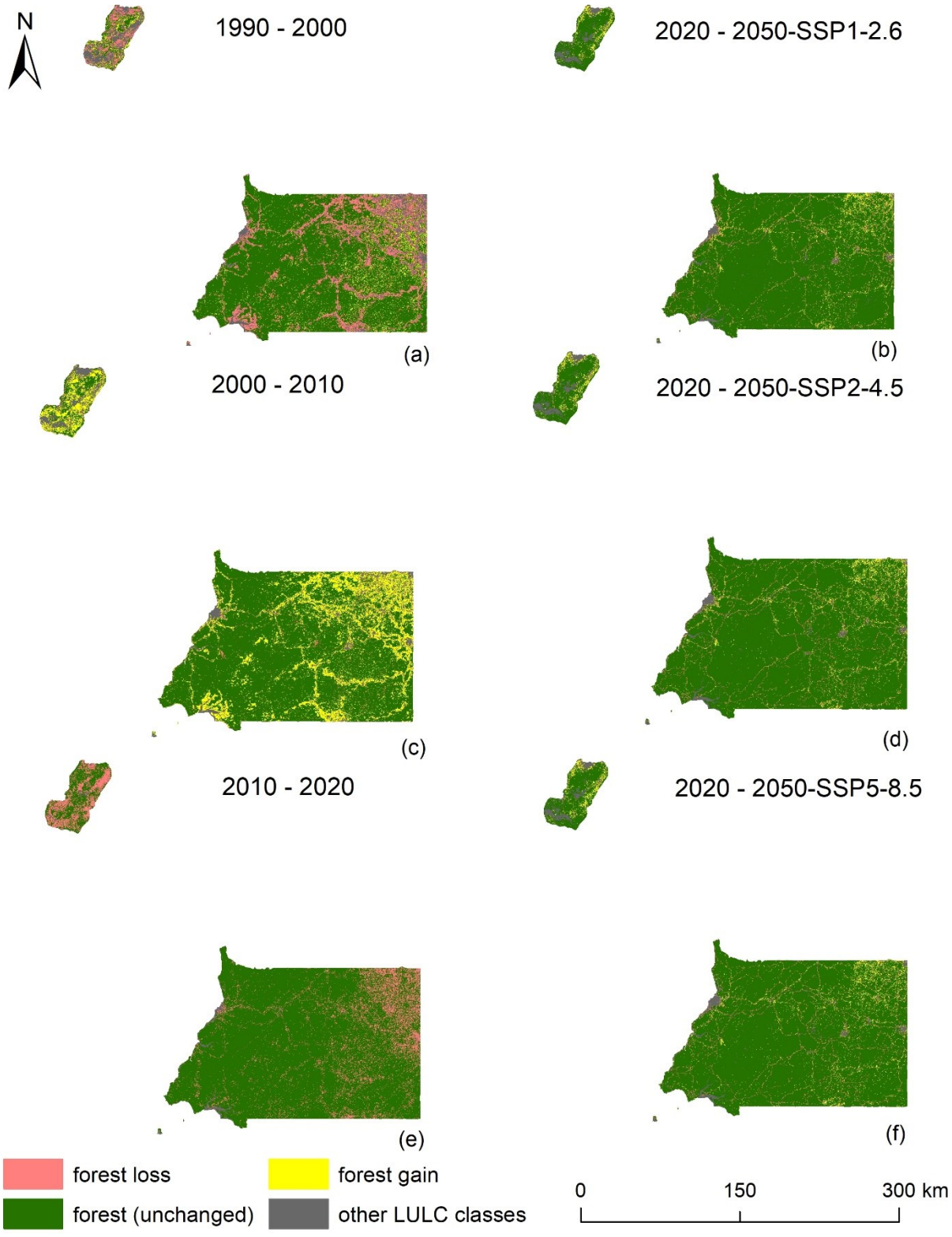

Figure S11e. Map of forest cover loss and gain in Equatorial Guinea, under all four change periods

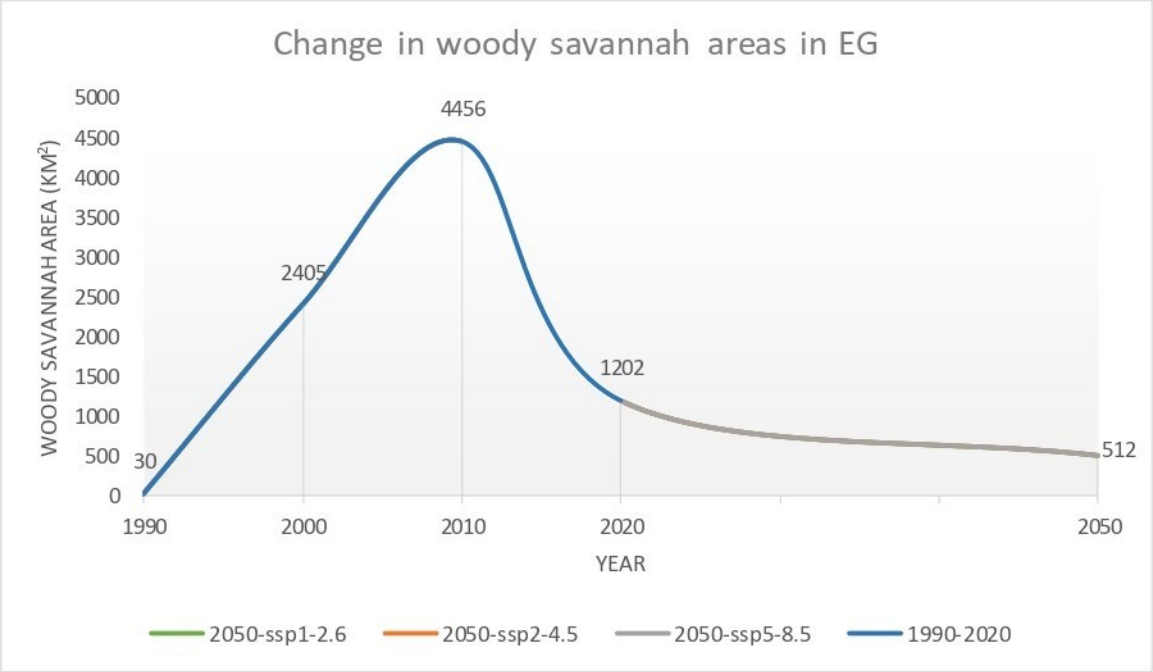

Figure S11f. Change in woody savannah areas within the DRC, under all four change periods

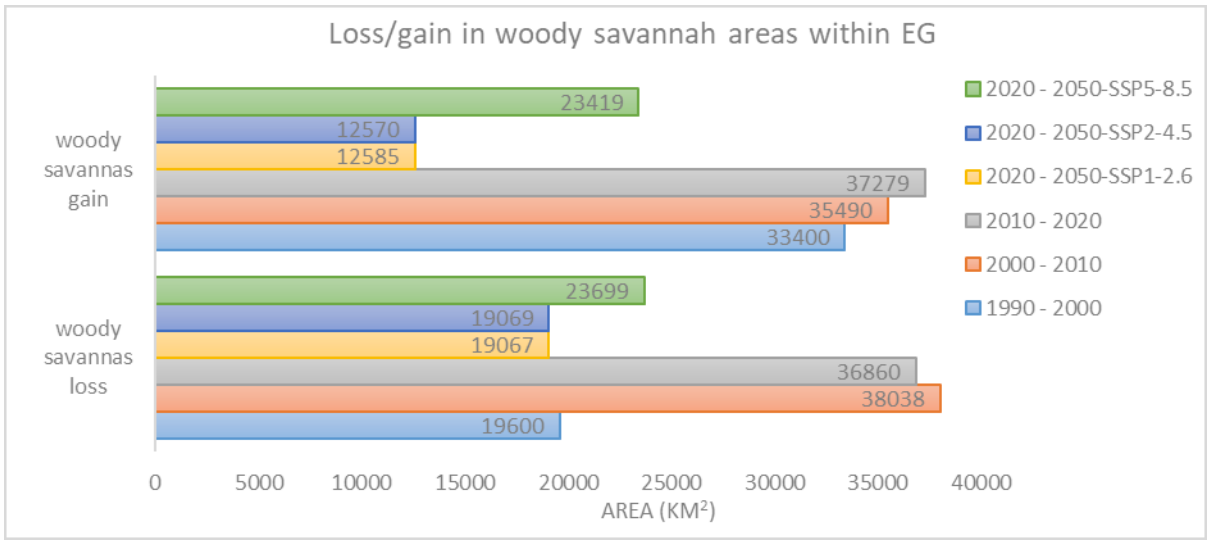

Figure S11g. Comparison in woody savannah loss and gain in Equatorial Guinea, across all four change periods

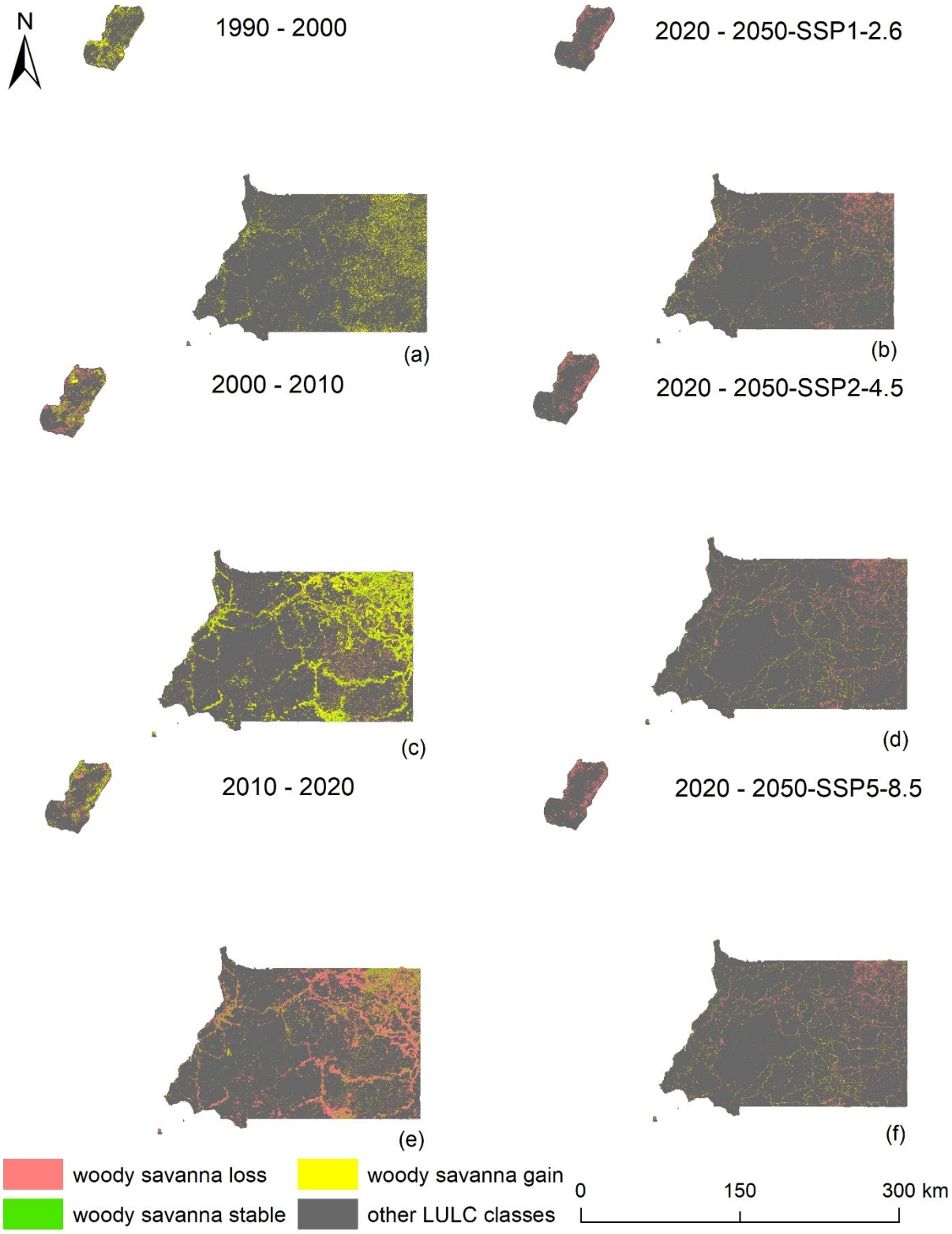

Figure S11h. Map of woody savannah loss and gain in Equatorial Guinea, under all four change periods

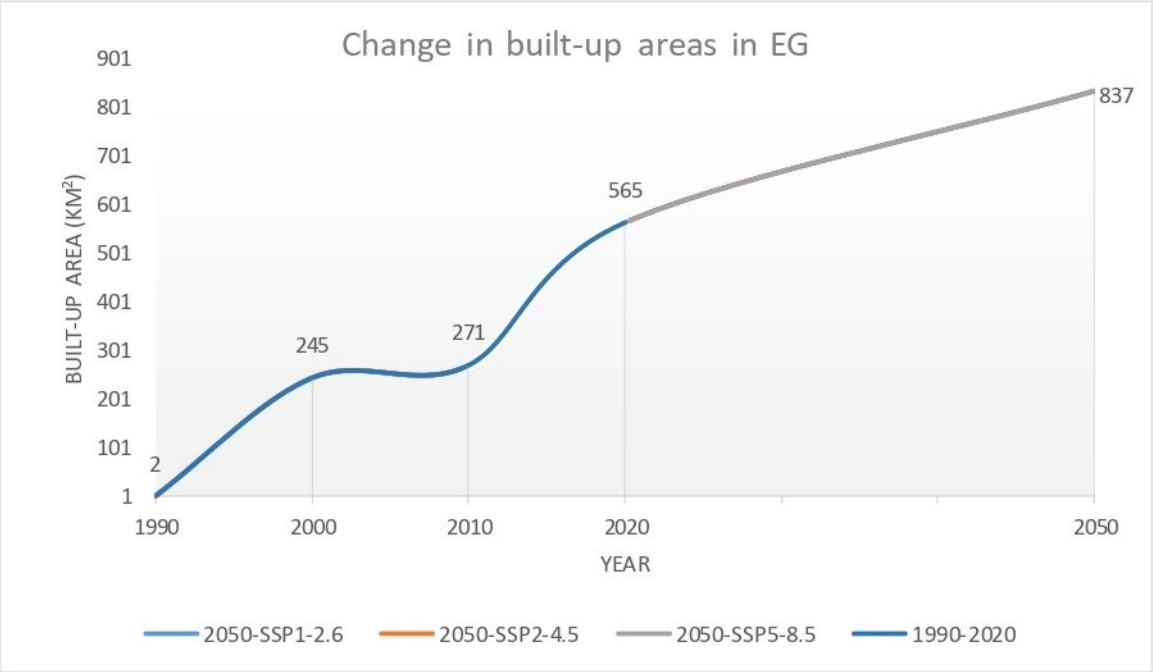

Figure S11i. Change in built-up areas within Equatorial Guinea, under all four change periods

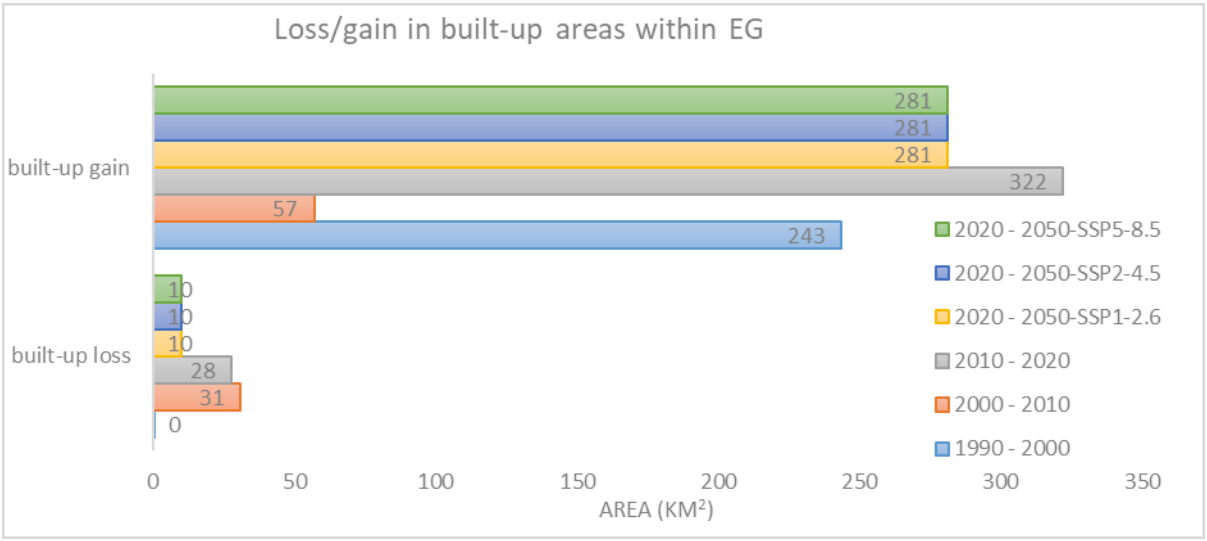

Figure S11j. Comparison in built-up area loss and gain in Equatorial Guinea, across all four change periods

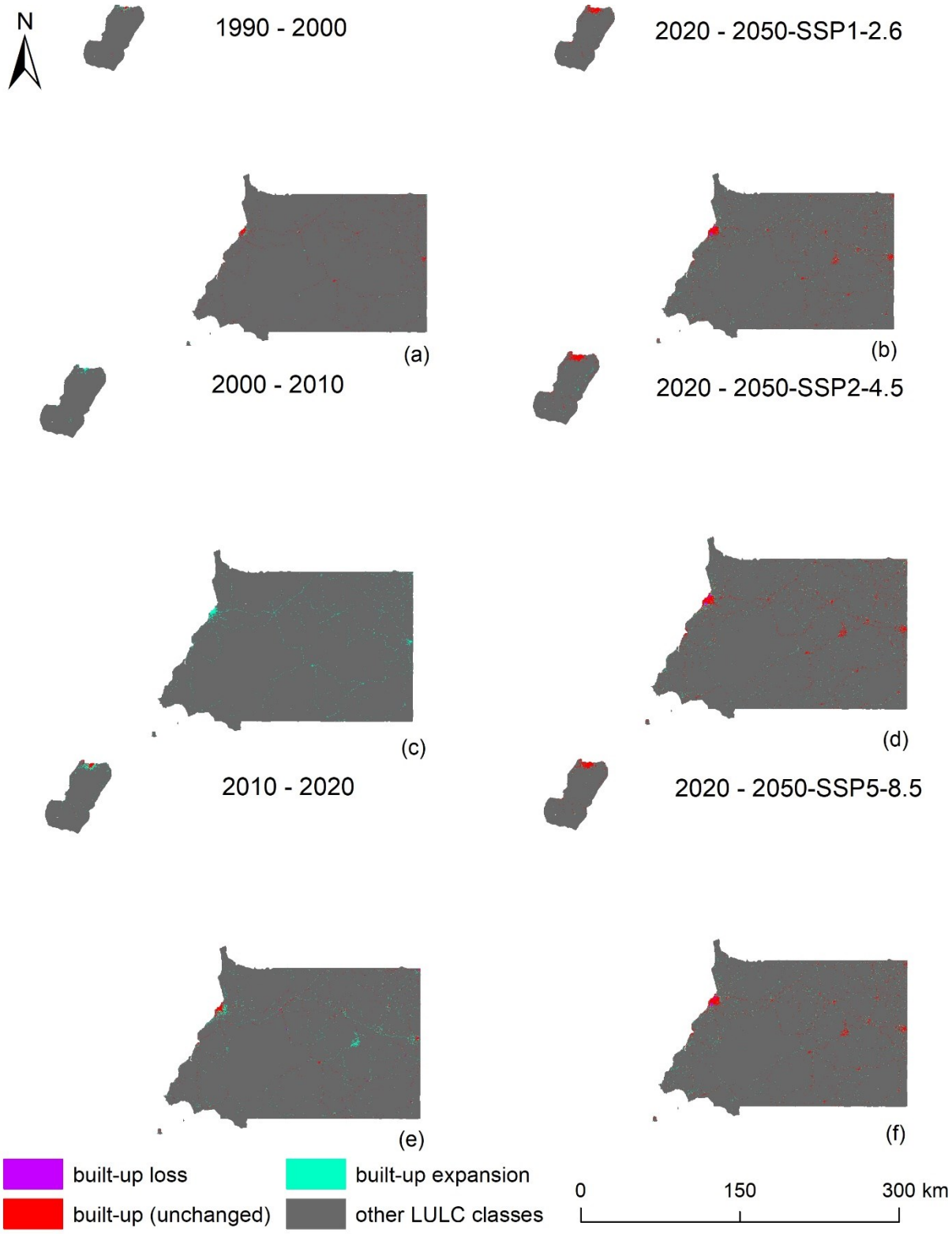

Figure S11k. Map showing loss and gains in built-up areas within Equatorial Guinea, under all four change periods

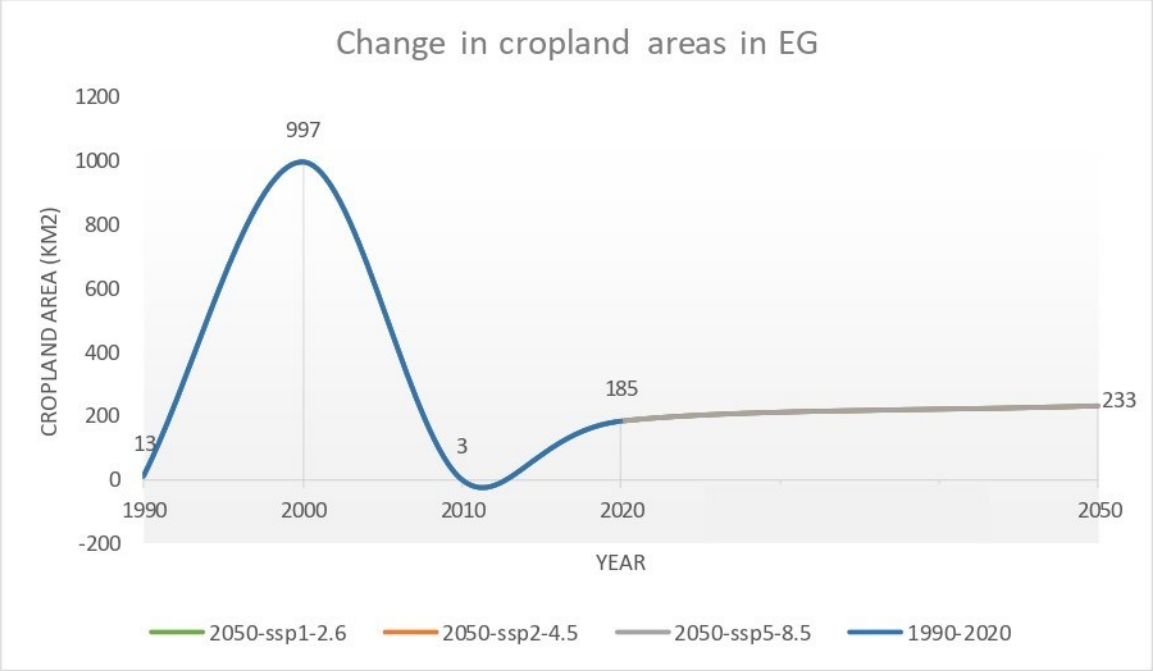

Figure S11l. Change in cropland areas within Equatorial Guinea, under all four change periods

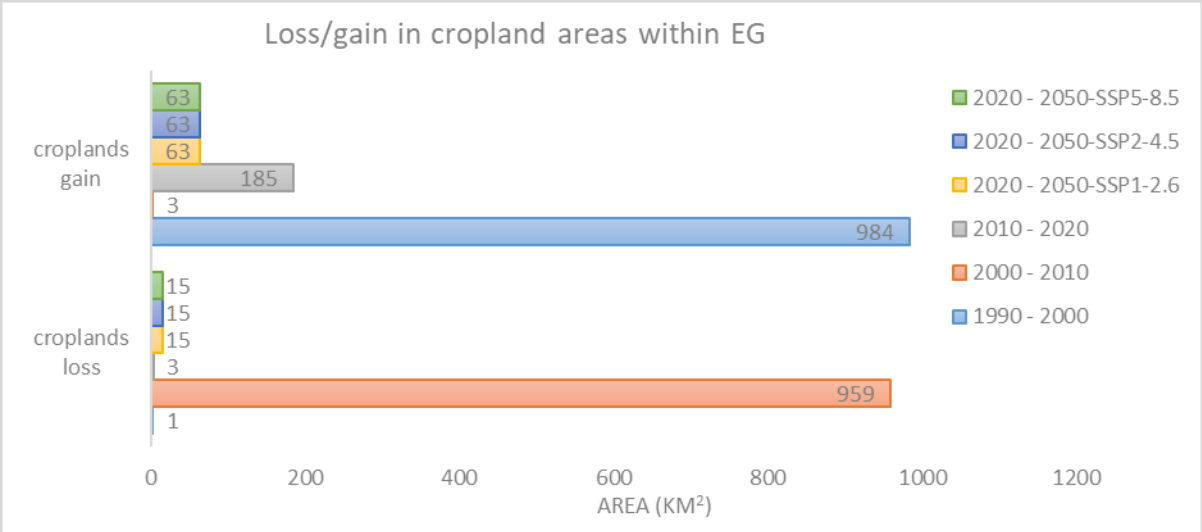

Figure S11m. Comparison in cropland area loss and gain in Equatorial Guinea, across all four change periods

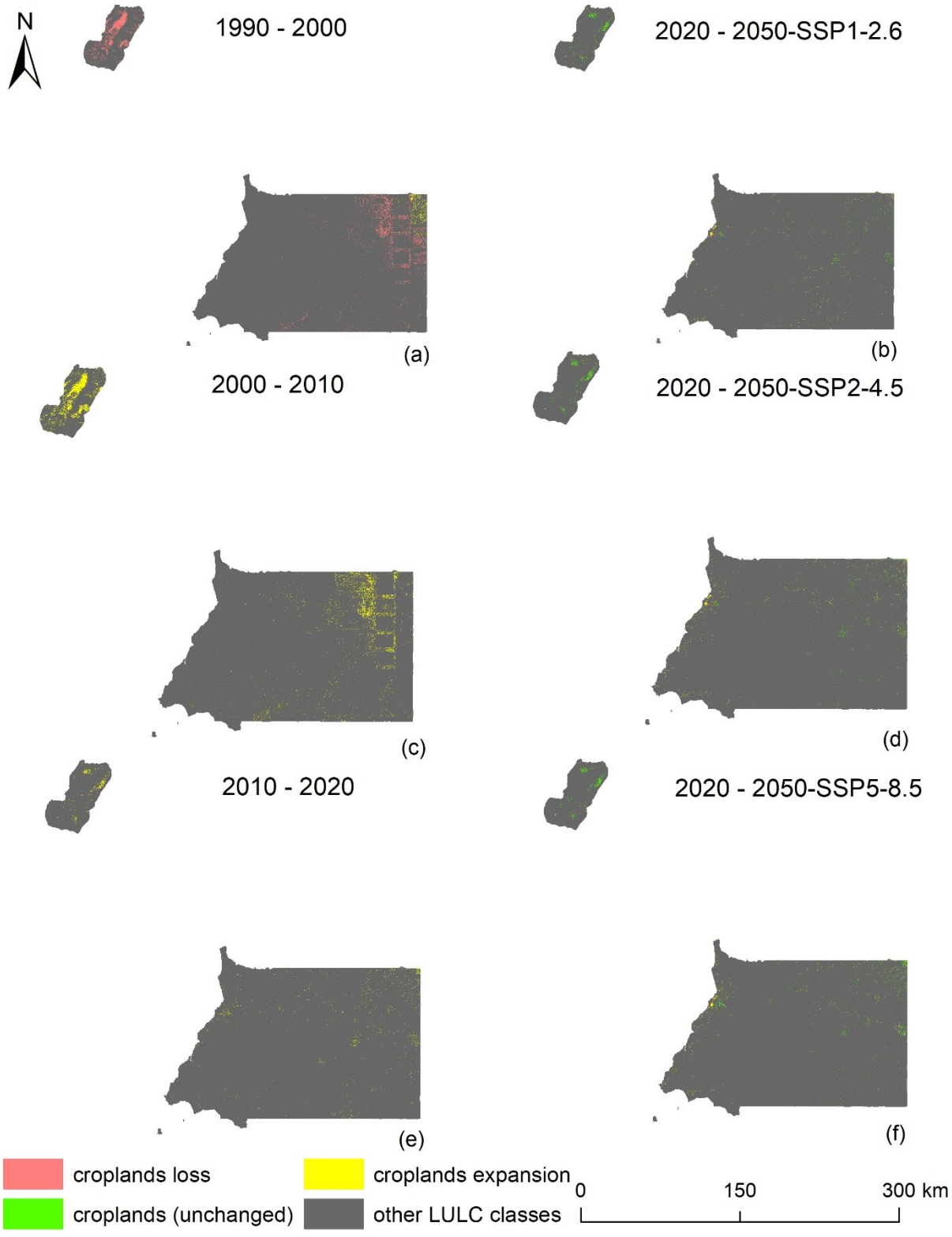

Figure S11n. Map of croplands gain/loss in Equatorial Guinea, under all four change periods

Table S24a. Area and proportion of land cover classes in each year of study in EG

	1990		2000		2010		2020		2050					
									SSP1-2.6		SSP2-4.5		SSP5-8.5	
LULC class	**Area (km2)**	**% Area**	**Area (km2)**	**% Area**	**Area (km2)**	**% Area**	**Area (km2)**	**% Area**	Area (km2)	% Area	Area (km2)	% Area	Area (km2)	% Area
croplands	13.1	0	996.9	3.7	3.2	0	185.3	0.7	233.4	0.9	233.4	0.9	233.4	0.9
dense forest	26739.6	98.7	22850.8	84.4	19669.4	73.2	24490	91.1	24896.1	92.6	24896.1	92.6	24896.1	92.6
grassland/savannas	1.9	0	42.1	0.2	58.9	0.2	24	0.1	5.7	0	5.7	0	5.7	0
open savannas/barelands	126.5	0.5	245.2	0.9	1758.6	6.5	149.6	0.6	135.5	0.5	135.5	0.5	135.5	0.5
built-up areas	1.6	0	244.9	0.9	270.9	1	565.1	2.1	836.5	3.1	836.5	3.1	836.5	3.1
water bodies	169.1	0.6	298.1	1.1	229.8	0.9	259.7	1.0	256.7	1	256.7	1	256.7	1
wetlands	0.2	0	1.9	0	437.2	1.6	1.2	0.0	1.2	0	1.2	0	1.2	0
woody savannas	30.1	0.1	2404.6	8.9	4456.2	16.6	1202.1	4.5	512	1.9	512	1.9	512	1.9
Total	27082	100	27084.6	100	26884.2	100	26877.1	100	26877.1	100	26877.1	100	26877.1	100

Table S24b. Quantified decadal changes in land cover patterns in EG, between 1990-2020

	1990-2000		2000-2010		2010-2020		2020-2050					
							SSP1-2.6		SSP2-4.5		SSP5-8.5	
LULC classes	**Area (km2)**	**% Area**	**Area (km2)**	**% Area**	**Area (km2)**	**% Area**	**Area (km2)**	**% Area**	**Area (km2)**	**% Area**	**Area (km2)**	**% Area**
croplands	983.8	3.6	-993.7	-3.7	182.1	0.7	48.1	0.2	48.1	0.2	48.1	0.2
dense forest	-3888.8	-14.4	-3181.4	-11.2	4820.6	18	406.1	1.5	406.1	1.5	406.1	1.5
grassland/savannas	40.2	0.1	16.8	0.1	-34.9	-0.1	-18.3	-0.1	-18.3	-0.1	-18.3	-0.1
open savannas/barelands	118.7	0.4	1513.4	5.6	-1609	-6.0	-14.1	-0.1	-14.1	-0.1	-14.1	-0.1
built-up areas	243.3	0.9	26	0.1	294.2	1.1	271.4	1.0	271.4	1.0	271.4	1.0
water bodies	129	0.5	-68.3	-0.2	29.9	0.1	-3.0	0.0	-3.0	0.0	-3.0	0.0
wetlands	1.7	0	435.2	1.6	-435.9	-1.6	0.0	0.0	0.0	0.0	0.0	0.0
woody savannas	2374.6	8.8	2051.6	7.7	-3254.1	-12.1	-690.1	-2.6	-690.1	-2.6	-690.1	-2.6

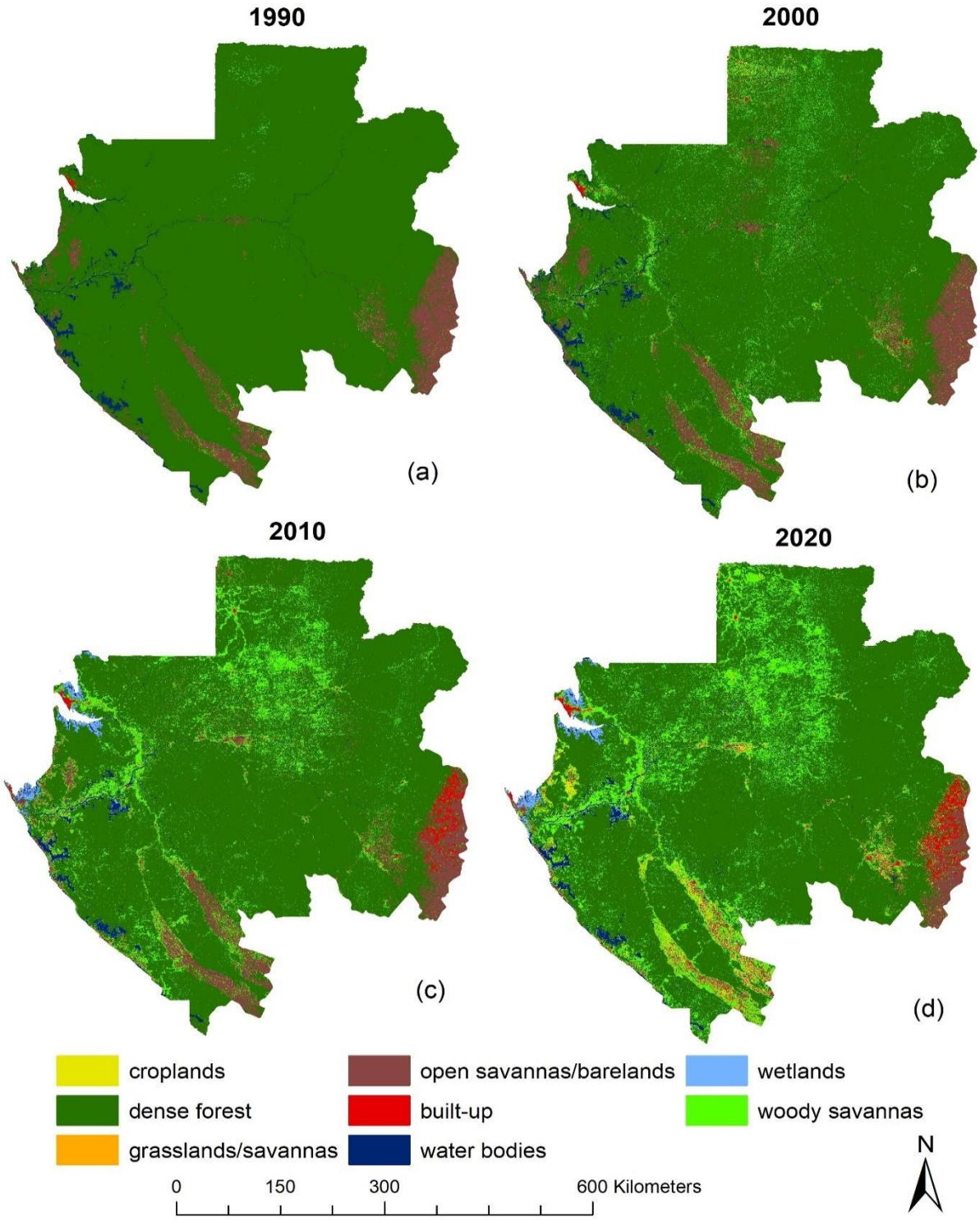

Figure S12a. Land cover classification maps for Gabon, for the years 1990, 2000, 2010, and 2020.

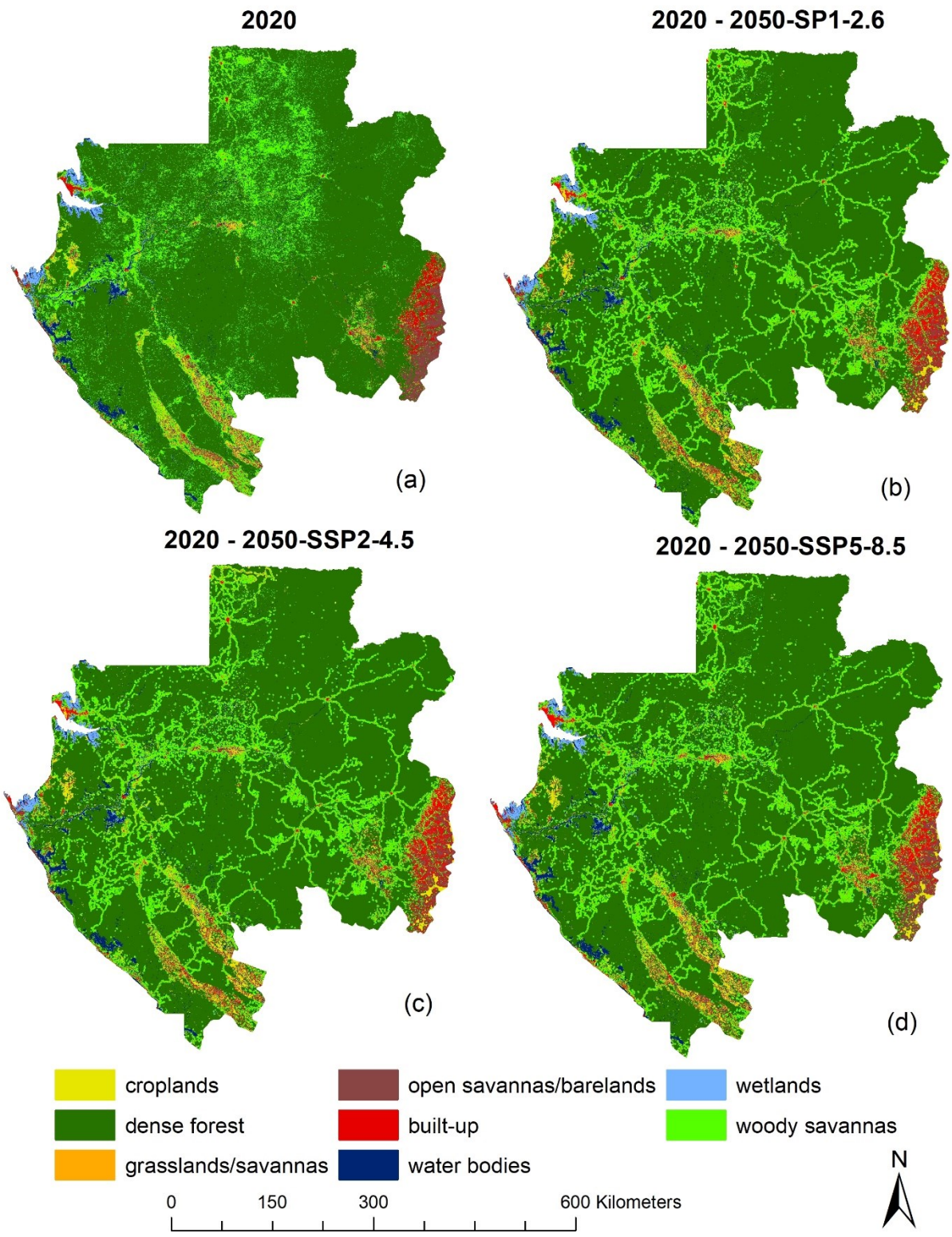

Figure S12b. Projected LULC maps of Gabon for the year 2050. Map shows projected results under all three climate change scenarios (SSP1-2.6, SSP2-4.5 and SSP5-8.5), with the year 2020 representing the baseline condition (for comparison purpose).

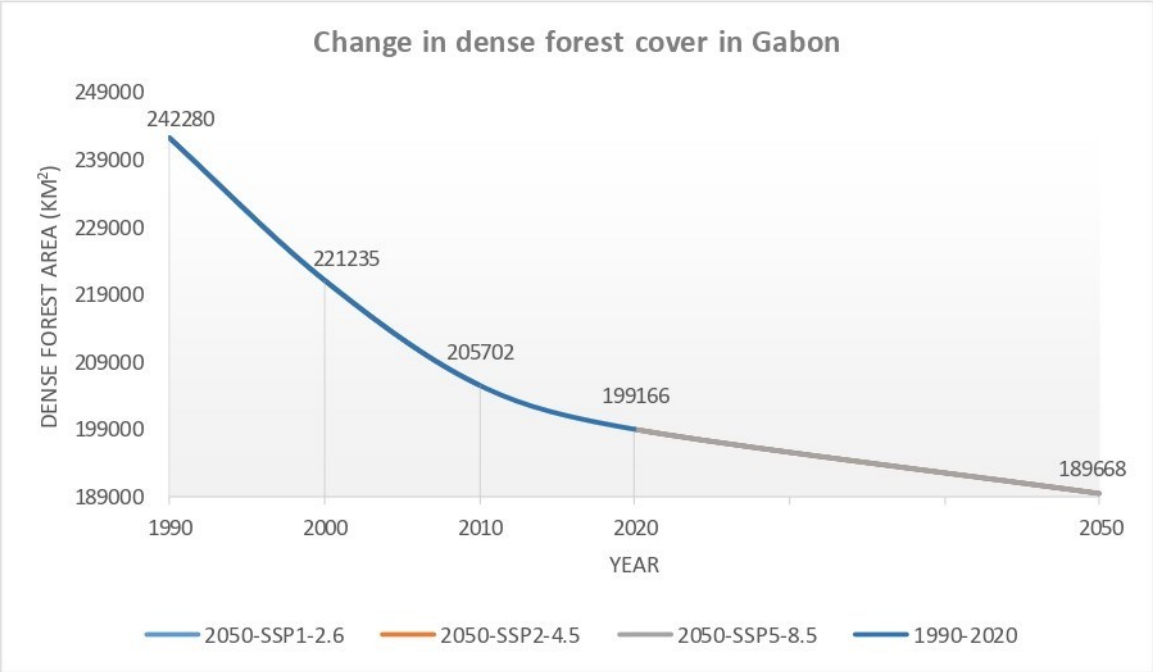

Figure S12c. Change in dense forest cover within Gabon, under all four change periods (1990-2000, 2000-2010, 2010-2020, and 2020-2050-under SSP1, SSP2, and SSP5 conditions).

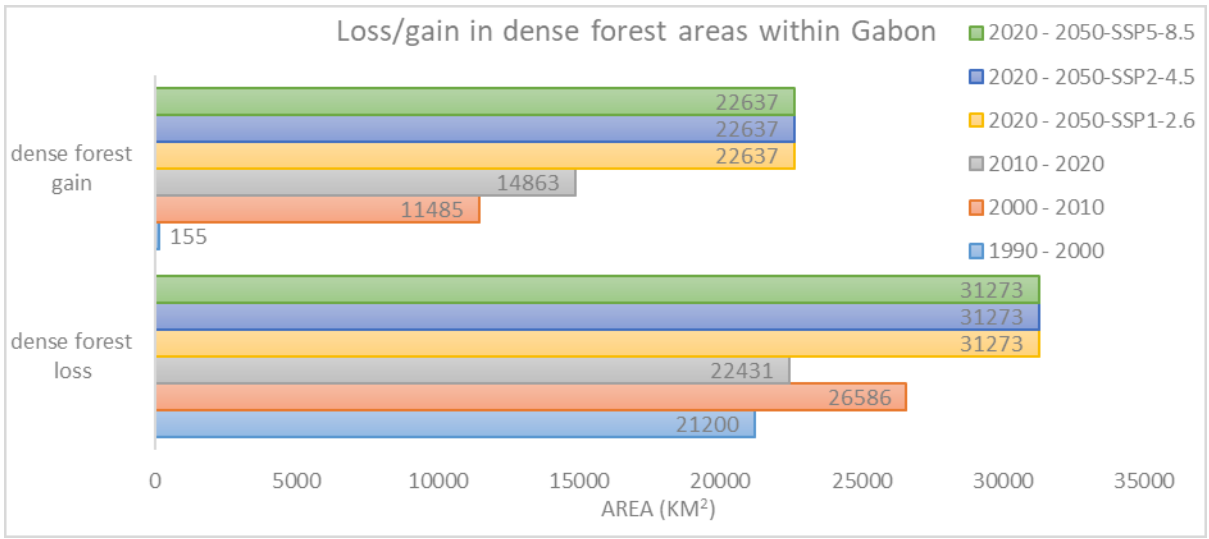

Figure S12d. Comparison in dense forest cover loss and gain in Gabon, across all four change periods

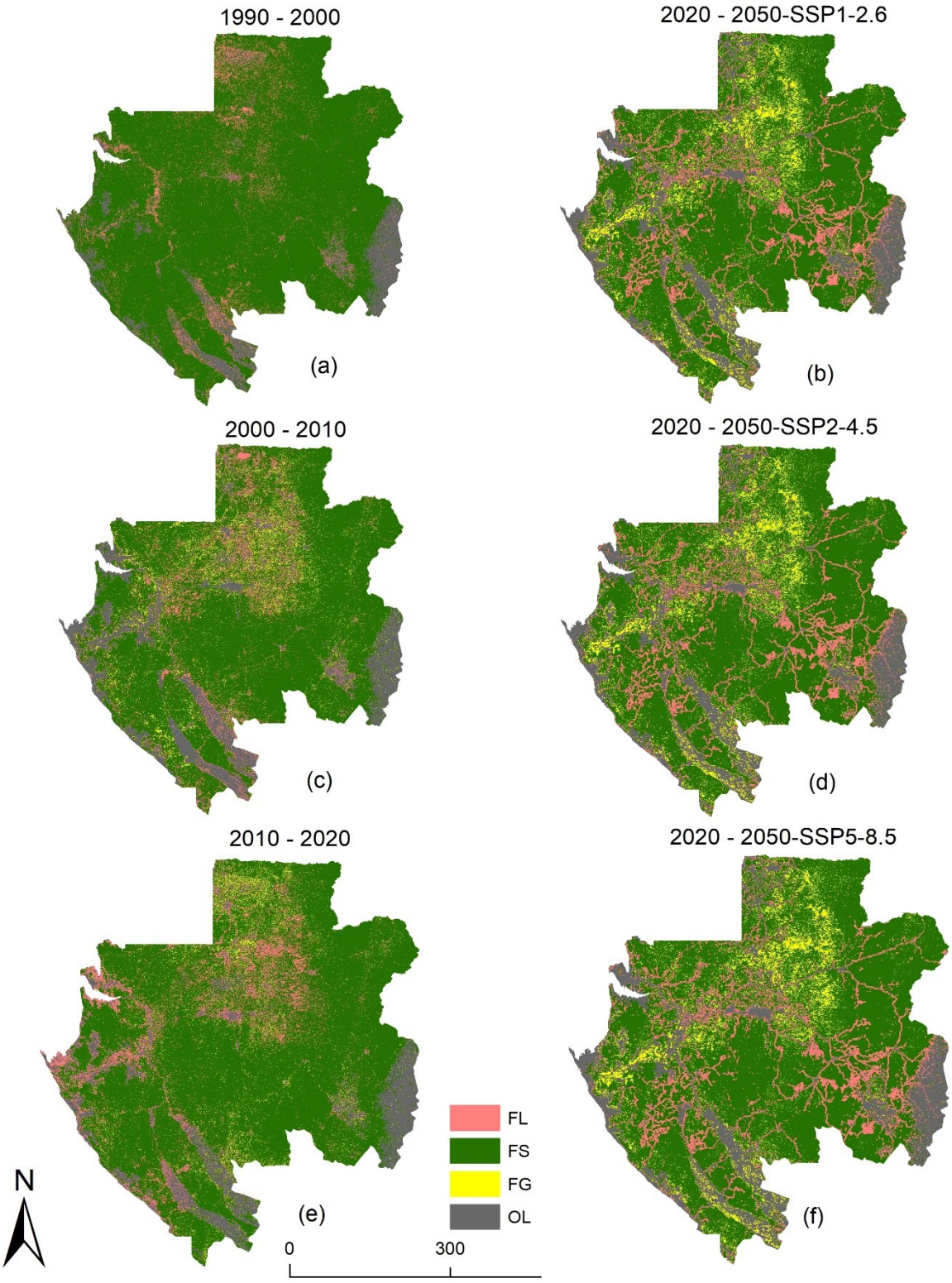

Figure S12e. Map of forest cover loss and gain in Gabon, under all four change periods. FL = forest loss; FS = forest stable (unchanged); FG = forest gain; OL = other LULC

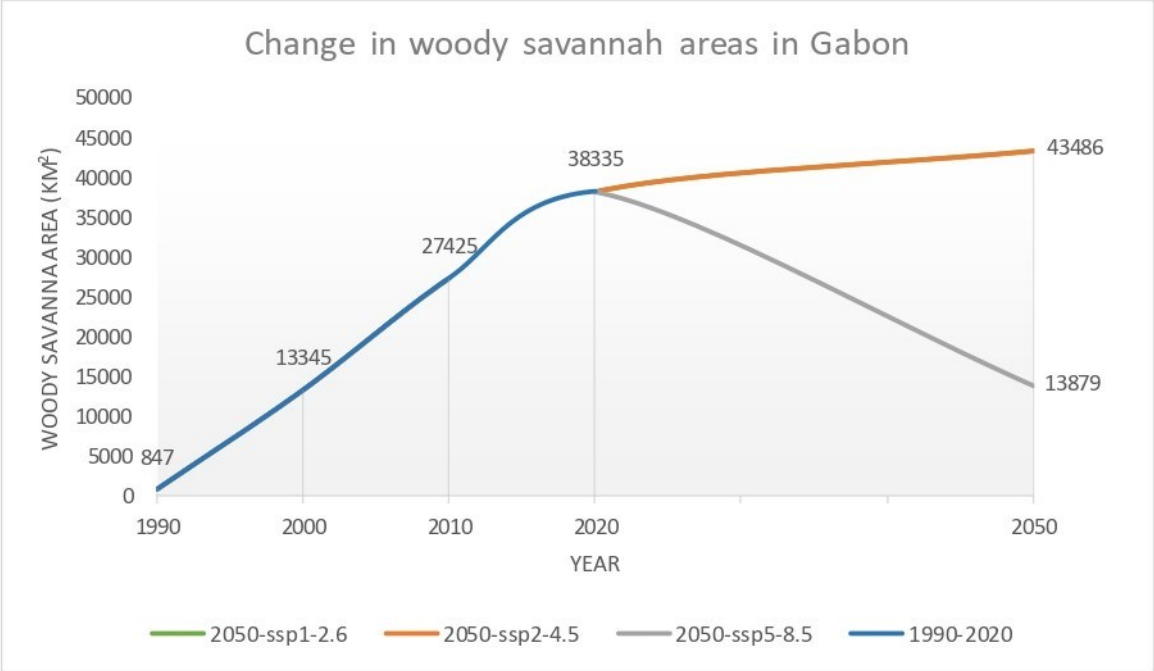

Figure S12f. Change in woody savannah areas within Gabon, under all four change periods

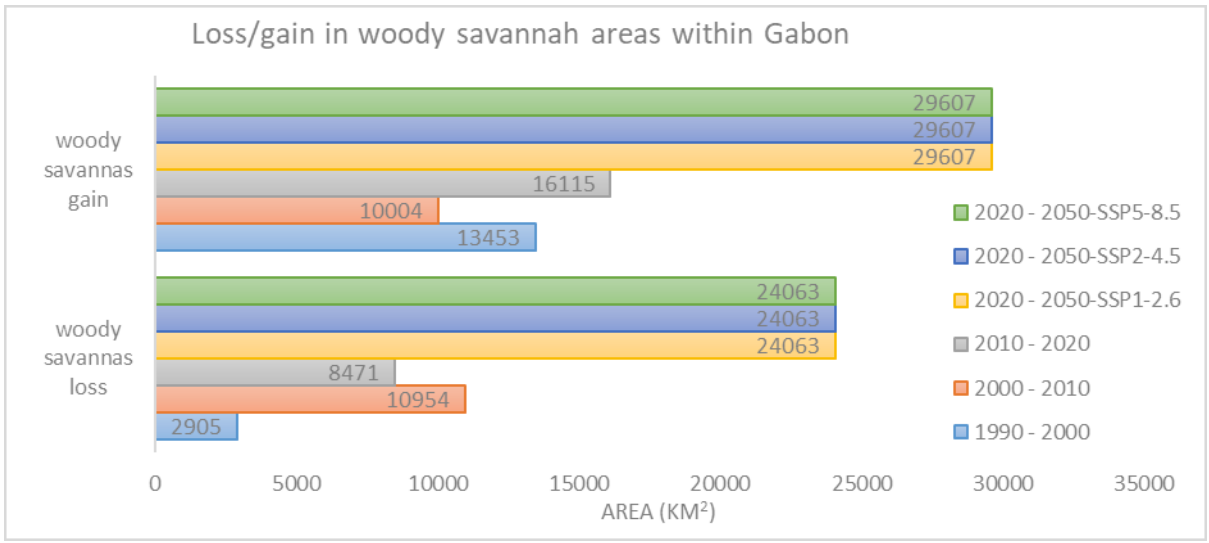

Figure S12g. Comparison in woody savannah loss and gain in Gabon, across all four change periods

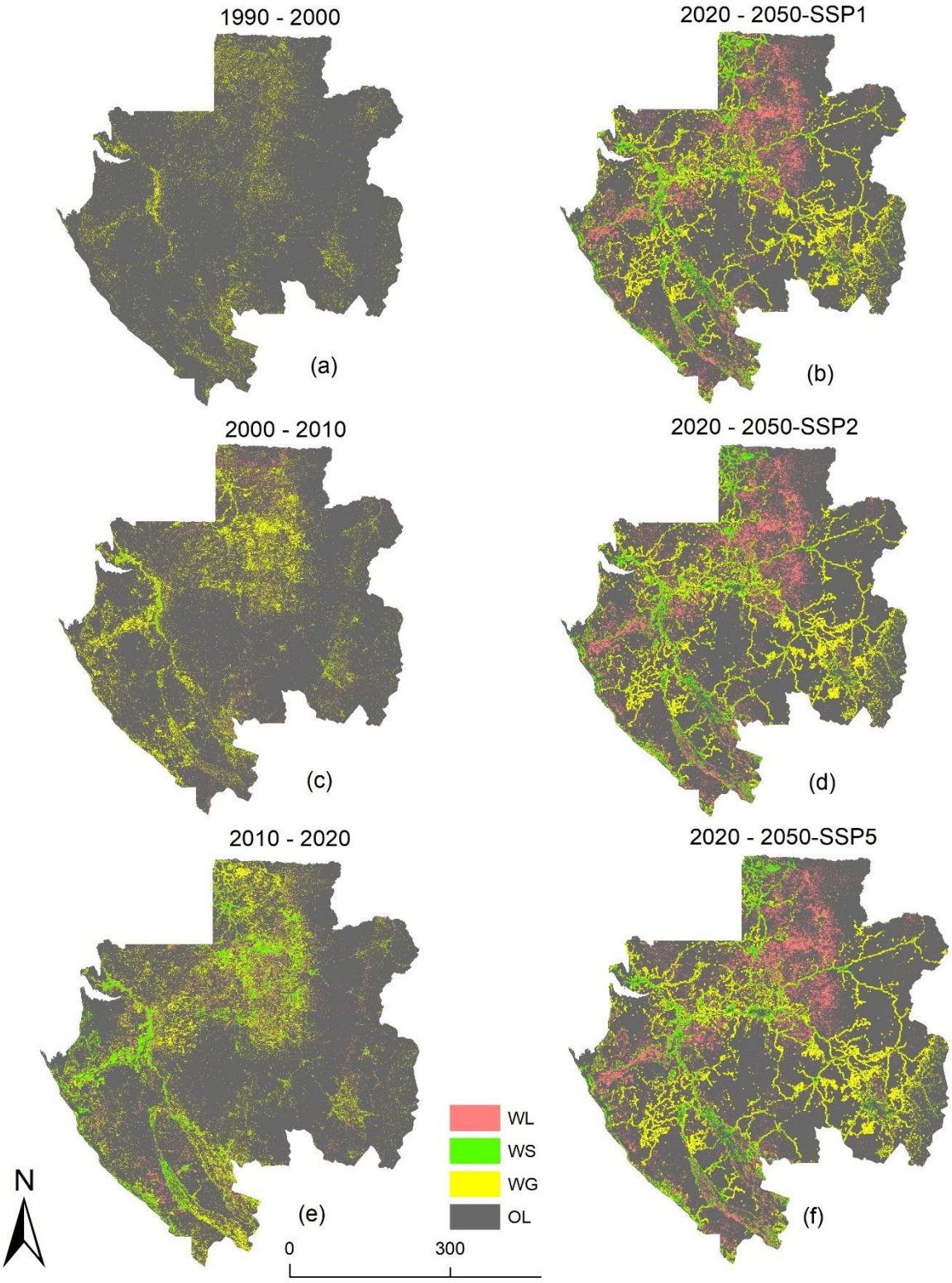

Figure S12h. Map of woody savannah loss and gain in Gabon, under all four change periods. WL = woody savannah loss; WS = woody savannah stable (unchanged); WG = woody savannah gain; OL = other LULC

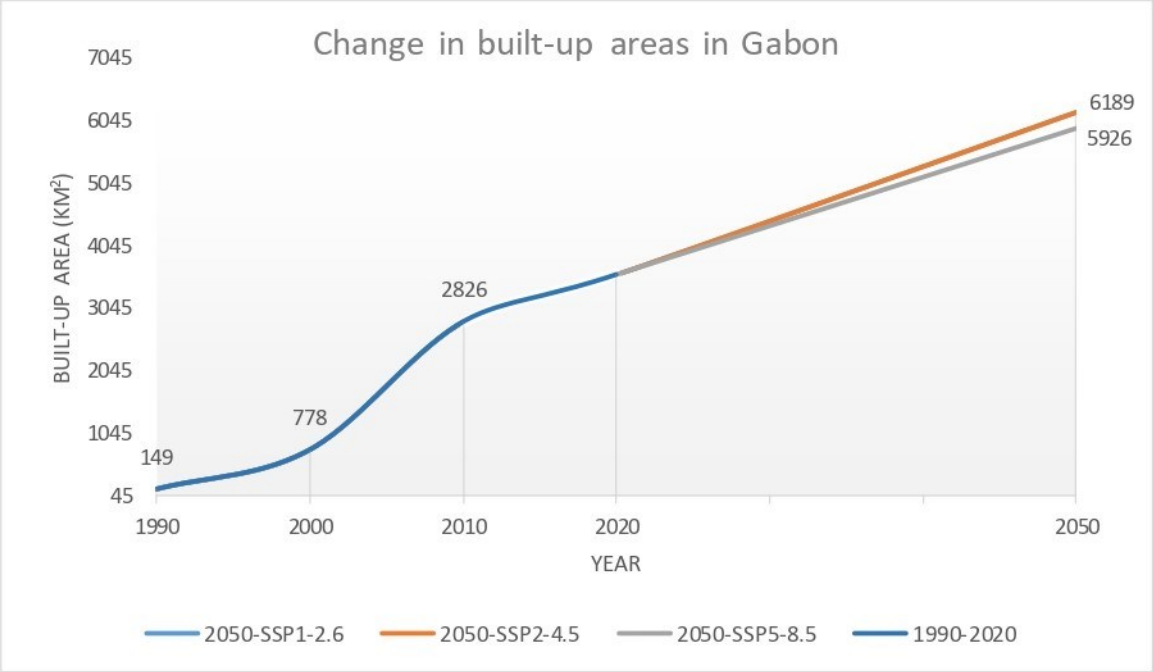

Figure S12i. Change in built-up areas within the Gabon, under all four change periods

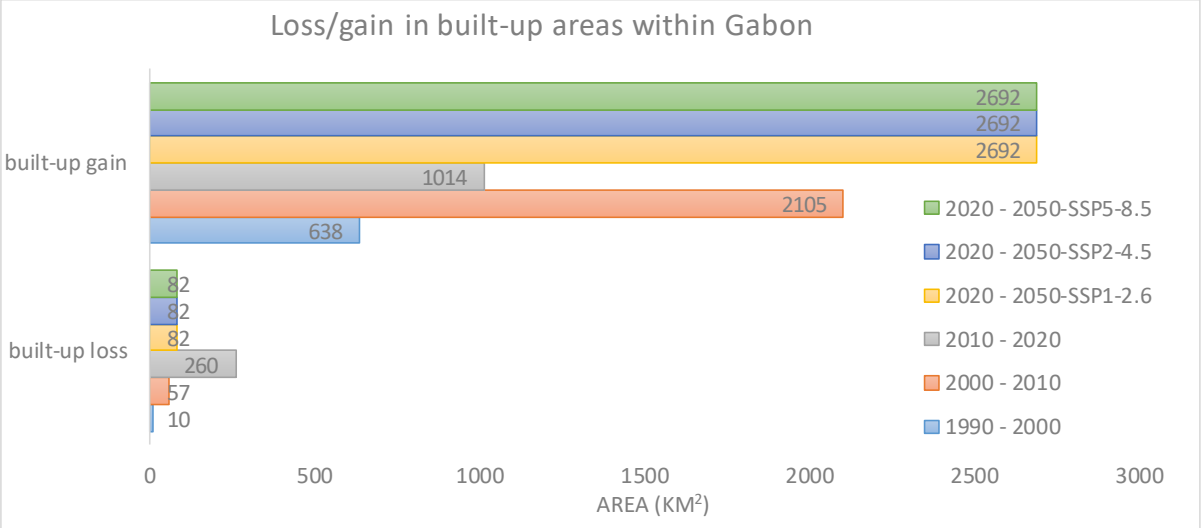

Figure S12j. Comparison in built-up area loss and gain in Gabon, across all four change periods

Figure S12k. Map showing loss and gains in built-up areas within Gabon, under all four change periods. BL = built-up area loss; BS = built-up area stable (unchanged): BE = built-up expansion; OL = other LULC classes

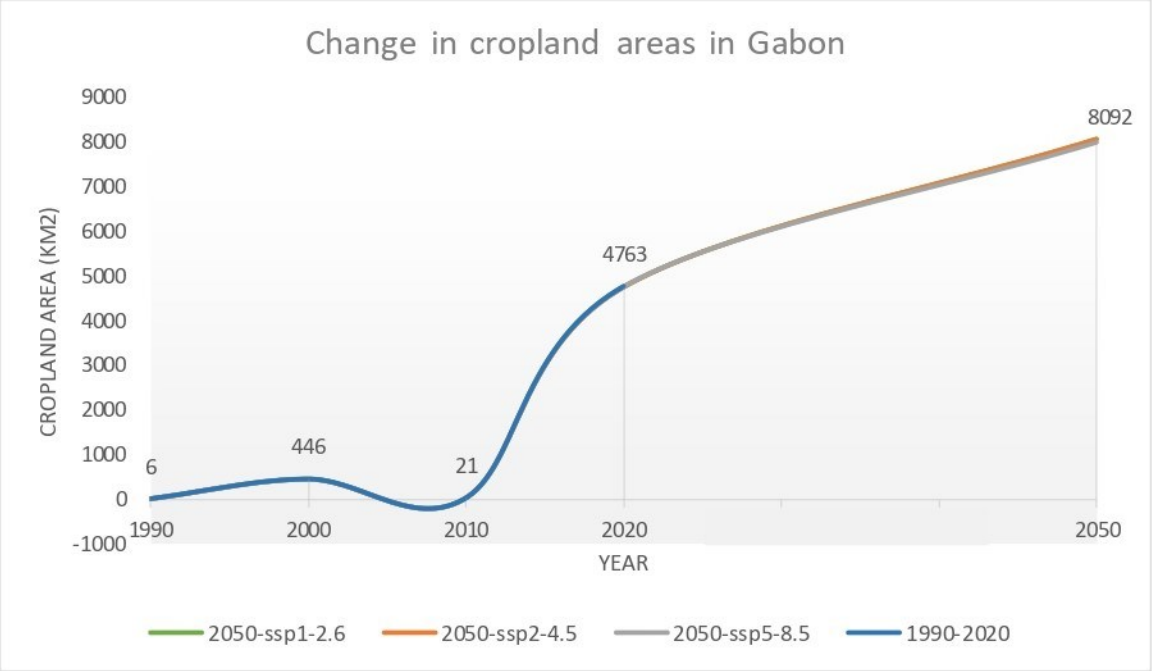

Figure S12l. Change in cropland areas within Gabon, under all four change periods

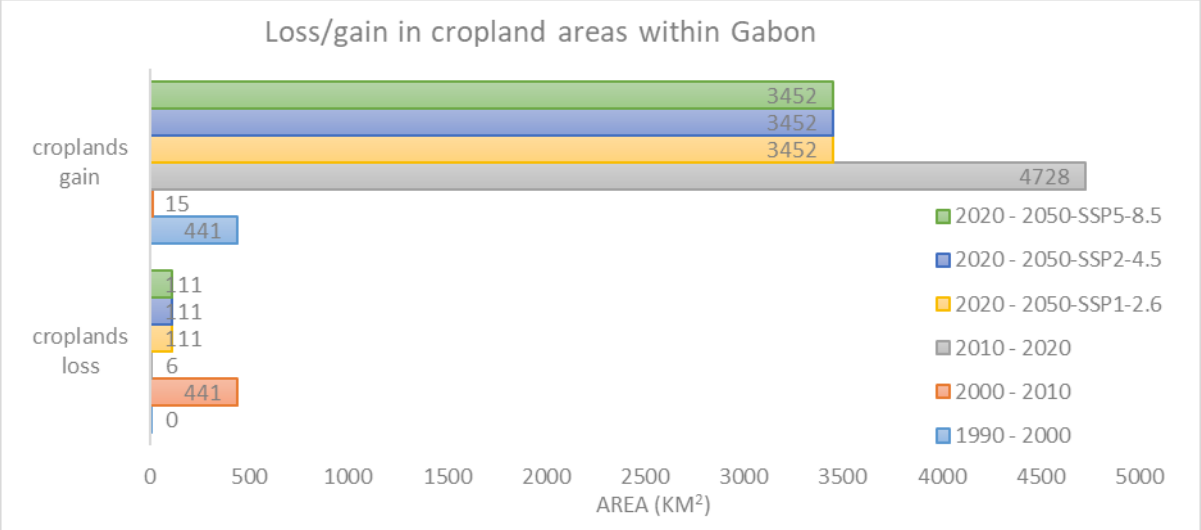

Figure S12m. Comparison in cropland area loss and gain in Gabon, across all four change periods

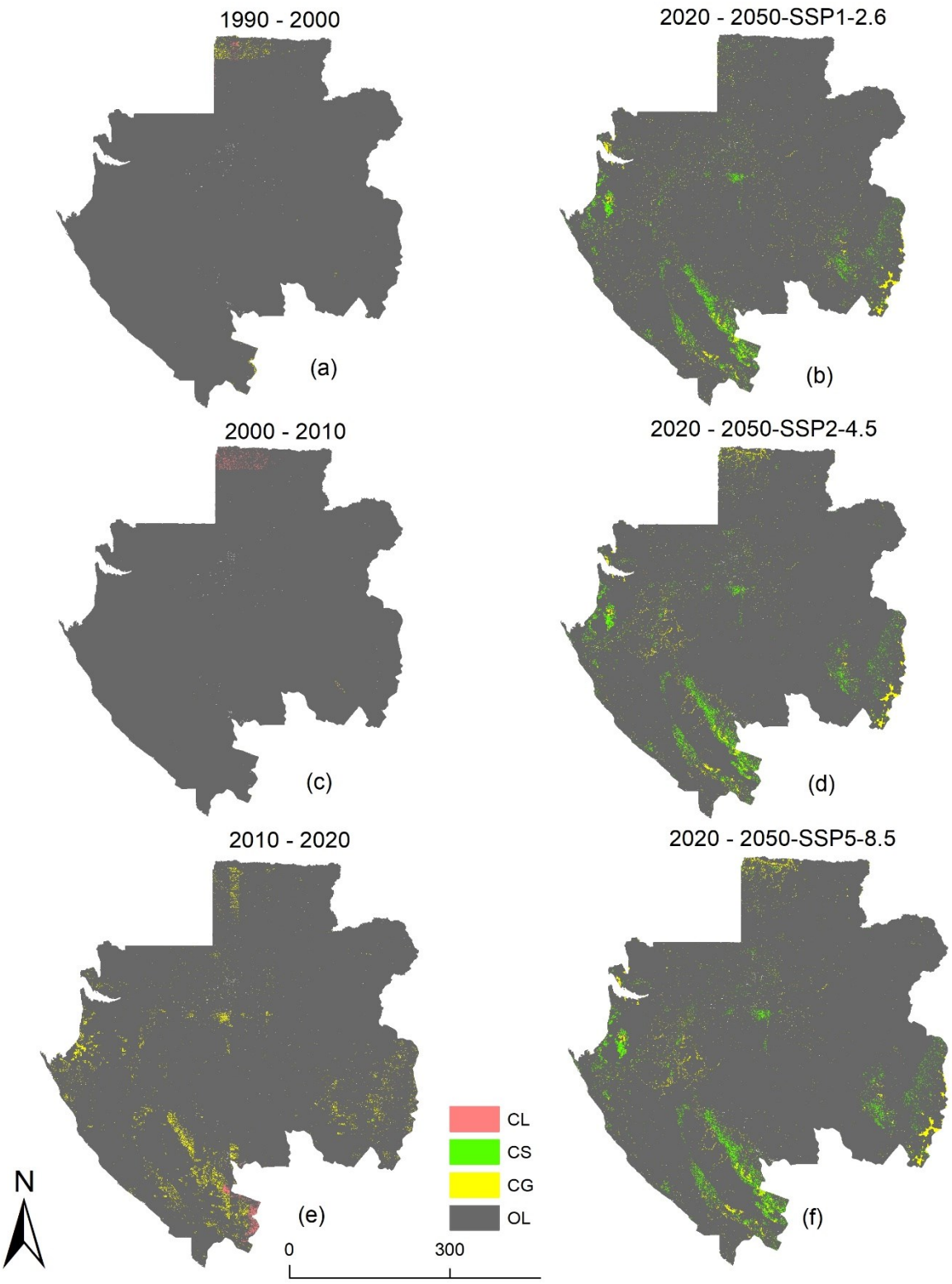

Figure S12n. Map of croplands gain/loss in Gabon, under all four change periods. CL = cropland area loss; CS = cropland area stable (unchanged); CG = cropland area gain; OL = other LULC classes

Table S25a. Area and proportion of land cover classes in each year of study in Gabon

	1990		2000		2010		2020		2050					
									SSP1		SSP2		SSP5	
LULC class	**Area (km2)**	**% Area**	**Area (km2)**	**% Area**	**Area (km2)**	**% Area**	**Area (km2)**	**% Area**	Area (km2)	% Area	Area (km2)	% Area	Area (km2)	% Area
croplands	5.5	0	446.1	0.2	20.5	0	4763	1.8	8091.5	3.1	8091.5	3.1	8004.9	3.4
dense forest	242279.9	91.8	221234.6	83.8	205702.3	78	199165.8	75.1	189667.8	71.9	189667.8	71.9	189667.8	81.2
grassland/savannas	76.1	0	267.2	0.1	212.3	0.1	1031.3	0.4	1169.9	0.4	1169.9	0.4	1030.2	0.4
open savannas/barelands	17362.8	6.6	22842.6	8.7	20889.7	7.9	10612.8	4	7926.9	3.0	7926.9	3.0	7926.9	3.4
built-up areas	149.3	0.1	777.6	0.3	2826.3	1.1	3583.2	1.4	6189.1	2.3	6189.1	2.3	5923.5	2.5
water bodies	3134.1	1.2	4929.5	1.9	4379.1	1.7	5224.1	2	5152.1	2.0	5152.1	2.0	5187.9	2.2
wetlands	14.3	0	26.6	0	2110.7	0.8	2345.8	0.9	2054.1	0.8	2054.1	0.8	2054.1	0.9
woody savannas	847.4	0.3	13345.2	5.1	27425.3	10.4	38334.5	14.5	43486.2	16.5	43486.2	16.5	13879.4	5.9
Total	263869.4	100	263869.4	100	263566.2	100	265060.3	100	263737.4	100	263737.4	100	233674.6	100

Table S25b. Quantified decadal changes in land cover patterns in Gabon, between 1990-2020

	1990-2000		2000-2010		2010-2020		2020-2050					
							SSP1		SSP2		SSP5	
LULC classes	**Area (km2)**	**% Area**	**Area (km2)**	**% Area**	**Area (km2)**	**% Area**	**Area (km2)**	**% Area**	**Area (km2)**	**% Area**	**Area (km2)**	**% Area**
croplands	440.6	0.2	-425.6	-0.2	4742.6	1.8	3328.5	1.3	3328.5	1.3	3241.9	1.6
dense forest	-21045.3	-8.0	-15532.3	-5.8	-6536.5	-2.9	-9498.0	-2.7	-9498.0	-2.7	-9498.0	6.6
grassland/savannas	191.1	0.1	-54.9	0.0	818.9	0.3	138.6	0.1	138.6	0.1	-1.1	0.1
open savannas/barelands	5479.8	2.1	-1952.9	-0.7	-10277.0	-3.9	-2685.9	-1.0	-2685.9	-1.0	-2685.9	-0.6
built-up areas	628.3	0.2	2048.7	0.8	756.9	0.3	2605.9	1.0	2605.9	1.0	2340.3	1.2
water bodies	1795.4	0.7	-550.3	-0.2	844.9	0.3	-72.0	0.0	-72.0	0.0	-36.2	0.3
wetlands	12.3	0.0	2084.1	0.8	235.0	0.1	-291.7	-0.1	-291.7	-0.1	-291.7	0.0
woody savannas	12497.8	4.7	14080.1	5.3	10909.2	4.1	5151.7	2.1	5151.7	2.1	-24455.1	-8.4

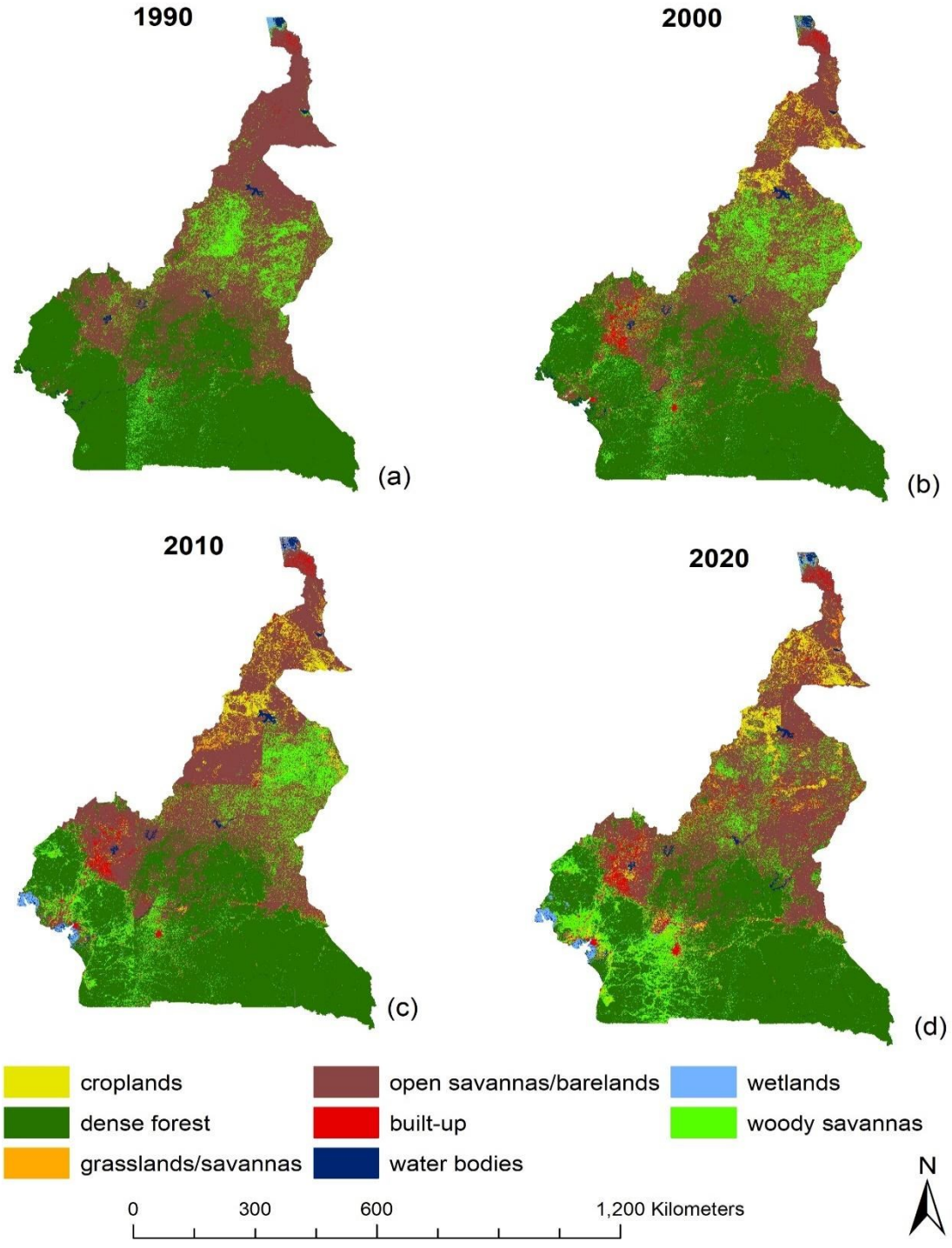

Figure S13a. Land cover classification maps for Cameroon, for the years 1990, 2000, 2010, and 2020.

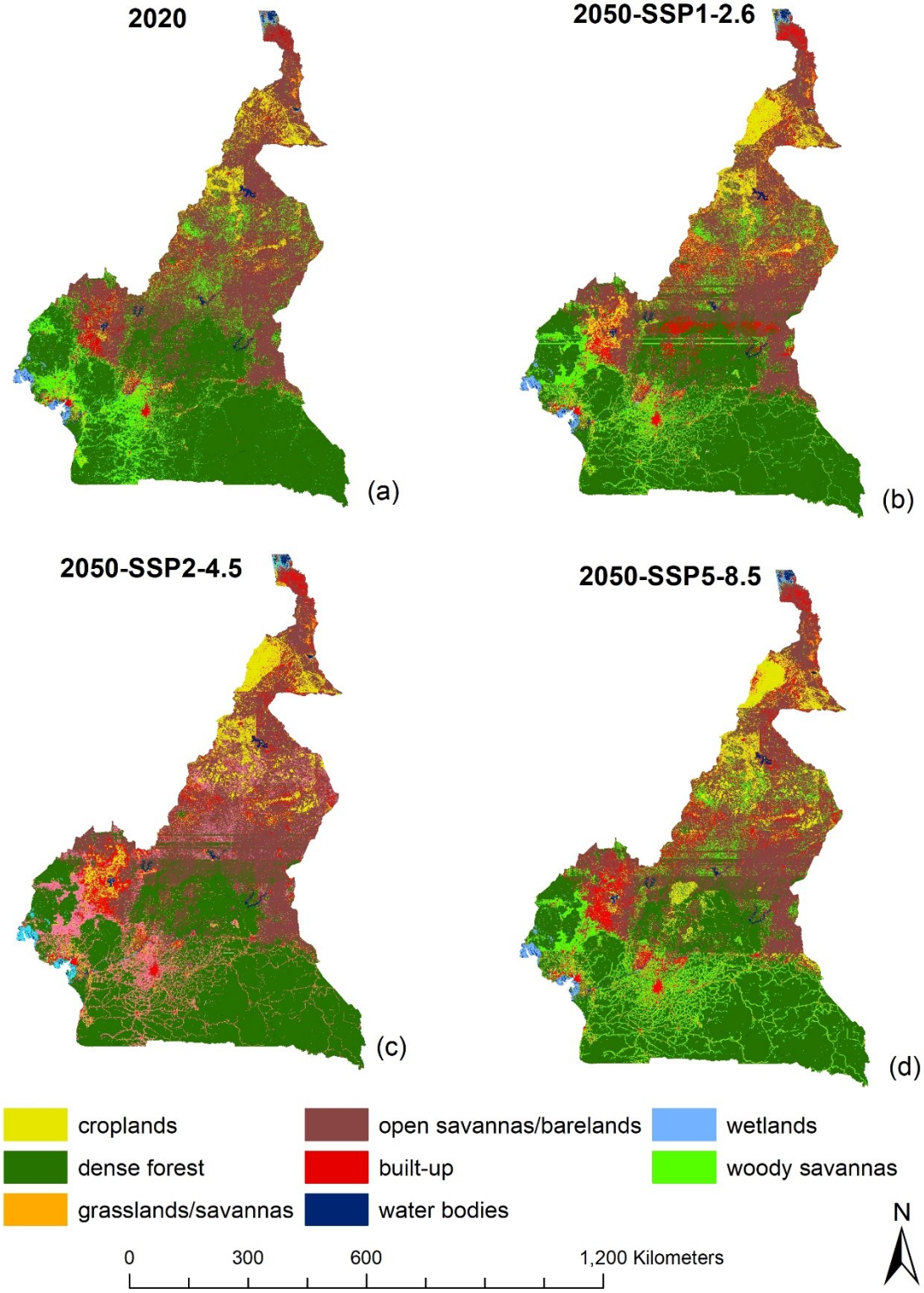

Figure S13b. Projected LULC maps of Cameroon for the year 2050. Map shows projected results under all three climate change scenarios (SSP1-2.6, SSP2-4.5 and SSP5-8.5), with the year 2020 representing the baseline condition (for comparison purpose).

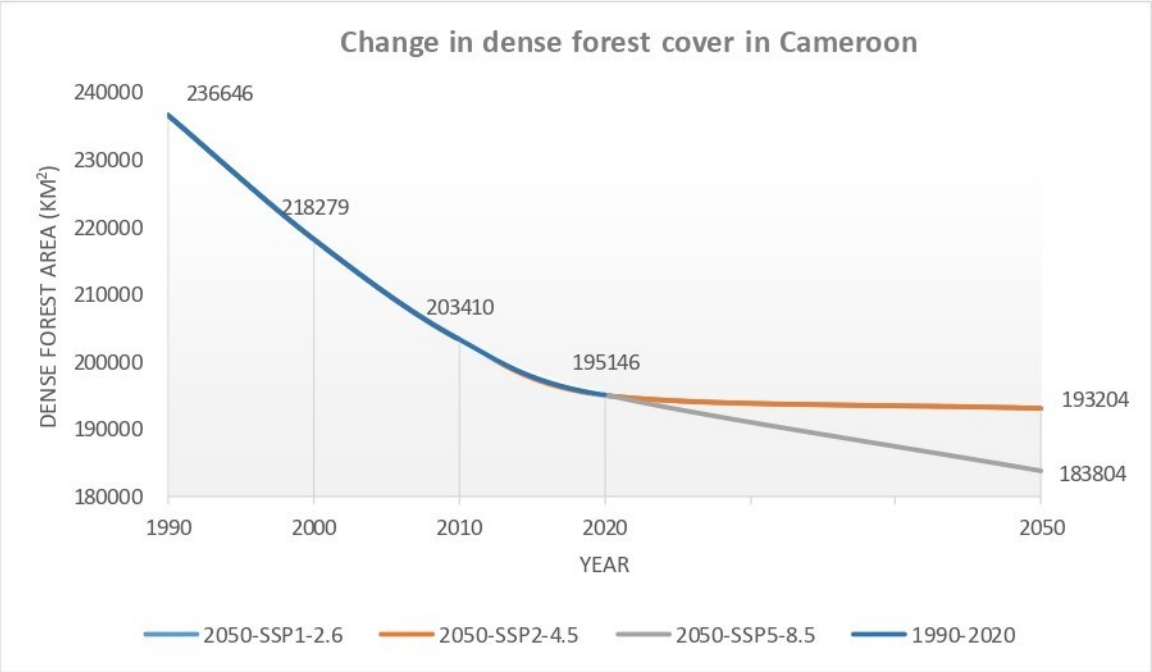

Figure S13c. Change in dense forest cover within Cameroon, under all four change periods (1990-2000, 2000-2010, 2010-2020, and 2020-2050-under SSP1-2.6, SSP2-4.5, and SSP5-8.5 climate change scenarios).

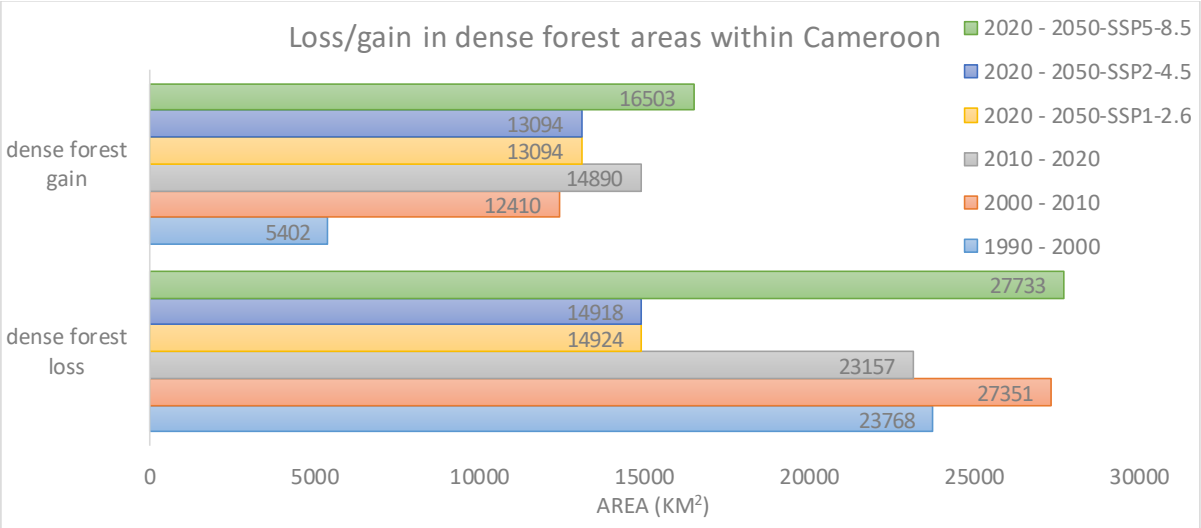

Figure S13d. Comparison in dense forest cover loss and gain in Cameroon, across all four change periods

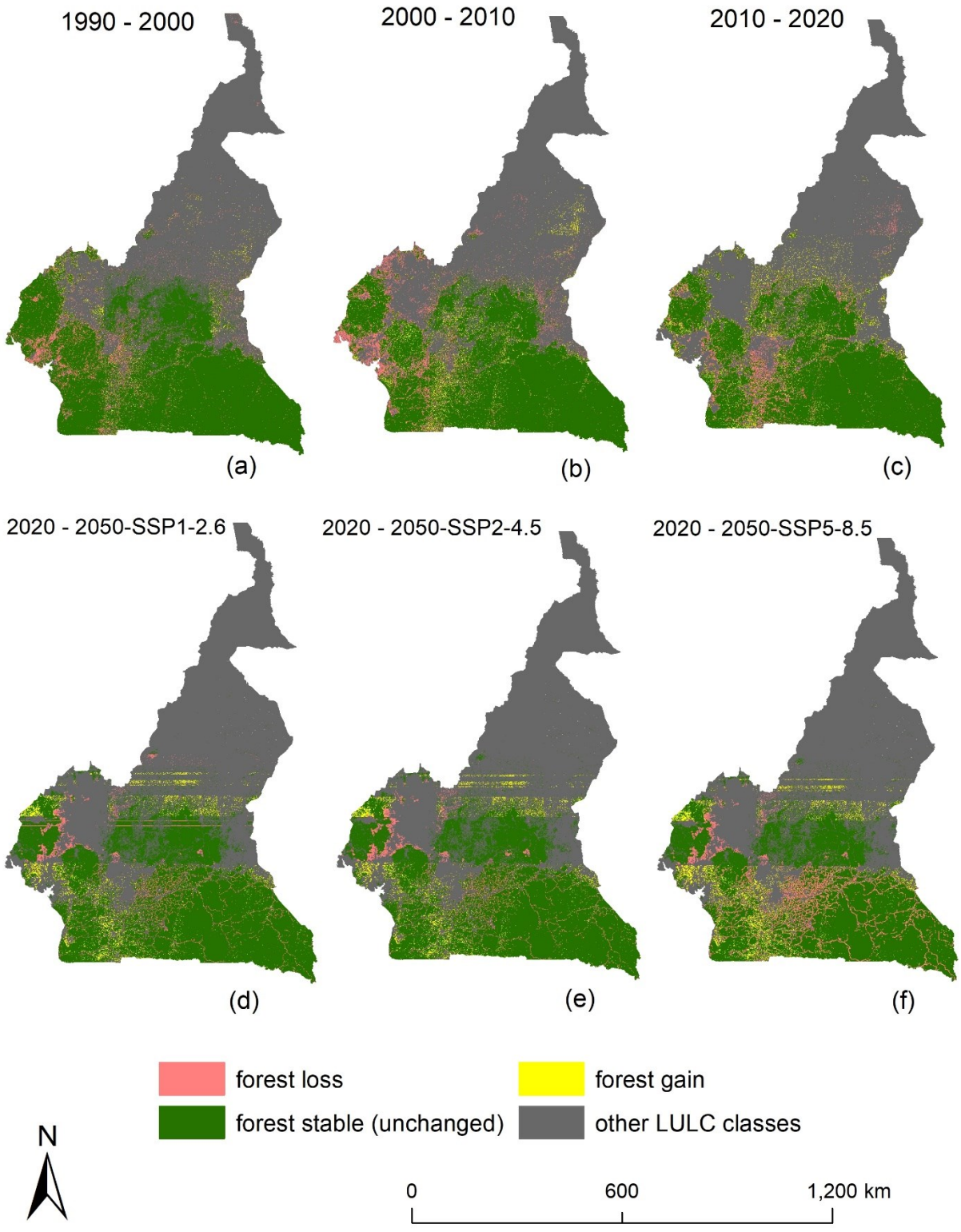

Figure S13e. Map of forest cover loss and gain in Cameroon, under all four change periods

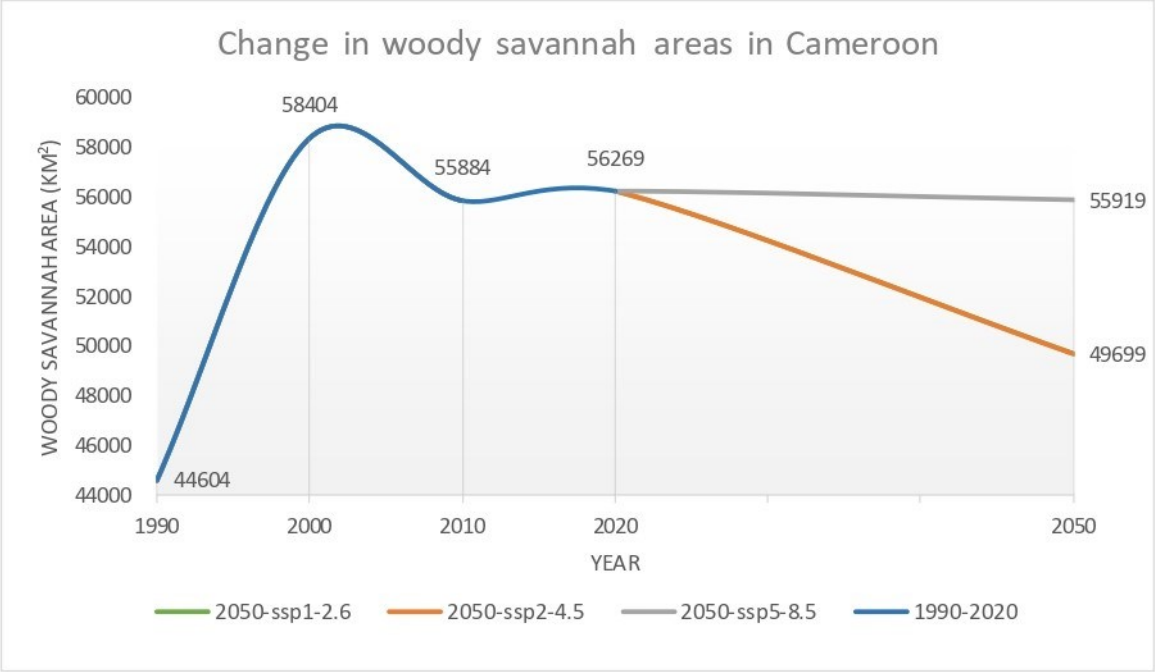

Figure S13f. Change in woody savannah areas within Cameroon, under all four change periods.

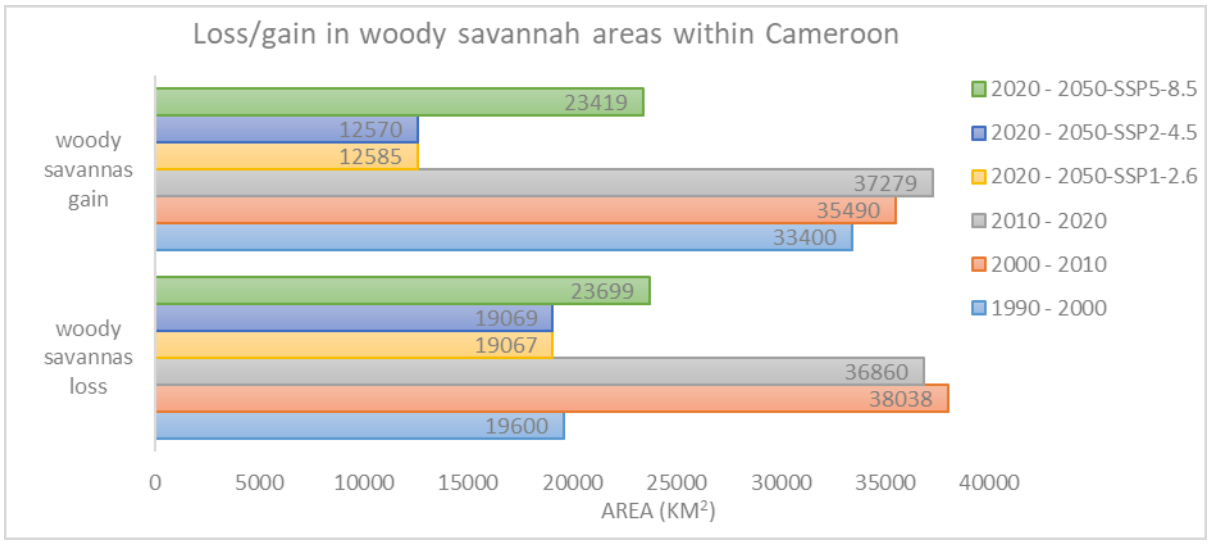

Figure S13g. Comparison in woody savannah loss and gain in Cameroon, across all four change periods

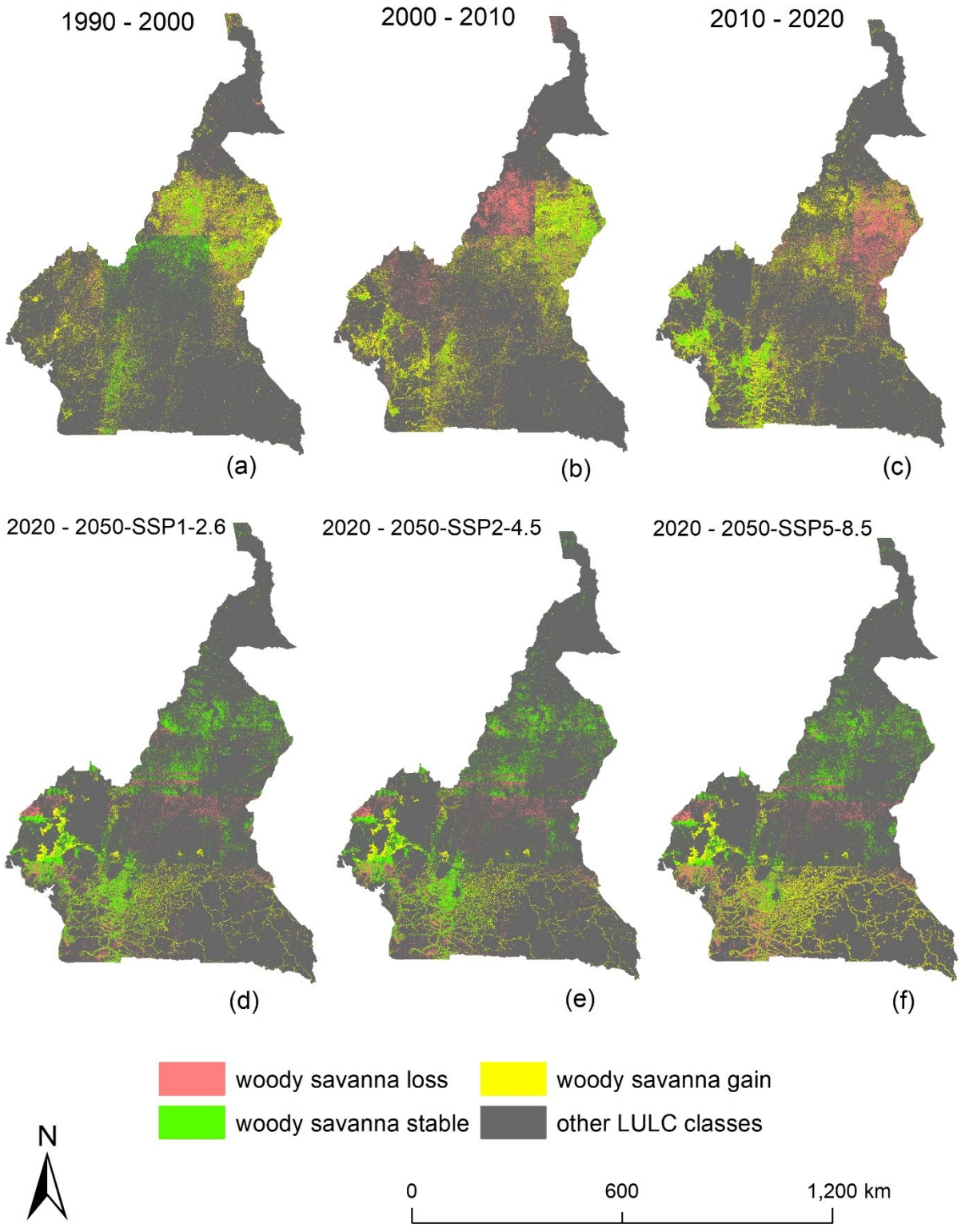

Figure S13h. Map of woody savannah loss and gain in Cameroon, under all four change periods

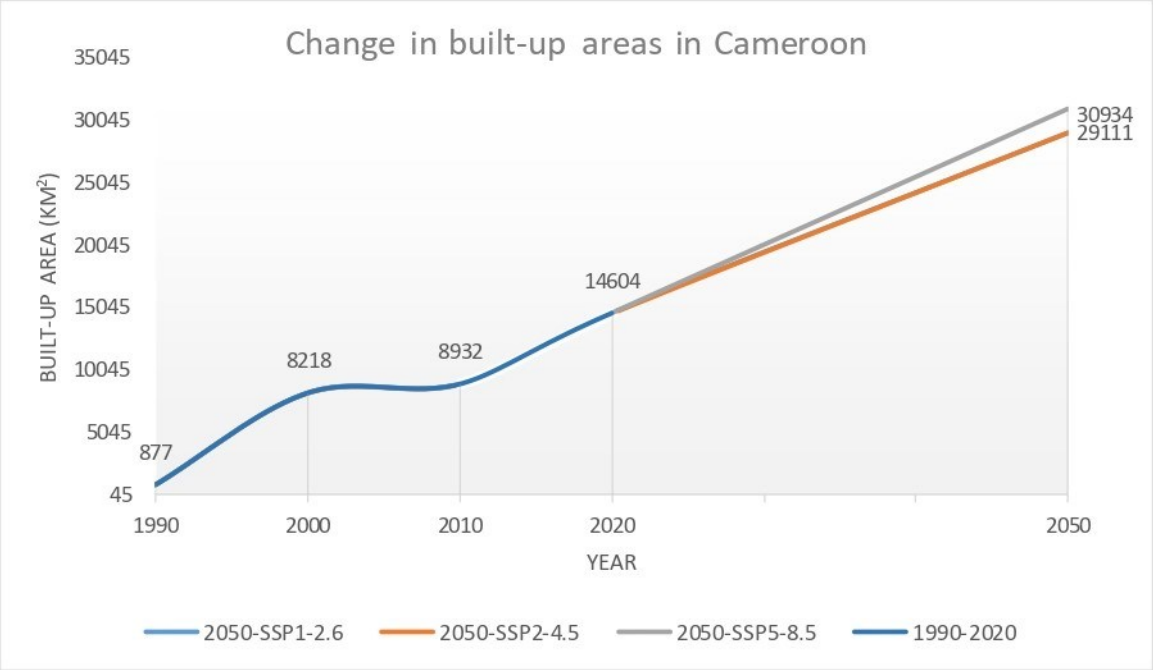

Figure S13i. Change in built-up areas within Cameroon, under all four change periods

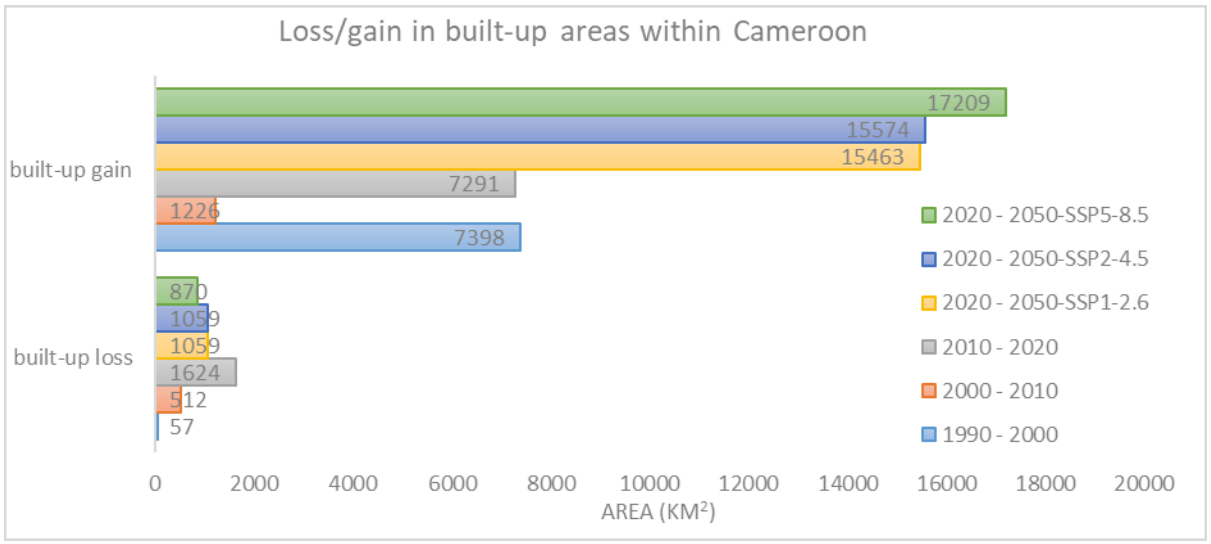

Figure S13j. Comparison in built-up area loss and gain in Cameroon, across all four change periods

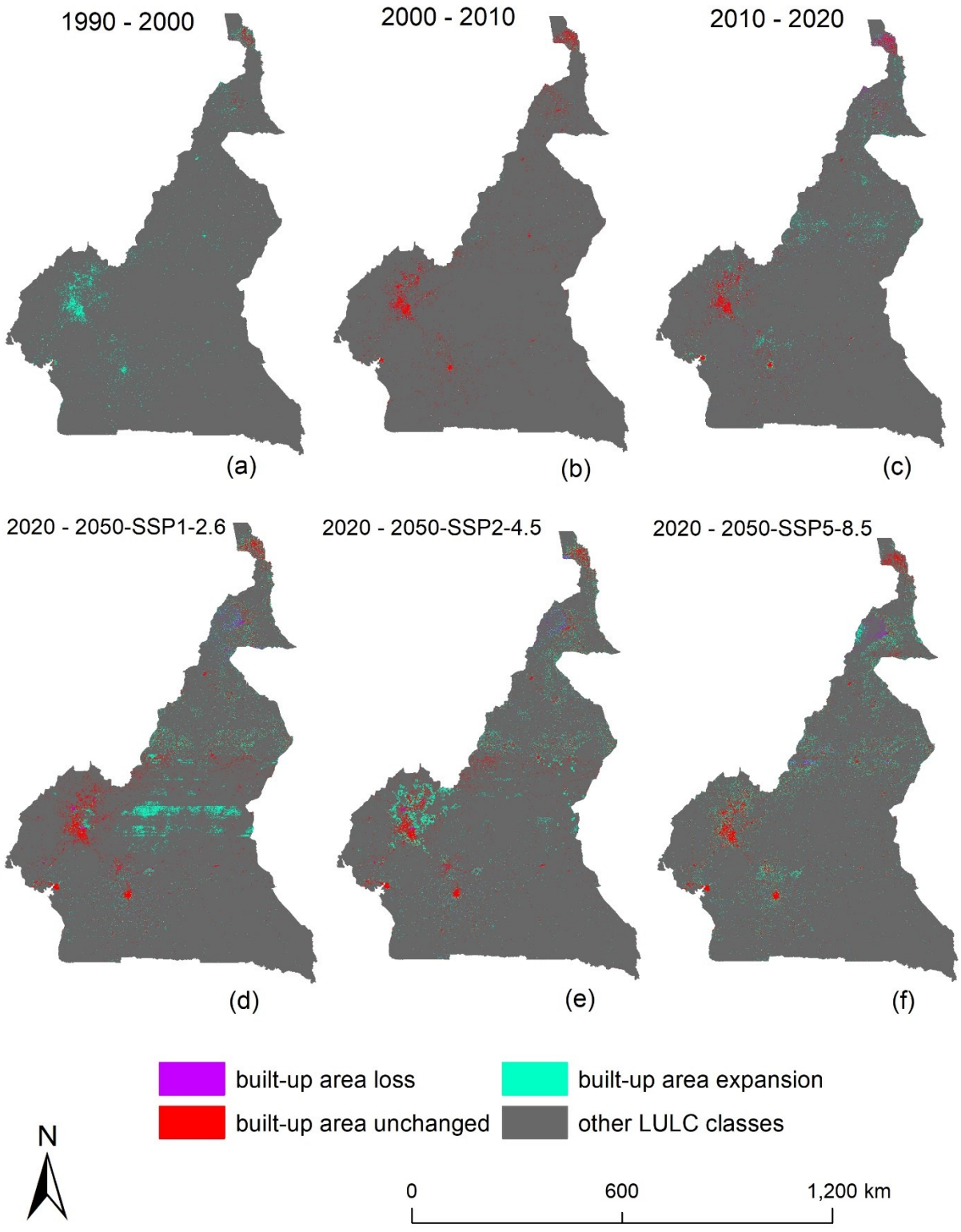

Figure S13k. Map showing loss and gains in built-up areas within Cameroon, under all four change periods

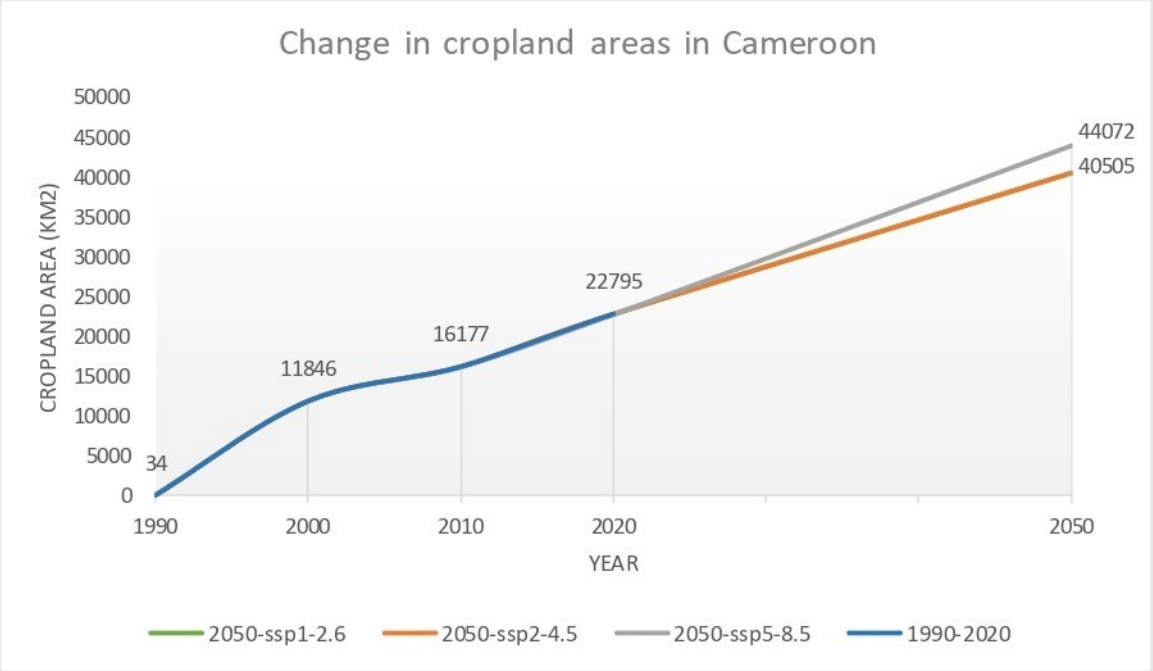

Figure S13l. Change in cropland areas within Cameroon, under all four change periods

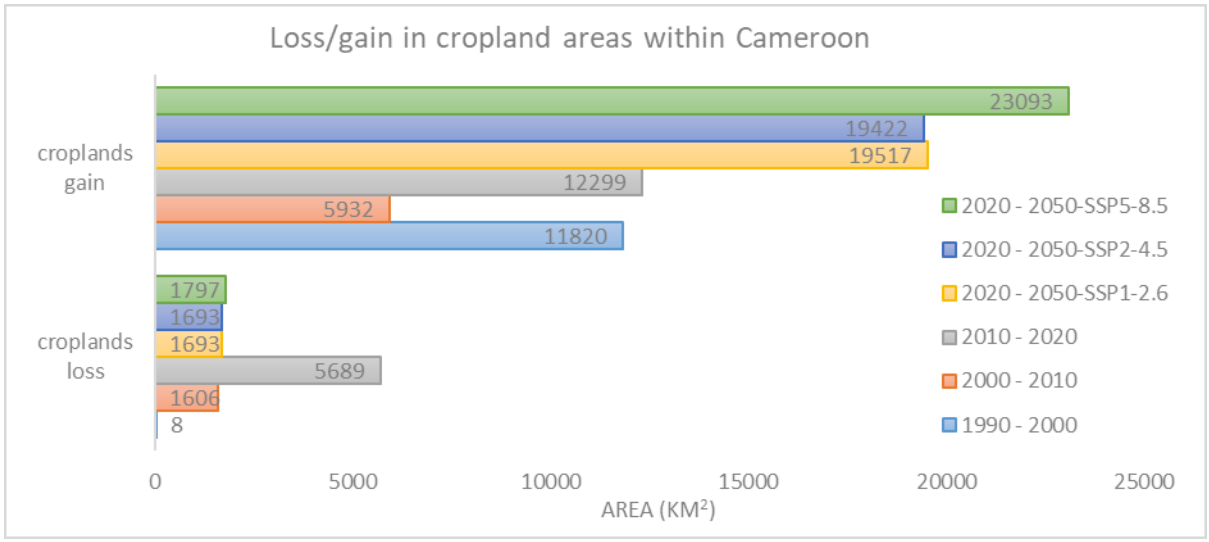

Figure S13m. Comparison in cropland area loss and gain in Cameroon, across all four change periods

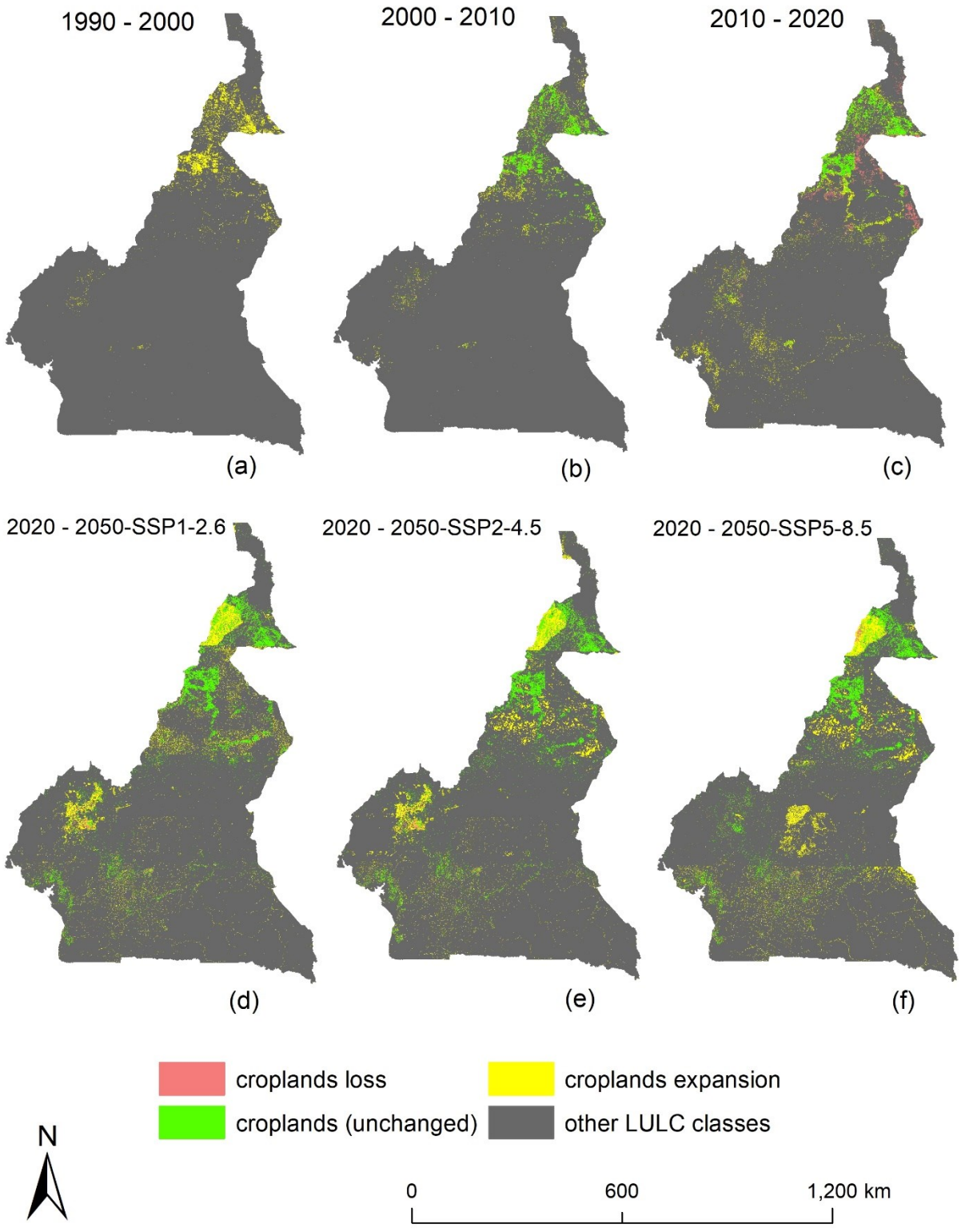

Figure S13n. Map of croplands gain/loss in Cameroon, under all four change periods

Table S26a. Area and proportion of land cover classes in each year of study in Cameroon

	1990		2000		2010		2020		2050					
									SSP1-2.6		SSP2-4.5		SSP5-8.5	
LULC class	**Area (km2)**	**% Area**	**Area (km2)**	**% Area**	**Area (km2)**	**% Area**	**Area (km2)**	**% Area**	Area (km2)	% Area	Area (km2)	% Area	Area (km2)	% Area
croplands	33.6	0	11846	2.5	16176.8	3.5	22795.3	4.9	40599.4	8.7	40504.6	8.7	44072.2	9.4
dense forest	236645.9	50.7	218279.3	46.8	203409.5	43.6	195146.1	41.8	193203.9	41.4	193209.6	41.4	183804.1	39.4
grassland/savannas	1775.1	0.4	2453.6	0.5	3293.6	0.7	3693.3	0.8	3108.6	0.7	3107.9	0.7	3339.8	0.7
open savannas/barelands	179040.7	38.4	163023.1	34.9	172200.1	36.9	167130.1	35.8	144000.1	30.9	143994.7	30.9	141579	30.3
built-up areas	876.7	0.2	8217.6	1.8	8932.3	1.9	14604.3	3.1	28999.7	6.2	29111.2	6.2	30934.3	6.6
water bodies	3100.2	0.7	4024.5	0.9	3595.9	0.8	3541.2	0.8	3352.5	0.7	3352.5	0.7	3362.3	0.7
wetlands	700	0.1	527.7	0.1	3431.1	0.7	3751.5	0.8	3564.9	0.8	3564.9	0.8	3534.2	0.8
woody savannas	44603.6	9.6	58403.9	12.5	55883.6	12	56268.7	12.1	49715.6	10.7	49699.2	10.7	55918.7	12
Total	466775.7	100	466775.7	100	466923	100	466930.4	100	466544.6	100	466544.6	100	466544.6	100

Table S26b. Quantified decadal changes in land cover patterns in Cameroon, between 1990-2020

	1990-2000		2000-2010		2010-2020		2020-2050					
							SSP1-2.6		SSP2-4.5		SSP5-8.5	
LULC classes	**Area (km2)**	**% Area**	**Area (km2)**	**% Area**	**Area (km2)**	**% Area**	**Area (km2)**	**% Area**	**Area (km2)**	**% Area**	**Area (km2)**	**% Area**
croplands	11812.4	2.5	4330.8	0.9	6618.5	1.4	17804.1	3.8	17709.3	3.8	21276.9	4.5
dense forest	-18366.5	-3.9	-14869.8	-3.2	-8263.4	-1.8	-1942.2	-0.4	-1936.5	-0.4	-11342	-2.4
grassland/savannas	678.6	0.1	840.0	0.2	399.7	0.1	-584.7	-0.1	-585.4	-0.1	-353.5	-0.1
open savannas/barelands	-16017.6	-3.4	9177.1	2.0	-5070.1	-1.1	-23130	-4.9	-23135.4	-4.9	-25551.1	-5.5
built-up areas	7340.9	1.6	714.8	0.2	5671.9	1.2	14395.4	3.1	14506.9	3.1	16330	3.5
water bodies	924.3	0.2	-428.6	-0.1	-54.7	0.0	-188.7	-0.1	-188.7	-0.1	-178.9	-0.1
wetlands	-172.3	0	2903.5	0.6	320.3	0.1	-186.6	0	-186.6	0	-217.3	0
woody savannas	13800.2	3	-2520.3	-0.5	385.1	0.1	-6553.1	-1.4	-6569.5	-1.4	-350	-0.1

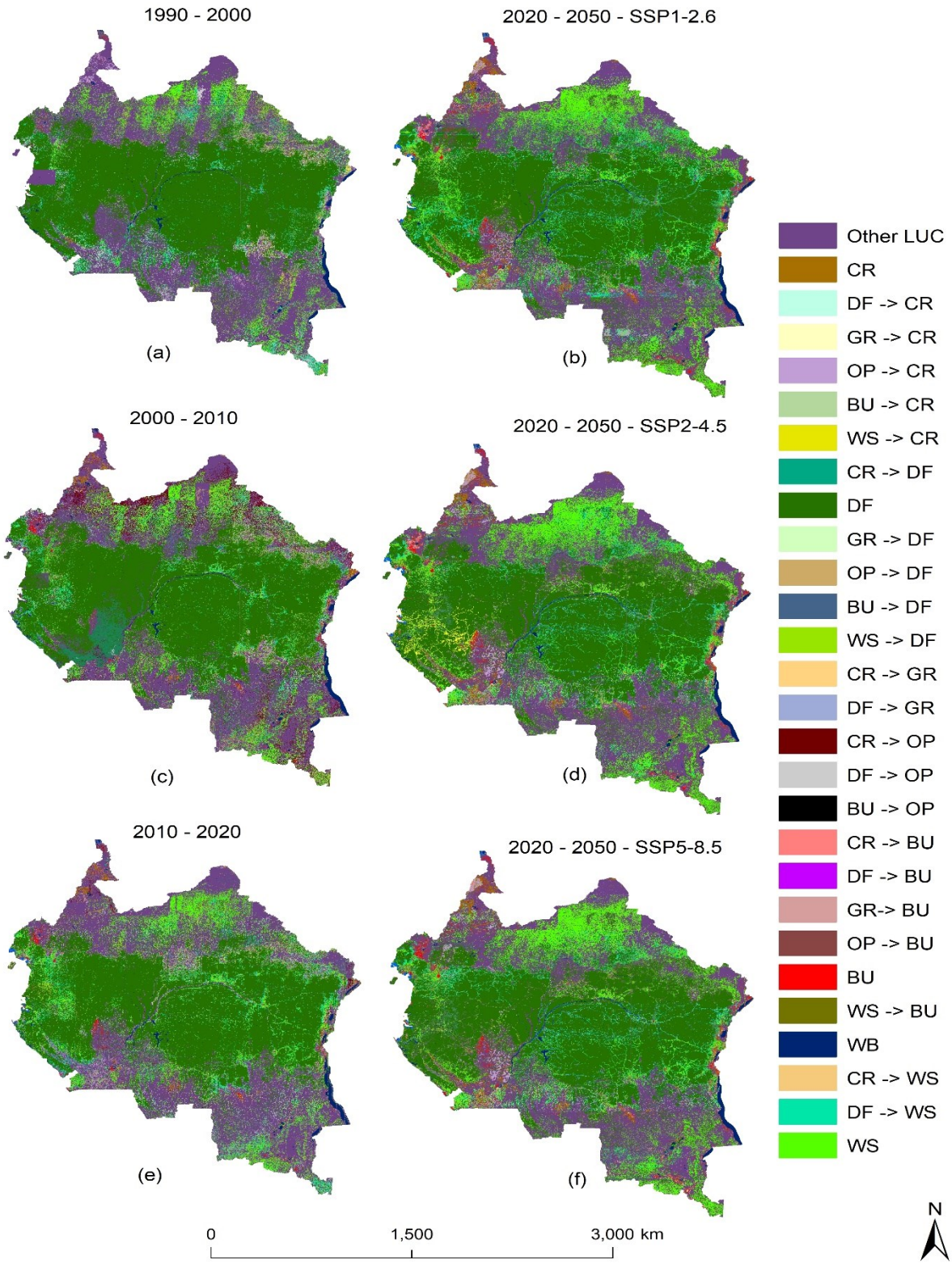

Figure S14. Land cover change detection map for the Congo Basin. Map shows detected changes from one land cover class in time (T1) to another in time (T2). Changes are shown for the most important LULC variables that can help support policy planning. * CR = Croplands; DF = Dense forest; GR = Grassland savannas; OP = Open savannas/barelands; WB = Water bodies; WL = Wetlands; WS = Woody savannas; BU = Built-up; Other LUC = Other Land use and Land cover classes

Table S27. Quantified areas of LULCC detection. Results are shown for the most important LULC variables that can help support policy planning.

LULCC categories	1990 - 2000	2000 - 2010	2010 - 2020	2020 - 2050 - SSP1-2.6	2020 - 2050 - SSP2-4.5	2020 - 2050 - SSP5-8.5
CR	1716.5	20790.1	22019.2	80081.6	79671.7	79567.5
DF -> CR	4993.9	1011.9	5608.6	19233.1	21425.7	23290.3
GR -> CR	190.9	760.5	1582.3	2509.4	2308.5	2151.2
OP -> CR	22595.6	10083.2	46550.8	60311.7	55841.8	61757
BU -> CR	13.7	140.6	935.5	2889.6	2860.4	2702.6
WS -> CR	3276.6	2473.4	8935.2	16099.7	14463.5	15801.2
CR -> DF	7.9	1759.9	742.2	0	0	1657
DF (unchanged)	1986951	1853177	1769114	1719433.2	1701767.4	1688956.3
GR -> DF	3017.8	10868.7	6792	13762.0	239.0	176.6
OP -> DF	74175.9	79180.8	70060.2	0	0	0
BU -> DF	3.4	118.5	1247.8	0	0	0
WS -> DF	59118.5	121462.4	129135.2	65746.2	65745.5	96643.8
CR -> GR	9.1	291.6	571.9	0	0.0	0
DF -> GR	19513	8561.1	11373.1	10075.3	9048.1	9145.6
CR -> OP	56.9	7773.5	8742.4	0	0	0
DF -> OP	132092	82981.1	77987	0	0	0
BU -> OP	335.4	960.9	2803.5	0	0	362.8
CR -> BU	77940.2	405.7	1685.1	5852.1	6262.1	6003.6
DF -> BU	3212.9	430.4	2708.4	7360.2	13029.2	12961.9
GR -> BU	176.2	93.2	404.5	916	709.9	2408.3
OP -> BU	13183.3	7159.9	17997.5	27896.8	23636	30897.2
BU (unchanged)	1294.9	18260.7	20275.1	43510.2	43539.5	41530.4
WS -> BU	1823.7	408.1	2976.6	6575.3	5508.6	8342.4
WB	48226.2	50590.7	29401.2	56715.5	56793.1	56782.4
WL	249.2	250.4	20363.1	11684.3	11717.7	11676.3
CR -> WS	9.7	1697.3	1160.8	0	0	0
DF -> WS	182873.5	168286.1	196065.5	212724.5	177286.4	149925.2
WS (unchanged)	202590.8	228902.4	262859.6	531645.6	555319.2	541228.5
Other LULCC	1275611	1434689	1386582	1192730.7	1214506.7	1209087.1

* CR = Croplands; DF = Dense forest; GR = Grassland savannas; OP = Open savannas/barelands; WB = Water bodies; WL = Wetlands; WS = Woody savannas; BU = Built-up areas

Appendix 3. Supplementary Materials for Chapter 4, Yuh et al. (2023)

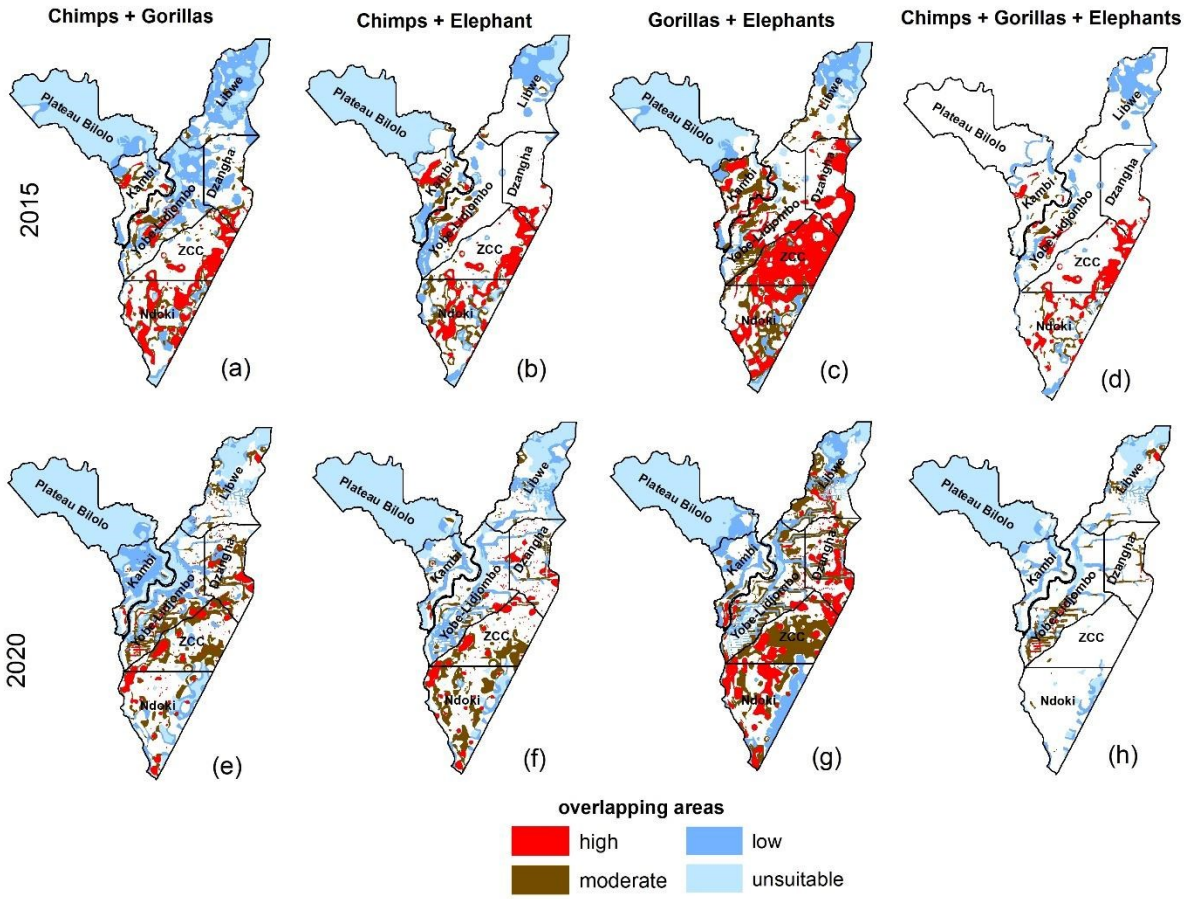

Figure S1. Map showing spatially overlapping habitat areas occupied by all three large mammal species in both years of study. Figures a – d and e – h show spatially overlapping areas between chimpanzees and gorillas, chimpanzees and elephants, gorillas and elephants, and chimpanzees, gorillas and elephants for the years 2015 and 2020 respectively. Areas are represented by high, low, moderate and unsuitable, with high = areas where highly suitable habitats overlap, moderate = areas where moderately suitable habitats overlap, low and unsuitable = areas where low and unsuitable habitats overlap respectively, and white = areas of no overlap.

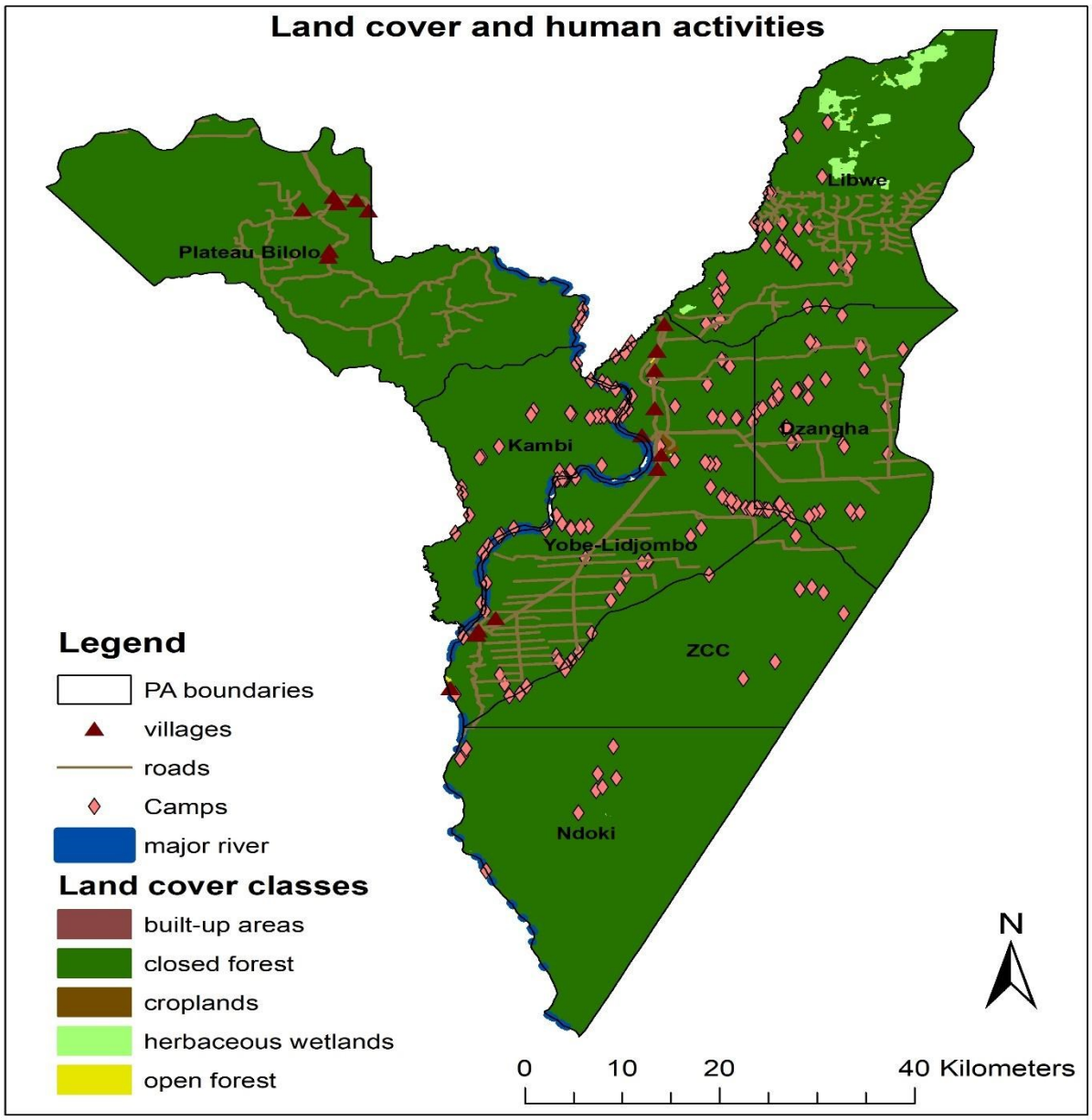

Figure S2. Land cover and human activities within the DSPAs. Land cover map extracted from the Copernicus 2019 global land cover data (https://land.copernicus.eu/global/products/lc)

Table S1. Area of overlapping priority habitats per PA sector

2015																				
Sectors	**Chimps + Gorillas (km^2)**					**Chimps + Elephants (km^2)**					**Gorillas + Elephants (km^2)**					**Chimps + Gorillas + Elephants (km^2)**				
	H	M	L	U	NO	H	M	L	U	NO	H	M	L	U	NO	H	M	L	U	NO
Dzanga	19	21	97	2	356	26	1	7	1	460	168	7	7	0	402	19	0	7	0	469
Ndoki	172	59	58	17	444	111	81	80	23	455	172	117	49	15	397	73	29	37	0	711
Plateau Bilolo	0	0	91	807	35	0	4	21	851	57	0	3	65	786	79	0	0	20	0	913
Libwe	0	8	371	142	171	0	6	188	106	383	5	32	163	115	369	0	2	169	0	613
Kambi	16	26	59	24	272	45	24	61	31	236	53	72	34	10	228	13	8	18	0	358
Yobe-Lidjobo	27	39	243	70	373	34	25	91	6	596	68	103	34	22	527	22	13	48	0	669
ZCC	111	20	6	0	447	127	8	4	0	445	421	28	3	0	132	109	3	3	0	469
2020																				
Dzanga	33	64	3	26	369	32	15	8	12	428	97	57	19	0	322	1	7	1	7	479
Ndoki	45	53	97	69	486	48	146	46	46	464	152	97	10	134	357	0	1	43	42	664
Plateau Bilolo	0	0	904	21	8	0	3	902	12	16	0	1	839	69	25	0	0	896	12	25
Libwe	7	21	203	51	402	0	9	273	84	318	19	88	110	108	359	6	15	170	30	463
Kambi	2	4	129	170	92	2	13	65	66	251	9	22	7	134	225	0	3	58	58	278
Yobe-Lidjobo	17	84	139	113	399	12	27	86	95	532	22	112	52	109	457	6	40	77	48	581
ZCC	47	142	16	18	361	50	98	2	1	433	104	263	11	0	206	0	1	2	1	580

* H = high, M = moderate, L = low, U = unsuitable, NO = no overlaps.

Table S2. Changes in Land cover patterns experienced within the DSPA between the years 2015 and 2019. Data extracted from the Copernicus 2015 and 2019 global land cover products.

	Year 2015		**Year 2020**		**Change (2020 – 2015)**	
Land cover class	Area (km^2)	% Area	Area (km^2)	% Area	Area (km^2)	% Area
Built-up areas	0.7	0	0.7	0	0	0
Closed forest	4556	98.9	4555	98.8	-0.1	0
croplands	5.1	0.1	5.1	0.1	0	0
Herbaceous wetlands	0.9	0	38.8	0.8	37.9	0.8
Herbaceous vegetations	35.9	0.7	0	0	-35.9	-0.7
Open forest	18.3	0.3	16.7	0.3	-1.6	0
Water bodies	0.8	0	0.9	0	0.1	0

Table S3. Acquired predictor variables and variable sources

Data category	Data type	Definition	source	Description
Land cover	Dense forest	Closed, dense, primary or undisturbed forests habitats with greater than 20% canopy cover	https://land.copernicus.eu/global/products/lc Buchhorn et al., (2020)	Datasets obtained from the Copernicus global land cover products for the periods 2015 – 2019, and at 100m resolution. Datasets were thus resampled at a fine scale resolution of 30m * 30m for analysis. River data were used in calculating distance to rivers using the ArcGIS Euclidean distance tool
	Open forest	Forests with open canopies of less than 10% density, and are sometimes disturbed.		
	Wetland vegetation	Swampy vegetation covers		
	Rivers	Flowing water bodies		
Climate	Maximum temperature	Highest daily temperatures measured at mean annual variations in ^{o}C	https://app.climateengine.org/climateEngine	Monthly TerraClimate datasets for the periods 2015 – 2020 downloaded from the google earth climate engine (a tool for visualizing and processing weather and climate data obtained from a compilation of different climatic simulations (e.g. TerraClimate, CFS reanalysis, ERA5 reanalysis, MERRA2 reanalysis). The datasets are generated at 4km resolution monthly
	Minimum temperature	Lowest daily temperatures measured at mean annual variations in ^{o}C		
	Annual precipitation	Measures of annual mean rainfall in mm.		
Topography	slope	A measure of landscape steepness or inclination	https://earthexplorer. usgs.gov/	Data extracted from the 2010 global multi-resolution digital terrain data created by the US Geological Survey.
	elevation	The height or altitude of a landscape above sea level		
Fragmentation and forest disturbance	Patch forests	relatively small and isolated forest fragments that cannot constitute intact forests but can generate large edge effects	Calculated from the 2015 – 2019 Copernicus land cover maps using the approach of Vogt et al. (2007)	The approach for extracting datasets involved an automated simulation of fore,st vs non-forest products in ArcGIS using the ArcGIS fragmentation tool. Datasets combined with open forests as composite indicators of forest disturbance data.
	Perforated forests	intact forest areas with relatively small perforations or developed holes that cause edge effects		
	Edge density	border effects between intact forests or isolated		

		forest patches or both		
Anti-patrol data	Eco-guard patrols	Vehicle, boat and foot patrols carried out by eco-guards to intercept illegal hunting, logging or mining activities in and out of Pas.	Obtained from the 2015 – 2020 WWF field patrol data stored in the Spatial Monitoring and Reporting Tool (SMART)	Patrol points were interpolated using the kernel density interpolation approach in ArcGIS.
Human pressure	Hunting	Capturing and killing of wild animals for food and other socioeconomic efforts	Obtained from the 2015 – 2020 WWF field patrol data stored in the Spatial Monitoring and Reporting Tool (SMART)	Data on human signs such as hunting, logging, roads, villages, camps, human presence and farming were interpolated using the kernel density interpolation approach in ArcGIS. PCAs performed and important variables combined into a single composite indicator of human pressure. Roads, camps and village data were also used in calculating distance to roads, villages and settlements using the ArcGIS Euclidean distance tool
	Logging and farming	Cutting of trees and forest vegetation for timber and farming		
	Camps	Temporary hurts built by hunters, loggers and minners for living during hunting, mining and logging activities		
	Villages	Building or group of buildings within rural settlements		
	Roads	Developmental corridors within forest habitats forming edge effects		

Table S4. Changes in Encounter Rates of Human Activities during 2015 and 2020 based on Survey data

Sectors	Hunting signs: Encounter Rate (Number/km)			All Human activities: Encounter Rate (Number/km)		
	2015	**2020**	**Change Rate (%)**	**2015**	**2020**	**Change Rate (%)**
Dzanga	0.172	0.18	4.92	1.806	1.93	6.86
Ndoki	0.078	0.058	-25.79	0.874	0.649	-25.73
Kambi	0.655	1.619	147.24	4.167	4.048	-2.86
Libwe	0.638	2.413	278.39	5.160	7.292	41.31
Plateau Bilolo	0.703	2.102	199.04	6.157	7.41	20.35
Yobe-Lidjombo	0.731	0.891	21.82	4.202	4.848	15.38
ZCC	0.555	0.420	-24.38	2.551	1.637	-35.84
Dzanga-Ndoki National Park	**0.124**	**0.225**	**81.45**	**1.331**	**1.462**	**9.84**
Special Reserve	**0.653**	**1.388**	**112.56**	**4.399**	**4.739**	**7.73**
DSPA	**0.496**	**1.020**	**105.65**	**3.484**	**3.701**	**6.23**

Table S5a. Pearson's correlation test and variance inflation factor (VIF) for predictors variables. Values in red represent strong correlations and high VIF (i.e. correlation coefficient, R > 0.5, and VIF > 5)

	slope	Elev	CF	dv	dr	dc	driv	edge	hp	HW	EP	pd	Tmax	Tmin	OF	Patch	Perf	prec	VIF
Slope	1																		1.7
Elev	0.37	1																	5.3
CF	0.02	-0.03	1																1.15
dv	-0.02	0.21	-0.02	1															11
dr	-0.21	-0.25	-0.01	0.57	1														6
dC	0.03	0.42	0.01	-0.11	-0.02	1													3.84
driv	-0.31	-0.3	0.02	0.4	0.88	-0.04	1												6.2
Edge	-0.01	-0.18	-0.19	-0.17	0.09	-0.1	0.01	1											2.8
hp	0.12	0.42	-0.02	-0.21	-0.35	0.41	-0.43	0.08	1										3.6
Hw	-0.12	-0.33	-0.0	0.03	0.0	-0.04	0.06	0.41	0.09	1									2.1
EP	0.11	-0.09	-0.05	-0.12	-0.16	-0.17	-0.12	0.07	-0.07	0.08	1								1.3
pd	-0.04	-0.02	-0.19	-0.15	-0.08	-0.01	-0.11	0.34	0.09	0.02	0.29	1							1.6
Tmax	-0.41	-0.95	0.02	-0.18	0.3	-0.43	0.37	0.23	-0.41	0.3	0.02	0.07	1						14.9
Tmin	0.12	-0.67	0.03	-0.01	0.29	-0.42	-0.71	0.18	-0.49	0.12	0.0	0.05	0.99	1					28.1
OF	-0.08	0.15	-0.19	-0.17	0.11	-0.1	-0.27	0.98	0.08	0.18	0.06	0.34	0.23	0.18	1				1.3
Patch	-0.03	0.2	-0.16	-0.2	-0.03	-0.08	-0.03	0.61	0.22	0.44	0.07	0.34	0.04	0.01	0.61	1			2.4
Perf	0.01	0.06	-0.02	-0.12	0.02	-0.06	-0.21	0.51	0.01	0.08	0.09	0.15	0.08	-0.8	0.51	0.09	1		1.2
prec	0.43	0.72	-0.05	0.31	-0.34	-0.09	-0.38	-0.14	0.24	0.19	0.11	-0.03	-0.8	-0.82	-0.14	-0.08	-0.07	1	29.2

*Elev = Elevation; CF = Closed or Dense forest; dv = distance to villages; dr = distance to roads; dc = distance to camps; driv = distance to rivers; hp = human pressure; Hw = herbaceous wetlands; EC = Eco-guard Patrols; pd = population density; Tmax = Maximum temperatures; Tmin = Minimum temperatures; OF = Open forest; Patch = Isolated forest patches; Perf = Perforated forests; Prec = Precipitation

Table S5b. VIF values for retained predictors from our correlation tests and PCA (Principal Component Analysis). Results show VIF values < 5, suggesting no collinearity or multi-collinearity between variables, hence no redundancy.

Retained predictors	Slope	Elevation	Dense forest	Distance to camps	Distance to roads	Disturbed forest	Eco-guard patrols	Maximum temperature	Human pressure
VIF	1.44	2.8	1.03	1.68	1.26	1.34	1.11	2.31	2.12

Table S6a. Cumulative patrol efforts per sector in the DSPA since 2017

Administrative designation	Sectors	Area Size (km²)	Number of Patrols	Number of Days	Number of Active hours in patrols (Hr)	Total distance on patrols (Km)	Number of Eco-guards involved in patrols	Man-Days
Dzanga-Ndoki National Park	**Dzanga**	497.7	565	2,381	13,639.5	20,835.6	116	13,641
	Ndoki	754.6	110	489	3,421.0	3,593.4	92	2,437
	Total NP	**1,252.2**	**675**	**2,870**	**17,060.4**	**24,429.1**	**208**	**16,078**
Special Reserve of Dzanga Sangha	**Kambi**	400.6	96	431	2,832.7	6,873.4	97	2,666
	Libwe	686.8	218	867	6,367.7	18,855.5	119	5,029
	Plateau Bilolo	938.4	13	24	70.8	917.1	47	136
	Yobé Lidjombo	756.3	1,162	3,977	20,440.3	84,305.7	126	22,959
	ZCC	587.5	187	625	3,763.5	12,386.3	100	3,593
	Total SR	**3,369.5**	**1,676**	**5,924**	**33,475.0**	**123,337.9**	**489**	**34,383**
Total DSPA		**4,621.7**	**2,351**	**8,794**	**50,535.5**	**147,767.0**	**697**	**50,461**

Table S6b. Patrol efforts per area size per sector in the DSPA since 2017

Administrative designation	Sectors	Area Size (km²)	Number of Patrols	Number of Days	Number of Active hours in patrols (Hr)	Total distance covered on patrols (Km)	Number of Eco-guards involved in patrols	Man-Days
Dzanga-Ndoki National Park	**Dzanga**	497.65	1.135	4.784	27.408	41.868	0.233	27.411
	Ndoki	754.57	0.146	0.648	4.534	4.762	0.122	3.230
	Total NP	**1,252.22**	**0.539**	**2.292**	**13.624**	**19.509**	**0.166**	**12.840**
Special Reserve of Dzanga Sangha	**Kambi**	400.56	0.240	1.076	7.072	17.160	0.242	6.656
	Libwe	686.80	0.317	1.262	9.272	27.454	0.173	7.322
	Plateau Bilolo	938.39	0.014	0.026	0.075	0.977	0.050	0.145
	Yobé Lidjombo	756.29	1.536	5.259	27.027	111.473	0.167	30.357
	ZCC	587.45	0.318	1.064	6.406	21.085	0.170	6.116
	Total SR	**3,369.49**	**0.497**	**1.758**	**9.935**	**36.604**	**0.145**	**10.204**
Total DSPA		**4,621.71**	**0.509**	**1.903**	**10.934**	**31.972**	**0.151**	**10.918**

Table S7a. Model evaluation results for ape and elephant suitability mapping for the year 2015

Chimpanzee suitability				
Methods	AUC	COR	TSS	Deviance
gam	0.8	0.37	0.52	0.74
glm	0.74	0.31	0.4	0.75
Chimpanzee nest suitability				
gam	0.82	0.43	0.55	0.71
glm	0.75	0.17	0.3	0.79
Gorilla suitability				
gam	0.79	0.31	0.32	1.36
glm	0.75	0.25	0.27	1.24
Gorilla nest suitability				
gam	0.8	0.41	0.48	1.03
glm	0.7	0.14	0.27	0.98
Elephant suitability				
gam	0.77	0.39	0.46	0.82
glm	0.7	0.19	0.27	0.94

Table S7b. Model evaluation results for ape and elephant suitability mapping for the year 2020

Chimpanzee suitability				
Methods	AUC	COR	TSS	Deviance
gam	0.76	0.42	0.4	0.91
glm	0.71	0.25	0.35	0.73
Chimpanzee nest suitability				
gam	0.78	0.47	0.46	0.85
glm	0.71	0.18	0.3	0.7
Gorilla suitability				
gam	0.76	0.47	0.37	1.06
glm	0.7	0.33	0.29	1.18
Gorilla nest suitability				
gam	0.86	0.58	0.57	0.58
glm	0.82	0.45	0.51	0.72
Elephant suitability				
gam	0.79	0.53	0.42	0.9
glm	0.72	0.42	0.33	1.01

*All models performed very well for both years of study, with AUC $\geq$ 0.7

References

Abegunde, V. O., & Obi, A. (2022). The role and perspective of climate smart agriculture in Africa: A scientific review. *Sustainability*, *14*(4), 2317. https://doi.org/10.3390/su14042317

Abernethy, K., Maisels, F., & White, L. J. T. (2016). Environmental issues in Central Africa. *Annual Review of Environment and Resources*, *41*(1), 1–33. https://doi.org/10.1146/annurev-environ-110615-085415

Achancho, V. (2013). Review and analysis of national investment strategies and agricultural policies in Central Africa: The case of Cameroun. In *Rebuilding West Africa's food potential* (A. Elbehri (ed.), pp. 117–148). FAO/IFAD. https://www.fao.org/3/i3222e/i3222e04.pdf

Adam, E., Mutanga, O., Odindi, J., & Abdel-Rahman, E. M. (2014). Land-use/cover classification in a heterogeneous coastal landscape using RapidEye imagery: Evaluating the performance of random forest and support vector machines classifiers. *International Journal of Remote Sensing*, *35*(10), 3440–3458. https://doi.org/10.1080/01431161.2014.903435

Aguiar, A. P. D., Câmara, G., & Escada, M. I. S. (2007). Spatial statistical analysis of land-use determinants in the Brazilian Amazonia: Exploring intra-regional heterogeneity. *Ecological Modelling*, *209*(2–4), 169–188. https://doi.org/10.1016/j.ecolmodel.2007.06.019

Aha, D. W., Kibler, D., & Albert, M. (1991). Instance-based learning algorithms. *Machine Learning, 6*(1), 37–66.

Akbulut, Y., Sengur, A., Guo, Y., & Smarandache, F. (2017). NS-k-NN: Neutrosophic Set-Based k-Nearest Neighbors Classifier. *Symmetry*, *9*(9), 179. https://doi.org/10.3390/sym9090179

Aleman, J. C., Blarquez, O., Gourlet-Fleury, S., Bremond, L., & Favier, C. (2017). Tree cover in Central Africa: Determinants and sensitivity under contrasted scenarios of global change. *Scientific Reports*, *7*(1), 41393. https://doi.org/10.1038/srep41393

Aloysius, N. R., Sheffield, J., Saiers, J. E., Li, H., & Wood, E. F. (2016). Evaluation of historical and future simulations of precipitation and temperature in Central Africa from CMIP5 climate models. *Journal of Geophysical Research: Atmospheres*, *121*(1), 130–152. https://doi.org/10.1002/2015JD023656

Alshari, E. A., Abdulkareem, M. B., & Gawali, B. W. (2023). Classification of land use/land cover using artificial intelligence (ANN-RF). *Frontiers in Artificial Intelligence*, *5*, 964279. https://doi.org/10.3389/frai.2022.964279

Ameray, A., Cavard, X., & Bergeron, Y. (2023). Climate change may increase Quebec boreal forest productivity in high latitudes by shifting its current composition. *Frontiers in Forests and Global Change*, *6*, 1020305. https://doi.org/10.3389/ffgc.2023.1020305

Anchang, J. Y., Prihodko, L., Kaptué, A. T., Ross, C. W., Ji, W., Kumar, S. S., Lind, B., Sarr, M. A., Diouf, A. A., & Hanan, N. P. (2019). Trends in woody and herbaceous vegetation in the Savannas of West Africa. *Remote Sensing*, *11*(5), 576. https://doi.org/10.3390/rs11050576

Andrén, H., & Andren, H. (1994). Effects of habitat fragmentation on birds and mammals in landscapes with different proportions of suitable habitat: A review. *Oikos*, *71*(3), 355. https://doi.org/10.2307/3545823

Arandjelovic, M., Head, J., Rabanal, L. I., Schubert, G., Mettke, E., Boesch, C., Robbins, M. M., & Vigilant, L. (2011). Non-Invasive genetic monitoring of wild central chimpanzees. *PLoS ONE*, *6*(3), e14761. https://doi.org/10.1371/journal.pone.0014761

Araújo, M. B., Cabeza, M., Thuiller, W., Hannah, L., & Williams, P. H. (2004). Would climate change drive species out of reserves? An assessment of existing reserve-selection methods: CLIMATE CHANGE AND RESERVES. *Global Change Biology*, *10*(9), 1618–1626. https://doi.org/10.1111/j.1365-2486.2004.00828.x

Ariom, T. O., Dimon, E., Nambeye, E., Diouf, N. S., Adelusi, O. O., & Boudalia, S. (2022). climate-smart agriculture in African countries: A review of strategies and impacts on smallholder farmers. *Sustainability*, *14*(18), 11370. https://doi.org/10.3390/su141811370

Armenteras, D., Murcia, U., González, T. M., Barón, O. J., & Arias, J. E. (2019). Scenarios of land use and land cover change for NW Amazonia: Impact on forest intactness. *Global Ecology and Conservation*, *17*, e00567. https://doi.org/10.1016/j.gecco.2019.e00567

Armenteras, D., Rudas, G., Rodriguez, N., Sua, S., & Romero, M. (2006). Patterns and causes of deforestation in the Colombian Amazon. *Ecological Indicators*, *6*(2), 353–368. https://doi.org/10.1016/j.ecolind.2005.03.014

Asner, G. P., Elmore, A. J., Olander, L. P., Martin, R. E., & Harris, A. T. (2004). Grazing systems, ecosystem responses, and global change. *Annual Review of Environment and*

Resources, *29*(1), 261–299. https://doi.org/10.1146/annurev.energy.29.062403.102142

Atkinson, P. M., & Tatnall, A. R. L. (1997). Introduction neural networks in remote sensing. *International Journal of Remote Sensing*, *18*(4), 699–709. https://doi.org/10.1080/014311697218700

Ayres, J. M., & Clutton-Brock, T. H. (1992). River boundaries and species range size in Amazonian primates. *The American Naturalist*, *140*(3), 531–537. https://doi.org/10.1086/285427

Balinga, M., Moses, S., Fombod, E., Sunderland, T. C., Chantal, S., & Asaha, S. (2006). *A preliminary assessment of the vegetation of the Dzanga Sangha Protected Area complex, Central African Republic*. WWF, Smithsonian Institution, Forests, Resources and People & CARPE. 124pp

Bakker, M. M., Govers, G., Kosmas, C., Vanacker, V., Oost, K. V., & Rounsevell, M. (2005). Soil erosion as a driver of land-use change. *Agriculture, Ecosystems & Environment*, *105*(3), 467–481. https://doi.org/10.1016/j.agee.2004.07.009

Barratt, C., Lester, J., Gratton, P., Onstein, R., Kalan, A., McCarthy, M., Bocksberger, G., White, L., Vigilant, L., Dieguez, P., Abdulai, B., Aebischer, T., Agbor, A., Assumang, A., Bailey, E., Bessone, M., Buys, B., Carvalho, J., Chancellor, R., … Kuhl, H. (2021). Quantitative estimates of glacial refugia for chimpanzees (*Pan troglodytes)* since the Last Interglacial (120,000 BP). *American Journal of Primatology*, *83*(10). https://doi.org/10.1002/ajp.23320

Basheer, S., Wang, X., Farooque, A. A., Nawaz, R. A., Liu, K., Adekanmbi, T., & Liu, S. (2022). Comparison of land use land cover classifiers using different satellite Imagery and machine learning techniques. *Remote Sensing*, *14*(19), 4978. https://doi.org/10.3390/rs14194978

Basnet, B., & Vodacek, A. (2015). Tracking land use/land cover dynamics in cloud prone areas using moderate resolution satellite data: a case study in Central Africa. *Remote Sensing*, *7*(6), 6683–6709. https://doi.org/10.3390/rs70606683

Beaumont, L. J., & Duursma, D. (2012). Global projections of 21st century land-use changes in regions adjacent to protected areas. *PLoS ONE*, *7*(8), e43714. https://doi.org/10.1371/journal.pone.0043714

Belgiu, M., & Drăguţ, L. (2016). Random forest in remote sensing: A review of applications and future directions. *ISPRS Journal of Photogrammetry and Remote Sensing*, *114*, 24–31. https://doi.org/10.1016/j.isprsjprs.2016.01.011

Blake, S., Deem, S. L., Strindberg, S., Maisels, F., Momont, L., Isia, I.-B., Douglas-Hamilton, I., Karesh, W. B., & Kock, M. D. (2008). Roadless wilderness area determines forest elephant movements in the Congo Basin. *PLoS ONE*, *3*(10), e3546. https://doi.org/10.1371/journal.pone.0003546

Blake, S., & Hedges, S. (2004). Sinking the Flagship: The case of forest elephants in Asia and Africa. *Conservation Biology*, *18*(5), 1191–1202. https://doi.org/10.1111/j.1523-1739.2004.01860.x

Blom, A. (2000). The monetary Impact of tourism on protected area management and the local economy in Dzanga-Sangha (Central African Republic). *Journal of Sustainable Tourism*, *8*(3), 175–189. https://doi.org/10.1080/09669580008667357

Bousquet, O., Boucheron, S., Lugosi, G. (2004). Introduction to statistical learning theory. In: Bousquet, O., von Luxburg, U., Rätsch, G. (eds) *Advanced lectures on machine learning*. *ML 2003*. Lecture Notes in Computer Science (169-207), vol 3176. Springer, Berlin, Heidelberg. https://doi.org/10.1007/978-3-540-28650-9_8

Brandt, M., Hiernaux, P., Rasmussen, K., Tucker, C. J., Wigneron, J.-P., Diouf, A. A., Herrmann, S. M., Zhang, W., Kergoat, L., Mbow, C., Abel, C., Auda, Y., & Fensholt, R. (2019). Changes in rainfall distribution promote woody foliage production in the Sahel. *Communications Biology*, *2*(1), 133. https://doi.org/10.1038/s42003-019-0383-9

Breiman. (2001a). Random forests. *Machine Learning*, *45*, 5–32.

Breiman, L. (2001b). Statistical modeling: The two cultures (with comments and a rejoinder by the author). *Statistical Science*, *16*(3). https://doi.org/10.1214/ss/1009213726

Brink, A. B., & Eva, H. D. (2009). Monitoring 25 years of land cover change dynamics in Africa: A sample based remote sensing approach. *Applied Geography*, *29*(4), 501–512. https://doi.org/10.1016/j.apgeog.2008.10.004

Britannica, n. d. (n.d.). *Britannica, T. (Ed.), n.d. Of Encyclopaedia (2022, September 2). Central Park. Encyclopedia Britannica.* https://www.britannica.com/place/Central-Park-New-York-City

Brown, J., & Yoder, A. (2015). Shifting ranges and conservation challenges for lemurs in the face of climate change. *Ecology and Evolution*, *5*(6), 1131–1142. https://doi.org/10.1002/ece3.1418

Buchhorn, M., Lesiv, M., Tsendbazar, N.-E., Herold, M., Bertels, L., & Smets, B. (2020). Copernicus global land cover layers—collection 2. *Remote Sensing*, *12*(6), 1044. https://doi.org/10.3390/rs12061044

Buckland, S. T., Anderson, D. R., Burnham, K. P., Laake, J. L., Borchers D. L., & Thomas, L. (2001). *Introduction to distance sampling: Estimating abundance of biological populations* (1st ed). Oxford University Press.

Büttner, G. CORINE (2014). Land cover and land cover change products. In: Manakos I., Braun M. (eds) *Land use and land cover mapping in Europe*: *Remote sensing and digital image processing*, vol 18. Springer, Dordrecht.

Bwangoy, J.-R. B., Hansen, M. C., Roy, D. P., Grandi, G. D., & Justice, C. O. (2010). Wetland mapping in the Congo Basin using optical and radar remotely sensed data and derived topographical indices. *Remote Sensing of Environment*, *114*(1), 73–86. https://doi.org/10.1016/j.rse.2009.08.004

Cafaro, P., Hansson, P., & Götmark, F. (2022). Overpopulation is a major cause of biodiversity loss and smaller human populations are necessary to preserve what is left. *Biological Conservation*, *272*, 109646. https://doi.org/10.1016/j.biocon.2022.109646

Campbell, J. B. (1996). *Introduction to remote sensing* (2nd ed.). Taylor and Francis.

Campbell, J. B., & Wynne, R. H. (2011). *Introduction to remote sensing* (5th ed.). Guilford Press.

Cardoso-Fernandes, J., Teodoro, A. C., Lima, A., & Roda-Robles, E. (2020). Semi-automatization of support vector machines to map lithium (Li) bearing pegmatites. *Remote Sensing*, *12*(14), 2319. https://doi.org/10.3390/rs12142319

Carozzi, M., Martin, R., Klumpp, K., & Massad, R. S. (2022). Effects of climate change in European croplands and grasslands: Productivity, greenhouse gas balance and soil carbon storage. *Biogeosciences*, *19*(12), 3021–3050. https://doi.org/10.5194/bg-19-3021-2022

Caselles, V., & López García, M. J. (1989). An alternative simple approach to estimate atmospheric correction in multitemporal studies. *International Journal of Remote Sensing*, *10*(6), 1127–1134. https://doi.org/10.1080/01431168908903951

Cerutti, P. O., & Tacconi, L. (2006). *Forests, illegality, and livelihoods in Cameroon*. Center for International Forestry Research Jl (CIFOR). https://pdfs.semanticscholar.org/304a/d82ad40d36fa0415b7c959ef9d09a9d2000c.pdf

Chang, Y., Hou, K., Li, X., Zhang, Y., & Chen, P. (2018). Review of land use and land cover change research progress. *IOP Conference Series: Earth and Environmental Science*, *113*, 012087. https://doi.org/10.1088/1755-1315/113/1/012087

Chase, M. J., Schlossberg, S., Griffin, C. R., Bouché, P. J. C., Djene, S. W., Elkan, P. W., Ferreira, S., Grossman, F., Kohi, E. M., Landen, K., Omondi, P., Peltier, A., Selier, S. A. J., & Sutcliffe, R. (2016). Continent-wide survey reveals massive decline in African savannah elephants. *PeerJ*, *4*, e2354. https://doi.org/10.7717/peerj.2354

Chaturvedi, R. K., Gopalakrishnan, R., Jayaraman, M., Bala, G., Joshi, N. V., Sukumar, R., & Ravindranath, N. H. (2011). Impact of climate change on Indian forests: A dynamic vegetation modeling approach. *Mitigation and Adaptation Strategies for Global Change*, *16*(2), 119–142. https://doi.org/10.1007/s11027-010-9257-7

Chavez, P. S. (1988). An improved dark-object subtraction technique for atmospheric scattering correction of multispectral data. *Remote Sensing of Environment*, *24*(3), 459–479. https://doi.org/10.1016/0034-4257(88)90019-3

Chavez, P. S. (1996). Image-based atmospheric corrections-revisited and improved. *Photogrammetric Engineering and Remote Sensing*, 62(9), 1025-1035.

Chen, J., Chang, K., Karacsonyi, D., & Zhang, X. (2014). Comparing urban land expansion and its driving factors in Shenzhen and Dongguan, China. *Habitat International*, *43*, 61–71. https://doi.org/10.1016/j.habitatint.2014.01.004

Chen, M., Vernon, C. R., Graham, N. T., Hejazi, M., Huang, M., Cheng, Y., & Calvin, K. (2020). Global land use for 2015–2100 at 0.05° resolution under diverse socioeconomic and climate scenarios. *Scientific Data*, *7*(1), 320. https://doi.org/10.1038/s41597-020-00669-x

Cheo, A. E., Voigt, H.-J., & Mbua, R. L. (2013). Vulnerability of water resources in northern Cameroon in the context of climate change. *Environmental Earth Sciences*, *70*(3), 1211–1217. https://doi.org/10.1007/s12665-012-2207-9

Chibeya, D., Wood, H., Cousins, S., Carter, K., Nyirenda, M. A., & Maseka, H. (2021). How do African elephants utilize the landscape during wet season? A habitat connectivity analysis for Sioma Ngwezi landscape in Zambia. *Ecology and Evolution*, *11*(21), 14916–14931. https://doi.org/10.1002/ece3.8177

Clarke, B. S. (2013). Special Issue on statistical learning: Special issue on statistical learning. statistical analysis and data mining. *The ASA Data Science Journal*, *6*(4), 271–272. https://doi.org/10.1002/sam.11201

Condro, A., Prasetyo, L., Rushayati, S., Santikayasa, I., & Iskandar, E. (2021). Predicting hotspots and prioritizing protected areas for Endangered primate species in Indonesia under changing climate. *Biology*, *10*(2). https://doi.org/10.3390/biology10020154

Congalton, R. G. (1991). A review of assessing the accuracy of classifications of remotely sensed data. *Remote Sensing of Environment*, *37*(1), 35–46. https://doi.org/10.1016/0034-4257(91)90048-B

Cook, M., Schott, J., Mandel, J., & Raqueno, N. (2014). Development of an operational calibration methodology for the Landsat thermal data archive and initial testing of the atmospheric compensation component of a Land Surface Temperature (LST) product from the archive. *Remote Sensing*, *6*(11), 11244–11266. https://doi.org/10.3390/rs61111244

Cortes, C., & Vapnik, V. (1995). Support-vector networks. *Machine Learning*, *20*(3), 273–297. https://doi.org/10.1007/BF00994018

Cox, P. M., Betts, R. A., Collins, M., Harris, P. P., Huntingford, C., & Jones, C. D. (2004). Amazonian forest dieback under climate-carbon cycle projections for the 21st century. *Theoretical and Applied Climatology*, *78*(1–3). https://doi.org/10.1007/s00704-004-0049-4

Cracknell, M. J., & Reading, A. M. (2014). Geological mapping using remote sensing data: A comparison of five machine learning algorithms, their response to variations in the spatial distribution of training data and the use of explicit spatial information. *Computers & Geosciences*, *63*, 22–33. https://doi.org/10.1016/j.cageo.2013.10.008

Critchlow, R., Plumptre, A. J., Alidria, B., Nsubuga, M., Driciru, M., Rwetsiba, A., Wanyama, F., & Beale, C. M. (2017). Improving law-enforcement effectiveness and efficiency in protected areas using ranger-collected monitoring data: Improved ranger efficiency in protected areas. *Conservation Letters*, *10*(5), 572–580. https://doi.org/10.1111/conl.12288

Critchlow, R., Plumptre, A. J., Driciru, M., Rwetsiba, A., Stokes, E. J., Tumwesigye, C., Wanyama, F., & Beale, C. M. (2015). Spatiotemporal trends of illegal activities from ranger-collected data in a Ugandan national park: Trends in illegal activities. *Conservation Biology*, *29*(5), 1458–1470. https://doi.org/10.1111/cobi.12538

Crooks, K. R., Burdett, C. L., Theobald, D. M., King, S. R. B., Di Marco, M., Rondinini, C., & Boitani, L. (2017). Quantification of habitat fragmentation reveals extinction risk in terrestrial mammals. *Proceedings of the National Academy of Sciences*, *114*(29), 7635–7640. https://doi.org/10.1073/pnas.1705769114

CSC. (2013). *Climate Change Scenarios for the Congo Basin*. [Haensler A., Jacob D., Kabat P., Ludwig F. (eds.)]. Climate Service Centre Report No. 11, Hamburg, Germany, ISSN: 2192-4058.

Cuni-Sanchez, A., White, L. J. T., Calders, K., Jeffery, K. J., Abernethy, K., Burt, A., Disney, M., Gilpin, M., Gomez-Dans, J. L., & Lewis, S. L. (2016). African savanna-forest boundary dynamics: A 20-year study. *PLoS ONE*, *11*(6), e0156934. https://doi.org/10.1371/journal.pone.0156934

Cutler, D. R., Edwards, T. C., Beard, K. H., Cutler, A., Hess, K. T., Gibson, J., & Lawler, J. J. (2007). Random forests for classification in ecology. *Ecology*, *88*(11), 2783–2792. https://doi.org/10.1890/07-0539.1

Da Cruz, D. C., Benayas, J. M. R., Ferreira, G. C., Santos, S. R., & Schwartz, G. (2021). An overview of forest loss and restoration in the Brazilian Amazon. *New Forests*, *52*(1), 1–16. https://doi.org/10.1007/s11056-020-09777-3

Dabija, A., Kluczek, M., Zagajewski, B., Raczko, E., Kycko, M., Al-Sulttani, A. H., Tardà, A., Pineda, L., & Corbera, J. (2021). Comparison of support vector machines and Random Forests for corine land lover mapping. *Remote Sensing*, *13*(4), 777. https://doi.org/10.3390/rs13040777

DeFries, R., Hansen, M., Steininger, M., Dubayah, R., Sohlberg, R., & Townshend, J. (1997). Subpixel forest cover in Central Africa from multisensor, multitemporal data. *Remote Sensing of Environment*, *60*(3), 228–246. https://doi.org/10.1016/S0034-4257(96)00119-8

Dejene, S. W., Mpakairi, K. S., Kanagaraj, R., Wato, Y. A., & Mengistu, S. (2021). Modelling continental range shift of the African elephant (*Loxodonta africana*) under a changing climate and land cover: Implications for future conservation of the species. *African Zoology*, *56*(1), 25–34. https://doi.org/10.1080/15627020.2020.1846617

Devos, C., Walsh, P. D., Arnhem, E., & Huynen, M.-C. (2008). Monitoring population decline: Can transect surveys detect the impact of the Ebola virus on apes? *Oryx*, *42*(03). https://doi.org/10.1017/S0030605308000161

deWasseige et al. (2009). *The forests of the Congo Basin: State of the forest 2008*. Luxembourg: Publications Office of the European Union.

De Wasseige, C., Tadoum, M., Eba'a Atyi, R., & Doumenge, C. (Eds.). *The forests of the Congo Basin: Forests and climate change*. Weyrich, Belgium: 128 p (2015).

Díaz-Pacheco, J., & Hewitt, R. (2014). Modelado de cambios de usos de suelo urbano a través de redes neuronales artificiales. Comparación con dos aplicaciones de software. GeoFocus. *International Review of Geographical Information Science and Technology*, *14*, 1–22.

Didham, R. K., Kapos, V., & Ewers, R. M. (2012). Rethinking the conceptual foundations of habitat fragmentation research. *Oikos*, *121*(2), 161–170. https://doi.org/10.1111/j.1600-0706.2011.20273.x

Diedhiou, A., Bichet, A., Wartenburger, R., Seneviratne, S. I., Rowell, D. P., Sylla, M. B., Diallo, I., Todzo, S., Touré, N. E., Camara, M., Ngatchah, B. N., Kane, N. A., Tall, L., & Affholder, F. (2018). Changes in climate extremes over West and Central Africa at 1.5 °C and 2 °C global warming. *Environmental Research Letters*, *13*(6), 065020. https://doi.org/10.1088/1748-9326/aac3e5

Douglas-Hamilton, I., Krink, T., & Vollrath, F. (2005). Movements and corridors of African elephants in relation to protected areas. *Naturwissenschaften*, *92*(4), 158–163. https://doi.org/10.1007/s00114-004-0606-9

Dove et al. (2021). *Climate risk country profile: Congo, Democratic Republic*. In The World Bank Group; World Bank. https://climateknowledgeportal.worldbank.org/sites/default/files/2021-06/15883-WB_Congo%2C%20Democratic%20Republic%20Country%20Profile-WEB.pdf

Drake, J. M., Randin, C., & Guisan, A. (2006). Modelling ecological niches with support vector machines. *Journal of Applied Ecology*, *43*(3), 424–432. https://doi.org/10.1111/j.1365-2664.2006.01141.x

Duan, R.-Y., Kong, X.-Q., Huang, M.-Y., Fan, W.-Y., & Wang, Z.-G. (2014). The Predictive performance and stability of six species distribution models. *PLoS ONE*, *9*(11), e112764. https://doi.org/10.1371/journal.pone.0112764

D'udine, F. A. C., Henson, D. W., & Malpas, R. C. (2016). *Wildlife law enforcement in Sub-Saharan African protected areas: A review of best practices*. IUCN, International Union for Conservation of Nature. https://doi.org/10.2305/IUCN.CH.2016.SSC-OP.58.en

Duro, D. C., Franklin, S. E., & Dubé, M. G. (2012). A comparison of pixel-based and object-based image analysis with selected machine learning algorithms for the classification of agricultural landscapes using SPOT-5 HRG imagery. *Remote Sensing of Environment*, *118*, 259–272. https://doi.org/10.1016/j.rse.2011.11.020

Durrieu de Madron, L., Fontez, B., & Dipapoundji, B. (2000). Dégâts d'exploitation et de débardage en fonction de l'intensité d'exploitation en forêt dense humide d'Afrique Centrale. *Bois et Forêts des Tropiques*. *264*. https://revues.cirad.fr/index.php/BFT/article/view/20052

Eastman, J. R., & Toledano, J. (2018). A short presentation of the Land Change Modeler (LCM). In M. T. Camacho Olmedo, M. Paegelow, J.-F. Mas, & F. Escobar (Eds.), *Geomatic Approaches for Modeling Land Change Scenarios* (pp. 499–505). Springer International Publishing. https://doi.org/10.1007/978-3-319-60801-3_36

Eba'a Atyi, R. (1998). *Cameroon's logging industry: Structure, economic importance and effects of devaluation* (OCCASIONAL PAPER No. 14). https://www.cifor.org/publications/pdf_files/OccPapers/OP-14.pdf

Elith, J., & Leathwick, J. R. (2009). Species distribution models: Ecological explanation and prediction across space and time. *Annual Review of Ecology, Evolution, and Systematics*, *40*(1), 677–697. https://doi.org/10.1146/annurev.ecolsys.110308.120159

Elith, J., Leathwick, J. R., & Hastie, T. (2008). A working guide to boosted regression trees. *Journal of Animal Ecology*, *77*(4), 802–813. https://doi.org/10.1111/j.1365-2656.2008.01390.x

Environment, C. A. R. P. for the. (2005). *The forests of the Congo Basin: A preliminary assessment*. CARPE. https://books.google.ca/books?id=-pPDNwAACAAJ

Ernst, C., Mayaux, P., Verhegghen, A., Bodart, C., Christophe, M., & Defourny, P. (2013). National forest cover change in Congo Basin: Deforestation, reforestation, degradation and regeneration for the years 1990, 2000 and 2005. *Global Change Biology*, *19*(4), 1173–1187. https://doi.org/10.1111/gcb.12092

Escobar, A. (2011). *Encountering development: The making and unmaking of the Third World* (Vol. 1). Princeton University Press.

Estrada, A. (2013). Socioeconomic contexts of primate conservation: Population, poverty, global economic demands, and sustainable land use: social contexts of primate conservation. *American Journal of Primatology*, *75*(1), 30–45. https://doi.org/10.1002/ajp.22080

Estrada, A., Garber, P. A., Rylands, A. B., Roos, C., Fernandez-Duque, E., Di Fiore, A., Nekaris, K. A.-I., Nijman, V., Heymann, E. W., Lambert, J. E., Rovero, F., Barelli, C., Setchell, J. M., Gillespie, T. R., Mittermeier, R. A., Arregoitia, L. V., de Guinea, M., Gouveia, S., Dobrovolski, R., … Li, B. (2017). Impending extinction crisis of the world's primates: Why primates matter. *Science Advances*, *3*(1), e1600946. https://doi.org/10.1126/sciadv.1600946

Eyring, V., Bony, S., Meehl, G. A., Senior, C. A., Stevens, B., Stouffer, R. J., & Taylor, K. E. (2016). Overview of the Coupled Model Intercomparison Project Phase 6 (CMIP6) experimental design and organization. *Geoscientific Model Development*, *9*(5), 1937–1958. https://doi.org/10.5194/gmd-9-1937-2016

Fa, J. E., Wright, J. H., Funk, S. M., Márquez, A. L., Olivero, J., Farfán, M. Á., Guio, F., Mayet, L., Malekani, D., Holo Louzolo, C., Mwinyihali, R., Wilkie, D. S., & Wieland, M. (2019). Mapping the availability of bushmeat for consumption in Central African cities. *Environmental Research Letters*, *14*(9), 094002. https://doi.org/10.1088/1748-9326/ab36fa

FAO. (2000). On definitions of forest and forest change. *Forest Resources Assessment Programme Working Paper 33, November, 2000*. https://www.fao.org/3/ad665e/ad665e00.htm

FAO. (2004). *Trade and sustainable forest management: Impacts and Interactions*. Food and Agriculture Organization. https://enb.iisd.org/crs/tsfm/

FAO. (2006). *Global Forest Resources Assessment 2006: Main report.* FAO.

FAO. (2018). *Global Forest Resources Assessment 2018: Main report*. FAO.

FAO. (2016). *Map accuracy assessment and area estimation: A practical guide*. National forest monitoring assessment working paper No.46/E. file:///D:/Downloads/a-i5601e.pdf

FAO. (2020). *Global Forest Resources Assessment 2020: Main report*. FAO. https://www.fao.org/forest-resources-assessment/2020/en/

Fisher, J. B., Sikka, M., Sitch, S., Ciais, P., Poulter, B., Galbraith, D., Lee, J.-E., Huntingford, C., Viovy, N., Zeng, N., Ahlström, A., Lomas, M. R., Levy, P. E., Frankenberg, C., Saatchi, S., & Malhi, Y. (2013). African tropical rainforest net carbon dioxide fluxes in the twentieth century. *Philosophical Transactions of the Royal Society B: Biological Sciences*, *368*(1625), 20120376. https://doi.org/10.1098/rstb.2012.0376

Fitzgerald, M., Coulson, R., Lawing, A. M., Matsuzawa, T., & Koops, K. (2018). Modeling habitat suitability for chimpanzees (*Pan troglodytes verus*) in the Greater Nimba Landscape, Guinea, West Africa. *Primates*, *59*(4), 361–375. https://doi.org/10.1007/s10329-018-0657-8

Fonteh, M. F. (2013). An assessment of impacts of climate change on available water resources and security in Cameroon. J*ournal of the Cameroon Academy of Sciences*, *11*(2&3), 145-156.

Forester, B. R., DeChaine, E. G., & Bunn, A. G. (2013). Integrating ensemble species distribution modelling and statistical phylogeography to inform projections of climate change impacts on species distributions. *Diversity and Distributions*, *19*(12), 1480–1495. https://doi.org/10.1111/ddi.12098

Fotang, C., Broring, U., Roos, C., Enoguanbhor, E., Abwe, E., Dutton, P., Schierack, P., Angwafo, T., & Birkhofer, K. (2021). Human activity and forest degradation threaten populations of the Nigeria-Cameroon chimpanzee (*Pan troglodytes ellioti*) in Western Cameroon. *International Journal of Primatology*, *42*(1), 105–129. https://doi.org/10.1007/s10764-020-00191-2

Fotso-Nguemo, T. C., Vondou, D. A., Pokam, W. M., Djomou, Z. Y., Diallo, I., Haensler, A., Tchotchou, L. A. D., Kamsu-Tamo, P. H., Gaye, A. T., & Tchawoua, C. (2017). On the added value of the regional climate model REMO in the assessment of climate change signal over Central Africa. *Climate Dynamics*, *49*(11–12), 3813–3838. https://doi.org/10.1007/s00382-017-3547-7

Franklin, J. (2010). *Mapping species distributions: spatial inference and Prediction*. Cambridge University Press

Franklin, J. (2013). Species distribution models in conservation biogeography: Developments and challenges. *Diversity and Distributions*, *19*(10), 1217–1223. https://doi.org/10.1111/ddi.12125

Frederick, K. D. (2002). *Water resources and climate change: The management of water resources,* vol. 2. Edward Elgar PublishingLtd, Cornwall, p. 528

Freund, Y., Schapire, R. E., et al. (1996) Experiments with a new boosting algorithm. In: Icml, Citeseer., 96, 148–156

Friedl, Mark, & Sulla-Menashe, Damien. (2019). *MCD12Q1 MODIS/Terra+Aqua Land Cover Type Yearly L3 Global 500m SIN Grid V006* [Data set]. NASA EOSDIS Land Processes DAAC. https://doi.org/10.5067/MODIS/MCD12Q1.006

Fry. J., Xian, G., Jin, S., Dewitz, J., Homer, C., Yang, L., Barnes, C., Herold, N., & Wickham, J. (2011). Completion of the 2006 national land cover database for the conterminous United States. *Photogrammetric Engineering and Remote Sensin*g 77, 859–64.

Gagniuc, P. A. (2017). *Markov chains: From theory to implementation and experimentation*. John Wiley & Sons.

Gandiwa, E., Heitkönig, I. M. A., Lokhorst, A. M., Prins, H. H. T., & Leeuwis, C. (2013). Illegal hunting and law enforcement during a period of economic decline in Zimbabwe: A case study of northern Gonarezhou National Park and adjacent areas. *Journal for Nature Conservation*, *21*(3), 133–142. https://doi.org/10.1016/j.jnc.2012.11.009

Gaveau, D. L. A., Sloan, S., Molidena, E., Yaen, H., Sheil, D., Abram, N. K., Ancrenaz, M., Nasi, R., Quinones, M., Wielaard, N., & Meijaard, E. (2014). Four decades of forest persistence, clearance and logging on Borneo. *PLoS ONE*, *9*(7), e101654. https://doi.org/10.1371/journal.pone.0101654

Gebhardt, S., Wehrmann, T., Ruiz, M., Maeda, P., Bishop, J., Schramm, M., Kopeinig, R., Cartus, O., Kellndorfer, J., Ressl, R., Santos, L., & Schmidt, M. (2014). MAD-MEX: Automatic wall-to-wall land cover monitoring for the Mexican REDD-MRV program using all Landsat data. *Remote Sensing*, *6*(5), 3923–3943. https://doi.org/10.3390/rs6053923

Geist, H. J., & Lambin, E. F. (2002). Proximate causes and underlying driving forces of tropical deforestation. *BioScience*, *52*(2), 143. https://doi.org/10.1641/0006-3568(2002)052[0143:PCAUDF]2.0.CO;2

Geist, H. J., & Lambin, E. F. (2004). Dynamic causal patterns of desertification. *BioScience*, *54*(9), 817. https://doi.org/10.1641/0006-3568(2004)054[0817:DCPOD]2.0.CO;2

Geler Roffe, T., Couturier, S., & García-Romero, A. (2022). Suitability of the global forest cover change map to assess climatic megadisturbance impacts on remote tropical forests. *Scientific Reports*, *12*(1), 11249. https://doi.org/10.1038/s41598-022-13558-7

Gessner, U., Machwitz, M., Esch, T., Tillack, A., Naeimi, V., Kuenzer, C., & Dech, S. (2015). Multi-sensor mapping of West African land cover using MODIS, ASAR and TanDEM-X/TerraSAR-X data. *Remote Sensing of Environment*, *164*, 282–297. https://doi.org/10.1016/j.rse.2015.03.029

Ghosh, A., & Joshi, P. K. (2014). A comparison of selected classification algorithms for mapping bamboo patches in lower Gangetic plains using very high resolution WorldView 2 imagery. *International Journal of Applied Earth Observation and Geoinformation*, *26*, 298–311. https://doi.org/10.1016/j.jag.2013.08.011

Gibson, L., Münch, Z., Palmer, A., & Mantel, S. (2018). Future land cover change scenarios in South African grasslands – implications of altered biophysical drivers on land management. *Heliyon*, *4*(7), e00693. https://doi.org/10.1016/j.heliyon.2018.e00693

Ginath Yuh, Y., N'Goran, P. K., Dongmo, Z. N., Tracz, W., Tangwa, E., Agunbiade, M., Kühl, H. S., Sop, T., & Fotang, C. (2020). Mapping suitable great ape habitat in and around the Lobéké National Park, South-East Cameroon. *Ecology and Evolution*, *10*(24), 14282–14299. https://doi.org/10.1002/ece3.7027

Gislason, P. O., Benediktsson, J. A., & Sveinsson, J. R. (2006). Random Forests for land cover classification. *Pattern Recognition Letters*, *27*(4), 294–300. https://doi.org/10.1016/j.patrec.2005.08.011

Gómez, C., White, J. C., & Wulder, M. A. (2016). Optical remotely sensed time series data for land cover classification: A review. *ISPRS Journal of Photogrammetry and Remote Sensing*, *116*, 55–72. https://doi.org/10.1016/j.isprsjprs.2016.03.008

Gomez-Zavaglia, A., Mejuto, J. C., & Simal-Gandara, J. (2020). Mitigation of emerging implications of climate change on food production systems. *Food Research International*, *134*, 109256. https://doi.org/10.1016/j.foodres.2020.109256

Gong, P., Wang, J., Yu, L., Zhao, Y., Zhao, Y., Liang, L., Niu, Z., Huang, X., Fu, H., Liu, S., Li, C., Li, X., Fu, W., Liu, C., Xu, Y., Wang, X., Cheng, Q., Hu, L., Yao, W., … Chen, J. (2013). Finer resolution observation and monitoring of global land cover: First mapping results with Landsat TM and ETM+ data. *International Journal of Remote Sensing*, *34*(7), 2607–2654. https://doi.org/10.1080/01431161.2012.748992

Gouveia, S., Souza-Alves, J., Rattis, L., Dobrovolski, R., Jerusalinsky, L., Beltrao-Mendes, R., & Ferrari, S. (2016). Climate and land use changes will degrade the configuration of the landscape for titi monkeys in eastern Brazil. *Global Change Biology*, *22*(6), 2003–2012. https://doi.org/10.1111/gcb.13162

Goward, S. N., Masek, J. G., Loveland, T. R., Dwyer, J. L., Williams, D. L., Arvidson, T., Rocchio, L. E. P., & Irons, J. R. (2021). Semi-centennial of Landsat observations & pending Landsat 9 launch. *Photogrammetric Engineering & Remote Sensing*, *87*(8), 533–539. https://doi.org/10.14358/PERS.87.8.533

Grainger, A. (2008). Difficulties in tracking the long-term global trend in tropical forest area. *Proceedings of the National Academy of Sciences*, *105*(2), 818–823. https://doi.org/10.1073/pnas.0703015105

Groves, C. P. (2001). *Primate taxonomy*. Smithsonian Institution Press.

Groves, C., & Game, E. T. (2016). *Conservation planning: Informed decisions for a healthier planet*. Roberts Publishers

Guermazi, E., Bouaziz, M., & Zairi, M. (2016). Water irrigation management using remote sensing techniques: A case study in Central Tunisia. *Environmental Earth Sciences*, *75*(3), 202. https://doi.org/10.1007/s12665-015-4804-x

Guisan, A., & Zimmermann, N. E. (2000). Predictive habitat distribution models in ecology. *Ecological Modelling*, *135*(2–3), 147–186. https://doi.org/10.1016/S0304-3800(00)00354-9

Hansen, M. C., Potapov, P. V., Moore, R., Hancher, M., Turubanova, S. A., Tyukavina, A., Thau, D., Stehman, S. V., Goetz, S. J., Loveland, T. R., Kommareddy, A., Egorov, A., Chini, L., Justice, C. O., & Townshend, J. R. G. (2013). High-resolution global maps of 21st-century forest cover change. *Science*, *342*(6160), 850–853. https://doi.org/10.1126/science.1244693

Hansen, M. C., Roy, D. P., Lindquist, E., Adusei, B., Justice, C. O., & Altstatt, A. (2008). A method for integrating MODIS and Landsat data for systematic monitoring of forest cover and change in the Congo Basin. *Remote Sensing of Environment*, *112*(5), 2495–2513. https://doi.org/10.1016/j.rse.2007.11.012

Hansen, M. C., Stehman, S. V., & Potapov, P. V. (2010). Quantification of global gross forest cover loss. *Proceedings of the National Academy of Sciences*, *107*(19), 8650–8655. https://doi.org/10.1073/pnas.0912668107

Hastie, T., Tibshirani, R., & Friedman, J. H. (2009). *The elements of statistical learning: Data mining, inference, and prediction* (2nd ed). Springer.

He, K., Fan, C., Zhong, M., Cao, F., Wang, G., & Cao, L. (2023). Evaluation of habitat suitability for Asian elephants in sipsongpanna under climate change by coupling multi-source remote sensing products with MaxEnt model. *Remote Sensing*, *15*(4), 1047. https://doi.org/10.3390/rs15041047

Heinicke, S., Mundry, R., Boesch, C., Amarasekaran, B., Barrie, A., Brncic, T., Brugière, D., Campbell, G., Carvalho, J., Danquah, E., Dowd, D., Eshuis, H., Fleury-Brugière, M.-C., Gamys, J., Ganas, J., Gatti, S., Ginn, L., Goedmakers, A., Granier, N., … Kühl, H.

S. (2019). Advancing conservation planning for western chimpanzees using IUCN SSC A.P.E.S.—The case of a taxon-specific database. *Environmental Research Letters*, *14*(6), 064001. https://doi.org/10.1088/1748-9326/ab1379

Hellwig, N., Walz, A., & Markovic, D. (2019). Climatic and socioeconomic effects on land cover changes across Europe: Does protected area designation matter? *PLoS ONE*, *14*(7), e0219374. https://doi.org/10.1371/journal.pone.0219374

Heydari, S. S., & Mountrakis, G. (2018). Effect of classifier selection, reference sample size, reference class distribution and scene heterogeneity in per-pixel classification accuracy using 26 Landsat sites. *Remote Sensing of Environment*, *204*, 648–658. https://doi.org/10.1016/j.rse.2017.09.035

Hill, R. A. (2006). Thermal constraints on activity scheduling and habitat choice in baboons. *American Journal of Physical Anthropology*, *129*(2), 242–249. https://doi.org/10.1002/ajpa.20264

Hill, S., & Winder, I. (2019). Predicting the impacts of climate change on *Papio* baboon biogeography: Are widespread, generalist primates "safe"? *Journal of Biogeography*, *46*(7), 1380–1405. https://doi.org/10.1111/jbi.13582

Homer, C., Dewitz, J., Fry, J., Coan, M., Hossain, N., Larson, C. et al. (2007). Completion of the 2001 national land cover database for the conterminous United States. *Photogrammetric Engineering and Remote Sensing*, 73(4), 337-341.

Homer, C. G., Dewitz, J. A., Yang, L., Jin, S., Danielson, P., Xian, G., Coulston, J., Herold, N. D., Wickham, J. D., & Megown, K. (2015). Completion of the 2011 national land cover database for the conterminous United States-Representing a decade of land cover change information. *Photogrammetric Engineering and Remote Sensing*, 81(5), 345-354.

Homer, C., Dewitz, J., Jin, S., Xian, G., Costello, C., Danielson, P., Gass, L., Funk, M., Wickham, J., Stehman, S., Auch, R., & Riitters, K. (2020). Conterminous United States land cover change patterns 2001–2016 from the 2016 national land cover database. *ISPRS Journal of Photogrammetry and Remote Sensing*, 162, 184-199.

Hughes, A. C., Tougeron, K., Martin, D. A., Menga, F., Rosado, B. H. P., Villasante, S., Madgulkar, S., Gonçalves, F., Geneletti, D., Diele-Viegas, L. M., Berger, S., Colla, S. R., De Andrade Kamimura, V., Caggiano, H., Melo, F., De Oliveira Dias, M. G., Kellner, E., & Do Couto, E. V. (2023). Smaller human populations are neither a

necessary nor sufficient condition for biodiversity conservation. *Biological Conservation*, *277*, 109841. https://doi.org/10.1016/j.biocon.2022.109841

Humle, T., Maisels, F., Oates, J.F., Plumptre, A., Williamson, E.A., 2016. *Pan troglodytes*. The IUCN red list of threatened species. e.T15933A10232667

Hurtt, G. C., Chini, L. P., Frolking, S., Betts, R. A., Feddema, J., Fischer, G., Fisk, J. P., Hibbard, K., Houghton, R. A., Janetos, A., Jones, C. D., Kindermann, G., Kinoshita, T., Klein Goldewijk, K., Riahi, K., Shevliakova, E., Smith, S., Stehfest, E., Thomson, A., … Wang, Y. P. (2011). Harmonization of land-use scenarios for the period 1500–2100: 600 years of global gridded annual land-use transitions, wood harvest, and resulting secondary lands. *Climatic Change*, *109*(1–2), 117–161. https://doi.org/10.1007/s10584-011-0153-2

IPCC. (2014). *Synthesis Report. Contribution of Working Groups I, II and III to the Fifth Assessment Report of the Intergovernmental Panel on Climate Change*.

IPCC, 2023: Summary for Policymakers. In: Climate Change 2023: *Synthesis Report. A Report of the Intergovernmental Panel on Climate Change. Contribution of Working Groups I, II and III to the Sixth Assessment Report of the Intergovernmental Panel on Climate Change* [Core Writing Team, H. Lee and J. Romero (eds.)]. IPCC, Geneva, Switzerland, 36 pages. (in press)

Isabirye-Basuta, G. M., & Lwanga, J. S. (2008). Primate populations and their interactions with changing habitats. *International Journal of Primatology*, *29*(1), 35–48. https://doi.org/10.1007/s10764-008-9239-8

IUCN. (2008). *Loxodonta africana*: Blanc, J.: The IUCN Red List of Threatened Species 2008: e.T12392A3339343 [Data set]. International Union for Conservation of Nature. https://doi.org/10.2305/IUCN.UK.2008.RLTS.T12392A3339343.en

IUCN. (2014). *Regional action plan for the conservation of western lowland gorillas and central chimpanzees 2015–2025*. Gland, Switzerland: IUCN SSC Primate Specialist Group. 54 pp.

IUCN. (2015). *Pan troglodytes ssp. ellioti*: Oates, J.F., Doumbe, O., Dunn, A., Gonder, M.K., Ikemeh, R., Imong, I., Morgan, B.J., Ogunjemite, B. & Sommer, V.: The IUCN Red List of threatened species 2016: e.T40014A17990330 [Data set]. International Union for Conservation of Nature. https://doi.org/10.2305/IUCN.UK.2016-2.RLTS.T40014A17990330.en

IUCN. (2016a). *Pan troglodytes ssp. troglodytes*: Maisels, F., Strindberg, S., Greer, D., Jeffery, K., Morgan, D.L. & Sanz, C.: The IUCN Red List of Threatened Species 2016: e.T15936A102332276 [Data set]. International Union for Conservation of Nature. https://doi.org/10.2305/IUCN.UK.2016-2.RLTS.T15936A17990042.en

IUCN. (2016b). *Pan paniscus*: Fruth, B., Hickey, J.R., André, C., Furuichi, T., Hart, J., Hart, T., Kuehl, H., Maisels, F., Nackoney, J., Reinartz, G., Sop, T., Thompson, J. & Williamson, E.A.: The IUCN Red List of Threatened Species 2016: e.T15932A102331567 [Data set]. International Union for Conservation of Nature. https://doi.org/10.2305/IUCN.UK.2016-2.RLTS.T15932A17964305.en

IUCN. (2016c). *Pan troglodytes*: Humle, T., Maisels, F., Oates, J.F., Plumptre, A. & Williamson, E.A.: The IUCN Red List of Threatened Species 2016: e.T15933A129038584 [Data set]. International Union for Conservation of Nature. https://doi.org/10.2305/IUCN.UK.2016-2.RLTS.T15933A17964454.en

IUCN. (2018). *Gorilla beringei ssp. beringei*: Hickey, J.R., Basabose, A., Gilardi, K.V., Greer, D., Nampindo, S., Robbins, M.M. & Stoinski, T.S: The IUCN Red List of threatened species 2018: e.T39999A17989719 [Data set]. International Union for Conservation of Nature. https://doi.org/10.2305/IUCN.UK.2018-2.RLTS.T39999A17989719.en

IUCN. (2020). *Loxodonta cyclotis*: Gobush, K.S., Edwards, C.T.T, Maisels, F., Wittemyer, G., Balfour, D. & Taylor, R.D.: The IUCN Red List of threatened species 2021: e.T181007989A204404464 [Data set]. International Union for Conservation of Nature. https://doi.org/10.2305/IUCN.UK.2021-1.RLTS.T181007989A204404464.en

Jachmann, H. (2008a). Illegal wildlife use and protected area management in Ghana. *Biological Conservation*, *141*(7), 1906–1918. https://doi.org/10.1016/j.biocon.2008.05.009

Jachmann, H. (2008b). Monitoring law-enforcement performance in nine protected areas in Ghana. *Biological Conservation*, *141*(1), 89–99. https://doi.org/10.1016/j.biocon.2007.09.012

Jensen, J. R. (2005). *Introductory digital image processing: A remote sensing perspective*. 3rd, Prentice Hall, Upper Saddle River, New Jersey.

Nelder, J. A., & Wedderburn, R. W. M. (1972). Generalized linear models. J*ournal of the Royal Statistical Society: Series A (General),* 135, 370–384.

Juárez-Orozco, S. M., Siebe, C., & Fernández y Fernández, D. (2017). Causes and effects of forest fires in tropical rainforests: A bibliometric approach. *Tropical Conservation Science*, *10*, 194008291773720. https://doi.org/10.1177/1940082917737207

Junker, J., Blake, S., Boesch, C., Campbell, G., Toit, L. du, Duvall, C., Ekobo, A., Etoga, G., Galat-Luong, A., Gamys, J., Ganas-Swaray, J., Gatti, S., Ghiurghi, A., Granier, N., Hart, J., Head, J., Herbinger, I., Hicks, T. C., Huijbregts, B., … Kuehl, H. S. (2012). Recent decline in suitable environmental conditions for African great apes. *Diversity and Distributions*, *18*(11), 1077–1091. https://doi.org/10.1111/ddi.12005

Kablan, Y. A., Diarrassouba, A., Mundry, R., Campbell, G., Normand, E., Kühl, H. S., Koné, I., & Boesch, C. (2019). Effects of anti-poaching patrols on the distribution of large mammals in Taï National Park, Côte d'Ivoire. *Oryx*, *53*(3), 469–478. https://doi.org/10.1017/S0030605317001272

Kanagaraj, R., Araujo, M. B., Barman, R., Davidar, P., De, R., Digal, D. K., Gopi, G. V., Johnsingh, A. J. T., Kakati, K., Kramer-Schadt, S., Lamichhane, B. R., Lyngdoh, S., Madhusudan, M. D., Ul Islam Najar, M., Parida, J., Pradhan, N. M. B., Puyravaud, J., Raghunath, R., Rahim, P. P. A., … Goyal, S. P. (2019). Predicting range shifts of Asian elephants under global change. *Diversity and Distributions*, *25*(5), 822–838. https://doi.org/10.1111/ddi.12898

Karume, K., Mondo, J. M., Chuma, G. B., Ibanda, A., Bagula, E. M., Aleke, A. L., Ndjadi, S., Ndusha, B., Ciza, P. A., Cizungu, N. C., Muhindo, D., Egeru, A., Nakayiwa, F. M., Majaliwa, J.-G. M., Mushagalusa, G. N., & Ayagirwe, R. B. B. (2022). Current practices and prospects of climate-smart agriculture in Democratic Republic of Congo: A Review. *Land*, *11*(10), 1850. https://doi.org/10.3390/land11101850

Kavzoglu, T., & Colkesen, I. (2009). A kernel functions analysis for support vector machines for land cover classification. *International Journal of Applied Earth Observation and Geoinformation*, *11*(5), 352–359. https://doi.org/10.1016/j.jag.2009.06.002

Keerthi, S. S., Shevade, S. K., Bhattacharyya, C., & Murthy, K. R. K. (2001). Improvements to Platt's SMO algorithm for SVM classifier design. *Neural Computation*, *13*(3), 637–649. https://doi.org/10.1162/089976601300014493

Kellner, C. J., Brawn, J. D., & Karr, J. R. (1992). What is habitat suitability and how should it be measured? In D. R. McCullough & R. H. Barrett (Eds.), *Wildlife 2001: Populations* (pp. 476–488). Springer Netherlands. https://doi.org/10.1007/978-94-011-2868-1_36

Khatami, R., Mountrakis, G., & Stehman, S. V. (2016). A meta-analysis of remote sensing research on supervised pixel-based land-cover image classification processes: General guidelines for practitioners and future research. *Remote Sensing of Environment*, *177*, 89–100. https://doi.org/10.1016/j.rse.2016.02.028

Kirilenko, A. P., & Sedjo, R. A. (2007). Climate change impacts on forestry. *Proceedings of the National Academy of Sciences*, *104*(50), 19697–19702. https://doi.org/10.1073/pnas.0701424104

Kleinschroth, F., Laporte, N., Laurance, W. F., Goetz, S. J., & Ghazoul, J. (2019). Road expansion and persistence in forests of the Congo Basin. *Nature Sustainability*, *2*(7), 628–634. https://doi.org/10.1038/s41893-019-0310-6

Knorn, J., Rabe, A., Radeloff, V. C., Kuemmerle, T., Kozak, J., & Hostert, P. (2009). Land cover mapping of large areas using chain classification of neighboring Landsat satellite images. *Remote Sensing of Environment*, *113*(5), 957–964. https://doi.org/10.1016/j.rse.2009.01.010

Kolden, C. A., & Abatzoglou, J. T. (2012). Wildfire consumption and interannual impacts by land cover in Alaskan boreal forest. *Fire Ecology*, *8*(1), 98–114. https://doi.org/10.4996/fireecology.0801098

Kongnso, M. E. (2022). Indigenous adaptation of pastoralists to climate variability and range land management in the Ndop Plain, North West Region, Cameroon. In E. E. Ebhuoma & L. Leonard (Eds.), *Indigenous knowledge and climate governance* (pp. 13–26). Springer International Publishing. https://doi.org/10.1007/978-3-030-99411-2_2

Kosheleff, V. P., & Anderson, C. N. K. (2009). Temperature's influence on the activity budget, terrestriality, and sun exposure of chimpanzees in the Budongo Forest, Uganda. *American Journal of Physical Anthropology*, *139*(2), 172–181. https://doi.org/10.1002/ajpa.20970

Kubat, M. (1999). Neural networks: A comprehensive foundation by Simon Haykin, Macmillan, 1994, ISBN 0-02-352781-7. *The Knowledge Engineering Review*, *13*(4), 409–412. https://doi.org/10.1017/S0269888998214044

Kühl, H., Maisels, F., Ancrenaz, M., & Williamson, E. A. (2008). *Best practice guidelines for surveys and monitoring of great ape populations*. IUCN. https://doi.org/10.2305/IUCN.CH.2008.SSC-OP.36.en

Kuhn, M., & Johnson, K. (2016). Applied predictive modeling. [in] Lo, C.P.; Choi, J. 2004. A hybrid approach to urban land use/cover mapping using Landsat 7 enhanced thematic mapper plus (ETM+) images. *International Journal of Remote Sensing*, 25, 2687-2700

Kumar, D. (2011). Monitoring forest cover changes using remote sensing and GIS: A global prospective. *Research Journal of Environmental Sciences*, *5*(2), 105–123. https://doi.org/10.3923/rjes.2011.105.123

Kyale, D., Ngene, S., & Maingi, J. (2011). Biophysical and human factors determine the distribution of poached elephants in Tsavo East National Park, Kenya. *Pachyderm*, 49, 48-60

Lambin, E. F., Turner, B. L., Geist, H. J., Agbola, S. B., Angelsen, A., Bruce, J. W., Coomes, O. T., Dirzo, R., Fischer, G., Folke, C., George, P. S., Homewood, K., Imbernon, J., Leemans, R., Li, X., Moran, E. F., Mortimore, M., Ramakrishnan, P. S., Richards, J. F., … Xu, J. (2001). The causes of land-use and land-cover change: Moving beyond the myths. *Global Environmental Change*, *11*(4), 261–269. https://doi.org/10.1016/S0959-3780(01)00007-3

Laurance, W. (2015). Emerging threats to tropical forests. *Annals of the Missouri Botanical garden*, 100(3), 159–169. https://doi.org/10.3417/2011087

Laurance, W. F., Carolina Useche, D., Rendeiro, J., Kalka, M., Bradshaw, C. J. A., Sloan, S. P., Laurance, S. G., Campbell, M., Abernethy, K., Alvarez, P., Arroyo-Rodriguez, V., Ashton, P., Benítez-Malvido, J., Blom, A., Bobo, K. S., Cannon, C. H., Cao, M., Carroll, R., Chapman, C., … Zamzani, F. (2012). Averting biodiversity collapse in tropical forest protected areas. *Nature*, *489*(7415), 290–294. https://doi.org/10.1038/nature11318

Laurance, W. F., Clements, G. R., Sloan, S., O'Connell, C. S., Mueller, N. D., Goosem, M., Venter, O., Edwards, D. P., Phalan, B., Balmford, A., Van Der Ree, R., & Arrea, I. B. (2014). A global strategy for road building. *Nature*, *513*(7517), 229–232. https://doi.org/10.1038/nature13717

Laurance, W. F., Goosem, M., & Laurance, S. G. W. (2009). Impacts of roads and linear clearings on tropical forests. *Trends in Ecology & Evolution*, *24*(12), 659–669. https://doi.org/10.1016/j.tree.2009.06.009

Leathwick, J. R., Rowe, D., Richardson, J., Elith, J., & Hastie, T. (2005). Using multivariate adaptive regression splines to predict the distributions of New Zealand's freshwater

diadromous fish. *Freshwater Biology*, *50*(12), 2034–2052. https://doi.org/10.1111/j.1365-2427.2005.01448.x

Lek, S., Delacoste, M., Baran, P., Dimopoulos, I., Lauga, J., & Aulagnier, S. (1996). Application of neural networks to modelling nonlinear relationships in ecology. *Ecological Modelling*, *90*(1), 39–52. https://doi.org/10.1016/0304-3800(95)00142-5

Lema, M. A., & Majule, A. E. (2009). Impacts of climate change, variability and adaptation strategies on agriculture in semi-arid areas of Tanzania: The case of Manyoni District in Singida Region, Tanzania. *African Journal of Environmental Science and Technology*, 3(8), 206-218.

Lescuyer, G., Cerutti, P. O., Tshimpanga, P., Biloko, F., Adebu-Abdala, B., Tsanga, R., Yembe-Yembe, R. I., & Essiane-Mendoula, E. (2014). *The domestic market for small-scale chainsaw milling in the Democratic Republic of Congo: Present situation, opportunities and challenges*. Center for International Forestry Research (CIFOR). https://doi.org/10.17528/cifor/005040

Leutner, B., Horning, N., & Leutner, M. B. (2017). Package 'RStoolbox'. R foundation for statistical computing, Version 0.1.

Li, J., & Convertino, M. (2021). Inferring ecosystem networks as information flows. *Scientific Reports*, *11*(1), 7094. https://doi.org/10.1038/s41598-021-86476-9

Li, W., Ciais, P., MacBean, N., Peng, S., Defourny, P., & Bontemps, S. (2016). Major forest changes and land cover transitions based on plant functional types derived from the ESA CCI Land Cover product. *International Journal of Applied Earth Observation and Geoinformation*, *47*, 30–39. https://doi.org/10.1016/j.jag.2015.12.006

Liang, X., Liu, X., Li, D., Zhao, H., & Chen, G. (2018). Urban growth simulation by incorporating planning policies into a CA-based future land-use simulation model. *International Journal of Geographical Information Science*, *32*(11), 2294–2316. https://doi.org/10.1080/13658816.2018.1502441

Liu, L., Zhang, X., Gao, Y., Chen, X., Shuai, X., & Mi, J. (2021). Finer-resolution mapping of global land cover: Recent developments, consistency analysis, and prospects. *Journal of Remote Sensing*, *2021*, 2021/5289697. https://doi.org/10.34133/2021/5289697

Liu, X., Liang, X., Li, X., Xu, X., Ou, J., Chen, Y., Li, S., Wang, S., & Pei, F. (2017). A future land use simulation model (FLUS) for simulating multiple land use scenarios

by coupling human and natural effects. *Landscape and Urban Planning*, *168*, 94–116. https://doi.org/10.1016/j.landurbplan.2017.09.019

López, L., Villalba, R., & Stahle, D. (2022). High-fidelity representation of climate variations by Amburana cearensis tree-ring chronologies across a tropical forest transition in South America. *Dendrochronologia*, *72*, 125932. https://doi.org/10.1016/j.dendro.2022.125932

Ludwig, F., Franssen, W., Jans, W., Beyenne, T., Kruijt, B., & SupitI. (2013). Climate change impacts on the Congo Basin region. In: *Climate change scenarios for the Congo Basin*. [Haensler A., Jacob D., Kabat P., Ludwig F. (eds.)]. Climate Service Centre Report No. 11, Hamburg, Germany, ISSN: 2192-4058.

MacQueen, J., et al. (1967). Some methods for classification and analysis of multivariate observations. In: *Proceedings of the fifth Berkeley symposium on mathematical statistics and probability*, 1, 281–297. Oakland, CA, USA

Magidi, J., Nhamo, L., Mpandeli, S., & Mabhaudhi, T. (2021). Application of the Random Forest classifier to map irrigated areas using Google Earth Engine. *Remote Sensing*, *13*(5), 876. https://doi.org/10.3390/rs13050876

Maingi, J. K., Mukeka, J. M., Kyale, D. M., & Muasya, R. M. (2012). Spatiotemporal patterns of elephant poaching in south-eastern Kenya. *Wildlife Research*, *39*(3), 234. https://doi.org/10.1071/WR11017

Maisels, F., Strindberg, S., Blake, S., Wittemyer, G., Hart, J., Williamson, E. A., Aba'a, R., Abitsi, G., Ambahe, R. D., Amsini, F., Bakabana, P. C., Hicks, T. C., Bayogo, R. E., Bechem, M., Beyers, R. L., Bezangoye, A. N., Boundja, P., Bout, N., Akou, M. E., … Warren, Y. (2013). Devastating decline of forest elephants in Central Africa. *PLoS ONE*, *8*(3), e59469. https://doi.org/10.1371/journal.pone.0059469

Malhi, Y., Adu-Bredu, S., Asare, R. A., Lewis, S. L., & Mayaux, P. (2013). African rainforests: Past, present and future. *Philosophical Transactions of the Royal Society B: Biological Sciences*, *368*(1625), 20120312. https://doi.org/10.1098/rstb.2012.0312

Mandrekar, J. N. (2010). Receiver operating characteristic curve in diagnostic test assessment. *Journal of Thoracic Oncology*, *5*(9), 1315–1316. https://doi.org/10.1097/JTO.0b013e3181ec173d

Mangaza, L., Sonwa, D. J., Batsi, G., Ebuy, J., & Kahindo, J.-M. (2021). Building a framework towards climate-smart agriculture in the Yangambi Landscape, Democratic Republic of Congo (DRC). *International Journal of Climate Change*

Strategies and Management, *13*(3), 320–338. https://doi.org/10.1108/IJCCSM-08-2020-0084

Matlhodi, B., Kenabatho, P. K., Parida, B. P., & Maphanyane, J. G. (2019). Evaluating land use and land cover change in the Gaborone Dam Catchment, Botswana, from 1984–2015 using GIS and Remote Sensing. *Sustainability*, *11*(19), 5174. https://doi.org/10.3390/su11195174

Matthews, E, & Grainger, A. (2003). Evaluation of FAO's Global Forest Resources Assessment from the user perspective. *Unasylva 53*, 42–55.

Mavah, G., Child, B., & Swisher, M. E. (2022). Empty laws and empty forests: Reconsidering rights and governance for sustainable wildlife management in the Republic of the Congo. *African Journal of Ecology*, *60*(2), 212–221. https://doi.org/10.1111/aje.12953

Mayaux, P. (2004). *A land cover map of Africa = Carte de l'occupation du sol de l'Afrique*. Office for Official Publications of the European Communities.

Mayaux, P., Grandi, G. F. D., Rauste, Y., Simard, M., & Saatchi, S. (2002). Large-scale vegetation maps derived from the combined L-band GRFM and C-band CAMP wide area radar mosaics of Central Africa. *International Journal of Remote Sensing*, *23*(7), 1261–1282. https://doi.org/10.1080/01431160110092894

Mayaux, P., Bartholome, E., Massart, M., Vancutsem, C. A. C., Nonguierma, A., Diallo, O., Pretorius, C., Thompson, M., Cherlet M., Pekel, J.-F., Defourny, P., Vasconcelos, M., Di Gregorio, A., Fritz, S., De Grandi, G., Elvidge, C., Vogt, P., & Belward, A. (2003). *A land cover map of Africa*. Luxembourg: Office for Official Publications of the European Communities and European Commission, Joint Research Centre, Luxembourg.

Mba, W. P., Longandjo, G.-N. T., Moufouma-Okia, W., Bell, J.-P., James, R., Vondou, D. A., Haensler, A., Fotso-Nguemo, T. C., Guenang, G. M., Tchotchou, A. L. D., Kamsu-Tamo, P. H., Takong, R. R., Nikulin, G., Lennard, C. J., & Dosio, A. (2018). Consequences of 1.5 °C and 2 °C global warming levels for temperature and precipitation changes over Central Africa. *Environmental Research Letters*, *13*(5), 055011. https://doi.org/10.1088/1748-9326/aab048

McCarthy, M. A. (2007). *Bayesian methods for ecology*. John Wiley & Sons

Megahed, Y., Cabral, P., Silva, J., & Caetano, M. (2015). Land cover mapping analysis and urban growth modelling using Remote Sensing techniques in greater Cairo region—

Egypt. *ISPRS International Journal of Geo-Information*, *4*(3), 1750–1769. https://doi.org/10.3390/ijgi4031750

Megevand, C., Mosnier, A., Hourticq, J., Sanders, K., Doetinchem, N., & Streck, C. (2013). *Deforestation trends in the Congo Basin: Reconciling economic growth and forest protection*. The World Bank. https://doi.org/10.1596/978-0-8213-9742-8

Mellor, A., Haywood, A., Stone, C., & Jones, S. (2013). The performance of Random Forests in an operational setting for large area sclerophyll forest classification. *Remote Sensing*, *5*(6), 2838–2856. https://doi.org/10.3390/rs5062838

Mendelsohn, R., Dinar, A., & Dalfelt, A. (2000). *Climate change impacts on African agriculture. Preliminary analysis prepared for the World Bank*, Washington, District of Columbia, pp. 25

Mengist, W. (2020). An overview of the major vegetation classification in Africa and the new vegetation classification in Ethiopia. *American Journal of Zoology,* 2(4), 51-62.

Merow, C., Smith, M. J., Edwards, T. C., Guisan, A., McMahon, S. M., Normand, S., Thuiller, W., Wüest, R. O., Zimmermann, N. E., & Elith, J. (2014). What do we gain from simplicity versus complexity in species distribution models? *Ecography*, *37*(12), 1267–1281. https://doi.org/10.1111/ecog.00845

Merow, C., Smith, M. J., & Silander, J. A. (2013). A practical guide to MaxEnt for modeling species' distributions: What it does, and why inputs and settings matter. *Ecography*, *36*(10), 1058–1069. https://doi.org/10.1111/j.1600-0587.2013.07872.x

Meyer, A., & Pie, M. (2022). Climate change estimates surpass rates of climatic niche evolution in primates. *International Journal of Primatology*, 43(1), 40–56. https://doi.org/10.1007/s10764-021-00253-z

Meyer, A., Pie, M., & Passos, F. (2014). Assessing the exposure of lion tamarins (*Leontopithecus spp*.) to future climate change. *American Journal of Primatology*, 76(6), 551–562. https://doi.org/10.1002/ajp.22247

Midekisa, A., Holl, F., Savory, D. J., Andrade-Pacheco, R., Gething, P. W., Bennett, A., & Sturrock, H. J. W. (2017). Mapping land cover change over continental Africa using Landsat and Google Earth Engine cloud computing. *PLoS ONE*, *12*(9), e0184926. https://doi.org/10.1371/journal.pone.0184926

Midekisa, A., Senay, G. B., & Wimberly, M. C. (2014). Multisensor earth observations to characterize wetlands and malaria epidemiology in Ethiopia. *Water Resources Research*, *50*(11), 8791–8806. https://doi.org/10.1002/2014WR015634

Mohajane, M., Essahlaoui, A., Oudija, F., El Hafyani, M., Hmaidi, A. E., El Ouali, A., Randazzo, G., & Teodoro, A. C. (2018). Land use/land cover (LULC) using Landsat data series (MSS, TM, ETM+ and OLI) in Azrou Forest, in the central middle atlas of Morocco. *Environments*, *5*(12), 131. https://doi.org/10.3390/environments5120131

Molinario, G., Hansen, M. C., Potapov, P. V., Tyukavina, A., Stehman, S., Barker, B., & Humber, M. (2017). Quantification of land cover and land use within the rural complex of the Democratic Republic of Congo. *Environmental Research Letters*, *12*(10), 104001. https://doi.org/10.1088/1748-9326/aa8680

Moore, D. L., & Vigilant, L. (2014). A population estimate of chimpanzees (*Pan troglodytes schweinfurthii*) in the Ugalla region using standard and spatially explicit genetic capture-recapture methods: Population Estimate of Ugalla Chimpanzees. *American Journal of Primatology*, *76*(4), 335–346. https://doi.org/10.1002/ajp.22237

Morgan, B. J. et al. (2011). *Regional action plan for the conservation of the Nigeria-Cameroon chimpanzee* (Pan troglodytes ellioti). IUCN/SSC Primate Specialist Group and Zoological Society of San Diego, CA, USA

Morgan, D., Mundry, R., Sanz, C., Ayina, C. E., Strindberg, S., Lonsdorf, E., & Kühl, H. S. (2018). African apes coexisting with logging: Comparing chimpanzee (*Pan troglodytes troglodytes*) and gorilla (*Gorilla gorilla gorilla*) resource needs and responses to forestry activities. *Biological Conservation*, *218*, 277–286. https://doi.org/10.1016/j.biocon.2017.10.026

Morgan, D., Strindberg, S., Winston, W., Stephens, C. R., Traub, C., Ayina, C. E., Ndolo Ebika, S. T., Mayoukou, W., Koni, D., Iyenguet, F., & Sanz, C. M. (2019). Impacts of selective logging and associated anthropogenic disturbance on intact forest landscapes and apes of Northern Congo. *Frontiers in Forests and Global Change*, *2*, 28. https://doi.org/10.3389/ffgc.2019.00028

Morgan, P., Heyerdahl, E. K., Strand, E. K., Bunting, S. C., Riser Ii, J. P., Abatzoglou, J. T., Nielsen-Pincus, M., & Johnson, M. (2020). Fire and land cover change in the Palouse Prairie–Forest Ecotone, Washington and Idaho, USA. *Fire Ecology*, *16*(1), 2. https://doi.org/10.1186/s42408-019-0061-9

Mosnier et al. (2016). *Modelling land use changes in the Democratic Republic of the Congo 2000– 2030*. www.redd-pac.org

Mu, J. E., Sleeter, B. M., Abatzoglou, J. T., & Antle, J. M. (2017). Climate impacts on agricultural land use in the USA: The role of socio-economic scenarios. *Climatic Change*, *144*(2), 329–345. https://doi.org/10.1007/s10584-017-2033-x

Naimi, B., & Araújo, M. B. (2016). sdm: A reproducible and extensible R platform for species distribution modelling. *Ecography*, *39*(4), 368–375. https://doi.org/10.1111/ecog.01881

Nasi, R., Taber, A., & Van Vliet, N. (2011). Empty forests, empty stomachs? Bushmeat and livelihoods in the Congo and Amazon Basins. *International Forestry Review*, *13*(3), 355–368. https://doi.org/10.1505/146554811798293872

Nedd, R., Light, K., Owens, M., James, N., Johnson, E., & Anandhi, A. (2021). A synthesis of land use/land cover studies: Definitions, classification systems, meta-studies, challenges and knowledge gaps on a global landscape. *Land*, *10*(9), 994. https://doi.org/10.3390/land10090994

Ngene, S. M., Van Gils, H., Van Wieren, S. E., Rasmussen, H., Skidmore, A. K., Prins, H. H. T., Toxopeus, A. G., Omondi, P., & Douglas-Hamilton, I. (2009). The ranging patterns of elephants in Marsabit Protected Area, Kenya: The use of satellite-linked GPS collars: The ranging patterns of elephants in Kenya. *African Journal of Ecology*, *48*(2), 386–400. https://doi.org/10.1111/j.1365-2028.2009.01125.x

Ngigi, S. N. (2009). *Climate change adaptation strategies: Water resources management options for smallholder farming systems in Sub-Saharan Africa*. The MDG Centre for East and Southern Africa, the Earth Institute at Columbia University, New York. Pp.189.

N'Goran, P. K., Boesch, C., Mundry, R., N'Goran, E. K., Herbinger, I., Yapi, F. A., & Kühl, H. S. (2012). Hunting, law enforcement, and African primate conservation: Primate hunting and law enforcement. *Conservation Biology*, *26*(3), 565–571. https://doi.org/10.1111/j.1523-1739.2012.01821.x 48(2), 386–400. https://doi.org/10.1111/j.1365-2028.2009.01125.x

N'Goran, K.P. (2015). *Méthodologie de collecte de données, inventaires de grands et moyens mammifères par distance sampling*. Document de travail, WWF Regional Office for Africa - Yaoundé Hub, Yaoundé, Cameroun

N'Goran, K.P., Nzooh Dongmo, Z., & Le-Duc Yeno, S. (2014). *Guide technique pour les protocoles d'inventaires fauniques de grands et moyens mammifères par distance*

sampling. Document de travail, WWF Regional Office for Africa - Yaoundé Hub, Yaoundé, Cameroun

N'Goran, K. P., Ndomba, D. L., & Beukou, G. B. (2016). *Rapport de l'inventaire des grands et moyens mammifères dans le segment RCA du paysage Tri-national de la Sangha*. Unpublished report. Bayanga, Central African Republic: Bureau Régional du WWF pour l'Afrique

N'Goran, K.P., Nzooh Dongmo, Z., & Le-Duc Yeno, S. (2017). *WWF biomonitoring activities from 2014 to 2016. Status of forest elephant and great apes in Central Africa priority sites*. Project Report, WWF Regional Office for Africa - Yaoundé Hub, Yaoundé, Cameroun. https://awsassets.panda.org/downloads/WWF_CA_Biomonitoring_23102017a.pdf

N'Goran, P. K., Boesch, C., Mundry, R., N'Goran, E. K., Herbinger, I., Yapi, F. A., & Kühl, H. S. (2012). Hunting, law enforcement, and African primate conservation: Primate hunting and law enforcement. *Conservation Biology, 26*(3), 565–571. https://doi.org/10.1111/j.1523-1739.2012.01821.x

Njidda. (2001). *Structures et dynamiques des espèces ligneuses dans les zones Sud Est du Parc National de Waza*. Mémoire du diplôme d'ingénieur des eaux et forêts. Université de Dschang.

Njidda. (2001). *Structures et dynamiques des espèces ligneuses dans les zones Sud Est du Parc National de Waza.* Mémoire du diplôme d'ingénieur des eaux et forêts. Université de Dschang.

Nkrumah, K. (1976). *Neo-colonialism: The last stage of imperialism* (6. print). International Publ.

Nuissl, H., & Siedentop, S. (2021). Urbanisation and land use change. In T. Weith, T. Barkmann, N. Gaasch, S. Rogga, C. Strauß, & J. Zscheischler (Eds.), *Sustainable land management in a European context* (Vol. 8, pp. 75–99). Springer International Publishing. https://doi.org/10.1007/978-3-030-50841-8_5

Nzooh Dongmo, Z. L., N'goran, K. P., Etoga, G., Belinga, J. P., Fouda, E., Bandjouma, M., & Dongmo, P. (2016a). *Les populations de grands et moyens mammifères dans le segment Cameroun du Paysage TRIDOM: Forêt de Ngoyla-Mintom, PN Boumba Bek et PN Nki et leurs zones périphériques*. Rapport Technique. Yaoundé, Cameroun.

Nzooh Dongmo, Z. L., Ngoran, K. P., Ekodeck, H., Kobla, A. S., Famegni, S., Sombambo, M., & Mengamenya, A. (2016b). *Les populations de grands et moyens mammifères*

dans le segment Lobéké et du Tri-National de la Sangha. Unpublished report. WWF/Sangha Tri-National Foundation/Ministry of Forestry and Wildlife, Yaoundé, Cameroon.

Oates et al. (2007). *Regional action plan for the conservation of the cross river gorilla (*Gorilla gorilla diehli*)*. IUCN/SSC Primate Specialist Group and Conservation International.

Oates, J. F., McFarland, K. L., Groves, J. L., Bergl, R. A., Linder, J. M., & Disotell, T. R. (2002). The cross river gorilla: Natural history and status of a neglected and critically endangered subspecies. In A. B. Taylor & M. L. Goldsmith (Eds.), *Gorilla biology* (1st ed., pp. 472–497). Cambridge University Press. https://doi.org/10.1017/CBO9780511542558.021

Ogunyiola, A., Gardezi, M., & Vij, S. (2022). Smallholder farmers' engagement with climate smart agriculture in Africa: role of local knowledge and upscaling. *Climate Policy*, *22*(4), 411–426. https://doi.org/10.1080/14693062.2021.2023451

Olén, N. B., & Lehsten, V. (2022). High-resolution global population projections dataset developed with CMIP6 RCP and SSP scenarios for year 2010-2100. *Data in brief*, *40*, 107804. https://doi.org/10.1016/j.dib.2022.107804

Olofsson, P., Foody, G. M., Herold, M., Stehman, S. V., Woodcock, C. E., & Wulder, M. A. (2014). Good practices for estimating area and assessing accuracy of land change. *Remote Sensing of Environment*, *148*, 42–57. https://doi.org/10.1016/j.rse.2014.02.015

Olson, D. M., Dinerstein, E., Wikramanayake, E. D., Burgess, N. D., Powell, G. V. N., Underwood, E. C., D'amico, J. A., Itoua, I., Strand, H. E., Morrison, J. C., Loucks, C. J., Allnutt, T. F., Ricketts, T. H., Kura, Y., Lamoreux, J. F., Wettengel, W. W., Hedao, P., & Kassem, K. R. (2001). Terrestrial ecoregions of the world: A new map of life on earth. *BioScience*, *51*(11), 933. https://doi.org/10.1641/0006-3568(2001)051[0933:TEOTWA]2.0.CO;2

Ordaz-Nemeth, I., Sop, T., Amarasekaran, B., Bachmann, M., Boesch, C., Brncic, T., Caillaud, D., Campbell, G., Carvalho, J., Chancellor, R., Davenport, T., Dowd, D., Eno-Nku, M., Ganas-Swaray, J., Granier, N., Greengrass, E., Heinicke, S., Herbinger, I., Inkamba-Nkulu, C., … Kuhl, H. (2021). Range-wide indicators of African great ape density distribution. *American Journal of Primatology*, 83(12). https://doi.org/10.1002/ajp.23338

Ordway, E. M., Naylor, R. L., Nkongho, R. N., & Lambin, E. F. (2019). Oil palm expansion and deforestation in Southwest Cameroon associated with proliferation of informal mills. *Nature Communications*, *10*(1), 114. https://doi.org/10.1038/s41467-018-07915-2

Pacheco, A. da P., Junior, J. A. da S., Ruiz-Armenteros, A. M., & Henriques, R. F. F. (2021). Assessment of k-Nearest Neighbor and Random Forest classifiers for mapping forest fire areas in Central Portugal using Landsat-8, Sentinel-2, and Terra Imagery. *Remote Sensing*, *13*(7), 1345. https://doi.org/10.3390/rs13071345

Paneque-Gálvez, J., Mas, J.-F., Moré, G., Cristóbal, J., Orta-Martínez, M., Luz, A. C., Guèze, M., Macía, M. J., & Reyes-García, V. (2013). Enhanced land use/cover classification of heterogeneous tropical landscapes using support vector machines and textural homogeneity. *International Journal of Applied Earth Observation and Geoinformation*, *23*, 372–383. https://doi.org/10.1016/j.jag.2012.10.007

Parent, J. (2009). *Landscape fragmentation analysis (version 2)*. University of Connecticut Press, USA

Partenariat pour les Forêts du Bassin du Congo-PFBC. (2006). *Les forêts du bassin du Congo: État des forêts 2006*. Partenariat pour 296 Chapter 12. Forest Fragmentation: Causes and Impacts. https://pfbc-cbfp.org/files/docs/Bassin%20du%20Congo/EdF/Les%20forets%20du%20Bassin%20du%20Congo%202006%20neu.pdf

Patrice Dkamela, G., & Nguiffo, S. (2022). The new turn in the militarization of conservation in Cameroon, Central Africa. In M. Ramutsindela, F. Matose, & T. Mushonga (Eds.), *The Violence of Conservation in Africa*. Edward Elgar Publishing. https://doi.org/10.4337/9781800885615.00016

Pedregosa, F., Varoquaux, G., Gramfort, A., Michel, V., Thirion, B., Grisel, O., Blondel, M., Müller, A., Nothman, J., Louppe, G., Prettenhofer, P., Weiss, R., Dubourg, V., Vanderplas, J., Passos, A., Cournapeau, D., Brucher, M., Perrot, M., & Duchesnay, É. (2012). *Scikit-learn: Machine Learning in Python*. https://doi.org/10.48550/ARXIV.1201.0490

Pelletier, C., Valero, S., Inglada, J., Champion, N., & Dedieu, G. (2016). Assessing the robustness of Random Forests to map land cover with high resolution satellite image time series over large areas. *Remote Sensing of Environment*, *187*, 156–168. https://doi.org/10.1016/j.rse.2016.10.010

Pereira, C., & Tsikata, D. (2021). Contextualising extractivism in Africa. *Feminist Africa*, *2*(1), 14-47

Peres, C. A., & Lake, I. R. (2003). Extent of nontimber resource extraction in tropical forests: Accessibility to game vertebrates by hunters in the Amazon Basin. *Conservation Biology*, *17*(2), 521–535. https://doi.org/10.1046/j.1523-1739.2003.01413.x

Pérez-Vega, A., Mas, J.-F., & Ligmann-Zielinska, A. (2012). Comparing two approaches to land use/cover change modeling and their implications for the assessment of biodiversity loss in a deciduous tropical forest. *Environmental Modelling & Software*, *29*(1), 11–23. https://doi.org/10.1016/j.envsoft.2011.09.011

Phillips, S. J., Anderson, R. P., & Schapire, R. E. (2006). Maximum entropy modeling of species geographic distributions. *Ecological Modelling*, *190*(3–4), 231–259. https://doi.org/10.1016/j.ecolmodel.2005.03.026

Phillips, S. J., & Dudík, M. (2008). Modeling of species distributions with Maxent: New extensions and a comprehensive evaluation. *Ecography*, *31*(2), 161–175. https://doi.org/10.1111/j.0906-7590.2008.5203.x

Philippe and Karume. (2019). Assessing forest cover change and deforestation hot-spots in the North Kivu Province, DR-Congo using remote sensing and GIS. 8(2), 39–54.

Plumptre, A. J. (2010). Eastern chimpanzee (*Pan troglodytes schweinfurthii*): Status survey and conservation action plan, 2010-2020. IUCN

Pörtner, H. O., Roberts, D. C., Adams, H., Adler, C., Aldunce, P., Ali, E., Ara Begum, R., Betts, R., Bezner Kerr, R., Biesbroek, R., Birkmann, J., Bowen, K., Castellanos, E., Cissé, G., Constable, A., Cramer, W., Dodman, D., Eriksen, S. H., Fischlin, A., ... Zaiton Ibrahim, Z. (2022). *Climate change 2022: Impacts, adaptation and vulnerability*. IPCC. https://edepot.wur.nl/565644

Potapov, P., Li, X., Hernandez-Serna, A., Tyukavina, A., Hansen, M. C., Kommareddy, A., Pickens, A., Turubanova, S., Tang, H., Silva, C. E., Armston, J., Dubayah, R., Blair, J. B., & Hofton, M. (2021). Mapping global forest canopy height through integration of GEDI and Landsat data. *Remote Sensing of Environment*, *253*, 112165. https://doi.org/10.1016/j.rse.2020.112165

Potapov, P., Turubanova, S., Hansen, M. C., Tyukavina, A., Zalles, V., Khan, A., Song, X.-P., Pickens, A., Shen, Q., & Cortez, J. (2022). Global maps of cropland extent and change show accelerated cropland expansion in the twenty-first century. *Nature Food*, *3*(1), 19–28. https://doi.org/10.1038/s43016-021-00429-z

Potapov, P. V., Turubanova, S. A., Hansen, M. C., Adusei, B., Broich, M., Altstatt, A., Mane, L., & Justice, C. O. (2012). Quantifying forest cover loss in Democratic Republic of the Congo, 2000–2010, with Landsat ETM+ data. *Remote Sensing of Environment*, *122*, 106–116. https://doi.org/10.1016/j.rse.2011.08.027

Poulsen, J. R., Koerner, S. E., Moore, S., Medjibe, V. P., Blake, S., Clark, C. J., Akou, M. E., Fay, M., Meier, A., Okouyi, J., Rosin, C., & White, L. J. T. (2017). Poaching empties critical Central African wilderness of forest elephants. *Current Biology*, *27*(4), R134–R135. https://doi.org/10.1016/j.cub.2017.01.023

Poulsen, J. R., Rosin, C., Meier, A., Mills, E., Nuñez, C. L., Koerner, S. E., Blanchard, E., Callejas, J., Moore, S., & Sowers, M. (2018). Ecological consequences of forest elephant declines for Afrotropical forests. *Conservation Biology*, *32*(3), 559–567. https://doi.org/10.1111/cobi.13035

Pouteau, R., Collin, A., & Stoll, B. (2011). *A comparison of machine learning algorithms for classification of tropical ecosystems observed by multiple sensors at multiple scales*. International Geoscience and Remote Sensing Symposium 2011: Vancouver, BC, Canada.

Pruetz, J. D., Marchant, L. F., Arno, J., & McGrew, W. C. (2002). Survey of savanna chimpanzees (*Pan troglodytes verus*) in southeastern Sénégal: Savanna chimpanzees in Sénégal. *American Journal of Primatology*, *58*(1), 35–43. https://doi.org/10.1002/ajp.10035

Qian, Y., Zhou, W., Yan, J., Li, W., & Han, L. (2014). Comparing machine learning classifiers for object-based land cover classification using very high resolution imagery. *Remote Sensing*, *7*(1), 153–168. https://doi.org/10.3390/rs70100153

Quinlan, J. R. (1993). Programs for machine learning. *Machine Learning* 4, 5.

Rahman, M., Jashimuddin, M., Kamrul, I., & Kumar Nath, T. (2016). Land use change and forest fragmentation analysis: A geoinformatics approach on Chunati Wildlife Sanctuary, Bangladesh. *Journal of Civil Engineering and Environmental Sciences*, *2*(1), 020–029. https://doi.org/10.17352/2455-488X.000010

Rainforest Foundation. (2021). *Roads to ruin: The emerging impacts of infrastructure development in Congo Basin forests*. https://www.rainforestfoundationuk.org/wp-content/uploads/2021/10/infrastructure-report.pdf

Ramutsindela, M., Matose, F., & Mushonga, T. (Eds.). (2022). *The violence of conservation in Africa: State, militarization and alternatives*. Edward Elgar Publishing.

R Core Team, 2016. *R: A language and environment for statistical computing*. R Foundation for Statistical Computing, Vienna, Austria. URL https://www.R-project.org/

R Core Team, 2022. *R:* A *language and environment for statistical computing*. R Foundation for Statistical Computing, Vienna, Austria. URL https://www.R-project.org/

Reed, K. E., & Fleagle, J. G. (1995). Geographic and climatic control of primate diversity. *Proceedings of the National Academy of Sciences*, *92*(17), 7874–7876. https://doi.org/10.1073/pnas.92.17.7874

Réjou-Méchain, M., Mortier, F., Bastin, J.-F., Cornu, G., Barbier, N., Bayol, N., Bénédet, F., Bry, X., Dauby, G., Deblauwe, V., Doucet, J.-L., Doumenge, C., Fayolle, A., Garcia, C., Kibambe Lubamba, J.-P., Loumeto, J.-J., Ngomanda, A., Ploton, P., Sonké, B., … Gourlet-Fleury, S. (2021). Unveiling African rainforest composition and vulnerability to global change. *Nature*, *593*(7857), 90–94. https://doi.org/10.1038/s41586-021-03483-6

Ritchie, H., & Roser, M. (2021). *Forests and Deforestation*. OurWorldInData.org. 'https://ourworldindata.org/forests-and-deforestation

Robson, A. S., Trimble, M. J., Purdon, A., Young-Overton, K. D., Pimm, S. L., & Van Aarde, R. J. (2017). Savanna elephant numbers are only a quarter of their expected values. *PLoS ONE*, *12*(4), e0175942. https://doi.org/10.1371/journal.pone.0175942

Rodriguez-Galiano, V. F., Ghimire, B., Rogan, J., Chica-Olmo, M., & Rigol-Sanchez, J. P. (2012). An assessment of the effectiveness of a Random Forest classifier for land-cover classification. *ISPRS Journal of Photogrammetry and Remote Sensing*, *67*, 93–104. https://doi.org/10.1016/j.isprsjprs.2011.11.002

Romijn, E., Lantican, C. B., Herold, M., Lindquist, E., Ochieng, R., Wijaya, A., Murdiyarso, D., & Verchot, L. (2015). Assessing change in national forest monitoring capacities of 99 tropical countries. *Forest Ecology and Management*, 352, 109–123. https://doi.org/10.1016/j.foreco.2015.06.003

Rood, E., Ganie, A. A., & Nijman, V. (2010). Using presence-only modelling to predict Asian elephant habitat use in a tropical forest landscape: Implications for conservation: Sumatran elephant habitat use in Indonesia. *Diversity and Distributions*, *16*(6), 975–984. https://doi.org/10.1111/j.1472-4642.2010.00704.x

Roy, J., Vigilant, L., Gray, M., Wright, E., Kato, R., Kabano, P., Basabose, A., Tibenda, E., Kühl, H. S., & Robbins, M. M. (2014). Challenges in the use of genetic mark-recapture to estimate the population size of Bwindi mountain gorillas (*Gorilla*

beringei beringei). *Biological Conservation*, *180*, 249–261. https://doi.org/10.1016/j.biocon.2014.10.011

Royal Collection Trust, n.d. Press Office, Royal Collection Trust, York House, St James's Palace, London, SW1A 1BQ T. +44 (0)20 7839 1377, press@royalcollection.org.uk, www.royalcollection.org.uk

Ruiz Pérez, M., Ezzine de Blas, D., Nasi, R., Sayer, J. A., Sassen, M., Angoué, C., Gami, N., Ndoye, O., Ngono, G., Nguinguiri, J.-C., Nzala, D., Toirambe, B., & Yalibanda, Y. (2005). Logging in the Congo Basin: A multi-country characterization of timber companies. *Forest Ecology and Management*, *214*(1–3), 221–236. https://doi.org/10.1016/j.foreco.2005.04.020

Sá, R. (2012). The trade and ethnobiological use of chimpanzee body parts in Guinea-Bissau. *Traffic Bulletin*, 24

Sales, L., Ribeiro, B., Chapman, C., & Loyola, R. (2020). Multiple dimensions of climate change on the distribution of Amazon primates. *Perspectives in Ecology and Conservation*, *18*(2), 83–90. https://doi.org/10.1016/j.pecon.2020.03.001

Samaniego, L., & Schulz, K. (2009). Supervised classification of agricultural land cover using a modified k-NN technique (MNN) and Landsat remote sensing imagery. *Remote Sensing*, *1*(4), 875–895. https://doi.org/10.3390/rs1040875

Sang, C. C., Olago, D. O., Nyumba, T. O., Marchant, R., & Thorn, J. P. R. (2022). Assessing the underlying drivers of change over two decades of land use and land cover dynamics along the standard gauge railway corridor, Kenya. *Sustainability*, *14*(10), 6158. https://doi.org/10.3390/su14106158

Sarfo, I., Shuoben, B., Otchwemah, H. B., Darko, G., Kedjanyi, E. A. G., Oduro, C., Folorunso, E. A., Alriah, M. A. A., Amankwah, S. O. Y., & Ndafira, G. C. (2022). Validating local drivers influencing land use cover change in Southwestern Ghana: A mixed-method approach. *Environmental Earth Sciences*, *81*(14), 367. https://doi.org/10.1007/s12665-022-10481-y

Sari, I. L., Weston, C. J., Newnham, G. J., & Volkova, L. (2021). Assessing accuracy of land cover change maps derived from automated digital processing and visual interpretation in tropical forests in Indonesia. *Remote Sensing*, *13*(8), 1446. https://doi.org/10.3390/rs13081446

Sarker, I. H. (2021). Machine learning: Algorithms, real-world applications and research directions. *SN Computer Science*, *2*(3), 160. https://doi.org/10.1007/s42979-021-00592-x

Sassen, M., van Soesbergen, A., Arnell, A. P., & Scott, E. (2022). Patterns of (future) environmental risks from cocoa expansion and intensification in West Africa call for context specific responses. *Land Use Policy*, *119*, 106142. https://doi.org/10.1016/j.landusepol.2022.106142

Savory, D. J., Andrade-Pacheco, R., Gething, P. W., Midekisa, A., Bennett, A., & Sturrock, H. J. W. (2017). Intercalibration and gaussian process modeling of nighttime lights imagery for measuring urbanization trends in Africa 2000–2013. *Remote Sensing*, *9*(7), 713. https://doi.org/10.3390/rs9070713

Serra, P., Pons, X., & Saurí, D. (2008). Land-cover and land-use change in a Mediterranean landscape: A spatial analysis of driving forces integrating biophysical and human factors. *Applied Geography*, *28*(3), 189–209. https://doi.org/10.1016/j.apgeog.2008.02.001

Sesink Clee, P. R., Abwe, E. E., Ambahe, R. D., Anthony, N. M., Fotso, R., Locatelli, S., Maisels, F., Mitchell, M. W., Morgan, B. J., Pokempner, A. A., & Gonder, M. K. (2015). Chimpanzee population structure in Cameroon and Nigeria is associated with habitat variation that may be lost under climate change. *BMC Evolutionary Biology*, *15*(1), 2. https://doi.org/10.1186/s12862-014-0275-z

Shelestov, A., Lavreniuk, M., Kussul, N., Novikov, A., & Skakun, S. (2017). Exploring Google Earth Engine platform for big data processing: Classification of multi-temporal satellite imagery for crop mapping. *Frontiers in Earth Science*, *5*. https://doi.org/10.3389/feart.2017.00017

Shi, D., & Yang, X. (2015). Support Vector Machines for land cover mapping from remote sensor imagery. In J. Li & X. Yang (Eds.), *Monitoring and modeling of global changes: A Geomatics Perspective* (pp. 265–279). Springer Netherlands. https://doi.org/10.1007/978-94-017-9813-6_13

Shi, Y., Wang, R., Fan, L., Li, J., & Yang, D. (2010). Analysis on land-use change and its demographic factors in the original-stream watershed of tarim river based on GIS and statistic. *Procedia Environmental Sciences*, *2*, 175–184. https://doi.org/10.1016/j.proenv.2010.10.021

Shutt, K. (2014). *Wildlife tourism and conservation: An interdisciplinary evaluation of gorilla ecotourism in Dzanga-Sangha, Central African Republic* (Doctoral dissertation, Durham University).

Silva, L. P. e, Xavier, A. P. C., da Silva, R. M., & Santos, C. A. G. (2020). Modeling land cover change based on an artificial neural network for a semiarid river basin in northeastern Brazil. *Global Ecology and Conservation*, *21*, e00811. https://doi.org/10.1016/j.gecco.2019.e00811

Smits, P. C., Dellepiane, S. G., & Schowengerdt, R. A. (1999). Quality assessment of image classification algorithms for land-cover mapping: A review and a proposal for a cost-based approach. *International Journal of Remote Sensing*, *20*(8), 1461–1486. https://doi.org/10.1080/014311699212560

Sonwa, D. J., Nkem, J. N., Idinoba, M. E., Bele, M. Y., & Jum, C. (2012). Building regional priorities in forests for development and adaptation to climate change in the Congo Basin. *Mitigation and Adaptation Strategies for Global Change*, *17*(4), 441–450. https://doi.org/10.1007/s11027-011-9335-5

State Parties of Cameroon, the Central African Republic and Congo, 2019. *Report of the State Party to the World Heritage Committee on the state of conservation of the Sangha Trinational (Cameroon, the Central African Republic and Congo)*. [online] State Parties of Cameroon, the Central African Republic and Congo. Available at: https://whc.unesco.org/en/list/1380/document.

Steffen, W., Broadgate, W., Deutsch, L., Gaffney, O., & Ludwig, C. (2015). The trajectory of the Anthropocene: The Great Acceleration. *The Anthropocene Review*, 2(1), 81–98. https://doi.org/10.1177/2053019614564785

Stokes, E., Strindberg, S., Bakabana, P., Elkan, P., Iyenguet, F., Madzoke, B., Malanda, G., Mowawa, B., Moukoumbou, C., Ouakabadio, F., & Rainey, H. (2010). Monitoring great ape and elephant abundance at large spatial scales: Measuring effectiveness of a conservation landscape. *PLoS ONE*, *5*(4). https://doi.org/10.1371/journal.pone.0010294

Stralberg, D., Wang, X., Parisien, M.-A., Robinne, F.-N., Sólymos, P., Mahon, C. L., Nielsen, S. E., & Bayne, E. M. (2018). Wildfire-mediated vegetation change in boreal forests of Alberta, Canada. *Ecosphere*, *9*(3), e02156. https://doi.org/10.1002/ecs2.2156

Strindberg, S., Maisels, F., Williamson, E. A., Blake, S., Stokes, E. J., Aba'a, R., Abitsi, G., Agbor, A., Ambahe, R. D., Bakabana, P. C., Bechem, M., Berlemont, A., Bokoto de Semboli, B., Boundja, P. R., Bout, N., Breuer, T., Campbell, G., De Wachter, P., Ella Akou, M., … Wilkie, D. S. (2018). Guns, germs, and trees determine density and distribution of gorillas and chimpanzees in Western Equatorial Africa. *Science Advances*, *4*(4), eaar2964. https://doi.org/10.1126/sciadv.aar2964

Struebig, M., Fischer, M., Gaveau, D., Meijaard, E., Wich, S., Gonner, C., Sykes, R., Wilting, A., & Kramer-Schadt, S. (2015). Anticipated climate and land-cover changes reveal refuge areas for Borneo's orang-utans. *Global Change Biology*, *21*(8), 2891–2904. https://doi.org/10.1111/gcb.12814

Sunderland-Groves. (2003). *Surveys of the cross river gorilla and chimpanzee populations in Takamanda Forest Reserve, Cameroon* (Vol. 1–8). Smithsonian Institution. file:///D:/Downloads/09-Sunderland-Grovesetal2003Takamandagorillas.pdf

Swets, J. A. (1988). Measuring the accuracy of diagnostic systems. *Science*, *240*(4857), 1285–1293. https://doi.org/10.1126/science.3287615

Tamoffo, A. T., Vondou, D. A., Pokam, W. M., Haensler, A., Yepdo, Z. D., Fotso-Nguemo, T. C., Tchotchou, L. A. D., & Nouayou, R. (2019). Daily characteristics of Central African rainfall in the REMO model. *Theoretical and Applied Climatology*, *137*(3–4), 2351–2368. https://doi.org/10.1007/s00704-018-2745-5

ATchobsala, A. A., & Mbolo, M. (2010). Impact of wood cuts on the structure and floristic diversity of vegetation in the peri-urban zone of Ngaoundere, Cameroon. *Journal of Ecology and The Natural Environment*, 2(11), 235-258.

Tchotsoua, M., 2006. *Evolution récente des territoires de l'Adamawa central : de la spatialisation à l'aide pour un développement maîtrisé*. Université d'Orléans. Ecole doctorale sciences de l'homme et de la société. HDR. Discipline (Géographie-Aménagement Environnement). p 267

Teodoro, A. C. (2015). Applicability of data mining algorithms in the identification of beach features/patterns on high-resolution satellite data. *Journal of Applied Remote Sensing*, *9*(1), 095095. https://doi.org/10.1117/1.JRS.9.095095

TerrSet. (2020). *TerrSet 2020 Geospatial monitoring and modeling software*. Clark Labs. https://clarklabs.org/terrset/

Thanh Noi, P., & Kappas, M. (2017). Comparison of Random Forest, k-Nearest Neighbor, and Support Vector Machine classifiers for land cover classification using Sentinel-2 Imagery. *Sensors*, *18*(2), 18. https://doi.org/10.3390/s18010018

Thakur, R., & Panse, P. (2022). Classification performance of land use from multispectral remote sensing images using Decision Tree, K-Nearest Neighbor, Random Forest and Support Vector Machine using EuroSAT data. *International Journal of Intelligent Systems and Applications in Engineering*, 10(1s), 67-77

Thomas, L., Buckland, S. T., Rexstad, E. A., Laake, J. L., Strindberg, S., Hedley, S. L., Bishop, J. R. B., Marques, T. A., & Burnham, K. P. (2010). Distance software: Design and analysis of distance sampling surveys for estimating population size. *Journal of Applied Ecology*, *47*(1), 5–14. https://doi.org/10.1111/j.1365-2664.2009.01737.x

Thomas, Y., & Bacher, C. (2018). Assessing the sensitivity of bivalve populations to global warming using an individual-based modelling approach. *Global Change Biology*, *24*(10), 4581–4597. https://doi.org/10.1111/gcb.14402

Thrasher, B., Wang, W., Michaelis, A., Melton, F., Lee, T., & Nemani, R. (2022). NASA global daily downscaled projections, CMIP6. *Scientific Data*, *9*(1), 262. https://doi.org/10.1038/s41597-022-01393-4

Törmä, M. (2013). Land cover classification of Finnish Lapland using decision tree classification algorithm. *The photogrammetric Journal of Finland*, 23(2)

Tranquilli, S., Abedi-Lartey, M., Abernethy, K., Amsini, F., Asamoah, A., Balangtaa, C., Blake, S., Bouanga, E., Breuer, T., Brncic, T. M., Campbell, G., Chancellor, R., Chapman, C. A., Davenport, T. R. B., Dunn, A., Dupain, J., Ekobo, A., Eno-Nku, M., Etoga, G., … Sommer, V. (2014). Protected areas in tropical Africa: Assessing threats and conservation activities. *PLoS ONE*, *9*(12), e114154. https://doi.org/10.1371/journal.pone.0114154

Tudge, S., Brittain, S., Kentatchime, F., Tagne, C., & Rowcliffe, J. (2021). The impacts of human activity on mammals in a community forest near the Dja Biosphere Reserve in Cameroon. *Oryx*. https://doi.org/10.1017/S0030605321000806

Tyukavina, A., Hansen, M. C., Potapov, P., Parker, D., Okpa, C., Stehman, S. V., Kommareddy, I., & Turubanova, S. (2018). Congo Basin forest loss dominated by increasing smallholder clearing. *Science Advances*, *4*(11), eaat2993. https://doi.org/10.1126/sciadv.aat2993

UNESCO (2015). *Report on the state of conservation of Sangha Trinational, Cameroon, the Central African Republic and Congo. State of conservation information system of the World Heritage Centre*. [online]. UNESCO World Heritage Centre, Paris, France. Available at: https://whc.unesco.org/en/list/1380/documents/

UNESCO (2017). *Report on the state of conservation of Sangha Trinational, Cameroon, the Central African Republic and Congo. State of conservation information system of the World Heritage Centre.* [online]. UNESCO World Heritage Centre, Paris, France. Available at: https://whc.unesco.org/en/list/1380/documents/

UNESCO (2019). *Report on the state of conservation of Sangha Trinational, Cameroon, the Central African Republic and Congo. State of conservation information system of the World Heritage Centre*. [online]. UNESCO World Heritage Centre, Paris, France. Available at: https://whc.unesco.org/en/list/1380/documents/

UNESCO/IUCN (2016). *Rapport de la mission de suivi réactif conjointe Centre du patrimoine mondial/UICN au Trinational de la sangha (République Centrafricaine, Cameroun et Congo), 15 – 25 octobre 2016*. IUCN and UNESCO World Heritage Centre, Gland, Switzerland and Paris, France. [online] Available at: https://whc.unesco.org/en/list/1380/documents/

United Nations, Department of Economic and Social Affairs, Population Division. (2022). *World population prospects*. United Nations. file:///D:/Downloads/WPP2022_Data_Sources.pdf

Upgupta, S., Sharma, J., Jayaraman, M., Kumar, V., & Ravindranath, N. H. (2015). Climate change impact and vulnerability assessment of forests in the Indian Western Himalayan region: A case study of Himachal Pradesh, India. *Climate Risk Management*, *10*, 63–76. https://doi.org/10.1016/j.crm.2015.08.002

Verhegghen, A. (2015). Review and combination of recent remote sensing based products for forest cover change in Cameroon. *International Forestry Review*, *18*, 14–25.

Verhegghen, A., Mayaux, P., de Wasseige, C., & Defourny, P. (2012). Mapping Congo Basin vegetation types from 300 m and 1 km multi-sensor time series for carbon stocks and forest areas estimation. *Biogeosciences*, *9*(12), 5061–5079. https://doi.org/10.5194/bg-9-5061-2012

Vermote, E., Justice, C., Claverie, M., & Franch, B. (2016). Preliminary analysis of the performance of the Landsat 8/OLI land surface reflectance product. *Remote Sensing of Environment*, *185*, 46–56. https://doi.org/10.1016/j.rse.2016.04.008

Vogt, P., Riitters, K. H., Estreguil, C., Kozak, J., Wade, T. G., & Wickham, J. D. (2007). Mapping spatial patterns with morphological image processing. *Landscape Ecology*, *22*(2), 171–177. https://doi.org/10.1007/s10980-006-9013-2

Volke, M. I., & Abarca-Del-Rio, R. (2020). Comparison of machine learning classification algorithms for land cover change in a coastal area affected by the 2010 Earthquake and Tsunami in Chile [Preprint]. *Natural Hazards and Earth System Sciences: Discussions*. Databases, GIS, Remote Sensing, Early Warning Systems and Monitoring Technologies. https://doi.org/10.5194/nhess-2020-41

Vu, T., Tran, D., Tran, H., Nguyen, M., Do, T., Ta, N., Cao, H., Pham, N., & Phan, D. (2020). An assessment of the impact of climate change on the distribution of the grey-shanked douc *Pygathrix cinerea* using an ecological niche model. *Primates*, *61*(2), 267–275. https://doi.org/10.1007/s10329-019-00763-8

Wall, J., Wittemyer, G., Klinkenberg, B., LeMay, V., Blake, S., Strindberg, S., Henley, M., Vollrath, F., Maisels, F., Ferwerda, J., & Douglas-Hamilton, I. (2021). Human footprint and protected areas shape elephant range across Africa. *Current Biology*, *31*(11), 2437-2445.e4. https://doi.org/10.1016/j.cub.2021.03.042

Walsh, S. J., Messina, J. P., Mena, C. F., Malanson, G. P., & Page, P. H. (2008). Complexity theory, spatial simulation models, and land use dynamics in the Northern Ecuadorian Amazon. *Geoforum*, *39*(2), 867–878. https://doi.org/10.1016/j.geoforum.2007.02.011

Walton. (2008). Subpixel urban land cover estimation: Comparing cubist, Random Forests, and support vector regression. *Photogrammetric Engineering & Remote Sensing*, *74*(10), 1213–1222.

Wang, H., Liu, Y., Wang, Y., Yao, Y., & Wang, C. (2023). Land cover change in global drylands: A review. *Science of The Total Environment*, *863*, 160943. https://doi.org/10.1016/j.scitotenv.2022.160943

Wang, Y., Jiang, D., Zhuang, D., Huang, Y., Wang, W., & Yu, X. (2013). Effective key parameter determination for an automatic approach to land cover classification based on multispectral remote sensing imagery. *PLoS ONE*, *8*(10), e75852. https://doi.org/10.1371/journal.pone.0075852

Wasser, S. K., Shedlock, A. M., Comstock, K., Ostrander, E. A., Mutayoba, B., & Stephens, M. (2004). Assigning African elephant DNA to geographic region of origin: Applications to the ivory trade. *Proceedings of the National Academy of Sciences*, *101*(41), 14847–14852. https://doi.org/10.1073/pnas.0403170101

Watson, R. T., Noble, I. R., Bolin, B., Ravindranath, N. H., Verardo, D. J., & Dokken, D. J. (2001). *Land use, land-use change and forestry: A special report of the Intergovernmental Panel on Climate Change*. Cambridge University Press

Watson, J. E. M., Grantham, H. S., Wilson, K. A., & Possingham, H. P. (2011). Systematic conservation planning: Past, present and future. In R. J. Ladle & R. J. Whittaker (Eds.), *Conservation Biogeography* (1st ed., pp. 136–160). Wiley. https://doi.org/10.1002/9781444390001.ch6

Wei, C., Huang, J., Mansaray, L., Li, Z., Liu, W., & Han, J. (2017). Estimation and mapping of winter oilseed rape LAI from high spatial resolution satellite data based on a hybrid method. *Remote Sensing*, *9*(5), 488. https://doi.org/10.3390/rs9050488

Weinhold, D., & Reis, E. (2008). Transportation costs and the spatial distribution of land use in the Brazilian Amazon. *Global Environmental Change*, *18*(1), 54–68. https://doi.org/10.1016/j.gloenvcha.2007.06.004

Wessels, K. J., Reyers, B., van Jaarsveld, A. S., & Rutherford, M. C. (2003). Identification of potential conflict areas between land transformation and biodiversity conservation in north-eastern South Africa. *Agriculture, Ecosystems & Environment*, *95*(1), 157–178. https://doi.org/10.1016/S0167-8809(02)00102-0

White, J. C., Wulder, M. A., Hermosilla, T., Coops, N. C., & Hobart, G. W. (2017). A nationwide annual characterization of 25 years of forest disturbance and recovery for Canada using Landsat time series. *Remote Sensing of Environment*, *194*, 303–321. https://doi.org/10.1016/j.rse.2017.03.035

Wilson, D. E., & Reeder, D. M. (Eds.). (2005). *Mammal species of the world: A taxonomic and geographic reference* (3rd ed). Johns Hopkins University Press.

Wittemyer, G., Elsen, P., Bean, W. T., Burton, A. C. O., & Brashares, J. S. (2008). Accelerated human population growth at protected area edges. *Science*, *321*(5885), 123–126. https://doi.org/10.1126/science.1158900

Wittemyer, G., Northrup, J. M., Blanc, J., Douglas-Hamilton, I., Omondi, P., & Burnham, K. P. (2014). Illegal killing for ivory drives global decline in African elephants. *Proceedings of the National Academy of Sciences*, *111*(36), 13117–13121. https://doi.org/10.1073/pnas.1403984111

Xia, J., Dalla Mura, M., Chanussot, J., Du, P., & He, X. (2015). Random subspace ensembles for hyperspectral image classification with extended morphological attribute profiles.

IEEE Transactions on Geoscience and Remote Sensing, *53*(9), 4768–4786. https://doi.org/10.1109/TGRS.2015.2409195

Xie, Y., Mei, Y., Guangjin, T., & Xuerong, X. (2005). Socio-economic driving forces of arable land conversion: A case study of Wuxian City, China. *Global Environmental Change*, *15*(3), 238–252. https://doi.org/10.1016/j.gloenvcha.2005.03.002

Yang, X. (2009). Artificial neural networks for urban modeling. *Manual of geographic information systems*, 647-658

Yang, Y., Yang, D., Wang, X., Zhang, Z., & Nawaz, Z. (2021). Testing accuracy of land cover classification algorithms in the Qilian mountains based on GEE cloud platform. *Remote Sensing*, *13*(24), 5064. https://doi.org/10.3390/rs13245064

Yeshaneh, E., Wagner, W., Exner-Kittridge, M., Legesse, D., & Blöschl, G. (2013). Identifying land use/cover dynamics in the Koga catchment, Ethiopia, from multi-scale data, and implications for environmental change. *ISPRS International Journal of Geo-Information*, *2*(2), 302–323. https://doi.org/10.3390/ijgi2020302

Ygorra, B., Frappart, F., Wigneron, J. P., Moisy, C., Catry, T., Baup, F., Hamunyela, E., & Riazanoff, S. (2021). Monitoring loss of tropical forest cover from Sentinel-1 time-series: A CuSum-based approach. *International Journal of Applied Earth Observation and Geoinformation*, *103*, 102532. https://doi.org/10.1016/j.jag.2021.102532

Yuh, Y. G., Dongmo, Z. N., N'Goran, P. K., Ekodeck, H., Mengamenya, A., Kuehl, H., Sop, T., Tracz, W., Agunbiade, M., & Elvis, T. (2019). Effects of land cover change on great apes distribution at the Lobéké National Park and its surrounding forest management units, South-East Cameroon. A 13 year time series analysis. *Scientific Reports*, *9*(1), 1445. https://doi.org/10.1038/s41598-018-36225-2

Zerrouki, N., Harrou, F., Sun, Y., & Hocini, L. (2019). A machine learning-based approach for land cover change detection using remote sensing and radiometric measurements. *IEEE Sensors Journal*, *19*(14), 5843–5850. https://doi.org/10.1109/JSEN.2019.2904137

Zgłobicki, W., Gawrysiak, L., Baran-Zgłobicka, B., & Telecka, M. (2016). Long-term forest cover changes, within an agricultural region, in relation to environmental variables, Lubelskie Province, Eastern Poland. *Environmental Earth Sciences*, *75*(20), 1373. https://doi.org/10.1007/s12665-016-6195-z

Zhang, H. K., & Roy, D. P. (2017). Using the 500 m MODIS land cover product to derive a consistent continental scale 30 m Landsat land cover classification. *Remote Sensing of Environment*, *197*, 15–34. https://doi.org/10.1016/j.rse.2017.05.024

Zhang, L., Ameca, E., Cowlishaw, G., Pettorelli, N., Foden, W., & Mace, G. (2019). Global assessment of primate vulnerability to extreme climatic events. *Nature Climate Change*, *9*(7), 554. https://doi.org/10.1038/s41558-019-0508-7

Zhao, X., Ren, B., Garber, P., Li, X., & Li, M. (2018). Impacts of human activity and climate change on the distribution of snub-nosed monkeys in China during the past 2000 years. *Diversity and Distributions*, *24*(1), 92–102. https://doi.org/10.1111/ddi.12657

Ziervogel, G., Cartwright, A., Tas, A., Adejuwon, J., Zermoglio, F., Shale, M., & Smith, B. (2008). *Climate change and adaptation in African agriculture*. Stockholm Environment Institute, March 2008, pp. 17-19

Ziegler, S., Fa, J. E., Wohlfart, C., Streit, B., Jacob, S., & Wegmann, M. (2016). Mapping bushmeat hunting pressure in Central Africa. *Biotropica*, *48*(3), 405–412. https://doi.org/10.1111/btp.12286

Zoungrana, B., Conrad, C., Amekudzi, L., Thiel, M., Da, E., Forkuor, G., & Löw, F. (2015). Multi-temporal Landsat images and ancillary data for land use/cover change (LULCC) detection in the Southwest of Burkina Faso, West Africa. *Remote Sensing*, *7*(9), 12076–12102. https://doi.org/10.3390/rs70912076